ANALYTICA CHIMICA ACTA

International monthly devoted to all branches of analytical chemistry
Revue mensuelle internationale consacrée à tous les domaines de la chimie analytique
Internationale Monatsschrift für alle Gebiete der analytischen Chemie

ELSEVIER PUBLISHING COMPANY
AMSTERDAM

Anal. Chim. Acta, Vol. 56, No. 3, 333–496, October 1971
Published monthly
Completing Volume 56

Publication Schedule for 1971

In the interests of rapid publication it has been found necessary to schedule 5 volumes for appearance in 1971. Since monthly publication will be maintained, this implies that 2 of the volumes will each consist of three issues, while 3 of the volumes will each consist of only 2 issues. The following provisional schedule applies:

Vol. **53**, No. **1**	January 1971	
Vol. **53**, No. **2**	February 1971	**(completing Vol. 53)**
Vol. **54**, No. **1**	March 1971	
Vol. **54**, No. **2**	April 1971	
Vol. **54**, No. **3**	May 1971	**(completing Vol. 54)**
Vol. **55**, No. **1**	June 1971	
Vol. **55**, No. **2**	July 1971	**(completing Vol. 55)**
Vol. **56**, No. **1**	August 1971	
Vol. **56**, No. **2**	September 1971	
Vol. **56**, No. **3**	October 1971	**(completing Vol. 56)**
Vol. **57**, No. **1**	November 1971	
Vol. **57**, No. **2**	December 1971	**(completing Vol. 57)**

Subscription price: $17.50 or Dfl. 63.— per volume plus postage. Total subscription price for 1971: $87.50 or Dfl. 315.— plus postage. Additional cost for copies by airmail available on request. For subscribers in the U.S.A. and Canada, 2nd class postage paid at New York, N.Y. For advertising rates apply to the publishers.

Subscriptions should be sent to:

ELSEVIER PUBLISHING COMPANY P.O. Box 211, Amsterdam, The Netherlands

---

GENERAL INFORMATION

Languages

Papers will be published in English, French or German.

Submission of papers

Papers should be sent to:

PROF. PHILIP W. WEST,
Coates Chemical Laboratories,
College of Chemistry and Physics,
Louisiana State University,
Baton Rouge 3,
La. 70803 (U.S.A.)

or to:

DR. A. M. G. MACDONALD,
Department of Chemistry,
The University,
P.O. Box 363
Birmingham B15 2TT (Great Britain)

Reprints

Fifty reprints will be supplied free of charge. Additional reprints (minimum 100) can be ordered at quoted prices. They must be ordered on order forms which are sent together with the proofs.

Kodak

For a copy of the new Eastman Catalog (No. 46)

or for any of the 6,000 chemicals it contains, contact one of these laboratory supply houses. EASTMAN Organic Chemicals are stocked locally in the continental U.S.A. by:

B&A
CURTIN
FISHER
HOWE & FRENCH
NORTH-STRONG
PREISER
SARGENT-WELCH
WILL/VW&R

For EASTMAN Organic Chemicals service elsewhere:

ARGENTINA
Cientifica Comercial Argentina S.A.C.I.
Buenos Aires

AUSTRALIA
H. B. Selby and Co., Pty., Ltd.
Adelaide
Brisbane
Hobart
Melbourne
Perth
Sydney
Ramsay Surgical Limited
Victoria

BELGIUM
s. a. Belgolabo
Overijse

BRAZIL
Atlantida Representacoes e Importacoes, Ltda.
Rio de Janeiro
Tennant Quimica S.A.
Sao Paulo

CANADA
Fisher Scientific Co., Ltd.
Edmonton
Montreal
Ottawa
Toronto
Vancouver
Sargent-Welch Scientific of Canada, Ltd.
Vancouver
Weston

DENMARK
H. Struers Chemiske Laboratorium
Copenhagen K

FINLAND
Havulinna Oy
Helsinki

FRANCE
Touzart & Matignon
Paris

W. GERMANY
Serva International Chemie-Handels GmbH & Co.
Heidelberg

GREECE
P. Bacacos S.A.
Athens

GUATEMALA
F. Krafka and Co., Ltd.
Emaoa

INDIA
Kodak Limited
Bombay

ISRAEL
Landseas Israel
Tel Aviv

ITALY
Prodotti Gianni, s.r.l.
Milan

JAPAN
Muromachi Kagaku Kogyo Kaisha, Ltd.
Tokyo
Nagase and Co., Ltd.
Tokyo

KOREA
The Sang Chung Commercial Co., Ltd.
Seoul

MEXICO
Alfonso Marhx, S.A.
Mexico 1, D. F.
Hoffmann-Pinther and Bosworth, S.A.
Mexico 1, D. F.

NETHERLANDS
N. V. Holland-Indie Agenturen Mij, HIAM
Amsterdam C

NEW ZEALAND
Kempthorne, Prosser & Co's.
New Zealand Drug Co., Ltd.
Wellington-Dunedin

NORWAY
Nerliens Kemisk Tekniske Aktieselskap
Oslo

PORTUGAL
Soquimica, Sociedad de Representacoes de Quimica
Lisbon

PUERTO RICO
Fisher Scientific Co.
Santurce

REPUBLIC OF CHINA
San Ho Instrument Co.
Taipei, Taiwan
Teh Ying Co., Ltd.
Taipei, Taiwan

REPUBLIC OF MALAWI
Baird and Tatlock (International) Ltd.
Blantyre

REPUBLIC OF SOUTH AFRICA
Baird and Tatlock S.A., Pty.
Johannesburg

REPUBLIC OF ZAMBIA
Baird and Tatlock (Zambia) Ltd.
Ndola

SWEDEN
KEBO AB
Stockholm 6

SWITZERLAND
Dr. Bender and Dr. Hobein AG
Zurich 6

UNITED KINGDOM
Kodak Limited
Kirkby, Liverpool

VENEZUELA
Equipos Cientificos y Educativos S.A.
Caracas

The catalog may also be obtained from:
Dept. 412L, Eastman Organic Chemicals,
Eastman Kodak Company, Rochester, N.Y. 14650, U.S.A.

19 ม.ค. 2515
ห้องสมุด กรมวิทยาศาสตร์

A NEW PUBLICATION

cell differentiation

An international journal for the rapid publication of original research papers on the aspects of cellular differentiation in eukaryotes

- CELL DIFFERENTIATION is an international journal which will serve its contributors by the rapid publication of novel research on aspects of cellular differentiation in eukaryotes.
- Papers will deal with molecular aspects of cell differentiation, regulatory devices active in the development of cellular traits, nucleo-cytoplasmic interactions, morphogenesis of subcellular elements, environmental influences on cellular activity and genome action in cellular development.
- The journal will provide rapid publication of original research papers not exceeding 3,000 words or the equivalent in diagrams, tables, illustrations and a list of references. The papers should be complete and essentially final reports meriting urgent publication.
- CELL DIFFERENTIATION will be published bimonthly at first, in volumes of approximately 360 pages.

Manuscripts should be sent to the Managing Editors:

Dr. H. D. Berendes, Managing Editor Cell Differentiation, Dept. of Biology, University of Nijmegen, Nijmegen, The Netherlands.

Dr. U. E. Loening, Managing Editor Cell Differentiation, Dept. of Zoology, University of Edinburgh, Edinburgh, Great Britain.

Subscription Information:
One volume of six issues per year initially. Volume 1 – 1972. Subscription price: Dfl. 70.00 or approx. US$ 20.00 + Dfl. 7.00 or approx. US$ 2.00 postage per volume.

Send your order to your usual supplier or direct to North-Holland Publishing Company.

North-Holland

Journal Division, P.O. Box 211,
Amsterdam - The Netherlands

291N

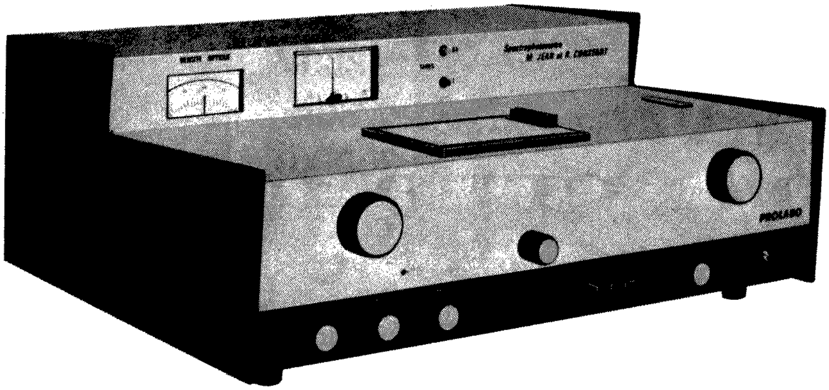
PROLABO

A New Elsevier Publication in Engineering

HEAT TRANSFER 1970

Papers presented at the Fourth International Heat Transfer Conference,
Paris – Versailles, 1970

Edited by U. GRIGULL and E. HAHNE, München, Germany

10 Volumes. 5102 pages, ISBN 0–444–999 39–6
Dfl. 650.00 (ca. $ 180.75) per set of 10 volumes.

These volumes contain the papers presented at the Fourth International Heat Transfer Conference held from August 31st to September 4th, 1970 at Paris-Versailles. The conference was sponsored by the General Assembly for Heat Transfer Conferences whose purpose it is to keep the sum total of knowledge in the field of heat transfer up to date and to provide a setting for reports and discussion on the subject within the framework of a four-yearly conference.

Approximately 350 contributions were selected to serve as a basis for thirty-six working sessions. The first eight volumes contain the papers presented at the conference, while volume nine covers the rapporteurs' critical review of them. A considerable portion of each working session was devoted to discussions and reports of these are published in volume ten.

CONTENTS: Vol. I: HEAT EXCHANGERS, 510 pages, 28 tables, 261 illus.
Vol. II: FORCED CONVECTION I, 522 pages, 20 tables, 376 illus.
Vol. III: FORCED CONVECTION II RADIATION, 590 pages, 15 tables, 399 illus.
Vol. IV: NATURAL CONVECTION RHEOLOGY, 550 pages, 23 tables, 273 illus., 4 plates, 4 photographs
Vol. V: BOILING I, 641 pages, 26 tables, 401 illus.
Vol. VI: BOILING II CONDENSATION, 534 pages, 22 tables, 336 illus.
Vol. VII: COMBINED HEAT TRANSFER, 500 pages, 21 tables, 222 illus.
Vol. VIII: ABSTRACTS OF THE PAPERS IN ENGLISH, FRENCH, GERMAN AND RUSSIAN LANGUAGE, 388 pages
Vol. IX: LECTURES OF THE RAPPORTEURS, 531 pages
Vol. X: DISCUSSIONS, 336 pages

Elsevier

Book Division, P.O. Box 211
Amsterdam - The Netherlands

133 E

vous
êtes
attendus

par

750
fabricants

une
profession qui
se prépare

depuis
18 mois

pour
vous recevoir
6 jours

du
6 au 11
déc.

une invitation qui ne se décline pas

Salon
du laboratoire 1971

Paris, porte de Versailles

6.11 déc. 1971

epiac

INDUSTRIAL ELECTROCHEMICAL PROCESSES

A Comprehensive Review of Past and Present Industrially Scaled Processes

Edited by A. T. KUHN, Lecturer in Electrochemistry, University of Salford, Lancashire, England

1971, xxiv + 632 pages, 56 tables, 144 illus., 1,805 lit.refs., Dfl. 165.00 (ca. $ 45.75)
ISBN 0-444-40885-1

This book will provide newcomers with an excellent idea of the scope of the field, and the basic principles involved, together with the relative importance of each area. The professional electrochemist will find a concise and up to date review of the scientific background, while the chemical engineer or industrial electrochemist will find the fullest available bibliography on the process of interest to him. There is a listing of key Patents and references. The second part of the book reviews the major components of the technology, and a final chapter examines the development of the industry on a country by country basis.

The contributing authors have compiled what is unquestionably the most authoritative and fully researched book yet written on the subject.

CONTENTS:

Production of Elemental Fluorine by Electrolysis. Electrochemical Fluorination. The Chlor-Alkali Industry. Industrial Water Electrolysis. Electrolytic Heavy Water Manufacture. The Electrowinning of Metals. Electrorefining in Aqueous Electrolytes. Electrorefining in Molten Salts. Electrochemical Machining. The Electrolytic Finishing of Metals. Electroforming. The Electrodeposition of Paint. Electrodialysis. Miscellaneous Industrial Processes. Electrodes for Industrial Processes. Diaphragms and Electrolytes. Cell Design. An International Survey of Industrial Electrochemical Processes.

CONTRIBUTORS:

B. A. Cooke, D. Gilroy, P. F. Hart, A. W. D. Hills, G. Isserlis, C. Jackson, R. J. Kendrick, A. T. Kuhn, D. Lawson, N. N. Ness, A. L. L. Palluel, A. J. Rudge, D. H. Smith, G. S. Solt, J. M. Steele, E. V. Tuck, B. J. Woodhall, P. M. Wright.

Elsevier
Book Division, P.O. Box 3489
Amsterdam - The Netherlands

119E

VERLAG
CHEMIE

Erhard Hornbogen

Durchstrahlungs-Elektronenmikroskopie fester Stoffe

Die Verwirklichung jeder technischen Idee erfordert geeignete Werkstoffe. Deren Verfügbarkeit entscheidet zunehmend häufiger über den Erfolg eines Konzepts und beeinflußt so das Ausmaß des technischen Fortschritts. Oft sind Werkstoffprobleme die eigentliche Schwierigkeit bei Projekten, deren grundlegende physikalische und konstruktive Zusammenhänge gelöst sind. So rückt die Optimierung vorhandener und die Entwicklung neuer Werkstoffe immer mehr in den Blickpunkt der technischen Entwicklung. Fragen nach Werkstoffen mit geeigneten Eigenschaften, nach ihrem Aufbau, ihrer Untersuchung und ihrer Anwendung stellen sich in allen Bereichen der Technik in zunehmendem Maße; sowohl Ingenieure als auch Wissenschaftler werden mit Ihnen konfrontiert. Zur Beantwortung dieser Frage soll die Buchreihe „Werkstoffe" beitragen, deren erster Band nun vorliegt.

Für Werkstoffentwicklungen ist es immer weniger sinnvoll, den früher allein üblichen empirischen Weg zu gehen. Es ist vielmehr zweckmäßig, die Eigenschaften eines Werkstoffes aus dem atomaren Aufbau abzuleiten. Voraussetzung dazu ist in jedem Fall, daß der mikroskopische Aufbau eines Stoffes lückenlos bekannt ist.

Das vorliegende Buch vermittelt eine Einführung, die praktisches Arbeiten im Labor ermöglichen soll. Es ist für alle gedacht, die die direkte Durchstrahlung mit Elektronen zur Untersuchung des Gefüges von Werkstoffen anwenden wollen. Bekanntlich sind solche Untersuchungen nicht ohne Kenntnisse über das Entstehen der Abbildungen möglich. Ziel des Buches ist es, ausgehend von einfachen Kontrastbedingungen – z. B. der Versetzung, des Stapelfehlers, der Antiphasengrenze – zu einem Verständnis der in der Praxis vorkommenden Gefüge zu gelangen.

Dieses Buch beschränkt sich auf die direkte Durchstrahlung der Werkstoffe. Diese Methode wird im ersten Kapitel in den Rahmen der anderen optischen Untersuchungsverfahren eingeordnet. Im Mittelpunkt stehen die Abbildungen mit Streuabsorption, d. h. Streuung der Elektronen in der Probe und Absorption dieser Elektronen in einer Objektiv-Aperturblende. Der hier am ausführlichsten behandelte Sonderfall ist der Beugungskontrast, d. h. Beugung in der kristallinen Probe und Absorption der gebeugten Strahlen in der Blende.

Den Abschluß des Bandes bildet je ein Abschnitt über Zusatzeinrichtungen zur Probebehandlung im Mikroskop und über Mikroskopie bei sehr hoher Spannung.

Band 1 der neuen Reihe „Werkstoffe – Aufbau, Eigenschaften, Untersuchung, Anwendung". Herausgegeben von G. Petzow und H. Warlimont. 1971. XI, 151 Seiten mit 109 Abbildungen und 17 Tabellen. Broschiert DM 31,50.

ISBN: 3-527-25386-6. LC Catalog Card No.: 71-150730

Wir übersenden Ihnen gern unseren Sonderprospekt.

VERLAG CHEMIE GMBH WEINHEIM/BERGSTR.

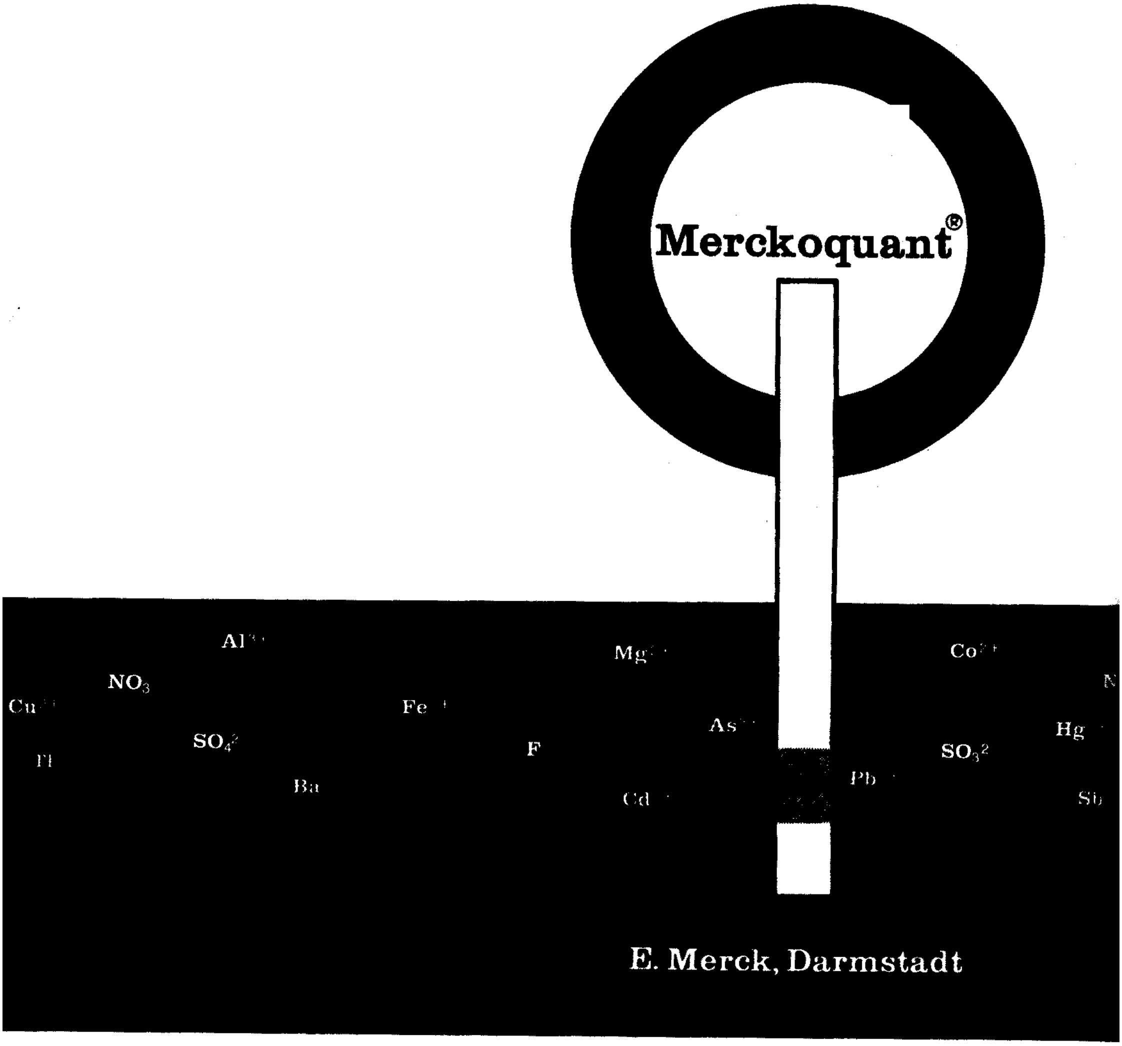
Merckoquant®
Al
NO
Cu
SO
Tl
Ba
Fe
F
Mg
Cd
As
Pb
Co
SO
Hg
Sb

Analytica Chimica Acta
Elsevier Publishing Company, Amsterdam
Printed in The Netherlands

AN ELECTRODE FOR THE DETERMINATION OF GLUTAMINE

G. G. GUILBAULT AND F. R. SHU
Department of Chemistry, Louisiana State University in New Orleans, New Orleans, La. 70122 (U.S.A.)

(Received 5th May 1971)

No direct and convenient method has so far been reported for the determination of glutamine. In order to determine this substance, glutamine is usually first hydrolyzed to glutamate. Following this deamination step:

$$\text{glutamine} \xrightarrow{\text{glutaminase}} \text{glutamate} + NH_3 \qquad (1)$$

the glutamate produced is determined by a second, coupled enzyme reaction with glutamic acid dehydrogenase. The fluorescent product, NADH, is measured, and equated to the concentration of glutamine present[1-3].

$$\text{glutamate} + \text{NAD} \xrightarrow[\text{dehydrogenase}]{\text{glutamic acid}} NH_3 + \text{oxoglutamate} + \text{NADH} \qquad (2)$$

Undoubtedly, the rather expensive NAD, as well as the tedious analysis procedure, are the major disadvantages of these analytical methods. In an attempt to develop a simple and accurate procedure for the analysis of glutamine, we have extended our research on enzyme electrode probes. In this paper, a new enzyme electrode, namely, the glutamine electrode, and its properties are reported.

There are essentially three types of glutaminase which can catalyze reaction (1)[4] and, hence, be used in an enzyme electrode.

1. The phosphate-activated enzyme of kidney (glutaminase I) has an optimum pH around 8.0[5]. Although this pH region is suitable for the operation of cation-sensitive electrodes with little hydronium ion interference, glutaminase I was not considered because of its thermal instability.

2. Glutaminase II is the designation given to the pyruvate-activated glutaminase. Because of the complicated reaction paths as well as the slow reaction rate, glutaminase II was also unsuitable for the enzyme electrode work.

3. Glutaminase III, as used in the current work, was a commercial enzyme prepared from bacteria. This type of glutaminase is a very effective catalyst for reaction (1). In addition, it is also relatively stable at room temperature.

EXPERIMENTAL

Apparatus and solutions

The glutamine electrode was made from either a Beckman 39137 cationic electrode or a Thomas 4923-Q10 potassium ion electrode. A standard fiber-junction saturated calomel electrode was used as the reference electrode. Millivolt measurements were made with a Beckman Zeromatic II pH-potentiometer connected to a recorder. The solution was stirred and maintained at 25.0 ± 0.1° during the measurement with a thermostated water jacket.

Stock solutions of glutamine (0.1 *M*) were prepared in the appropriate buffers using triply distilled water. In order to achieve maximum buffer capacity, two types of buffer were used at various pH values. TRIS–phosphate buffer was used for measurements at pH 6–7 while TRIS–acetate buffer was used for the preparation of pH 5–6 solutions. The concentration of both buffers was 0.3 *M* with respect to TRIS.

L-Glutaminase used in this work was purchased from NBC. This enzyme was prepared from E. Coli and was claimed to have an optimum pH value of 4.9. The enzyme was stored in a freezer at −5° before use.

Preparation of glutamine electrode

The cationic electrodes were used to monitor ammonium ions. A piece of nylon stocking was placed over the glass bulb and was fixed with rubber bands. This electrode was then immersed into the enzyme solution containing about 150 mg of enzyme per ml of buffer, making sure that all of the pores of the netting were filled with the solution. A film of dialysis paper was finally used to trap the enzyme from diffusing into the solution. The enzyme electrode was soaked and stirred in the buffer solution for 1 h before use.

RESULTS AND DISCUSSION

Effect of the cation sensor

In the course of a search for a more selective cationic electrode for ammonium ion, the response and selectivity characteristics of a new electrode recently marketed by A. H. Thomas Company were determined. As defined by Eisenman[6], the selectivity ratio, *K*, can be expressed as

$$E\begin{pmatrix}\mathrm{M}_2^+ = 0.1\ M \\ \mathrm{M}_1^+ = 0\end{pmatrix} - E\begin{pmatrix}\mathrm{M}_2^+ = 0 \\ \mathrm{M}_1^+ = 0.1\ M\end{pmatrix} = \frac{RT}{F}\ln K_{\mathrm{M}_1^+/\mathrm{M}_2^+} \qquad (3)$$

where *E* represents the potential reading in the unit of volts and *R*, *T*, *F* have their usual thermodynamic meaning. The selectivity ratios for the Beckman 39137 and Thomas 4923-Q10 electrodes are listed in Table I. A comparison of these two cationic electrodes on the basis of the selectivity ratios for ammonium ion indicates that the new Thomas electrode is probably made from a type of glass similar to that used in the manufacture of the Beckman 39137 electrode. In addition, it can be seen that the order of selectivity of the Thomas electrode is $\mathrm{Ag^+ > H^+ > K^+ > NH_4^+ > Na^+ > Li^+}$, which is quite different from that claimed by the manufacturer: $\mathrm{K^+ > Ag^+, H^+ > Na^+, NH_4^+}$. Since the selectivity ratios for ammonium ion are very similar for both electrodes, both electrodes were used in subsequent work. The calibration curves for ammonium ions of both electrodes were found to superimpose each other almost exactly in preliminary studies.

TABLE I

THE SELECTIVITY OF THE CATION-SENSITIVE ELECTRODES

Cations[a]	*Selectivity*[b] K_{M^+/NH_4^+}	
	Beckman[c] 39137	*Thomas* 4923-*Q*10
K^+	0.416	0.476
Li^+	83.5	42.8
Na^+	4.03	2.65
H^+	0.468	0.288
Ag^{+}[d]	0.402	0.186
Mg^{2+}	$2.6 \cdot 10^4$	$1.01 \cdot 10^3$

[a] $[M^{n+}] = 0.1$ *M*, TRIS–HNO_3 buffer, pH 7.0 (except that for H^+), [TRIS] = 0.1 *M*. [b] Eqn. (3). [c] Ref. 8. [d] TRIS–HNO_3 salt bridge used to prevent fouling of S.C.E.

pH effect

The effect of pH on the electrode response is shown in Fig. 1. As indicated by these calibration curves, the decrease of the slope as the pH of the solution is lowered is undoubtedly attributable to the hydronium ion interference. This type of interference can be demonstrated more distinctively by comparing these curves with those obtained for ammonium ions at various pH values as shown in Fig. 2. Since the variation of the slope with pH is approximately the same for both sets of curves, it can be concluded that a higher pH region would be preferable for the operation of the

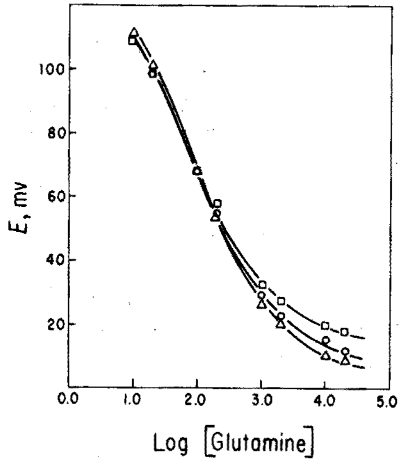

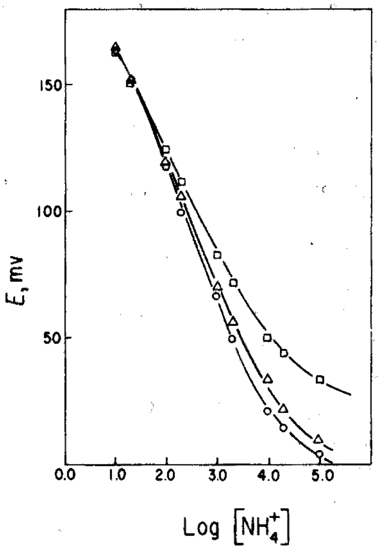

Fig. 1. Calibration curves for the glutamine electrode at various pH values. (□) pH 5.0, slope 40 mV/decade; (○) pH 5.5, slope 45 mV/decade; (△) pH 6.0, slope 48 mV/decade.

Fig. 2. Effect of pH on response of the cation electrode to [NH_4^+]. (□) pH 5.0, slope 42 mV/decade; (△) pH 6.0, slope 48 mV/decade; (○) pH 7.0, slope 52 mV/decade.

glutamine electrode, in order to reduce the hydronium ion interference. On the other hand, however, increasing the pH of a solution significantly reduces the effectiveness of the glutaminase catalysis of reaction (1). The effect of pH on the enzyme activity is shown in Fig. 3. As a result of the extremely slow response of the glutamine electrode (more than 8 min to reach a steady-state reading at pH 6.0), any effort to reduce the hydronium ion interferences can be successful only at the sacrifice of the enzymic activity.

By comparing Figs. 1 and 3, one can conclude that a pH of 5.5 would be a good compromise choice.

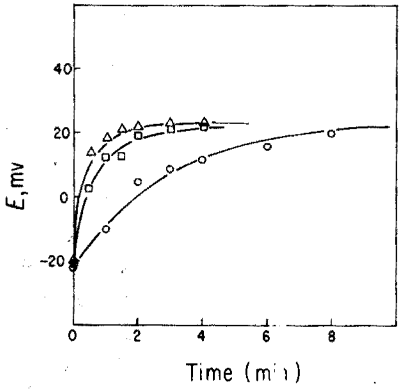

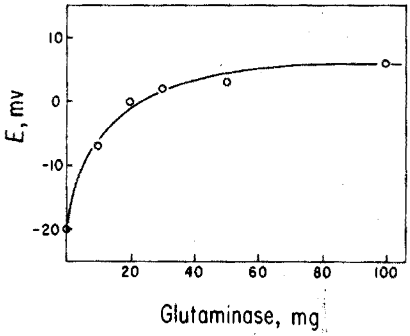

Fig. 3. Effect of pH on the response of the glutamine electrode. [Glutamine] = $5.0 \cdot 10^{-3}$ *M*. (△) pH 5.0; (□) pH 5.5; (○) pH 6.0.

Fig. 4. Effect of glutaminase concentration on the steady-state potential reading of a glutamine electrode. pH = 5.5, [glutamine] = 10^{-3} *M*.

Concentration of glutaminase

The influence of increasing enzyme concentration on reaction (1) is shown in Fig. 4. In this test, the substrate concentration was kept constant at 10^{-3} *M* while the enzyme concentration was varied from 0 to 100 mg. The parabolic electrode response curves show that only a small improvement can be achieved by further increase of the enzyme concentration above 30 mg per 100 ml of solution at the defined conditions of pH 5.5, [glutamine] = 10^{-3} *M* and 25°. Proportionally, a 30 mg ml^{-1} enzyme solution would be sufficiently concentrated for preparing the enzyme electrode probe, provided that the substrate concentration is always less than 0.1 *M*. However, as suggested by Guilbault and Hrabankova[7], the stability of this type of enzyme electrode can be greatly improved by a further increase in the enzyme concentration. Consequently, the concentration of glutaminase used in the electroprobe was 150 mg ml^{-1} through all this work.

Stability of glutamine electrode

The calibration curve of a freshly prepared glutamine electrode was found to be reproduced exactly through an 8-h period of continuous operation. The sensitivity of the electrode was reduced in the second day even when the electrode was stored at 5° overnight. Calibration curves of a glutamine electrode on four consecutive days are

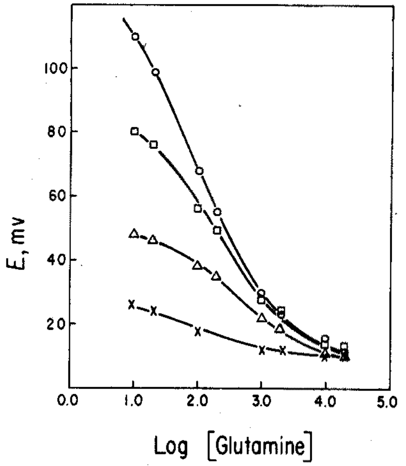

Fig. 5. Stability of the glutamine electrode. pH = 5.5. (○) 1st day; (□) 2nd day; (△) 3rd day; (×) 4th day.

shown in Fig. 5.

The observed instability of the glutamine electrode can be attributed either to mechanical leakage of the enzyme from the electrode into the solution, or to the decomposition of the enzyme. In an attempt to minimize the mechanical loss of the enzyme from the electroprobe, an attempt was made to immobilize glutaminase on the glass bulb of the electrode with acrylamide gel according to the procedure originally described by Guilbault and Montalvo[8-10]. However, the immobilized glutamine electrode shows no response at all to variation of the glutamine concentration. Presumably, this is due to photodeactivation of the enzyme. Since an excess amount of enzyme was added in the preparation of the electroprobe to compensate for any mechanical loss of the enzyme, the decrease of the electrode sensitivity must result from the deterioration of the enzyme with time.

Sensitivity and selectivity

The concentration limit of the glutamine electrode is 10^{-4} *M*. Above this limit, the electrode response to the logarithm of the glutamine concentration is linear with slopes of 40, 45, and 48 mV/decade at pH values of 5.0, 5.5, and 6.0, respectively (Fig. 1). Since these values are in agreement with the ammonium ion calibration curves (Fig. 2), the discrepancy between the observed slope of the glutamine electrode with the Nernstian coefficient, 59.2 mV, is apparently inherited from the property of the ammonium ion sensor, *i.e.*, the glass cationic electrode. Of course, the hydronium ion interference is the predominant factor in the electrode response. On the other hand, the nonlinear deviation in the region of 10^{-4} *M* substrate concentration is much greater for the glutamine electrode than that for the ammonium electrode, indicating that the enzymic conversion of glutamine to glutamate is incomplete in this concentration region.

As has been pointed out previously[7], any monovalent cation which can be sensed by the Beckman glass cationic electrode will interfere with the glutamine measurements. However, this type of interference can be greatly reduced if a proper method is available to remove these cations, *e.g.* cation-exchange resin[11].

So far as the enzyme specificity is concerned, the glutaminase employed in the current study does not deaminate or deamidate urea, glutamic acid, D,L-lysine, L-alanine, D,L-leucine, D,L-arginine, and D,L-citrullin. However, L-asparagine undergoes deamination under the catalytic effect of glutaminase to a small extent. Calculated on the basis of eqn. (3), the selectivity ratio of this glutamine electrode for L-glutamine in the presence of L-asparagine is 50.

The financial assistance of the National Science Foundation, Grant No. GB-12669, and the National Institutes of Health, Grant No. 5 RO1 GM17268-02, is gratefully acknowledged.

SUMMARY

An enzyme electrode specific for glutamine is described. The electrode is prepared by entrapping glutaminase on a nylon net between a layer of cellophane and a Beckman 39137 or Thomas 4923-Q10 cation electrode. The electrode responds to glutamine over the concentration range 10^{-1}–10^{-4} M with a response time of only 1–2 min. The electrode can be used continuously for about 12 h.

RÉSUMÉ

On décrit une électrode-enzyme spécifique pour le dosage de la glutamine. Elle se prépare en fixant la glutaminase sur un réseau de nylon, entre une couche de cellophane et une électrode cationique Beckman 39137 ou Thomas 4923-Q10. On peut ainsi effectuer des déterminations de glutamine de 10^{-1}–10^{-4} M avec un temps de réponse de 1–2 min seulement. Cette électrode peut être utilisée en continu pendant environ 12 h.

ZUSAMMENFASSUNG

Es wird eine für Glutamin spezifische Enzymelektrode beschrieben. Sie wird hergestellt, indem Glutaminase auf ein Nylonnetz aufgebracht wird, das sich zwischen einer Cellophanschicht und einer Kationenelektrode vom Typ Beckman 39137 oder Thomas 4923-Q10 befindet. Die Elektrode reagiert auf Glutamin im Konzentrationsbereich 10^{-1}–10^{-4} M mit einer Ansprechzeit von nur 1–2 min und kann etwa 12 h lang ununterbrochen benutzt werden.

REFERENCES

1 H. Holzer and H. D. Soling, *Z. Biochem.*, 336 (1962) 201.
2 J. M. Sowerby and J. H. Ottaway, *Biochem. J.*, 99 (1966) 246.
3 G. G. Guilbault, S. H. Sadar and R. McQueen, *Anal. Chim. Acta*, 45 (1969) 1.
4 C. Long (Editor), *Biochemist's Handbook*, E. + F.N. Spon, London, 1961.
5 M. C. Otey, S. M. Binnbaum and J. P. Greenstein, *Arch. Biochem. Biophys.*, 49 (1954) 245.
6 G. Eisenman, *Glass Electrodes for Hydrogen and Other Cations*, Marcel Dekker, New York, 1967, p. 726.
7 G. G. Guilbault and E. Hrabankova, *Anal. Chem.*, 42 (1970) 1779.
8 G. G. Guilbault, R. K. Smith and J. G. Montalvo, *Anal. Chem.*, 41 (1969) 600.
9 G. G. Guilbault and J. G. Montalvo, *J. Amer. Chem. Soc.*, 92 (1970) 2533.
10 G. G. Guilbault and J. G. Montalvo, *Anal. Lett.*, 2 (1969) 283.
11 G. G. Guilbault and E. Hrabankova, *Anal. Chim. Acta*, 52 (1970) 287.

Analytica Chimica Acta
Elsevier Publishing Company, Amsterdam
Printed in The Netherlands

THE SIMULTANEOUS DETERMINATION OF CARBON AND OXYGEN IN ELECTROPLATED GOLD BY HELIUM-3 ACTIVATION

C. K. KIM AND M. J. VASILE
Bell Telephone Laboratories, Incorporated, Murray Hill, N.J. 07974 (U.S.A.)

(Received 16th April 1971)

The co-deposition of an organic polymer in gold electroplates that contain hardening agents such as cobalt or nickel has been firmly established by previous studies[1]. Polymer deposition also occurs in unalloyed gold electroplates when the cathode efficiency during plating is low. The carbon content in gold electroplates has been determined by a microchemical combustion technique with a sensitivity limit of about 1 μg[2]. Infrared spectroscopy on sublimed samples of the polymer indicates the presence of $-C{\equiv}N$ and $-C-H$ structural units.

The principal objectives of previous studies were to establish the presence of the polymeric material in the bulk of the electroplate and to correlate the presence and amount of polymer with bath composition or plating conditions. Attempts to analyze the polymer by vacuum-fusion techniques have been made, but a complete study by this technique is lacking. Spark-source mass spectrometry has been applied to study the polymeric impurities in gold electroplates[3], but quantitative analysis by this technique requires either calibration standards for each impurity element detected or a detailed knowledge of the arc parameters that control the vaporization and ionization of the material under study.

The present study is the result of a search to find an alternative and convenient method for analyzing the impurity content in gold electroplates. Inducing nuclear transmutations to radioactive isotopes by high-energy (10 MeV) ^{3}He ions is a particularly attractive method since two elements, carbon and oxygen, may be determined simultaneously. The nuclear reactions involved are $^{12}C(^{3}He,\alpha)^{11}C$, and $^{16}O(^{3}He,p)^{18}F$. The ^{11}C and ^{18}F nuclides decay by positron emission with half-lives of 20.8 and 112 min, respectively. This analytical technique is very sensitive and, in this case, yields absolute results without chemical separations. Helium-3 activation is nondestructive and therefore the samples of gold electroplate with known amounts of carbon and oxygen can be used in other experiments.

EXPERIMENTAL

Gold was electroplated from commercially supplied hard gold plating baths to a thickness of about 25 μm on 2 × 2 × 0.04 cm high-purity copper substrates. Several types of alloyed hard gold electroplates were examined, as well as one type of pure soft gold electroplate[4] which was plated to a thickness of 50 μm. The data describing the electroplated samples are given in Table I. The copper substrates were chemically polished in a nitric–phosphoric acid mixture before plating. Clean platinum anodes

TABLE I

DATA ON ELECTROPLATED SAMPLES

Gold plate type	*Thickness (μm)*	*Approximate atom-% hardening element*	*Atom-% carbon by combustion*
Type 1[a]	25	1.0 -0.7 Ni	3-7
Type 2[a]	25	0.27-0.67 Ni	3-7
Type 3[a]	25	1.0 -1.7 Co	3-5
Type 4[a]	25	0.27-0.67 Co	3-5
Soft, citrate	50	None	<0.2

[a] Proprietary plating solutions which are commercially supplied.

and Pyrex cells were always used in the plating operations. The plating current density was *ca.* $5 \cdot 10^{-3}$ A cm^{-2}, and the cathode efficiency for the hard gold electroplates was estimated to be 30-40%. The electroplated surfaces were thoroughly rinsed in distilled water, dried, and subsequently coated with a 0.5-μm layer of evaporated copper to minimize the possibility of contamination from handling or background gases in the accelerator.

The samples were irradiated in a Tandem Van de Graaf accelerator. A 10-MeV ^{3}He beam was collimated to a diameter of about 6 mm at the target. The beam current was of the order of 1 μA, and the irradiations were carried out until a total charge of 60 μC reached the target. The target assembly was a Faraday cup collector with secondary electron suppression, which insured that the total charge registered on the current integrator was due only to incident ^{3}He ions.

Following irradiation, the samples were immersed in a 1+1 nitric acid-water mixture to remove the copper coating. The decay of the ^{11}C and ^{18}F nuclides was measured by coincidence counting of the 0.51-MeV quanta resulting from positron annihilation. The radioactive decay was followed until several half-lives of the ^{18}F nuclide were evident or until sufficient data were available to resolve completely the multicomponent decay curves.

The significance of the contribution of adsorbed contaminants and residual gases in the accelerator to the total disintegration rate was tested by irradiating gold foil (99.99% pure) and etching the surface of the gold foil after irradiation. Estimates of the thickness of gold removed by aqua regia etching were obtained by sample weight loss. Decay rates were measured just before and immediately following the etching.

The standards used for oxygen and carbon determinations were chosen on the basis of similarities between the atomic number and density of the standard matrix to that of gold. Hot pressed disks (2.5 cm in diameter and 3 mm in thickness) of tantalum carbide and tungsten carbide were used as carbon standards, and a thorium oxide crystal was used as an oxygen standard. N.B.S. certified samples of low-alloy steel were also investigated as possible carbon standards since their carbon contents are in the range of those in gold electroplates.

RESULTS AND DISCUSSION

The concentrations of carbon and oxygen in the gold electroplate were calculated by means of the thick target comparator method of Ricci and Hahn[5]. The equation used for computation was:

$$N_x = R_s Q_s N_s D_x / Q_x R_x D_x \tag{1}$$

where N_x, N_s = the number of carbon or oxygen atoms cm^{-3} in the unknown and standard, respectively;
Q_x, Q_s = total charge delivered to the unknown and standard;
R_x, R_s = range of 10-MeV ^3He ions, in μm, in the unknown and standard;
D_x, D_s = disintegration rates of the unknown and standard at a given time after cessation of bombardment.

The thick target approximation is valid for the gold electroplates used in this study since the range of 10-MeV ^3He ions for reaction with ^{12}C or ^{16}O in gold is *ca.* 18 μm. Range values for the carbide and oxide standards were computed on a weight fraction basis from tabulated data for elemental substances[6,7]. Range data for ^3He ions in tungsten could not be found, so the range was assumed to be the same as in tantalum, since their atomic numbers differ only by one. The relevant quantities for the standards and gold itself are given in Table II.

TABLE II

RANGE DATA FOR STANDARDS AND GOLD

Standard	*Density ($g\ cm^{-3}$)*	*Range ($g\ cm^{-2} \cdot 10^2$)*	*Range (μm)*	N_S[a]
TaC	15.6	4.2	29.6	$4.4 \cdot 10^{22}$
WC	14.2	4.2	27.0	$4.8 \cdot 10^{22}$
Low-alloy steels				
NBS 1162	7.75	2.6	33.6	$1.4 \cdot 10^{21}$
NBS 1168	7.76	2.6	33.6	$0.92 \cdot 10^{21}$
ThO_2	10.0	4.3	43.0	$4.56 \cdot 10^{22}$
Au	19.3	4.95	25.6	—

[a] N_S = Number of atoms cm^{-3} of carbon or oxygen in the standard matrix.

Figure 1 shows a resolved composite decay curve for a cobalt-hardened gold electroplate. The half-lives measured from the plot are 112 min for ^{18}F and 20 min for ^{11}C. All hard gold electroplates and gold foils exhibited decay curves similar to that shown in Fig. 1, with a spread in the half-lives of about ± 1 min. Samples of soft gold electroplate (*ca.* 50 μm thick) did not clearly show the characteristic 112-min half-life of ^{18}F decay in their very low-level activity. Prolonged counting of the decay revealed a third component with a half-life of 9.5 h, which most likely results from the reaction $^{65}Cu(^3He,2n)^{66}Ga$. The half-life of ^{66}Ga is 9.45 h. Once this decay component was established, it was possible to resolve the remaining curve into its components arising from ^{18}F and ^{11}C. The very small amount of ^{66}Ga observed may arise from the recoil of activated copper in the evaporated protective film or from the substrate, though the latter should occur only if there are cracks or voids in the plating, which is unlikely. It may also result from very low-level contamination of the gold plate with copper.

Table III shows a comparison of the results obtained for carbon using the

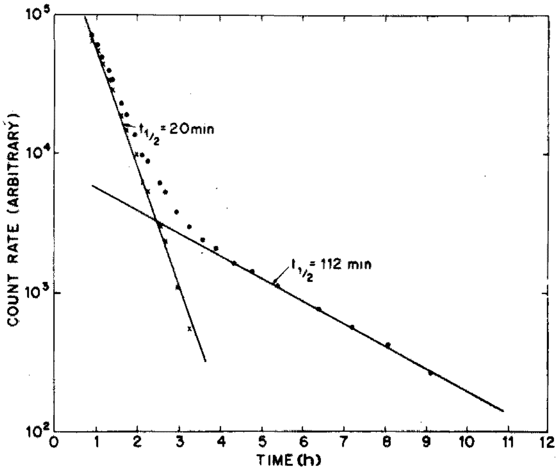

Fig. 1. Resolved two-component decay curve obtained after irradiation of a cobalt hardened gold electroplate.

TABLE III

NUMBER OF CARBON ATOMS $cm^{-3} \cdot 10^{-21}$

Sample number	*Gold plate*	*Standard*			
		TaC	*WC*	*NBS* 1162	*NBS* 1168
1	Type 1	1.41	1.54	1.24	1.25
2	Type 1	1.23	1.34	1.08	1.09
3	Type 2	0.79	0.86	0.69	0.70
4	Type 3	1.94	2.12	1.70	1.72
5	Type 3	1.90	2.07	1.67	1.68
6	Type 4	1.15	1.26	1.01	1.02
7	Type 4	2.03	2.22	1.78	1.80

low-alloy steel standards as well as the tantalum carbide and tungsten carbide. The steel standards contain different amounts of carbon (see Table II), but both yield essentially the same results. They are lower than the results from tantalum carbide by a factor of 0.89 and lower than those from tungsten carbide by a factor of 0.81. The iron in the low-alloy steel undergoes the reaction $^{56}Fe(^{3}He,2n)^{57}Ni$, and the resulting ^{57}Ni nuclide makes the use of low-alloy steel as a standard very inconvenient, since the decay must be followed for at least two days to obtain an accurate resolution of the decay components from ^{18}F and ^{11}C. The possibility of introducing an error in the carbon disintegration rate is enhanced by the extrapolations necessary to resolve the ^{11}C decay component. The low-alloy steels are also a less attractive choice as carbon standards because of the wide disparities in atomic number and density between the iron and gold matrices. In spite of these difficulties, the agreement between the results from the low-alloy steel standards and those from the more favorable standards of high atomic number and high density is reasonably good.

Table IV contains the results of the carbon and oxygen determinations for

TABLE IV

RESULTS FOR CARBON AND OXYGEN IN GOLD PLATES

Sample number	*Atoms cm^{-3}*					
	Gold plate	*C (by TaC)*	*O*	*C/O*	*Atom-% C*	*Atom-% O*
1	Type 1	$1.41 \cdot 10^{21}$	$3.25 \cdot 10^{20}$	4.3	2.52	0.58
2	Type 1	$1.23 \cdot 10^{21}$	$2.85 \cdot 10^{20}$	4.3	2.20	0.51
3	Type 2	$0.79 \cdot 10^{21}$	$2.70 \cdot 10^{20}$	2.9	1.36	0.47
4	Type 3	$1.94 \cdot 10^{21}$	$5.22 \cdot 10^{20}$	3.7	3.46	0.93
5	Type 3	$1.90 \cdot 10^{21}$	$5.48 \cdot 10^{20}$	3.5	3.39	0.98
6	Type 4	$1.15 \cdot 10^{21}$	$4.56 \cdot 10^{20}$	2.5	1.98	0.79
7	Type 4	$2.03 \cdot 10^{21}$	$8.03 \cdot 10^{20}$	2.5	3.50	1.38
8	Soft, citrate	$6.6 \cdot 10^{18}$	$2.1 \cdot 10^{19}$	0.31	$1.1 \cdot 10^{-2}$	$3.6 \cdot 10^{-2}$
9	Repeat 6	$1.38 \cdot 10^{21}$	$5.29 \cdot 10^{20}$	2.6	2.38	0.91
10	Repeat 5	$1.97 \cdot 10^{21}$	$5.11 \cdot 10^{20}$	3.9	3.52	0.91

several types of hard gold plates and one soft gold plate. The carbon analyses are those based on the tantalum carbide standards only because the tungsten carbide range was estimated. These were used to calculate the atom percent carbon and the carbon:oxygen ratio. The results from the tungsten carbide standard would be about 10% greater. The analyses for carbon by ^{3}He activation are in the same range as those by combustion in previous studies (see Table I)[1]. No direct comparison between the two methods can be made with the available data because of the rather wide variations that can occur for any given type of electroplate, even if it is plated under apparently identical conditions[1].

Sample numbers 9 and 10 in Table IV are repeat determinations of sample numbers 6 and 5, respectively. The carbon content measured in the repeat of sample 6 was 20% higher while the oxygen content was 19% higher. The repeat of sample 5 showed increases of 3.7% and 3.9% for carbon and oxygen, respectively. The most probable source of irreproducibility as severe as that found for sample 6 is the positioning of the irradiated specimen with respect to the axis of the two coincidence detectors. The integrator that monitors the ^{3}He beam current is reproducible to at least ±1%, and the counting apparatus was found to be reproducible to about ±4% in measurements with a ^{22}Na standard (positron emitter, half-life = 2.6 years). A self-centering specimen mount for irradiation and counting should insure a better alignment of the center of the irradiated zone and the axis of the counters than was achievable in this study, and should improve the precision of the results.

The contribution of surface-adsorbed carbon and oxygen to the total analysis was estimated by irradiating 99.99% pure gold foil with no evaporated copper film. Figure 2a shows the fraction of the original activity remaining after successive surface etching, as a function of depth. The depth is only approximate, since aqua regia does not etch the surface uniformly. For comparison, the recoil depth profile of ^{18}F in stacked aluminum foil absorbers obtained by Lamb *et al.*[8], expressed in the same way is shown in Fig. 2b. The functional dependence is quite similar and suggests that the actual bulk impurity level in gold plates is lower than one would calculate from disintegration rate measurements without surface etching. This is undoubtedly the case for pure samples, such as 99.99% gold foil or soft gold electroplate with an

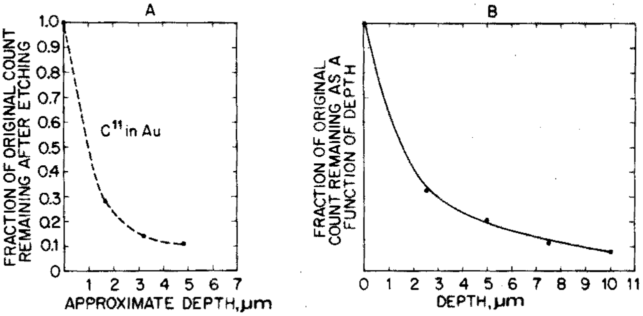

Fig. 2. (A) The fraction of the original count due to ^{11}C as a function of depth in a gold foil after successive etching. (B) Recoil data of ^{18}F in Al, converted to the same scales as in Fig. 2A (data of Lamb *et al.*[8]).

impurity level of 0.01% or lower.

It is interesting to note that the sample of soft gold electroplate had a carbon: oxygen ratio of 0.3, while all the hard gold plates had carbon:oxygen ratios greater than 2. This is consistent with the probability that most of the radioactive decay obtained in the "pure" samples originates from recoiled surface species, either adsorbed or in chemical combination, since the dominant background element in the accelerator is oxygen. This becomes significant when the bulk impurity level is of the order of 0.01%, *i.e.*, one part in 10^4 on an atomic basis. The use of thin evaporated metal films, *e.g.* copper, will help to reduce the effect by trapping recoiled nuclides but will not eliminate it. Recoil of activated surface species makes no difference in the analysis of the hard gold samples, since their impurity levels and disintegration rates are several orders of magnitude higher.

Interference from nuclear reactions with nuclides other than ^{12}C which also yield ^{11}C must be considered. These reactions are $^{9}Be(^{3}He,n)^{11}C$, $^{10}B(^{3}He,d)^{11}C$, $^{14}N(^{3}He,\alpha d)^{11}C$, and $^{16}O(^{3}He,2\alpha)^{11}C$. The probability of occurrence of beryllium or boron in these gold electroplates is so small that these interferences need not be considered seriously. The reactions with ^{14}N and ^{16}O are important possibilities; however, the cross-sections for these reactions are negligible for incident ^{3}He energies less than 10 MeV[9]. Interferences in the oxygen determination from the reactions $^{23}Na(^{3}He,2\alpha)^{18}F$ and $^{27}Al(^{3}He,3\alpha)^{18}F$ may also be regarded as insignificant for 10-MeV helium-3 particles.

The authors would like to acknowledge Mr. T. A. Palumbo for plating the specimens and Mrs. G. B. Munier for several helpful discussions.

SUMMARY

The carbon and oxygen contents in several types of hard electroplated gold and one type of soft gold plate have been determined by helium-3 activation analysis. The results for carbon are in the same range as those obtained from combustion analyses on similar samples. The carbon-to-oxygen ratio was found to vary from 2.5 to about 4 for hard gold plates. The maximum bulk level of carbon and oxygen in a soft gold electroplate was found to be about 10^{-2} atom-%. The technique requires no chemical separations and can easily detect impurities at the p.p.m. level.

RÉSUMÉ

L'analyse par activation à l'hélium-3 a permis de doser le carbone et l'oxygène dans plusieurs types d'ors durs électroplaqués et dans un type de dépôt d'or mou. Les résultats obtenus pour le carbone sont dans le même ordre de grandeur que ceux obtenus par combustion d'échantillons similaires. Le rapport carbone/oxygène varie de 2.5 à 4 pour les dépôts d'or dur. Cette technique ne nécessite pas de séparations chimiques. Des impuretés, en quantité de l'ordre du p.p.m., peuvent facilement être décelées.

ZUSAMMENFASSUNG

Die Kohlenstoff- und Sauerstoffgehalte in verschiedenen Sorten galvanisch hergestellter Hartgoldplattierung und in einer Sorte Weichgoldplattierung wurden durch Helium-3-Aktivierungsanalyse bestimmt. Die Kohlenstoffwerte liegen im selben Bereich wie die durch Verbrennungsanalysen mit ähnlichen Proben erhaltenen Ergebnisse. Das Verhältnis von Kohlenstoff zu Sauerstoff variierte bei Hartgoldüberzügen zwischen 2.5 und 4. Der maximale Gesamtgehalt von Kohlenstoff und Sauerstoff in einer Weichgoldplattierung betrug etwa 10^{-2} Atom-%. Das Verfahren erfordert keine chemischen Abtrennungen und erlaubt den Nachweis von Verunreinigungen im p.p.m.-Bereich.

REFERENCES

1 G. B. Munier, *Plating*, 56 (1969) 1151; and private communication.
2 T. F. Egan, *Microchem. J.*, 13 (1968) 646.
3 M. J. Vasile and D. L. Malm, to be published.
4 R. A. Ehrhardt, *Proc. Amer. Electroplaters' Soc.*, 47 (1960) 78.
5 E. Ricci and R. L. Hahn, *Anal. Chem.*, 37 (1965) 742; 39 (1967) 794.
6 C. F. Williamson, J. P. Boujot and J. Picard, *Centre d'Etudes Nucléaires de Saclay, Rapport CEA-R3042*, 1966.
7 G. Friedlander, J. W. Kennedy and J. M. Miller, *Nuclear and Radiochemistry*, 2nd Edn., John Wiley, New York, 1965.
8 J. F. Lamb, D. M. Lee and S. S. Markowitz, *Anal. Chem.*, 42 (1970) 212.
9 T. Nozaki, *1968 Intern. Conf. on Modern Trends in Activation Analysis*, preprints, 1968, pp. 930–935.

Analytica Chimica Acta
Elsevier Publishing Company, Amsterdam
Printed in The Netherlands

DETERMINATION OF THE URANIUM CONTENT IN SEA WATER BY A FISSION TRACK METHOD WITH CONDENSED AQUEOUS SOLUTION

TETSUO HASHIMOTO
Research Reactor Institute, Kyoto University, Kumatori-cho, Sennan-gun, Osaka (Japan)

(Received 15th April 1971)

The uranium content in sea water is of considerable interest for oceanographers and nuclear scientists as an eventual source of nuclear energy. The uranium content in sea-water samples from different places and different depths has already been determined occasionally. Wilson *et al.*[1] compared the uranium content for several sea-water samples applying three different analytical methods. Those were an isotopic dilution method, a fluorimetric method and pulse polarography[2]. From these methods the authors found average uranium values of 3.33 μg l^{-1} in all sea-water samples. However, all these methods are very complicated because a careful purification from many other elements is essential after the uranium collection from bulk sea water; for example, in the case of pulse polarography, molybdenum has to be removed completely.

Therefore simple analytical techniques giving correct values of the mean uranium content in sea water are required[3]. Since Price and Walker determined micro amounts of uranium by fission tracks with a suitable dielectric detector[4], many applications of the basic procedure have been reported: for example, the determination of the average uranium content in pellets made from powdered rocks[5-7], in plant ashes[8], and in liquid samples measuring thin deposits of the evaporated liquid[9-11]. However, these methods gave erroneous results sometimes, mainly because of heterogeneous fission track distributions resulting from a heterogeneous distribution of uranium in the individual minerals and an agglomeration of the uranium atoms during evaporation.

In the present experiments, homogeneous track distributions and accurate results were obtained with solutions containing trace amounts of uranium and muscovite as track-recording material in a quartz ampoule during neutron irradiation. After a simple coprecipitation, the uranium content in sea water was determined by this track method by measuring a solution. This method is simple, direct, rapid, and cheap.

EXPERIMENTAL

Reagents and apparatus

Aluminium nitrate solution. 250 g of $Al(NO_3)_3 \cdot 9H_2O$ (Wako Pure Chemical Industries, Ltd) was dissolved in 200 ml of nitric acid (7+93, v/v).

Standard uranium solution. Uranyl nitrate ($UO_2(NO_3)_2 \cdot 6H_2O$, City Chemical Corp., U.S.A.) was dissolved in nitric acid (7+93, v/v) to give solutions with 0.1, 0.5, 1, 4, and 10 μg U ml^{-1}.

Muscovite. The clear and slightly stained muscovite blocks (Bihar, India) were washed with dilute nitric acid in order to remove fissile nuclides from the surface.

Optical microscope. A binocular research microscope (Shimazu Co.) with a 400-fold of magnification was used.

Other chemicals were of analytical-reagent grade.

Sampling of sea water

Sea-water samples were collected from a channel in Osaka Bay, where sea water was always mixed well by a strong tidal current. To study absorption losses of uranium, two sea-water samples were collected in polyethylene bottles, and one of them was acidified immediately with 20 ml of concentrated nitric acid per liter of sea water.

Coprecipitation of uranium

In two samples (No. 1, 2) from the acidified sea water, two (No. 3, 4) from the original sea water and in one distilled water sample (No. 5) as reagent blank, the trace amounts of uranium were coprecipitated with aluminium phosphate[12]. The solutions (1 l each) were evaporated to about 500 ml; 0.2 ml of the aluminium nitrate solution and 0.8 ml of aqueous 10% (w/v) ammonium dihydrogen phosphate solution were added. The solution was acidified with concentrated nitric acid and boiled to remove the carbon dioxide present as carbonate ion in the solution, because uranium forms a stable tricarbonate complex, $[UO_2(CO_3)_3]^{4-}$, which causes poor yields of the chemical collection, especially in case of sea water[13]. Then, the solution was adjusted to the pH where a methyl red indicator just turns yellow by adding CO_2-free ammonia and an ammonium acetate–acetic acid solution. The aluminium phosphate precipitate was digested for about 12 h and collected by centrifugation. The same precipitation procedure was applied once more to the supernatant solutions of No. 1 and 3 in order to check the coprecipitation yield giving the additional samples (No. 6, 7). The precipitate was dissolved in 1+3 (v/v) nitric acid to give just 2 ml of solution.

Preparation of irradiation samples

An aliquot of the solution (*ca.* 0.1 ml) was pipetted into the quartz ampoule (outer diam. 5 mm, inner diam. 3.6 mm), into which small muscovite pieces (3 × 5 mm) were inserted before sealing. The quartz ampoule was sealed carefully to about 30 mm length with a propane–oxygen burner.

Neutron irradiation

About ten quartz ampoules were placed in a large polyethylene capsule (rabbit). Cotton was used as a shock absorber to prevent the destruction of ampoules. The samples were irradiated in the pneumatic tube (Pn-2) of the Kyoto University Reactor (KUR); the fluxes of thermal, epithermal and fast neutrons were $2.75 \cdot 10^{13}$, $1.09 \cdot 10^{12}$ and $6.0 \cdot 10^{12}$ n cm^{-2} sec^{-1}, respectively. During the 15-min irradiation period, the γ-dose rate was $3 \cdot 10^{7}$ R and the temperature 80°.

Chemical etching procedure and track counting

After cooling for 2 days, the quartz ampoules were crushed to obtain the muscovite pieces. Those were etched with a 46% hydrofluoric acid solution for 1 h at room temperature[14]. The fission tracks on the muscovite surface were observed under an optical microscope with a magnification of 40 × 10 ~ 15. The fission track density was determined from a microphotograph.

RESULTS AND DISCUSSION

The heterogeneous distribution of uranium in individual minerals, and the great variety of the uranium content in different rock-forming minerals, may cause such considerable clustering of the tracks that it becomes very difficult to determine the average uranium content by a fission track method with powdered rocks or ashes[5]. The samples obtained by depositing or drying of test solutions on the track-recording materials always showed non-uniform clustering tracks indicating agglomeration of uranium atoms during the evaporation[10].

Immersion of muscovite into the aqueous solution during the neutron irradiation gave homogeneous distributions of fission tracks as seen in Fig. 1a–c. These

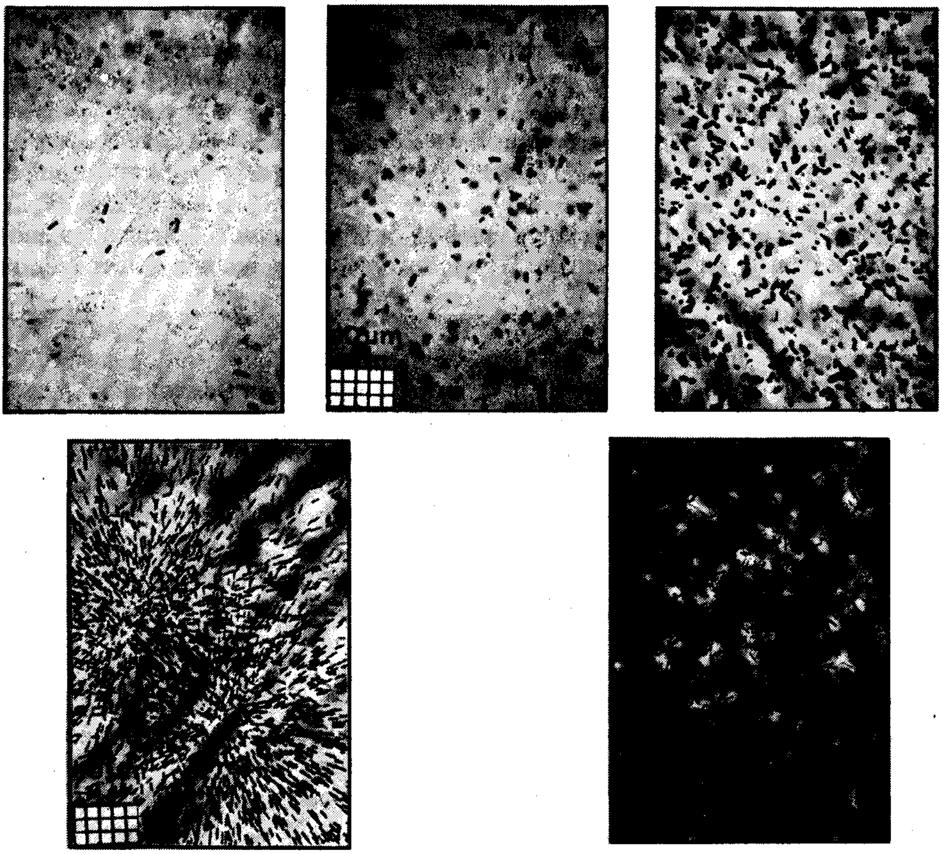

Fig. 1. Distribution of fission tracks obtained from aqueous solutions containing uranium. (a) 0.1 μg U ml^{-1}; 1.6·10^{4} tracks cm^{-2}. (b) 0.1 μg U ml^{-1}; 1.2·10^{5} tracks cm^{-2}. (c) 10 μg U ml^{-1}; 1.2·10^{6} tracks cm^{-2}. (d) Hollow tracks from alkaline Th solution. (e) Heterogeneous tracks from pH 6.8 U solution.

solutions were prepared from the standard uranium solutions (7+93 v/v nitric acid), where uranium was present as uranyl ion. However, in neutral and alkaline solutions, uranium tends to form colloidal particles with high adsorptive activity on the muscovite surface similar to thorium as shown in Fig. 1d, e. Therefore, in the final method, only acidic solutions were used.

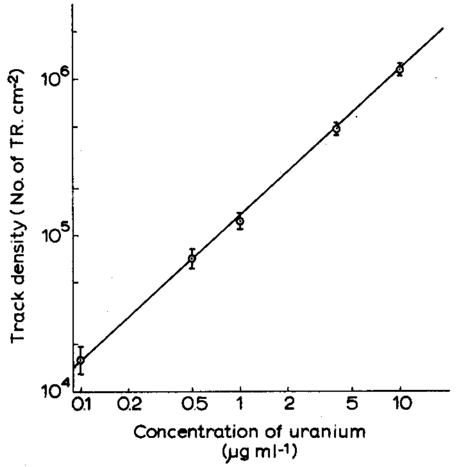

Fig. 2. Change of track density in aqueous samples as a function of uranium concentration. Irradiation condition: Pn-2 of KUR for 15 min at 5-MW operation.

Figure 2 shows the linear relationship between the uranium concentration and fission track density on the muscovite. The following equation could be derived:

$$\rho = 4.85 \cdot 10^{-12} C\phi \tag{1}$$

where ρ, C, and ϕ were the track density (cm^{-2}), the uranium concentration ($\mu g\ ml^{-1}$), and the total thermal neutron flux ($n\ cm^{-2}$), respectively. From this equation, it can be seen that trace amounts of uranium such as $4 \cdot 10^{-3}$ $\mu g\ ml^{-1}$ can be determined easily with a total neutron flux of $5 \cdot 10^{16}$ $n\ cm^{-2}$ and countable track densities of about 10^3 cm^{-2}. Under such conditions, even an original sea-water sample itself (approximately estimated as $3 \cdot 10^{-3}$ $\mu g\ ml^{-1}$) could be used for the determination of the uranium content. However, the limits are given by the uranium content in the muscovite ($2 \cdot 10^{-2} \sim 8 \cdot 10^{-4}$ $\mu g\ g^{-1}$)[15] used as a track-recording material and the difficulty of long-term neutron irradiations of solutions. Therefore, in this work, the uranium in sea water was coprecipitated with aluminium phosphate.

The influence of thorium, which is the only natural nuclide undergoing a fission reaction with reactor neutrons besides uranium, was taken into consideration from the point of view of the nuclear properties and its abundance in sea water. The thorium content in sea water is very small ($n \cdot 10^{-4}$ $\mu g\ l^{-1}$)[16]. Moreover, thorium undergoes a fission reaction (fission cross-section, 0.078 barn, for fast neutrons) only with neutrons faster than 1.2 MeV[17], which amount to less than one tenth of the thermal neutrons at the irradiation position used. Thus, the effects of thorium were negligible.

The influence of the specific gravity of solutions was examined also by a composite solution (1.07 in specific gravity) containing $7 \cdot 10^{-2}$ g of aluminium nitrate and 4 μg of uranium per ml of solution. The number of fission tracks decreased nearly 7 %. Hence the decrease of the track number caused by the aluminium phosphate used as the precipitating agent ($4 \cdot 10^{-2}$ g ml^{-1}) was estimated as less than 4 %.

TABLE I

URANIUM CONTENT OF SEA WATER DETERMINED BY A FISSION TRACK METHOD

Sample number	*Track density* (cm^{-2})	*Uranium content* ($\mu g\ l^{-1}$)
No. 1 sea water	$2.37 \cdot 10^5$	3.48
No. 2 sea water	$2.28 \cdot 10^5$	3.40
No. 3 sea water	$2.23 \cdot 10^5$	3.28
No. 4 sea water	$2.35 \cdot 10^5$	3.44
Average uranium content in sea water		3.40 ± 0.12
No 5 distilled water	$< 2.2 \cdot 10^3$	$< 3.2 \cdot 10^{-2}$
No. 6 sup. of No. 1	$< 2.2 \cdot 10^3$	$< 3.2 \cdot 10^{-2}$
No. 7 sup. of No. 3	$< 2.2 \cdot 10^3$	$< 3.2 \cdot 10^{-2}$

The uranium content in sea water determined by this method is given in Table I. Fig. 3 shows the homogeneous distribution of fission tracks on the muscovite pieces which had been immersed in the condensed sea-water solutions. The track density and the uranium contents are given in Table I. From the comparison of samples No. 1 and 3 with No. 6 and 7, the complete coprecipitation of uranium with aluminium phosphate was confirmed, as had been reported previously[2,12]. The uranium content in the supernatants after one step of coprecipitation is very small and appears to be equal to the blank solution (No. 5).

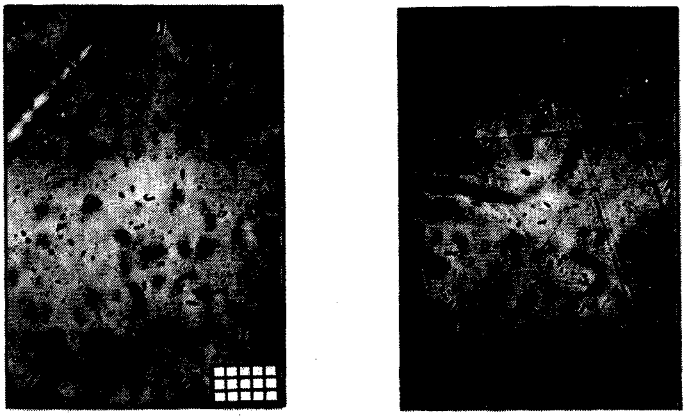

Fig. 3. Typical fission track patterns of condensed sea water samples. (a) Sample No. 2; (b) sample No. 3.

There is no difference between the acidified (No. 1, 2) and the original sea-water samples (No. 3, 4). Though it had been assumed that some losses might occur in unacidified samples owing to adsorption[3], the results here showed no difference if polyethylene bottles were used as containers and relatively fresh sea water was examined (here 15 days after the collection).

The average uranium content of 3.40 ± 0.12 μg l^{-1} is in good agreement with the value 3.33 ± 0.08 μg l^{-1} determined by Wilson *et al.*[1] as the average value of samples originated from Weymouth Bay and from various depths in the Bay of Biscay. As Rona *et al.*[18] have assumed already, the present work indicates very strongly that the uranium content in normal sea water is constant within the limits of experimental error, irrespective of the location and depth. The determination of the uranium content in sea water by fission track counting of condensed solutions after a simple coprecipitation procedure, without any further chemical purification, proves to be very convenient. This method has another advantage as the required amount of sea water is very small. Only 50-ml portions of sea water were used in this work.

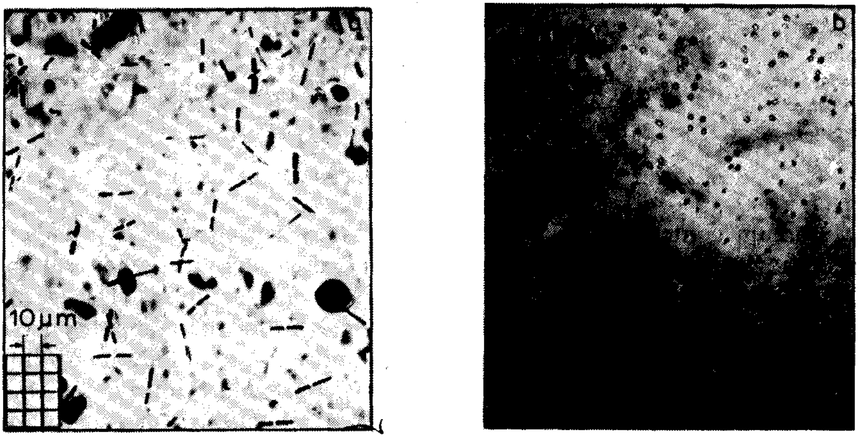

Fig. 4. (a) Microphotograph of typical binary fission track pairs in a muscovite sandwich. (b) Fission tracks on a surface of quartz ampoule.

Figure 4a shows binary fission tracks of the uranium brought between two muscovite pieces by capillary action during the neutron irradiation. These binary fission tracks are interesting for the investigation of fission phenomena, such as the determination of the mass and energy distribution between two correlated fission fragments[19,20]. Figure 4b shows the fission tracks on the surface of the quartz ampoule after etching with hydrofluoric acid solution (2+3, v/v) at room temperature for 5 min. It can be seen that the quartz ampoule itself could be used as fission track-recording material, just as muscovite, glass or some plastic materials.

The author is indebted to Prof. M. Sakanoue, Prof. S. Iwata, Prof. Y. Kiso, and Dr. E. Falk for reading the manuscript and making valuable suggestions and to Miss Y. Tanaka for her technical assistance.

SUMMARY

The uranium content in sea water was determined by counting the fission tracks on muscovite immersed in a condensed aqueous solution during the reactor neutron irradiation. For the condensation from sea water, uranium was coprecipitated with aluminium phosphate. After the precipitate had been dissolved in a small amount of dilute nitric acid, an aliquot of this solution in a quartz ampoule was taken up by a piece of muscovite and irradiated with reactor neutrons (KUR). After etching of the muscovite with hydrofluoric acid solution, a microphotograph was taken. The fission fragment tracks on the muscovite surface were counted and the sea-water samples were compared with standard uranium solutions. The uranium content in sea water could be determined easily as 3.40 ± 0.12 μg l^{-1} without any further chemical purification.

RÉSUMÉ

Une méthode radiochimique est proposée pour le dosage de l'uranium dans l'eau de mer. On procède à une concentration de l'uranium par coprécipitation à l'aide de phosphate d'aluminium. Le précipité est dissous dans un faible volume d'acide nitrique dilué. Une aliquote est irradiée dans un réacteur neutronique (KUR). On peut ainsi doser des teneurs en uranium de 3.40 ± 0.12 μg l^{-1} sans aucune autre purification chimique.

ZUSAMMENFASSUNG

Der Urangehalt in Meerwasser wurde bestimmt, indem die Kernspaltungs-Bahnspuren auf Muskovit gezählt wurden, der während der Reaktorneutronenbestrahlung in eine angereicherte wässrige Lösung eingetaucht war. Für die Anreicherung wurde das Uran mit Aluminiumphosphat mitgefällt. Nach Auflösung des Niederschlages in einer kleinen Menge verdünnter Salpetersäure wurde ein Aliquot dieser Lösung in einer Quarzampulle durch ein Stück Muskovit aufgenommen und mit Reaktorneutronen (KUR) bestrahlt. Nach Anätzen des Muskovits mit Flüsssäure wurde eine Mikrophotographie aufgenommen. Die Bahnspuren der Spaltfragmente auf der Muskovitoberfläche wurden gezählt und die Meerwasserproben mit Standard-Uranlösungen verglichen. Der Urangehalt in Meerwasser wurde zu 3.40 ± 0.12 μg l^{-1} ermittelt, wobei keine weitere chemische Reinigung erforderlich war.

REFERENCES

1 J. D. Wilson, R. K. Webster, G. W. C. Milner, G. A. Barnett and A. A. Smales, *Anal. Chim. Acta*, 23 (1960) 505.
2 G. W. C. Milner, J. D. Wilson, G. A. Barnett and A. A. Smales, *J. Electroanal. Chem.*, 2 (1961) 25.
3 R. Spence, *Talanta*, 15 (1968) 1307.
4 P. B. Price and R. M. Walker, *Appl. Phys. Lett.*, 2 (1963) 23.
5 D. E. Fisher, *Anal. Chem.*, 42 (1970) 414.
6 T. Hashimoto, S. Hayashi and S. Iwata, *Japan Analyst*, 19 (1970) 1538.
7 K. K. Bertine, L. H. Chan and K. K. Turekian, *Geochim. Cosmochim. Acta*, 34 (1970) 641.
8 Kh. Abdullaev, B. B. Zakhvataev and V. P. Perelygin, *Radiobiologiya*, 8 (1968) 765.
9 R. L. Fleischer and D. B. Lovett, *Geochim. Cosmochim. Acta*, 32 (1968) 1126.
10 A. V. Murali, P. P. Parekh and M. Sankardas, *Anal. Chim. Acta*, 50 (1970) 71.
11 E. Doerschel and W. Stolz, *Radiochem. Radioanal. Lett.*, 4 (1970) 277.
12 A. P. Smith and F. S. Grimaldi, *U.S. Geol. Surv. Bull.*, 1006 (1957) 125.
13 H. J. Riedel, *Kerntechnik*, 12 (1970) 16.
14 T. Hashimoto, *Japan Analyst*, 19 (1970) 508.
15 P. B. Price and R. M. Walker, *J. Geophys. Res.*, 68 (1963) 4847.
16 B. L. K. Somayajulu and E. D. Goldberg, *Earth Planet. Sci. Lett.*, 1 (1966) 102.

17 D. A. Hilton and D. Reed, *Intern. J. Appl. Radiation Isotopes*, 17 (1966) 335.
18 E. Rona, L. O. Gilpatrick and L. M. Jeffrey, *Trans. Amer. Geophys. Union*, 37 (1956) 697.
19 M. Ait-Salem, H. Gerhardt, F. Goennen, H. Hipp and H. Paap, *Nucl. Instr. Methods*, 60 (1968) 45.
20 L. Medveczky and G. Somogyi, *Radiation Effects*, 5 (1970) 51.

Analytica Chimica Acta
Elsevier Publishing Company, Amsterdam
Printed in The Netherlands

RADIOCHEMICAL DETERMINATION OF PLUTONIUM IN SEA WATER, SEDIMENTS AND MARINE ORGANISMS

KAI M. WONG*
Woods Hole Oceanographic Institution, Woods Hole, Mass. 02543 (U.S.A.)

(Received 7th May 1971)

Various procedures are available for the determination of plutonium in aqueous samples, sediments and biological organisms. However, none is really adequate for low-level analysis because they have either low sensitivity or they are cumbersome for analysis of large samples.

In sea water analysis, the ion-exchange method[1] is suitable only for small volumes (5 l or less) and consequently the sensitivity is low for fall-out plutonium; the bismuth phosphate coprecipitation method[2] requires separation at temperatures of 80–100° which is impractical for processing samples of 50 l or more; and the iron(III) hydroxide method[3] used to coprecipitate plutonium from 50–200 l samples at room temperature usually shows low recovery.

The procedure described in this paper is a modification of the iron(III) hydroxide method to separate plutonium from sea water by coprecipitation with iron(II) hydroxide and the recovery is significantly improved.

Of the many procedures available for separation of plutonium in soil and sediments[4-8] and in biological samples[9-11], those involving complete dissolution usually give low sensitivity because only a small amount of sample can be processed conveniently. The leaching method[7], which is capable of treating kilogram amounts of soil, is more suitable for low-level analysis. The leaching method, with nitric and hydrochloric acids, has been compared with the sodium carbonate fusion and the hydrofluoric–perchloric acid total dissolution methods[12] and the results showed no significant difference between methods of analysis for fall-out plutonium in several types of soil samples. Therefore this method was adopted for sediment analysis; it is also applicable to the analysis of biological samples after they have been dry-ashed.

EXPERIMENTAL

Reagents

All the reagents used were of reagent grade. All water was distilled and then deionized on a Dowex-50 cation-exchange column.

Iron carrier solution. 50 mg Fe^{3+} ml^{-1} in 0.5 *M* hydrochloric acid.

Plutonium-236 *tracer.* Standardized, 2–3 d.p.m. ml^{-1} in 1 *M* nitric acid. This need not be kept clean of ^{228}Th and other α-active daughters since the procedure

---

* Present address: Scripps Institution of Oceanography, La Jolla, Calif. 92037, U.S.A.

provides good decontamination.

Anion-exchange resin. AG 1-X8, 100–200 mesh, Bio-Rad Lab., Richmond, Calif.

Counting apparatus

The α-spectrometer system consisted of an ORTEC 300 mm^2, 100-μm depletion-depth, lithium-drifted silicon surface-barrier detector mounted in a chamber connected to a vacuum system, a detector bias supply (ORTEC Mod. No. 428), a FET preamplifier (ORTEC No. 109A), a power supply (ORTEC No. 115), a linear amplifier (Canberra No. 1416) and a 512-channel pulse-height analyzer (Nuclear Data No. 120) connected to a typewriter readout. With a scale expander (Canberra No. 1461), a 128-channel analyzer (Nuclear Data No. 110) may also be used.

Procedure for sea water

Sea-water samples of 50–60 l collected at depths of 0–700 m from the North Atlantic Ocean (1967–1969) contained sufficient ^{239}Pu activity for convenient determination; however, much lower activity was observed for deeper samples[13].

Clean thoroughly the sample barrel (top, side, handles, caps, etc.) of all dust, dirt and loose material. Weigh the sample in the original barrel and transfer the sea water to a polyethylene container of the appropriate size (100–300 l capacity). Weigh the empty barrel to determine the weight of the sample. Observe any unusual appearance in the sample (*e.g.* color, particulate matter, etc.). This information may be useful to establish contamination, if any, of the sample. Add *ca.* 500 ml of 3 *M* hydrochloric acid to the empty barrel, recap, rotate the barrel on its side a few times, and leave for at least 2–3 h. Combine the acid rinse with the sample. Rinse the empty barrel twice with about 1 l of deionized water and combine with the sample.

Add 10 ml of iron carrier and 1 ml of standardized plutonium-236 (2–3 d.p.m.) tracer. Stir the sample with tank nitrogen for about 1 h. Add 100 ml of 2 *M* sodium hydrogensulfite and stir with tank nitrogen for about 30 min. Add a second 100 ml of the sulfite solution and sufficient 15 *M* ammonia solution (300–400 ml) to make the solution basic; mix well. Cover the sample securely and allow the precipitate to settle overnight.

Carefully siphon off the main fraction of the supernate and transfer the hydroxide slurry to a 3-l beaker. Cover the beaker with aluminum foil or plastic wrap and let the hydroxide settle. Decant and centrifuge the remaining supernate. Dissolve the hydroxide with a minimal amount of 16 *M* nitric acid. Estimate the volume of the solution and add an equal volume of 16 *M* nitric acid. Transfer the solution to a 400-ml beaker and dilute the solution to *ca.* 100 ml with 8 *M* nitric acid. Add 5 ml of 30% hydrogen peroxide, cover the beaker with a watch glass, and heat on a hot plate at 90–100° until the peroxide has decomposed. Cool the sample to room temperature, add 1 g of solid sodium nitrite, mix, leave for 30 min and then proceed with the plutonium purification.

Procedure for sediments

Usually 50–100 g of dried shallow water sediments give sufficient fall-out ^{239}Pu activity for convenient counting. Samples from the lower sections of cores (below 10 cm) or of oceanic sediments may require a larger aliquot; the ^{239}Pu concentration in the 10–12 cm section of the core is usually about 1/10 the concentration of the surface section.

It was found that the addition of hydrochloric acid in the leaching step is necessary only for sediment samples of low salinity. Most marine sediments contain sufficient chloride for complete leaching of plutonium from the sample using only nitric acid.

Weigh out a 100-g aliquot of dried sediment, transfer it to a 3-l beaker, wet the sample with water, and add 1 ml of standardized plutonium-236 tracer. Carefully add 200 ml of 16 *M* nitric acid and 100 ml of 12 *M* hydrochloric acid, slowly stir the sample and allow the mixture to react at room temperature. If foaming becomes appreciable, control it with the addition of a few drops of *n*-octanol. When the reaction subsides, cover the beaker with a watch glass, heat gently, then to near boiling (90–100°) and digest the sample for about 2 h with occasional stirring.

Add 300 ml of 1 *M* nitric acid and 25 ml of 30% hydrogen peroxide and continue heating (90–100°) until the peroxide has decomposed. Cool the sample, filter through a glass fiber filter paper and wash the residue with *ca.* 50 ml of hot 1 *M* nitric acid. Transfer the residue back to the 3-l beaker and repeat the entire process from the addition of concentrated nitric and hydrochloric acids. Combine the filtrate and acid rinses and evaporate (90–100°) until salts begin to form. Estimate the volume of the solution, add an equal volume of 1 *M* nitric acid, dilute to 1 l with 8 *M* nitric acid, and cool to room temperature. Add *ca.* 10 g of solid sodium nitrite, mix and leave for 30 min before proceeding with the plutonium purification.

Procedure for marine organisms

The concentration of fall-out plutonium in marine organisms is quite variable; a range from 0.004 d.p.m. kg^{-1} in fish tissue to more than 10 d.p.m. kg^{-1} in certain seaweeds has been observed[14]. For optimal sample counting rate, the activity should be about 0.5–5 d.p.m. Lower activity would require too long counting whereas higher activity could unnecessarily increase the chance of cross-contamination between samples.

Table I, which may be used as a guide for the selection of the proper sample size, lists the average ^{239}Pu concentrations in some marine organisms of the Atlantic Ocean collected in 1970[14]. Similar ranges of ^{239}Pu concentration have also been found in some Pacific organisms[15].

TABLE I

AVERAGE PLUTONIUM-239 CONCENTRATION OF MARINE ORGANISMS IN THE ATLANTIC OCEAN[14]

Organisms	*^{239}Pu (d.p.m. per kg wet wt.)*
Sargasso weed	13
Mixed Zooplankton	3
Starfish, *Asterias forbesi*	2
Mussels and clams, shell	0.6
meat	0.3
Fish, guts	0.9
bone	0.3
liver	0.1
meat	0.004

Weigh the wet organisms (dissected if necessary), take out the proper aliquot, dry to constant weight at 105°, and ash at 450–475° until all the organic material has oxidized. Do not ash above 500°[5]. Weigh the ash. Transfer the ash to a glass beaker. Since carbonates are formed during ashing, the initial reaction of the ash with acid is very vigorous; allow sufficient room in the selection of beaker so that spattering loss is minimized. Wet the ashed sample with water and add 1 ml of standardized plutonium-236 tracer. Proceed with the digestion and separation of plutonium as described in the procedure for sediments.

Plutonium purification procedure

Pass the sample solution obtained by the above steps through an anion-exchange column pre-conditioned with 8 *M* nitric acid. For sea-water samples, use 10 ml of wet resin in a 1-cm i.d. × 20 cm column, and for sediment samples use 25 ml of wet resin in a 1.5-cm i.d. × 30 cm column.

Allow the sample solution to drain to the top of the resin at a flow rate of about 10 ml min^{-1}. Using a 2-ml disposable glass pipet, rinse the column wall with 8 *M* nitric acid; drain the rinse solution carefully to the top of the resin. Repeat the rinse and draining step once. Elute the column with 30 ml of 8 *M* nitric acid, drain carefully to the top of the resin and discard the eluate. Elute as above with 30 ml of 12 *M* hydrochloric acid and discard this eluate.

Elute the plutonium with a solution of 30 ml of 16 *M* hydrochloric acid and 1 ml of 1 *M* ammonium iodide. Mix this eluant solution just before use. Collect the eluate in a 100-ml beaker, and evaporate below boiling to dryness on a hot plate. Remove the ammonium salts by evaporation with several portions of 2–3 ml each of 16 *M* nitric acid and 12 *M* hydrochloric acid. Rinse the wall of the beaker with each addition of acid. When the ammonium salts have evaporated, add a final rinse of 2–3 ml of 12 *M* hydrochloric acid, and evaporate the sample to dryness.

Add 5 ml of 12 *M* hydrochloric acid, warm the solution on a hot plate for a few minutes, and transfer to a 50-ml centrifuge tube. Rinse the beaker twice with 2–3 ml of 12 *M* hydrochloric acid and combine the solutions. Add *ca.* 100 mg of solid sodium nitrite, stir with a glass stirring rod, and allow to react for about 30 min. Centrifuge at low speed for 2–3 min. Transfer the supernate to the top of small ion-exchange column, loaded with 2 ml of wet AG 1-X8 resin preconditioned with 12 *M* hydrochloric acid. Drain the solution to the top of the resin, and rinse the tube and column walls twice with 1-ml portions of hydrochloric acid, draining carefully to the top of the resin each time. Wash the column with 20 ml of 12 *M* hydrochloric acid. Discard the eluate. Elute the plutonium with 20 ml of 12 *M* hydrochloric acid and 1 ml of 1 *M* ammonium iodide (mixed just before use).

Collect the plutonium eluant in a 50-ml beaker, and slowly evaporate to remove the ammonium salts as described above.

Electroplate the plutonium on stainless steel plating discs as described previously[3], count, and resolve the activity by α-spectrometry.

RESULTS AND DISCUSSION

This procedure has routinely been inserted into the sequential scheme[3] for analysis of fall-out radionuclides in sea water and other marine samples. The iron(II) hydroxide precipitation is made just after the removal of cesium with ammonium molybdophosphate (AMP); tests have shown that AMP carries no detectable plutonium from samples in the concentration range encountered.

The plutonium procedure requires 2–3 days for sediment or ashed organism samples and 3–4 days for sea water. In routine analysis two sets of 4 parallel samples can be processed in one week by a trained technician.

Sensitivity

The sensitivity of the procedure is respectively: 0.004 d.p.m. per 100 l of sea water (for a 50-l sample), 0.02 d.p.m. per kg of sediments (for 100 g of dried sediments), and 0.002 d.p.m. per kg (for 1 kg of fresh organisms); this is based on a two σ background uncertainty, a counting time of 48 h, and a counting efficiency of 38 %.

Chemical recovery

No radiochemical procedure in routine use today is quantitative for fall-out plutonium in large samples. Procedures based on "average" chemical yield from spiked analyses to correct for chemical loss are not reliable. Neither accidental nor intrinsic loss in such procedures can be accurately corrected. Therefore, cyclotron produced plutonium-236 tracer, free from other plutonium isotopes, is used in this laboratory for monitoring recovery of plutonium in analysis.

On thirty samples of 5–60 l of sea water, analyzed by the present procedure, the average plutonium recovery was 52 ± 18 %; even higher recoveries, up to 85 %, were obtained in the smaller volume samples. This compares to 25 ± 14 % (on 38 samples) by the iron(III) hydroxide method[3].

The average recovery on 75 samples of sediments and ashed organisms was 63 ± 20 % (range 30–99 %) by the given leaching method. Changing the sample size between 50 and 400 g of dried sediments showed no systematic effect on the recovery.

A possible explanation for the low recovery in the iron(III) hydroxide procedure is that the plutonium is lost through the formation of plutonium(IV) polymers. Plutonium(IV) ions are known to form polymers very readily in many solutions at low acid concentrations[5,16,17]. The chemical behavior of the polymers is significantly different from that of the ionic forms. Plutonium(IV) polymers are difficult to filter, extract, or coprecipitate because the size and charge of the colloidal particles vary unpredictably under many conditions.

This procedure avoids the difficulty encountered with plutonium(IV) polymers, by reduction of Pu(IV) to Pu(III) with sulfite and then separating the plutonium from sea water by coprecipitation with iron(II) hydroxide. Sodium hydrogensulfite or gaseous sulfur dioxide are both effective for the depolymerization and reduction of colloidal plutonium in acidic solution[17].

Polymerization loss of plutonium in the analysis of sediments and organisms is small, if not negligible, because the sample solution is maintained at a high acid concentration throughout the procedure.

Absolute values

The data presented here were all normalized to the disintegration rate, corrected for radioactive decay, of a plutonium-236 solution calibrated at the Health and Safety Laboratory, USAEC, in June 1965. At present there is some uncertainty about the absolute value of this solution.

TABLE II

ANALYSIS OF SEA WATER

Sample no.	*Location*	*Date*	^{239}*Pu* (*d.p.m. per 1000 kg*)[a]	*Std. dev.*
228	27°47′N 67°35′W	Dec. 1968	1.5±0.5	
331	27°47′N 67°35′W	Dec. 1968	2.6±0.5	0.6
332	27°47′N 67°35′W	Dec. 1968	2.6±0.7	
267	36°23′N 70°3′W	June 1969	2.6±0.8	
268	36°23′N 70°3′W	June 1969	2.3±0.5	0.7
269	36°23′N 70°3′W	June 1969	1.4±0.2	
270	36°23′N 70°3′W	June 1969	3.1±1.1	
389	WHOI Aquarium	Aug. 1970	2.9±0.8	0.3
390	line	Aug. 1970	2.5±0.4	
207	IAEA STD. 1	1970	123±5	
208	Seawater 1	1970	116±5	13
209	Seawater 1	1970	144±8	
210	Seawater 1	1970	118±6	
211	Seawater 2	1970	316±18	
212	Seawater 2	1970	298±12	11
213	Seawater 2	1970	324±21	
214	Seawater 2	1970	313±15	

[a] The ± values are the 1 σ of the counting error.

TABLE III

ANALYSIS OF SEDIMENTS

Sample no.	*Location*	*Date*	^{239}*Pu* (*d.p.m. per kg dry wt.*)[a]	*Std. dev.*
13	Cape Cod, Mass.	1968	72±7	6
13-R	Cape Cod, Mass.	1968	80±2	
16	Cape Cod, Mass.	1968	82±6	1
16-R	Cape Cod, Mass.	1968	84±2	
202	Bombay, India	1970	374±15	7
203	Bombay, India	1970	389±15	
204	Bombay, India	1970	374±15	

[a] The ± values are the 1 σ of the counting error.

Replicate analysis

Analyses of sea water, sediments and organisms are shown in Tables II–IV. The average standard deviation of the replicates is well within the 1 σ counting error of the samples (except for sea-water samples No. 207–210).

Contamination and blank activity

Little or no plutonium-239 contamination was found in reagent and simulated sea-water blanks (Table V). The simulated sea-water samples were obtained from deep oil well brine known to be free of fall-out radioactivities. The average ^{239}Pu concen-

TABLE IV

ANALYSIS OF ORGANISMS

Sample no.	*Organisms*	*^{239}Pu (d.p.m. per kg wet wt.)*[a]	*Std. dev.*
27	Shark liver	0.28 ± 0.07	0.05
41	Shark liver	0.21 ± 0.06	
32	Shark bone	0.025 ± 0.012	0.007
32-R	Shark bone	0.035 ± 0.014	
40	Blue mussels	0.33 ± 0.12	0.02
57	Blue mussels	0.36 ± 0.05	

[a] The ± values are the 1σ of the counting error.

TABLE V

PLUTONIUM-239 ACTIVITY IN REAGENT AND SIMULATED SEA-WATER BLANKS

Sample	*^{239}Pu (d.p.m. per sample)*
Reagent blanks	0.005 ± 0.005
	0.017 ± 0.015
	0.007 ± 0.007
Simulated sea-water blank	−0.005 ± 0.010
	0.010 ± 0.02
	−0.010 ± 0.02
Average	0.004 ± 0.010

tration of 6 such blanks (50 l), processed along with regular sea-water samples, was 0.004 ± 0.010 d.p.m. per sample, or about a factor of 2 above the detection limit.

The present detector background (5.00–5.20 MeV) for ^{239}Pu was less than one count per 24 h. The average detector background activity over an extended period of about 10,000 min was 4 counts, or 0.0004 ± 0.0002 c.p.m., near the region of the ^{239}Pu α-spectrum. Similar background activity was also found near the regions of the α-peaks of ^{238}Pu (5.30–5.50 MeV) and ^{236}Pu (5.60–5.80 MeV). This level of background activity is an exception rather than a general rule for most solid-state detectors. Much higher background has been observed in some solid-state detectors because of contamination with ^{241}Am used by the manufacturer for their calibration[13]. The present detectors were purchased from the manufacturer before any test with ^{241}Am. Such detectors are not hard to obtain, but the requirement must be explicitly specified to the manufacturer.

The average counting rate of the samples was about 0.5 c.p.m.; build-up of detector contamination from recoil atoms was negligible in about 15 months of operation. This is consistent with recoil studies of α-emitters with daughters of long half-lives such as the decay products of the plutonium isotopes[18].

In the determination of plutonium-238, a serious decontamination problem was encountered. Figure 1 shows a typical α-spectrum of the major peaks of ^{236}Pu, ^{238}Pu and ^{239}Pu; on this are superimposed the peaks, with the same detector and geometry, of thorium-228, and radium-224 in this energy region. It is clear that ^{238}Pu, the least abundant of the plutonium isotopes measured, is seriously interfered with by ^{228}Th, which is present, as a decay product, in the ^{236}Pu tracer, as well as being very rich in most recent marine sediments, and detectable in marine organisms. Radium-224 is no problem in the method described since it does not follow plutonium in the hydroxide precipitation.

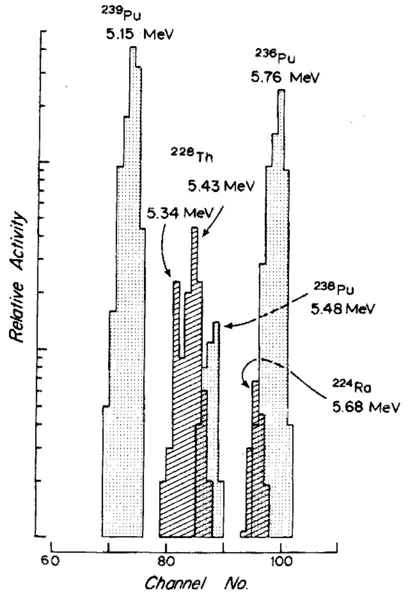

Fig. 1. α-Spectrum of ^{239}Pu, ^{238}Pu, ^{236}Pu, ^{228}Th and ^{224}Ra.

Thorium, however, does follow plutonium in the hydroxide precipitates and is not effectively cleaned up by the nitric acid elution (necessary for separation of iron from plutonium) on the anion-exchange column, nor, on this column, by hydrochloric acid elution: Stubborn traces of thorium continue to elute after many column-volumes of this acid. This is probably because of strong adsorption of thorium–nitrate complexes in the interstitial cavities of the resin beads, where the hydrochloric acid wash may be physically restricted. Use of a second anion column, equilibrated with hydrochloric acid, has proved necessary and effective: On this column plutonium adheres until eluted with hydrochloric acid–ammonium iodide whereas thorium is quickly washed out with concentrated acid.

Other parameters

Two kinds of material, platinum and stainless steel, were studied for the mounting of plutonium for α-spectrometry. Stainless steel discs were chosen because they are considerably less costly than platinum and the quality of the plated sample is not significantly different from that of the platinum disc in terms of both α-resolution and adhesion of plutonium to the plate.

The resolution of the spectrometer used for the 5.76-MeV α-emission of ^{236} Pu is 60 ± 5 keV (FWHM) on stainless steel discs as compared to 65 ± 5 keV for platinum discs. A plutonium-236 source electroplated on a stainless steel disc and used as a detector standard over a period of 32 months showed loss of neither activity (other than its normal decay) nor resolution.

Adsorption loss of plutonium on several laboratory wares was also checked. Known amounts of plutonium-236 standard were evaporated in Pyrex beakers, Teflon beakers, ceramic and Vycor crucibles with hydrochloric–nitric acid mixtures; the standard was then transferred to an electroplating apparatus, electroplated and counted. No significant difference was found in these standards from one that was directly electroplated.

The author is very grateful to Dr. V. T. Bowen for his advice and encouragement. This work was supported by the U.S. Atomic Energy Commission under contract AT(30-1)-2174. Contribution No. 2712 from the Woods Hole Oceanographic Institution.

SUMMARY

A radiochemical procedure is described for the determination of plutonium in large samples of sea water, sediments and organisms with a sensitivity of 0.004 d.p.m. per 100 l of sea water (for a 50-l sample), 0.02 d.p.m. per kg of sediments (100-g sample) and 0.002 d.p.m. per kg of marine organisms (1-kg sample). An iron(II) hydroxide coprecipitation method is used for the concentration of plutonium in sea water. A nitric–hydrochloric acid leaching method is adapted for the treatment of sediments and ashed organisms. Factors influencing the recovery, contamination and blank activity are discussed.

RÉSUMÉ

Une méthode radiochimique est décrite pour le dosage du plutonium dans des échantillons d'eaux de mer, de sédiments et d'organismes marins, avec des sensibilités de 0.004 d.p.m./100 l (prise d'échantillon 50 l), 0.02 d.p.m./kg (prise de 100 g) et 0.002 d.p.m./kg (prise de 1 kg) respectivement. Le plutonium est concentré par coprécipitation avec l'hydroxyde de fer(II). Un traitement au mélange acide nitrique–acide chlorhydrique est proposé pour sédiments et cendres d'organismes. Divers paramètres sont examinés.

ZUSAMMENFASSUNG

Es wird ein radiochemisches Verfahren beschrieben, mit dem Plutonium in grossen Proben von Meerwasser, Sedimenten und Organismen mit einer Empfindlichkeit von 0.004 d.p.m./100 l in Meerwasser (bei einer 50 l-Probe), 0.02 d.p.m./kg in Sedimenten (100 g-Probe) und 0.002 d.p.m./kg in maritimen Organismen (1 kg-Probe) bestimmt werden kann. Für die Anreicherung des Plutoniums in Meerwasser wird eine Eisen(II)-hydroxid-Mitfällungsmethode angewendet. Sedimente und veraschte Organismen werden mit einem Gemisch von Salpeter- und Salzsäure ausgezogen. Die Faktoren, die den erfassten Anteil, die Kontamination und Blindaktivität beeinflussen, werden diskutiert.

REFERENCES

1 M. G. LAI AND H. A. GOYA, *USNRDL–TR-67-73*, Naval Radiological Defense Laboratory, San Francisco, Calif., 1967.
2 U. HOLLSTEIN, H. M. HOOGMA AND J. KOOI, *Health Phys.*. 8 (1962) 49.
3 K. M. WONG, V. E. NOSHKIN AND V. T. BOWEN, in Y. NISHIWAKI AND R. FUKAI, *Reference Methods for Marine Radioactivity Studies*, International Atomic Energy Agency, Vienna, 1970, p. 119.
4 M. C. BERTOLI, *Anal. Chem.*, 39 (1967) 375.
5 G. H. COLEMAN, *The Radiochemistry of Plutonium*, Natl. Acad. Sci., Natl. Res. Counc. Publication NAS-NS 3058, 1965, p. 7.
6 J. H. HARLEY (Editor), *Manual of Standard Procedures*, Health and Safety Laboratory, U.S. At. Energy Comm. NYO-4700, 1967.
7 N. CHU, *Anal. Chem.*, 43 (1971) 449.
8 E. I. GEIGER, *Health Phys.*, 1 (1959) 405.
9 W. J. MAJOR, R. A. WESSMAN, R. MELGARD AND L. LEVENTHAL, *Health Phys.*, 10 (1964) 957.
10 T. Y. TORIBARA, C. PREDMORE AND P. A. HARGRAVE, *U.S. At. Energy Comm. Res. and Devel. Rept. UR-606*, 1962.
11 F. W. BRUENGER, B. J. STOVER AND D. R. ATHERTON, *Anal. Chem.*, 35 (1963) 1671.
12 P. W. KREY AND E. P. HARDY, *U.S. At. Energy Comm. Res. and Devel. Rept. HASL-235*, (1970) 16.
13 V. T. BOWEN, K. M. WONG AND V. E. NOSHKIN, *J. Marine Res.*, 29 (1971) 1.
14 K. M. WONG, J. C. BURKE AND V. T. BOWEN, submitted to *Health Phys.*
15 K. C. PILLAI, R. C. SMITH AND T. R. FOLSOM, *Nature*, 203 (1964) 568.
16 M. S. MILYUKOVA, N. I. GUSEV, I. G. SENTYURIN AND I. S. SKLYARENKO, *Analytical Chemistry of the Elements—Plutonium*, Ann Arbor-Humphrey Science Publications, Ann Arbor, London, 1969.
17 J. B. ANDELMAN AND T. C. ROZZELL, in R. F. GOULD, *Radionuclides in the Environment*, American Chemical Society Publications, Washington, D. C., 1970.
18 C. W. SILL AND D. G. OLSON, *Anal. Chem.*, 42 (1970) 1596.

Anal. Chim. Acta, 56 (1971) 355–364

Analytica Chimica Acta
Elsevier Publishing Company, Amsterdam
Printed in The Netherlands

DETERMINATION OF THALLIUM BY PHOTON ACTIVATION ANALYSIS

L. W. MASTERS AND G. J. LUTZ
Analytical Chemistry Division, National Bureau of Standards, Washington, D.C. 20234 (U.S.A.)

(Received 12th May 1971)

Thallium has been determined by the thermal neutron reaction $^{203}Tl(n,\gamma)^{204}Tl$ in a variety of matrices including meteorites[1,2], rocks[3], sea water[4], zinc and zinc salts[5], and, in a case of thallium poisoning, in hair and nails[6]. Sensitivities claimed are a small fraction of a microgram. Hoste *et al.*[7] have evaluated the possible error involved in the determination of thallium in the presence of large amounts of lead, due to the reaction $^{204}Pb(n,p)^{204}Tl$.

^{204}Tl decays exclusively by β-emission and thus requires a rigorous and frequently lengthy separation. In addition, it has a half-life of 3.8 years, effectively precluding decay measurements for assurance of radiochemical purity with respect to long-lived interferences.

In view of this, Talat-Erben and Okar[8] suggested the use of the reaction $^{203}Tl(n,2n)^{202}Tl$ with reactor neutrons. The product nuclide has a half-life of 12.0 days and a γ-ray of 439-keV energy is associated with 95% of the electron capture. There are, in addition, mercury X-rays of *ca.* 88 keV energy. The threshold for the reaction is about 9 MeV and Talat-Erben and Okar found the sensitivity to be about 20 μg for irradiations conducted for 30 h in close proximity to the fuel elements in a total flux of about 10^{13} n cm^{-2} sec^{-1}.

Oka and Kato[9] have used photons from a linear accelerator operated with an electron energy of 15 MeV to induce the reaction $^{203}Tl(\gamma,n)^{202}Tl$ and have measured nondestructively thallium in indium and gallium with a NaI(Tl) detector. Sensitivities of about 10 μg for thallium in the indium matrix and about 0.1% in the gallium matrix were possible.

In this paper, the determination of thallium in glass spiked with many elements and in zinc and zinc compounds by means of the (γ,n) reaction and a radiochemical separation, is described. The threshold for the reaction is about 8.8 MeV and the cross-section is estimated to rise to a peak of 600–700 mb at an energy of about 15 MeV.

EXPERIMENTAL

Equipment

The samples were irradiated in the 45-degree facility of the NBS electron linear accelerator. The converter target and the pneumatic transfer system have been described previously[10]. The accelerator electron energy was 35 MeV and the beam current was about 30 μA. Counting was done with a 37 cm^3 or 60 cm^3 Ge(Li) detector or a 5 × 5 in well type NaI(Tl) detector with a multichannel analyzer.

Irradiation of glass samples

These samples were from the Office of Standard Reference Materials of the National Bureau of Standards. The NBS is currently certifying a series of standard glasses containing 61 trace elements. The standard glasses were prepared by adding to a base glass composed of 72% SiO_2, 12% CaO, 14% Na_2O and 2% Al_2O_3, 61 elements to give a series of four glasses containing nominally 0.02, 1, 50 and 500 p.p.m. of each of the elements. They are designated with the Standard Reference Material numbers 610 through 617[11].

The samples, in the form of discs, about 1.5 cm in diameter and 1 mm thick, were rinsed in ethanol and dilute nitric acid and broken into small pieces. The samples were individually encapsulated in polyethylene snap cap vials of about 1.3 cm^3 volume. Accurately weighed discs of copper were taped to each end of the vials as flux monitors. The vials were placed in screw-cap aluminum rabbits and irradiated individually. Standards of thallium(I) sulfate were packaged in the same manner and irradiated separately. Samples were usually irradiated for a few hours depending on the level of thallium expected.

Separation of thallium in glass samples

It had been observed in a previous investigation of solvent extraction properties of benzyl and octyl alcohol[12], that of some thirty elements tested, only thallium(III) and gold(III) were extracted quantitatively from strongly acidic solutions into benzyl alcohol and octyl alcohol. Mercury was extracted to the extent of about 35% in benzyl alcohol, but less than 1% into octyl alcohol. Thallium(I) did not extract into either alcohol. These considerations were applied to the separation of thallium from the glass samples.

The samples, after irradiation, were dissolved in 10 ml of 70% perchloric acid with a few ml of hydrofluoric acid and *ca.* 20 mg of thallium(I) sulfate carrier. Thallium(I) was oxidized to thallium(III) by the addition of a small amount of potassium chlorate solution. The mixture was diluted to 30 ml with distilled water, cooled to room temperature and extracted twice with 15-ml portions of octyl alcohol that had previously been washed with dilute perchloric acid. The separatory funnels were centrifuged for a few minutes to expedite separation of phases. The combined organic phases were washed three times with 6 *M* hydrochloric acid and collected in a polyethylene bottle and counted with a Ge(Li) detector. The use of a Ge(Li) detector permits the counting of thallium without a separation of gold, if the amount of gold is not so large that the 430-keV γ-ray of ^{196}Au interferes with the 439-keV line of ^{202}Tl. If necessary, the gold can be separated before the extraction by adding gold(III) carrier and reducing gold to the metal with sulfur dioxide.

A portion of the thallium(I) sulfate standard was treated and extracted under similar conditions.

Irradiation and separation of thallium for zinc samples

The samples and thallium standards were packaged in a similar manner to the glass samples. The activations were performed with bremsstrahlung from energy slits used in a physics experiment. Electron energies were usually in excess of 50 MeV, but because the samples could not be positioned close to the source of photons, intensity was substantially reduced from that in the activation analysis facility.

TABLE I

PERCENTAGE EXTRACTION OF THALLIUM AND ZINC FROM HYDROCHLORIC ACID SOLUTIONS INTO EQUAL VOLUMES OF BENZYL ALCOHOL AND OCTYL ALCOHOL

HCl concn. (M)	*% Extracted*			
	Benzyl alcohol		*Octyl alcohol*	
	Thallium	*Zinc*	*Thallium*	*Zinc*
1.0	100	0.1	77.6	0.6
2.0	100	0.9	88.9	2.5
3.0	99.5	2.7	92.1	5.5
4.0	99.8	3.0	97.9	8.1
6.0	100	4.6	99.8	14.5

The activated samples were dissolved in concentrated hydrochloric acid and *ca.* 20 mg of thallium carrier was added. Thallium(I) was oxidized to thallium(III) by the addition of hydrogen peroxide and the sample was heated to expel excess of peroxide. The solution was diluted with distilled water to give a final hydrochloric acid concentration of about 1 *M*. The solution was cooled to room temperature and extracted twice with 15-ml portions of benzyl alcohol that had been equilibrated with 1 *M* hydrochloric acid. The separatory funnels were centrifuged at *ca.* 1000 r.p.m. for a few minutes to expedite separation of phases. The organic phase was washed several times with 1 *M* hydrochloric acid in which were dissolved zinc and copper carriers. On occasion, final traces of zinc could not be washed out. In these cases, it was necessary to delay counting until the 14-h ^{69m}Zn had completely decayed. ^{69m}Zn has a γ-ray at 440 keV which interferes with thallium counting.

The reason for the choice of benzyl alcohol as an extractant for the zinc samples can be seen in Table I. To achieve a quantitative extraction of thallium from a hydrochloric acid solution into octyl alcohol, an acid concentration of approximately 6 *M* is required. At this acid strength, a substantial amount of zinc is also extracted. However, when the extraction is into benzyl alcohol, it may be conducted at an acid concentration of 1 *M* for complete extraction of thallium and zinc extraction is minimized.

RESULTS AND DISCUSSION

Analytical results of the standard reference glass samples are shown in Table II

TABLE II

DETERMINATION OF THALLIUM IN STANDARD REFERENCE GLASS SAMPLES

Sample number	*Certified value*	*Results obtained by photon activation (p.p.m.)*[a]
95 GCG	61.8	63 ± 3
95 GCE	15.7	14 ± 1
95 G	0.27	0.22 ± 0.03

[a] Uncertainties are standard deviation.

and are compared with the certified values obtained by isotope dilution mass spectrometry. The accuracy of the method as shown by the agreement with mass spectrometry is in the range usually obtained with photon activation analysis. Table III gives some results of thallium determination in zinc and zinc compounds. These irradiations were conducted with bremsstrahlung from the electron scattering experiment with a loss of sensitivity and hence precision.

TABLE III

DETERMINATION OF THALLIUM IN ZINC AND ZINC SALTS

Sample	*Results obtained by photon activation analysis (p.p.m.)*[a]
Zinc metal	1.7 ± 0.2
Zinc chloride	2.8 ± 0.4
Zinc acetate	7.2 ± 0.7

[a] Uncertainties are standard deviation.

There are a number of detection methods of potential use for counting the ^{202}Tl activity. These include counting of the 439-keV γ-ray or the mercury X-rays with either a Ge(Li) or a NaI(Tl) well detector as well as gross γ-ray counting with a NaI(Tl) well detector. The sensitivities for these five modes of counting were calculated according to the method of Currie[13]. The results are shown in Table IV. The calculations are based on the method of counting shown in the first column. The minimum detectable activity, shown in the third column, is based on counting sample and background for 20 h each. The fourth column, detection efficiency, reflects not only

TABLE IV

SENSITIVITIES FOR THALLIUM FOR VARIOUS DETECTOR SYSTEMS

(Irradiation conditions: 10-h bombardment, 30-μA beam current and 35-MeV electrons. Counting conditions: background and sample each counted for 20 h)

Detection method	*Background (counts h^{-1})*	*Minimum detectable activity (counts h^{-1})*	*Detection efficiency (counts h^{-1} μg^{-1})*	*Minimum mass detectable (μg)*
Hg X-rays 66 cm^3 Ge(Li)	840	30	180	0.17
439-keV γ-rays 60 cm^3 Ge(Li)	60	8	60	0.13
Hg X-rays 5 × 5 in well NaI(Tl)	7600	90	960	0.09
439-keV γ-rays 5 × 5 in well NaI(Tl)	4500	70	1380	0.05
Gross γ-ray counting 5 × 5 in well NaI(Tl)	34800	195	3000	0.07

detector system efficiency, but also the conditions of irradiation. These calculations are based on a 10-h irradiation with 35-MeV electrons and an average beam current of 30 μA. The counting sample configuration is 20 ml of solution placed at the most favorable geometry. The irradiation configuration is the average of a *ca.* 10-cm^3 volume which could accommodate several samples simultaneously. The fifth column, minimum mass detectable, is the ratio of the values in the third and fourth columns. These sensitivities refer to counting with no interferences. Other possible detector systems include counting the mercury X-rays with a thin NaI(Tl) detector, reducing the efficiency somewhat and the background substantially, or coincidence counting the γ-ray and X-rays with two NaI(Tl) detectors, reducing the detection efficiency still further, but virtually eliminating detector background.

The possibility of systematic error caused by the interfering reactions ^{204}Pb-$(\gamma,n^{d}p)^{202}$Tl and ^{204}Pb$(\gamma,2n)^{202}$Pb. (^{202}Pb $\xrightarrow{\varepsilon}$ ^{202}Tl) was investigated. Samples of a very pure lead salt and a thallium salt were irradiated with a known relative intensity with bremsstrahlung from 35-MeV electrons. The lead salt was dissolved and, after about 20 h, any thallium activity induced in the lead was extracted with benzyl alcohol, counted and compared with the ^{202}Tl activity induced in the thallium. No ^{202}Tl was observed in the lead sample and, based on the smallest amount detectable, it was determined that 10^6 times as much lead as thallium in a sample would cause an error of less than 10%.

The authors thank the NBS LINAC operators for the very fine services performed.

SUMMARY

The determination of trace amounts of thallium by the thermal neutron reaction ^{203}Tl$(n,\gamma)^{204}$Tl is complicated because ^{204}Tl is a pure β-emitter, requiring a lengthy and rigorous separation. In addition the half-life of ^{204}Tl is too long to permit decay measurements. A photon activation analysis method has been developed for this determination. Bremsstrahlung from a beam of 35-MeV electrons induces the photonuclear reaction ^{203}Tl$(\gamma,n)^{202}$Tl. The detection limit is of the nanogram order. There are no interfering photonuclear reactions from lead.

RÉSUMÉ

Le dosage de traces de thallium par la réaction neutronique, thermique ^{203}Tl$(n, \gamma)^{204}$Tl est compliquée par le fait que ^{204}Tl est un pur émetteur β, exigeant une séparation longue et rigoureuse. En outre, la période de ^{204}Tl est trop longue pour permettre des mesures de désintégration. Une méthode d'analyse par activation au moyen de photons a été mise au point. La détection limite est de l'ordre du nanogramme. Il n'y a pas d'interférence photonucléaire du plomb.

ZUSAMMENFASSUNG

Die Bestimmung von Thalliumspuren durch die mit thermischen Neutronen ablaufende Reaktion ^{203}Tl$(n, \gamma)^{204}$Tl ist schwierig, da ^{204}Tl ein reiner β-Strahler ist,

der eine langwierige und sorgfältige Abtrennung erfordert. Ausserdem ist die Halbwertszeit von ^{204}Tl für Zerfallsmessungen zu lang. Für die Bestimmung wurde eine Methode der Photonenaktivierungsanalyse entwickelt. Bremsstrahlung von 35 MeV-Elektronen führt zu der photonuklearen Reaktion $^{203}\mathrm{Tl}(\gamma, n)^{202}\mathrm{Tl}$. Die Nachweisgrenze liegt im Nanogrammbereich. Störende photonukleare Reaktionen mit Blei treten nicht auf.

REFERENCES

1 W. D. Ehmann and J. R. Huizenga, *Geochim. Cosmochim. Acta*, 17 (1959) 125.
2 G. W. Reed, K. Kigoshi and A. Turkevich, *Geochim. Cosmochim. Acta*, 20 (1960) 122.
3 D. F. C. Morris and R. A. Killick, *Talanta*, 4 (1960) 51.
4 A. D. Matthews and J. P. Riley, *Anal. Chim. Acta*, 48 (1969) 25.
5 D. Gibbons and D. Lawson, *Proc. 1965 Intern. Conf. on Modern Trends in Activation Analysis, College Station*, p. 172–174.
6 G. Henke and G. Bohn, *Arch. Toxikol.*, 25 (1969) 48.
7 J. Op De Beeck, A. Speecke and J. Hoste, *Radiochim. Acta*, 4 (1965) 32.
8 M. Talat-Erben and S. Okar, *CNAEM-39*, Sept. 1966, P.K.I., Hava Alani, Istanbul, Turkey.
9 Y. Oka and T. Kato, *Nippon Kagaku Zasshi*, 87 (1966) 1057.
10 F. A. Lundgren and G. J. Lutz, *Trans. Amer. Nucl. Soc.*, (1967) 89.
11 *Price and Availability Listing of Standard Reference Materials*, NBS Special Publ. 260, Suppl. July 1970, Government Printing Office, Washington, D.C. 20402.
12 L. W. Masters, in P. D. LaFleur, *Activation Analysis Section: Summary of Activities, July 1968 to June 1969*, NBS Technical Note 508, Government Printing Office, Washington, D.C. 20402, 1970, p. 115–122.
13 L. A. Currie, *Anal. Chem.*, 40 (1968) 586.

Analytica Chimica Acta
Elsevier Publishing Company, Amsterdam
Printed in The Netherlands

A KINETIC METHOD OF DETERMINATION OF CALCIUM IN THE PRESENCE OF MAGNESIUM

SHIGENOBU FUNAHASHI, SHINKICHI YAMADA AND MOTOHARU TANAKA
Laboratory of Analytical Chemistry, Faculty of Science, Nagoya University, Chikusa-ku, Nagoya 464 (Japan)

(Received 15th April 1971)

The difference in stability constants of EGTA ((ethyleneglycol)bis(2-aminoethylether)-N,N,N′,N′-tetraacetate) complexes of calcium and magnesium forms a basis of a selective determination of calcium. Thus methods for the indirect polarographic and photometric determination of calcium have been elaborated[1,2], consideration being made of the following substitution reaction:

$$\mathrm{M_IY + M_{II} + }n\mathrm{A \rightleftharpoons M_IA_}n\mathrm{ + M_{II}Y}$$

where M_I and M_{II} refer to metals, Y an aminopolycarboxylate, and A a complexing agent.

Recently Paush and Margerum[3] have reported that metal exchange reactions between lead(II) and alkaline earth metal complexes of CyDTA (*trans*-1,2-diaminocyclohexane-N,N,N′,N′-tetraacetate) proceed at sufficiently different rates to permit the differential kinetic determination of mixtures of magnesium, calcium, strontium and barium.

The present paper describes a method of determination of calcium in the presence of magnesium based on the effect of calcium on the rate of the ligand substitution reaction (1).

$$\text{Cu-EGTA} + \text{PAR} \rightleftharpoons \text{Cu-PAR} + \text{EGTA} \qquad (1)$$

where PAR refers to 4-(2-pyridylazo)resorcinol.

RATE OF THE REACTION

The kinetics of the ligand substitution reaction of copper(II)–EGTA complex with PAR has been studied[4]. In order to force equilibrium (1) to the right, the reaction was done in ligand buffers[5] of $EGTA^{4-}$ with excess of alkaline earth metal ions; their roles in the reaction have been quantitatively assessed. Under conditions where copper(II) and PAR form the 1 : 2 complex, $Cu(PAR)_2^{2-}$, the rate law of the substitution reaction can be expressed as follows:

$$\begin{aligned}\mathrm{d}[\mathrm{Cu(PAR)_2^{2-}}]/\mathrm{d}t &= k_{0(\mathrm{M,H,PAR})}[\mathrm{Cu(EGTA)^{2-}}]\\ &= k_1^{\mathrm{M}}[\mathrm{Cu(EGTA)^{2-}}][\mathrm{M^{2+}}][\mathrm{OH^-}]\\ &\quad + k_2[\mathrm{Cu(EGTA)^{2-}}][\mathrm{HPAR^-}]\\ &\quad + k_3[\mathrm{Cu(EGTA)^{2-}}][\mathrm{PAR^{2-}}]\\ &\quad + k_4^{\mathrm{M}}[\mathrm{Cu(EGTA)^{2-}}][\mathrm{M^{2+}}][\mathrm{HPAR^-}]\\ &\quad + k_5^{\mathrm{M}}[\mathrm{Cu(EGTA)^{2-}}][\mathrm{M^{2+}}][\mathrm{PAR^{2-}}] \qquad (2)\end{aligned}$$

where $EGTA^{4-}$, PAR^{2-} and M^{2+} refer to tetravalent EGTA, divalent PAR and alkaline earth metal ion, respectively and $k_{0(M,H,PAR)}$ is the conditional rate constant involving concentrations of alkaline earth metal ion, hydrogen ion and PAR.

PRINCIPLE OF DETERMINATION

Under the present experimental conditions, the predominant species of PAR is the singly charged species ($HPAR^-$), as is evident from the stability constant of PAR[6], and PAR is in large excess in comparison with copper ion. The conditional rate constant can therefore be rewritten as the following equation:

$$k_{0(M,H,PAR)} = \left\{ k_1^M \frac{K_w}{[H^+]} + \left(k_4^M + \frac{k_5^M}{[H^+]K_{HPAR}} \right) C_{PAR} \right\} [M^{2+}] + \left(k_2 + \frac{k_3}{[H^+]K_{HPAR}} \right) C_{PAR} \tag{3}$$

where C_{PAR} refers to the total concentration of PAR, $K_w = [H^+][OH^-]$, and $K_{HPAR} = [HPAR^-]/[H^+][PAR^{2-}]$. As can be seen from eqn. (3), if the concentrations of hydrogen ion and PAR are kept constant, the conditional rate constant $k_{0(M,H,PAR)}$ is a linear function of the concentration of the alkaline earth metal ion.

Effect of magnesium ion

The effect of magnesium ion on the determination of calcium ion can be predicted from the reaction mechanism[4]. The reaction proceeds through dinuclear–diligand complexes involving copper, alkaline earth metal, EGTA and PAR (or hydroxide ion) and the rate of this reaction path is proportional to the stability constant of the complex of the alkaline earth metal ion with the segment of the EGTA partially released from the copper(II)–EGTA complex. Thus the concentration ratio of Cu(EGTA)Ca to Cu(EGTA)Mg is given by the following relation:

$$\frac{[Cu(EGTA)Ca]}{[Cu(EGTA)Mg]} = \frac{K^{Ca}_{Cu(EGTA)Ca}[Ca^{2+}]}{K^{Mg}_{Cu(EGTA)Mg}[Mg^{2+}]}$$

where $K^{Ca}_{Cu(EGTA)Ca}$ and $K^{Mg}_{Cu(EGTA)Mg}$ refer to the stability constants of dinuclear intermediates Cu(EGTA)Ca and Cu(EGTA)Mg, respectively. N-(Methoxyethyl)iminodiacetate being considered as a segment of EGTA, $K^{Ca}_{Cu(EGTA)Ca}$ and $K^{Mg}_{Cu(EGTA)Mg}$ can be approximated as the stability constants[7] of calcium and magnesium with N-(methoxyethyl)iminodiacetate. Then we have the following relation:

$$\frac{[Cu(EGTA)Ca]}{[Cu(EGTA)Mg]} = \frac{K_{CaL}[Ca^{2+}]}{K_{MgL}[Mg^{2+}]} = \frac{10^{4.53}[Ca^{2+}]}{10^{3.31}[Mg^{2+}]} = 10^{1.22}\frac{[Ca^{2+}]}{[Mg^{2+}]} \tag{4}$$

where L^{2-} refers to N-(methoxyethyl)iminodiacetate. The effect of magnesium on the determination of calcium can be predicted from eqn. (4): error from the presence of a comparable amount of magnesium does not seem to exceed 10%.

RESULT AND DISCUSSION

When the total concentration of PAR (C_{PAR}) and pH are kept constant, the

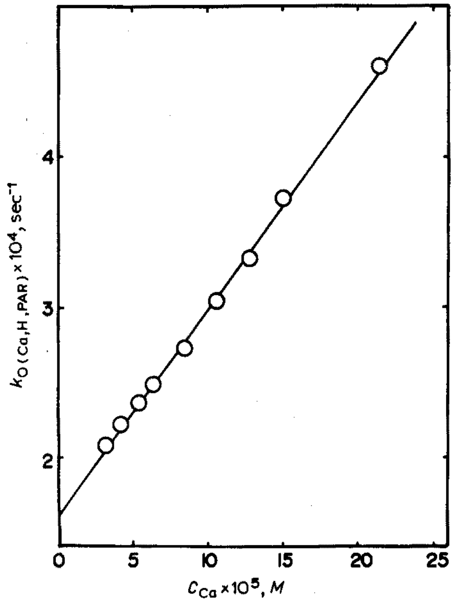

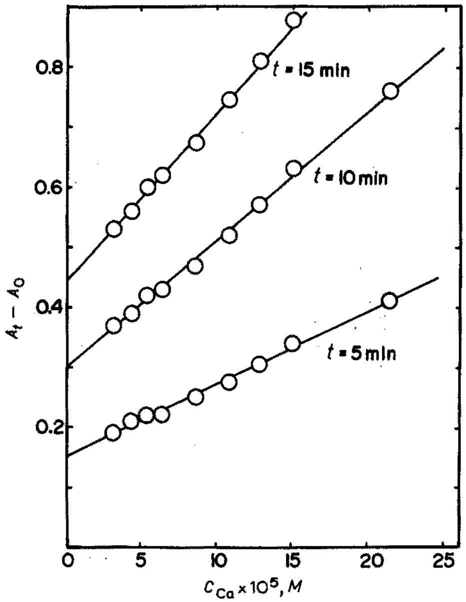

Fig. 1. A calibration curve for the determination of calcium based on conditional rate constants. Conditions: $C_{Cu} = 1.00 \cdot 10^{-5}$ M, $C_{EGTA} = 2.00 \cdot 10^{-5}$ M, $C_{PAR} = 1.00 \cdot 10^{-4}$ M, pH 9.15 (borate buffer), 25°.

Fig. 2. Calibration curves for the determination of calcium based on change in the absorbance during a definite time. Under the same conditions as described in Fig. 1.

conditional rate constants are proportional to the concentration of the alkaline earth metal ion. When the conditional rate constants are plotted against the concentration of alkaline earth metal ion, a straight line with an intercept is obtained. One such plot for calcium ion is presented in Fig. 1. Consequently the concentration of calcium ion can be determined by evaluating the conditional rate constants in this reaction system. However, the amount of copper(II)–PAR complex produced during a definite time is proportional to the calcium concentration. In Fig. 2, the difference in the measured absorbance of the reaction system at 0 and at *t* minutes $(A_t - A_0)$ is plotted against the concentration of calcium: the plot is used as a calibration curve. The effect of magnesium ion is shown in Table I, where are given conditional rate constants and the difference in absorbance in the presence of magnesium.

TABLE I

EFFECT OF MAGNESIUM ION

($C_{Cu} = 1.00 \cdot 10^{-5}$ M, $C_{EGTA} = 2.00 \cdot 10^{-5}$ M, $C_{PAR} = 1.00 \cdot 10^{-4}$ M, $C_{Ca} = 2.13 \cdot 10^{-5}$ M, pH 9.15 (borate buffer), 25°)

$C_{Mg}(\cdot 10^5\ M)$	$k_{O(M,H,PAR)}(\cdot 10^4\ sec^{-1})$	$A_{10} - A_0$	$A_{15} - A_0$
0.00	1.88 ± 0.10	0.345 ± 0.010	0.500 ± 0.010
2.43	1.90	0.352	0.507
4.86	2.00	0.375	0.535
9.73	2.22	0.411	0.579

A_0, A_{10} and A_{15} refer to the absorbance of the reaction system at 515 nm at 0, 10 and 15 min after the start of the reaction, respectively. As can be seen from Table I, at least the same amount of magnesium ion coexisting with calcium ion does not interfere with the determination of calcium. The influence of anions is presented in Table II. Ammonium ion interferes with the reaction, but can be tolerated up to $10^{-4}\,M$. Heavy metal ions interfere with the reaction, and must be previously separated.

TABLE II

EFFECT OF FOREIGN IONS

($C_{Cu}=1.00\cdot10^{-5}\,M$, $C_{EGTA}=2.00\cdot10^{-5}\,M$, $C_{PAR}=1.00\cdot10^{-4}\,M$, $C_{Ca}=2.13\cdot10^{-4}\,M$, pH 9.15 (borate buffer), 25°)

Foreign ions	*Concn.* (*M*)	*Ca*$^{2+}$ *found* ($\cdot10^4\,M$)	*Recovery* (%)
HPO_4^{2-}	10^{-4}	2.19	103
	10^{-3}	2.17	102
	10^{-2}	1.50	70
Cl^-	10^{-4}	2.19	103
	10^{-3}	2.13	100
	10^{-2}	2.30	108
HCO_3^-	10^{-4}	2.17	102
	10^{-2}	2.34	110
SO_4^{2-}	10^{-3}	2.13	100
	10^{-2}	1.90	89
F^-	$4\cdot10^{-4}$	2.19	103
NO_3^-	10^{-2}	2.19	103
NH_4^+	10^{-4}	2.17	102
	10^{-3}	2.25	106
	10^{-2}	4.20	197

Determination of calcium in natural water

Small amounts of heavy metal ions present in natural waters can be removed by extraction as their oxinates with chloroform at pH 5 and pH 9. Successful elimination of some heavy metals is shown in Table III.

TABLE III

ELIMINATION OF HEAVY METAL IMPURITIES

($C_{Cu}=1.00\cdot10^{-5}\,M$, $C_{EGTA}=2.00\cdot10^{-5}\,M$, $C_{PAR}=1.00\cdot10^{-4}\,M$, pH 9.15 (borate buffer), 25°)

Ions[a]	*Ca*$^{2+}$ *taken* ($\cdot10^4\,M$)	*Ca*$^{2+}$ *found* ($\cdot10^4\,M$)	*Recovery* (%)
Ca^{2+}	1.57	1.50	96
Ca^{2+}, Fe^{3+}	1.57	1.59	101
Ca^{2+}, Mn^{2+}	1.73	1.75	101
Ca^{2+}, Cu^{2+}	1.49	1.56	105
Ca^{2+}, Al^{3+}	1.49	1.46	98
Ca^{2+}, Zn^{2+}	1.49	1.55	104
Ca^{2+}, Mix.[b]	1.49	1.54	103

[a] The concentration of heavy metal ions is of the order of $10^{-4}\,M$.

[b] A mixture of Fe^{3+}, Mn^{2+}, Cu^{2+}, Al^{3+} and Zn^{2+}.

An underground water, in the campus of Nagoya University, was found to contain $2.43 \cdot 10^{-4}$ *M* of calcium. This value was checked by compleximetric titration with a standard EDTA solution with 2-hydroxy-1-(2-hydroxy-4-sulfo-1-naphthylazo)-3-naphthoic acid as indicator. The titrimetric result was in agreement with the kinetic result within experimental error, and added amounts of calcium were quantitatively recovered (Table IV).

TABLE IV

DETERMINATION OF CALCIUM IN AN UNDERGROUND WATER

($C_{Cu} = 1.00 \cdot 10^{-5}\,M$, $C_{EGTA} = 2.00 \cdot 10^{-5}\,M$, $C_{PAR} = 1.00 \cdot 10^{-4}\,M$, pH 9.15 (borate buffer), 25°)

Ca^{2+} added ($\cdot 10^4\,M$)	*Ca^{2+} found* ($\cdot 10^4\,M$)	*Recovery* (%)
0.00	2.43	—
2.13	4.52	98
4.28	6.59	97

EXPERIMENTAL

Reagents

Magnesium perchlorate. Reagent-grade magnesium oxide was dissolved in perchloric acid and excess of perchloric acid was removed by heating with an infrared lamp. Heavy metal impurities were extracted by the same procedure as in the case of calcium perchlorate[4]. The concentration of the magnesium perchlorate solution was determined compleximetrically with a standard EDTA solution with eriochrome black T as indicator.

Disodium hydrogen phosphate. Heavy metal impurities in sodium phosphate were extracted as oxinates with chloroform at pH 9. The same procedure was followed in the case of sodium chloride, sodium bicarbonate, sodium sulfate and sodium nitrate.

Methods of preparation of the other reagents (copper perchlorate, calcium perchlorate, PAR, EGTA, borax and sodium hydroxide) have been described previously[4].

Apparatus

Radiometer PHM-4d (Copenhagen) with a glass electrode (Type G 202) and a calomel electrode (Type K 401).

Hitachi Perkin-Elmer 139-UV-VIS Spectrophotometer with 5.1-cm cell thermostated at 25±0.2°.

Hitachi Recorder QPD 53.

Sharp Model TEB-10 Thermoelectric Circulating Bath.

Recommended procedures

Preparation of sample solution. Pipet into a clean, dry 200-ml separatory funnel, 50 ml of sample solution containing no more than 10^{-3} *M* calcium ion and 1 ml of 1% oxine–perchloric acid solution. Extract heavy metal ions as oxinates with chloroform at pH 5 and at pH 9. Then wash the aqueous phase three times with pure chloroform, bubble nitrogen gas to expel residual chloroform and dilute to 100 ml in a volumetric flask.

Measurement. Pipet into a clean, dry 100-ml cell for absorbance measurement 50 ml of sample solution, and 20 ml of copper(II)–EGTA solution containing $5 \cdot 10^{-5} M$ copper(II) perchlorate, $10^{-4} M$ EGTA and 0.1 M sodium borate. Dilute to 90 ml. Place the solution in the thermostated cell compartment of a spectrophotometer. After thermal equilibrium, initiate the substitution reaction by the addition of 10 ml of $10^{-3} M$ PAR solution. Record the absorbance at 515 nm as a function of the reaction time. Find the concentration of calcium ion by consulting the calibration curves previously constructed.

SUMMARY

A kinetic method of determination of calcium in the presence of magnesium is described. The method is based on the effect of calcium ion on the rate of the ligand substitution reaction of Cu(II)–EGTA with PAR. Calcium ion in the range 10^{-5}–$10^{-3} M$ can be photometrically determined in the presence of magnesium.

RÉSUMÉ

On décrit une méthode cinétique pour le dosage du calcium, en présence de magnésium. Elle est basée sur l'influence des ions calcium sur la vitesse de réaction de substitution complexométrique Cu(II)–EGTA avec PAR. On peut ainsi doser des concentrations en calcium de l'ordre de 10^{-5} à $10^{-3} M$, photométriquement, en présence de magnésium.

ZUSAMMENFASSUNG

Es wird eine kinetische Methode zur Bestimmung von Calcium in Gegenwart von Magnesium beschrieben. Die Methode beruht auf dem Einfluss, den Calciumionen auf die Geschwindigkeit der Ligandensubstitutionsreaktion von Cu(II)–EGTA mit PAR ausüben. Calciumionen im Bereich 10^{-5}–$10^{-3} M$ können in Gegenwart von Magnesium photometrisch bestimmt werden.

REFERENCES

1 G. Nakagawa and M. Tanaka, *Talanta*, 9 (1962) 847.
2 G. Nakagawa, I. Namiki and M. Tanaka, *Talanta*, 13 (1966) 1135.
3 J. B. Paush and D. W. Margerum, *Anal. Chem.*, 41 (1969) 226.
4 S. Funahashi, S. Yamada and M. Tanaka, *Inorg. Chem.*, 10 (1971) 257.
5 M. Tanaka, *Anal. Chim. Acta*, 29 (1963) 193.
6 W. J. Geary, G. Nickless and F. H. Pollard, *Anal. Chim. Acta*, 27 (1962) 71.
7 G. Schwarzenbach, G. Anderegg, W. Schneider and H. Senn, *Helv. Chim. Acta*, 38 (1955) 1147.

Analytica Chimica Acta
Elsevier Publishing Company, Amsterdam
Printed in The Netherlands

THERMAL ANALYSIS OF SODIUM METABISULFITE

MYRON MALANCHUK
Division of Health Effects Research, U.S. Environmental Protection Agency, Air Pollution Control Office, Cincinnati, Ohio 45237 (U.S.A.)

(Received 22nd April 1971)

Sodium metabisulfite, $Na_2S_2O_5$, was investigated as a part of a study of the role of sulfur dioxide in the effects of air pollution on health. Although the compound itself may not be directly involved as a major air pollutant, the chemistry associated with its thermal decomposition becomes important in understanding the possibilities of interactions between sulfur dioxide and aerosol particles. It is the bound form of SO_2, then, that must be considered as an air pollutant in determining its adverse health effects or control methods. It also is important to determine whether bound sulfur dioxide reaches the respiratory tract in a more, or a less hazardous form, *e.g.* whether it enters the lungs in an oxidizable state or perhaps as a metal sulfate.

Erdey *et al.*[1] described the thermal decomposition of sodium metabisulfite (sodium pyrosulfite) as a loss of sulfur dioxide followed by an oxidation of sodium sulfite. Cleghorn and Davies[2] used i.r. spectral data to suggest that there is an interval in the decomposition process when the evolution of sulfur dioxide and the oxidation of sodium sulfite proceed simultaneously. Cotton and Wilkinson[3] referred to a possible equilibrium between metabisulfite and the hydrogen sulfite, $NaHSO_3$. A possible decomposition intermediate, sodium peroxide, Na_2O_2, is oxidized to the superoxide, NaO_2, under conditions of elevated pressures and temperatures[3]. Thermogravimetric analysis (TGA) showed[4], on the other hand, that NaO_2 forms Na_2O_2 in air within the temperature range 200°–340°.

The formation and presence of one or more of these oxide components is thought to be involved in the decomposition process and, consequently, to affect the thermal analysis record.

Thermal decomposition of sodium metabisulfite is expected to yield sulfur dioxide with a corresponding loss in weight at *ca.* 150°. Further decomposition might be expected at a much higher temperature. The rate and the temperature range of decomposition varies with the atmosphere and with the rate of heating imposed upon the compound. An oxygen-containing atmosphere, for example, would probably cause an increase in weight through oxidation of the sample.

Sodium hydrogen sulfite preparations might be considered to be chiefly metabisulfite, and for all practical purposes, to act like it[5]. The preparation of the hydrogen sulfite involves an equilibrium between the hydrogen sulfite and the metabisulfite forms that results in a mixture of the two, that can be found even in the reagent grade[6].

EXPERIMENTAL

Reagent-grade compounds (Fisher Scientific Company) were used for the decomposition studies. The heat treatments of the samples involved two different procedures.

In the first method, a thermogravimetric system was used. The arrangement included a Cahn RG electrobalance with Fisher TGA accessory and Fisher model 260F furnace, and an F & M model 240M power proportioning temperature programmer[7]. A Cahn time derivative computer was coupled with a Honeywell 1-mV strip recorder for a sensitive check on the changes in the weight tracing recorded by the electrobalance. In the latter recording, the weight of sample was plotted against sample (tube) temperature by a Moseley Autograf model 7001 AM, X–Y recorder.

In preparation for the heating cycle, a 3–4 mg sample was placed in a platinum stirrup pan that was suspended within a "hangdown" quartz tube surrounded by the furnace heating element. A concentric quartz flow tube was arranged within the hangdown tube in a manner that would allow a controlled flow of gas to sweep over the sample and into an exhaust port. In every case, the gas (air, nitrogen or helium) was supplied from a cylinder through Teflon tubing at a flow rate of 0.1 l min^{-1}. The heating rates were 1°, 5°, or 10° min^{-1}. The sample container was a hemisphere-shaped platinum dish with a capacity of *ca.* 0.05 cm^3. The tip of a Fisher platinel thermocouple was adjusted to stay within 1 mm of the bottom of the sample container during the thermal treatment; it was this TC arrangement that was used to measure the temperature recorded on the abscissa scale of the X–Y plot. The ordinate was used to record the sample weight changes.

One of the arrangements of the Fisher TGA accessory permits a corrosive gas to be picked up by the sweep gas and to be passed over the sample without backflow into the balance chamber. In some of the runs, this arrangement was used to put sulfur dioxide (10% in N_2) in contact with a sample in order to check for a possible specific reaction during the heating process.

In several runs, the effluent gas from the TGA compartment was led into an absorption tube to entrap evolved gases for determination. In one procedure, sulfur dioxide produced during the heating process was absorbed in hydrogen peroxide solution and titrated with standard alkali[8]. The pressure of the sweep gas (helium) helped push the gas through the absorption system.

In the second method of heat treatment, macroquantities of sulfite were handled. Usually, 5- and 10-g samples were weighed on a Mettler-type H-15 balance and transferred to porcelain evaporating dishes. The sample dishes were then positioned in the middle of a Thermolyne-type 1500 furnace with stepless heat input control, and kept there for a measured period of time (2–8 h). The temperature was adjusted to a level estimated to bring about a reaction that would result in a definite weight change in the sample. The furnace atmosphere was ambient air, subject to changes effected by evolved gas(es); and affected by diffusion and convection processes permitted by leaks around the furnace door and by the open annular space at the back of the furnace through which the termocouple projected. At the end of the heat treatment, the container of sample was removed into the room environment and allowed to cool to near ambient temperature before being weighed. The samples were analyzed for sulfites by iodimetry[9] and for sulfates by nephelometric measurement of the barium salt[10] with a Turner model 110 fluorometer.

RESULTS

A study of the thermogravimetric record for sodium metabisulfite in air (50° min^{-1}) (Fig. 1, curve A) showed the metabisulfite sample starting to lose weight from

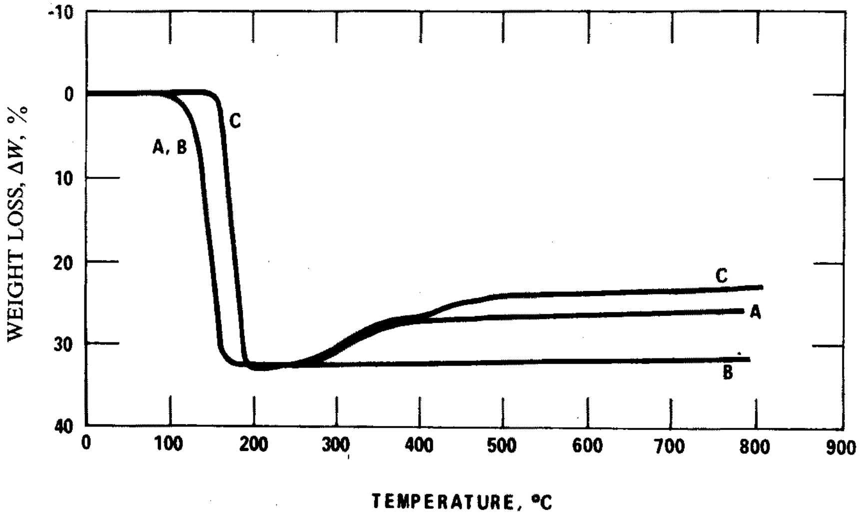

Fig. 1. TGA trace of sodium metabisulfite, $Na_2S_2O_5$.

gas evolution at 85–90°. The decrease was completed at 180°. The same loss was observed (Fig. 1, curve B) when inert atmospheres of helium and of nitrogen were maintained in the sample environment. A similar result also occurred in a reduced pressure atmosphere ($<$ 5 mm Hg). In that case, the weight loss began at a slightly lower temperature than in the case of the atmospheric pressure condition (air, helium, nitrogen).

When the effluent sweep gases were analyzed for evolved sulfur dioxide, the amount evolved was found equivalent to 33 % of the original weight of metabisulfite.

A second weight change, an increase, appeared in the air atmosphere, but not in the inert gas or the evacuated environment (Fig. 1, curves A, B); that change started at 255° and terminated at 415°.

When sulfur dioxide was added to the volume of air sweeping over the sample (*ca.* 3.5 % SO_2 by volume of the total sweep gas), the weight change gained an increment that was completed at 510° (Fig. 1, curve C). The loss of weight during the earlier decomposition step, seen also in curve A, did not begin until 150° and then proceeded at an accelerated rate to its completion at about 190° (curve C).

The cooling curves, for all practical purposes, backtracked along the straight line portions of the curves for the latter stages of heating and along the extensions of these lines, to room temperature. There were no further weight changes during the cooling process.

Reheating the sample to the same high temperature produced no further weight change; the heat-treated sample was gravimetrically stable over the whole temperature range.

The differential thermal analysis (DTA) of sodium metabisulfite (heating rate

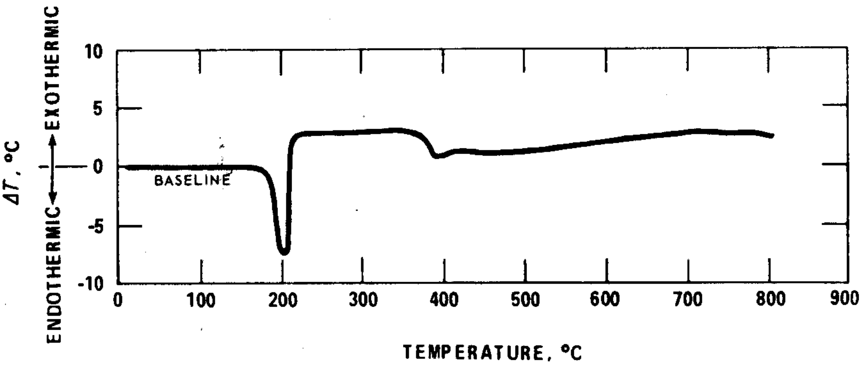

Fig. 2. DTA trace of sodium metabisulfite, $Na_2S_2O_5$.

2° min^{-1}) (Fig. 2) indicated two endothermic peaks. The first was approximately coincident with the initial decrease in sample weight as seen on the TGA record of curve C; the atmosphere around the sample in the DTA run was primarily self-evolved sulfur dioxide. The second peak appeared at the plateau of curve C at about 400°, near the end of the weight increase on the TGA record for the metabisulfite in air.

The TGA trace for sodium hydrogen sulfite sampled from a reagent bottle, so closely resembled the recorded changes for metabisulfite, that the sample was considered to be the same substance.

The results of the studies made on the macroquantities of metabisulfite confirmed the results obtained from the microsamples on the TGA system. Only end-point results were obtained. Thus, the samples heated to no more than 150° showed weight losses nearly quantitative with the release of one SO_2 molecule from each hydrogen sulfite molecule (Table I, sample A). Those samples, like sample C of Table I, treated at 400–450° had a lower net loss of weight. The products of the samples heated at such a temperature level produced a bright yellow surface coating, and the

TABLE I

RESULTS OF HEAT TREATMENTS OF 10-g SAMPLES OF SODIUM METABISULFITE, $Na_2S_2O_5$

Sample	*Heat treatment*	*Weight loss* (%)	*Equivalent* Na_2SO_3[a] *by iodimetric titration* (%)
A	2 h at 150°	33	81
B	2 h at 150°, cooling to 25°, rise (2–3 h) 25–400°.	27	0
C	Rise (2–3 h) 25–400°	31	30
D	2 h at 1000°	25	0

[a] Equivalent Na_2SO_3 values represent the titration values of the samples referred to reagent Na_2SO_3.

odor of hot sulfur. The yellowish hue disappeared a few minutes after the samples were withdrawn from the furnace into the room environment. Quantitative measurements for sulfur content, such as turbidimetry, were not attempted on the cooled product. However, when a 1–2 g portion of sample C was added to about 10 cm^3 of distilled water, a faint opalescence appeared in the solution. Samples heated to 1000° (sample D, Table I) had the smallest net weight loss.

Samples subjected to intermediate temperatures, between sample A and sample D varied between A and D in weight loss and in corresponding values of Na_2SO_3 equivalent.

DISCUSSION

The initial weight change for the heat-treated metabisulfite in air (Fig. 1) must represent the evolution of sulfur dioxide. The recorded loss is quantitatively equivalent to the loss of one molecule of sulfur dioxide from one molecule of the metabisulfite.

$$Na_2S_2O_5 \rightarrow SO_2\uparrow + Na_2SO_3 \qquad (1)$$

Based on molecular composition, the theoretical weight of sulfur dioxide in the pure salt is 33.6%; the TGA recording indicated a 33.0% to 33.5% loss. Gas evolution analysis confirmed the presence of such an amount of evolved sulfur dioxide. The change was recorded on the DTA trace as an endothermic process (Fig. 2).

The second weight change, seen in the TGA trace for metabisulfite sample in an atmosphere of air, was an increase of about 5.5%. There was no weight increase in the inert gas environment. A simple oxidation of the sulfite from reaction (1) to the sulfate form would require an atom of oxygen.

$$Na_2SO_3 + \tfrac{1}{2}O_2 \rightarrow Na_2SO_4 \qquad (2)$$

However, the additional weight of the combined oxygen would have been registered as an 8.4% rise on the TGA tracing if the samples had been completely converted.

A check of the DTA curve showed that a second peak occurred during the temperature interval coinciding with the weight increase mentioned above. The peak appeared as an endothermic process, indicating a probable second decomposition step. In addition, the yellow surface on the macroquantities of metabisulfite heated in the Thermolyne furnace suggested the presence of elemental sulfur, which would have been a product of a decomposition process.

An alternative reaction could account for the results:

$$Na_2SO_3 + \tfrac{1}{2}O_2 \rightarrow Na_2O_2 + \underset{\displaystyle S + O_2}{\underset{\downarrow}{SO_2}} \rightarrow Na_2SO_4 \qquad (3)$$

The heat of reaction for each of the steps indicated is given in Table II. These values were calculated for a temperature of 255°, the point at which the second weight change began on the TGA trace. Since the effect of temperature on the heats of reaction was estimated to be practically insignificant for the listed equations, it was assumed that the values would change little in the temperature range covering the entire weight increase.

The endothermic steps suggested by eqns. (4) and (5) (Table II) could appear on the DTA trace. The extent of the recorded change would be modified by a simultaneous oxidation reaction of exothermic character.

The extent of the decomposition of sulfur dioxide would affect the complete conversion of the sodium salt into the final sulfate form. In the case of applying sulfur dioxide to the sweep gas contacting the sample, the additional weight increase was enough to represent complete recovery of total sulfate. There was an overall weight increase of about 8.5%, equal to the amount predicted by eqn. (2). The partial pressure of the sulfur dioxide in the atmosphere could have suppressed the reaction of eqn. (4). Also, whatever amount of sodium peroxide might have formed could have reacted with the sulfur dioxide in the atmosphere to form the sulfate.

The results of the TGA study of reagent sodium hydrogen sulfite showed weight changes consistent with the molecular weight of the metabisulfite. There was no distinctive peak for the weight loss suggested by the reaction:

$$2\,NaHSO_3 \rightarrow Na_2S_2O_5 + H_2O \qquad (7)$$

In the sulfur dioxide evolution step in the 90–180° interval, the weight loss was a little less than that obtained in the decomposition of $Na_2S_2O_5$. Sodium bisulfite supplies, however, have been found to be mixtures of the hydrogen sulfite, $NaHSO_3$, and the metabisulfite, $Na_2S_2O_5$. If the initial, decomposition step for $NaHSO_3$ is quantitated according to reactions (7) and (1), and that for $Na_2S_2O_5$ is measured by reaction (1), mixtures of the two compounds would show the weight losses listed in the second column of Table III. Oxidation of the Na_2SO_3 product according to eqn. (2) would yield the sulfate form that would be equated with the percentage weight losses shown in the third column. The weight loss of about 30% found in the first step of decomposition of the $NaHSO_3$ sample was short of the range listed for the mixtures in Table III (column 2). The final value of 26.0% placed the hydrogen sulfite sample close to the level for pure $Na_2S_2O_5$ (0 : 2 ratio), indicated in column 3. The 26.0% weight loss

TABLE II

HEATS OF REACTION FOR PROCESSES POSTULATED IN THE HEAT TREATMENT OF SODIUM METABISULFITE, $Na_2S_2O_5$

Reaction	*Equation no.*	ΔH_{528} *(kcal/mole)*
$Na_2SO_3 + \frac{1}{2}O_2 \rightarrow Na_2O_2 + SO_2$	4	69.0
$SO_2 \rightarrow S + O_2$	5	70.1
$Na_2O_2 + SO_2 \rightarrow Na_2SO_4$	6	−139.3
$Na_2SO_3 + \frac{1}{2}O_2 \rightarrow Na_2SO_4$	2	−70.3

TABLE III

THEORETICAL WEIGHT LOSSES FROM THERMAL DECOMPOSITION OF MIXTURES OF $NaHSO_3$ AND $Na_2S_2O_5$

Molecular ratio $NaHSO_3 : Na_2S_2O_5$	*Weight loss for* 90–180° *interval* (%)	*Final weight loss after oxidation by* O_2 (%)
0:2	33.7	25.3
1:2	35.6	26.6
2:2	36.5	27.4
2:1	37.5	28.5
2:0	39.4	31.8

also appeared on the TGA measurements for pure $Na_2S_2O_5$. It would appear then that the hydrogen sulfite supply was chiefly in the metabisulfite form, $Na_2S_2O_5$.

In the treatments of the macrosamples (Table I), the heating periods and the temperature levels apparently allowed gas diffusion rates to control the final resulting composition leading to the sulfate form. For example, sample B, Table I, appeared to lose one equivalent weight of sulfur dioxide during the first heating step at 150°; a weight loss of 33 % was recorded. With the additional step to the higher temperature of 400°, it appeared, according to the iodimetric titration, to be completely converted to a non-sulfite form. The net weight loss, 27.0 %, indicated incomplete sulfate conversion, since the stoichiometric conversion value is 25.0 %. Nephelometric analysis confirmed an intermediate stage of conversion. The packing density and the porosity of the bulk sample probably influenced the overall decomposition effects by creating dissimilar atmospheres around the particles within the sample bulk and over the top surface. The bulk particles had an essentially pure sulfur dioxide atmosphere during the decomposition step, whereas the surface particles had much more of an air atmosphere. As a result, the sample may have undergone completely different reactions above and below the surface. Some idea of the possible variations in reactions is indicated by the differences between curve A and curve C (Fig. 1). In curve C, with the partial pressure of sulfur dioxide in the sweep gas, decomposition was delayed and oxidation was more complete than in curves A and B.

These results of product composition analysis agreed with those for the TGA samples previously described.

SUMMARY

Thermal decomposition of sodium metabisulfite in air involves two major weight changes before the final formation of sodium sulfate. The first is an endothermic process, in which sulfur dioxide is evolved, leaving a residue of sodium sulfite. The second change leads to the formation of sodium sulfate by oxidation of the sulfite. There are, however, intermediate decomposition reactions, occurring at the second change, which lead to the formation of elemental sulfur and to incomplete recovery of the original sulfur in the final sulfate product.

RÉSUMÉ

La décomposition thermique du métabisulfite de sodium à l'air comprend deux changements de poids principaux avant la formation finale de sulfate de sodium. Le premier est un processus endothermique, avec départ de dioxyde de soufre, et résidue de sulfite de sodium. Le deuxième changement conduit à la formation de sulfate de sodium par oxydation du sulfite. Il y a cependant des réactions de décomposition intermédiaires se produisant au deuxième stade, et conduisant à la formation de soufre élémentaire et à une perte en soufre dans le sulfate final obtenu.

ZUSAMMENFASSUNG

Bei der thermischen Zersetzung von Natriummetabisulfit in Luft werden zwei grössere Gewichtsänderungen vor der Bildung von Natriumsulfat als Endprodukt

beobachtet. Die erste ist ein endothermer Prozess, bei welchem Schwefeldioxid freigesetzt wird und Natriumsulfit zurückbleibt. Bei der zweiten Gewichtsänderung bildet sich Natriumsulfat durch Oxidation des Sulfits. Es treten jedoch bei der zweiten Gewichtsänderung intermediäre Zersetzungsreaktionen auf, durch die elementarer Schwefel entsteht und der ursprüngliche Schwefel nur unvollständig in das Endprodukt Sulfat übergeht.

REFERENCES

1 L. Erdey, J. Simon, S. Gal and G. Liptay, *Talanta*, 13 (1966) 67.
2 H. P. Cleghorn and M. B. Davies, *J. Chem. Soc.*, A (1970) 137.
3 F. A. Cotton and G. Wilkinson, *Advanced Inorganic Chemistry*, Interscience, New York, 1962.
4 *Technical Bulletin T-102*, Mettler Instrument Corp., Princeton, N.J.
5 P. Stecher (Editor), *The Merck Index*, 8th Edn., Merck and Company, Rahway, N.J., 1968.
6 *Reagent Chemicals*, American Chemical Society Specifications, 4th Edn., 1968.
7 *Bulletin 10-560-100*, Fisher Scientific Company, Pittsburgh, Pa., 1962.
8 S. Hochheiser, *Methods of Measuring and Monitoring Sulfur Dioxide*, Public Health Service publication No. 999-AP-6, Cincinnati, Ohio, 1964, p. 9.
9 W. C. Pierce and E. L. Haenisch, *Quantitative Analysis*, John Wiley, New York, 1937.
10 H. J. Kelly and L. B. Rodgers, *Anal. Chem.*, 27 (1955) 759.

Analytica Chimica Acta
Elsevier Publishing Company, Amsterdam
Printed in The Netherlands

DETERMINATION OF DIISOPROPYL PHOSPHITE IN SEBACATE-BASE LUBRICANTS

DETERMINATION OF PHOSPHORUS IN DIISOPROPYL PHOSPHITE

GEORGE NORWITZ, MICHAEL GALAN AND MARTIN E. EVERETT
Frankford Arsenal, Philadelphia, Pa. 19137 (U.S.A.)

(Received 14th April 1971)

Sebacate-base lubricants are becoming increasingly important because of their usefulness over extremes of high and low temperatures. In addition to di-(2-ethylhexyl) sebacate, these lubricants frequently contain diisopropyl phosphite $(CH_3H_7O)_2OPH$ (extreme pressure additive), lithium stearate (thickener), barium petroleum sulfonate (detergent and rust inhibitor), and a phenolic or amine compound (antioxidant). A typical sebacate-base lubricant (containing $1.0 \pm 0.2\%$ diisopropyl phosphite) is described in MIL-L-46000B[1].

An urgent need has arisen for accurate methods for the determination of diisopropyl phosphite in sebacate-base lubricants (the government specifications for these lubricants do not give analytical methods). Also there was urgent need for an analytical method for the determination of phosphorus in diisopropyl phosphite used in the manufacture of the lubricants.

It was not found feasible to determine the diisopropyl phosphite as such in the lubricant, so attention was concentrated on methods based on the phosphorus content of the lubricant.

Many methods have been proposed for the determination of phosphorus in petroleum-base lubricants and organic materials; however, these methods are not entirely satisfactory when applied to the determination of phosphorus in sebacate-base lubricants.

ASTM[2] describes gravimetric and spectrophotometric methods for the determination of phosphorus in lubricating oil and lubricating oil additives. In these methods the organic matter is destroyed and the phosphorus is converted to phosphate ion by treatment with sulfuric acid, nitric acid, and hydrogen peroxide in a Kjeldahl flask; the hydrogen peroxide is then decomposed by evaporation to fumes of sulfuric acid. In the gravimetric method the phosphate is determined by precipitation as magnesium ammonium phosphate; if interferences are present, the phosphorus is first precipitated as ammonium molybdophosphate and then as magnesium ammonium phosphate. In the spectrophotometric method, the vanadomolybdophosphate color, developed in a sulfuric acid solution, is used. These ASTM methods give excellent results for the ordinary petroleum-base lubricants. However, they gave low and erratic results for sebacate-base lubricants. Possibly, the reason for these low results is that the prolonged fuming with sulfuric acid required to destroy the sebacate causes volatilization of phosphorus. Also, the presence of the barium and lithium salts can cause loss of phosphorus because of sintering of phosphorus to the glass. ASTM[2] specifically mentions that lubricants containing barium or lead salts can give low results because of this sintering effect.

DETERMINATION OF DIISOPROPYL PHOSPHITE IN SEBACATE-BASE LUBRICANTS

Titrimetric method

Reagents. Ammonium molybdate solution. Prepare Solution No. 1 by transferring 100 g of molybdic acid (85% MoO_3) to a 600-ml beaker containing 240 ml of water. Mix and add 140 ml of ammonia solution (0.88) while stirring vigorously. When dissolution is complete, filter through a Whatman No. 40 filter paper, add 60 ml of nitric acid, and cool. Prepare Solution No. 2 by adding 400 ml of nitric acid to 960 ml of water in a 2-l beaker and cooling. Add Solution No. 1 to Solution No. 2 while stirring constantly. Add 0.1 g of diammonium hydrogen phosphate and let stand at least 24 h. Filter through a Whatman No. 40 filter paper before using. This solution must be prepared fresh every 2 weeks.

Standard sodium hydroxide solution (0.15 M). Standardize against potassium acid phthalate.

Standard nitric acid (0.15 M)

Procedure. Mix the lubricant thoroughly and transfer *ca.* 1 g (accurately weighed) to a 250-ml beaker with a spoon or a thief. Add 25 ml of concentrated nitric acid and 10 ml of perchloric acid (72%), cover with a watch glass, and evaporate to strong fumes of perchloric acid. Add nitric acid dropwise to the fuming solution until the solution is colorless. The final volume of the perchloric acid should be about 5 ml (as judged by comparison with 5 ml of water contained in a 250-ml beaker). If necessary, add more perchloric acid or boil off perchloric acid to attain this volume. Remove the beaker from the hot plate, add 25 ml of water, and swirl. If the solution is not clear, filter through a Whatman No. 40 paper and wash with water.

Transfer the solution to a 300-ml Erlenmeyer flask. Dilute to about 55 ml with water and add 5 ml of concentrated nitric acid. Add 150 ml of ammonium molybdate reagent at one stroke and swirl immediately. Insert a tight-fitting rubber stopper and immediately shake for 30 sec. Allow to stand for 2–2.5 h (no longer) with occasional shaking.

Filter through a Whatman No. 42 filter paper. Transfer the precipitate and wash the flask thoroughly with 1% potassium nitrate solution. Wash the filter paper and precipitate thoroughly 12 times with 1% potassium nitrate solution. Place paper and precipitate back into the original flask and add 20.00 ml of standard 0.15 M sodium hydroxide solution with a pipet around the sides of the flask. Stopper the flask and swirl until the precipitate has dissolved. Wash down the stopper and sides of the flask and dilute to about 100 ml with CO_2-free water. Add 2 drops of phenolphthalein indicator solution (1%) and titrate with 0.15 M nitric acid to the disappearance of the pink color. Ascertain the ml of sodium hydroxide solution equivalent to 1 ml of nitric acid by pipetting 20.00 ml of the standard 0.15 M sodium hydroxide solution into a flask, diluting to about 100 ml, and titrating with the nitric acid.

Calculate as follows:

$$\% \text{ diisopropyl phosphite} = \frac{(A-BC)M \cdot 0.007295}{W} \cdot 100$$

where A = ml of sodium hydroxide solution added to sample, B = ml of nitric acid required to titrate sample, C = ml of sodium hydroxide solution equivalent to 1 ml of nitric acid, M = molarity of sodium hydroxide solution, W = g of sample, and $0.007295 = 0.001360 \cdot 5.364$.

Gravimetric method

Precipitate the phosphorus as described above. Filter the precipitated ammonium molybdophosphate through a tared sintered glass crucible of fine porosity, transfer, and wash 10 times with 1% nitric acid solution. Dry at 120° for 90 min, cool in a desiccator, and weigh.

Calculate as follows:

$$\% \text{ diisopropyl phosphite} = \frac{0.08926P}{W} \cdot 100$$

where P = g of precipitate, W = g of sample, and $0.08926 = 0.01664 \cdot 5.364$.

Spectrophotometric method

Reagents. Standard phosphorus solution (1 *ml* = 0.40 *mg P*). Dry potassium dihydrogen phosphate for 1 h at 105°, cool in a desiccator, dissolve 1.7575 g in water, and dilute to 1 l in a volumetric flask.

Ammonium vanadate solution (0.25%). Dissolve 2.5 g of ammonium vanadate (NH_4VO_3) in about 500 ml of hot water, cool, and dilute to 1 l.

Ammonium molybdate solution (5%). Dissolve 50 g of ammonium molybdate ($(NH_4)_6Mo_7O_{24} \cdot 4H_2O$) in hot water, cool, and dilute to 1 l. Filter before using.

Preparation of calibration curve. Transfer 2.0, 3.0, 4.0, 5.0, 6.0, 7.0, 8.0, 9.0, and 10.0 ml of standard phosphorus solution, measured with a semimicro buret, to 250-ml beakers. Carry along a reagent blank. Add 8 ml of perchloric acid (72%), evaporate to fumes of perchloric acid, and fume for about 1 min. Cool and wash into 100-ml volumetric flasks with sufficient water to bring the volume to about 60 ml. Adjust the temperature to $21° \pm 2°$. Add 10.0 ml of ammonium vanadate solution (0.25%) and swirl. Add 15.0 ml of ammonium molybdate solution (5%) and swirl. Dilute to the mark with water and allow to stand for 40 ± 5 min from the time of the addition of the ammonium molybdate solution. Measure the absorbance at 470 nm against the reagent blank. Plot absorbance against mg of phosphorus.

Procedure. Proceed as described in the first paragraph of the titrimetric method but adjust the volume of perchloric acid after the fuming to about 8 ml.

Transfer the solution to a 100-ml volumetric flask, add the ammonium vanadate and ammonium molybdate solutions, and measure the color as described under the preparation of calibration curve. Determine the mg of phosphorus by referring to the calibration curve.

Calculate as follows:

$$\% \text{ diisopropyl phosphite} = \frac{5.364M}{10W}$$

where M = mg of phosphorus found from curve, and W = g of sample.

DETERMINATION OF PHOSPHORUS IN DIISOPROPYL PHOSPHITE

Titrimetric method

Reagents. Same as for the titrimetric determination of diisopropyl phosphite in sebacate-base lubricants except that 0.3 M sodium hydroxide is used.

Procedure. Pipet *ca.* 1 ml of the diisopropyl phosphite (equivalent to about 1 g of sample) into a tared 10-ml beaker. Weigh the beaker plus sample immediately and calculate the exact weight of sample by difference. Wash the sample into a 250-ml beaker with 1–2 ml of water from a wash bottle and then rinse the 10-ml beaker with a total of 25 ml of concentrated nitric acid (added in three portions). Add 1 ml of bromine and allow to stand for 2 h or more. Add 10 ml of perchloric acid (72 %) and warm gently at the edge of the hot plate for 30 min. Evaporate to fumes of perchloric acid at moderate heat and fume for about 5 min. Cool, add about 50 ml of water, cool again, and dilute to 250 ml in a volumetric flask. Pipet a 15-ml aliquot (equivalent to about 0.06 g of sample) into a 300-ml Erlenmeyer flask and add 35 ml of water, 4 ml of perchloric acid (72 %), and 5 ml of concentrated nitric acid. Precipitate the phosphorus and titrate as described in the titrimetric method for diisopropyl phosphite in lubricants except that 40.00 ml of 0.3 M sodium hydroxide is used.

Calculate as follows:

$$\%\ \text{phosphorus} = \frac{(A-BC)M\cdot 0.001360}{W}\cdot 100$$

where the symbols have the same meaning as on p. 386.

Gravimetric method

Precipitate the phosphorus as described in the titrimetric method for phosphorus in diisopropyl phosphite. Filter and dry the precipitate as described in the gravimetric method for diisopropyl phosphite in sebacate-base lubricants.

Calculate as follows:

$$\%\ \text{phosphorus} = \frac{0.01664P}{W}\cdot 100$$

where the symbols have the same meaning as on p. 386.

DISCUSSION AND RESULTS

Extensive experimental work established the optimal conditions of acidity, volume, temperature, amount of reagent, and time of standing for the precipitation of the phosphorus for the titrimetric and gravimetric methods. The use of an acidic solution of ammonium molybdate saturated with ammonium molybdophosphate by the addition of ammonium phosphate and filtration[3] was found to be desirable.

The empirical factor (1 ml of 1 M NaOH = 0.001360 g P) established for the titrimetric method by use of standard phosphate solution was significantly different from the theoretical factor (1 ml of 1 M NaOH = 0.001347 g P[4]).

Drying the precipitate at 120° for 90 min for the gravimetric method was found to be optimal. The empirical factor for the $(NH_4)_3PO_4\cdot 12MoO_3$ precipitate (0.01664) obtained by use of standard phosphate solution was significantly different from the theoretical factor (0.01651).

Potassium dihydrogen phosphate is a satisfactory primary standard for phosphorus in establishing the empirical factors. Analysis of this chemical for phosphorus by precipitation as magnesium ammonium phosphate and ignition to the pyrophosphate, with a 0.25-g sample, gave practically theoretical results (the theoretical phosphorus content is 22.76%). It was not necessary to recrystallize the potassium dihydrogen phosphate; however, it should be dried at 105° for 1 h.

The acidity of the perchloric acid solution used in the development of the color in the spectrophotometric method was about 1.6 *M*. According to the work of previous investigators[5-8] who used perchloric acid medium for the vanadomolybdophosphate color, the acidity is not critical.

It is recommended that the calibration curve for the vanadomolybdophosphate color be prepared by fuming aliquots of the standard phosphate solution with perchloric acid as in the method. The calibration curve so prepared had a slightly different slope from a calibration curve prepared from solutions that were not fumed.

As judged by the use of nitric–perchloric acid medium for the determination of diisopropyl phosphite in lubricants, it would seem that the use of a mixture of nitric and perchloric acids for the determination of phosphorus in diisopropyl phosphite would offer no problems. However, this did not prove to be the case, since low and erratic results were obtained. The method is successful for the determination of the diisopropyl phosphite in the lubricants possibly because of the presence of the high boiling sebacate or possibly because of the catalytic effect of other components of the lubricant. It was found that good results were obtained for phosphorus in diisopropyl phosphite titrimetrically and gravimetrically if the sample were digested with nitric acid and bromine and then evaporated to fumes of perchloric acid. It is believed that this method was successful because the bromine prevents reduction of the diisopropyl phosphite to volatile compounds of phosphorus (such as phosphine).

Some work was carried out on the application of the spectrophotometric method to the determination of the phosphorus in diisopropyl phosphite. However, the accuracy was not adequate for assay purposes.

TABLE I

RESULTS FOR DIISOPROPYL PHOSPHITE IN SEBACATE-BASE LUBRICANTS

Sample	*Diisopropyl phosphite (%)*			*Sample*	*Diisopropyl phosphite (%)*		
	Titrimetric	*Gravimetric*	*Spectrophotometric*		*Titrimetric*	*Gravimetric*	*Spectrophotometric*
1	0.95	0.97	0.89	6	0.91	0.91	0.86
	0.91	0.98	0.90		0.89	0.91	0.90
2*	2.75	2.87	2.91	7	2.63	2.49	2.52
	2.71	2.79	2.86		2.68	2.54	2.53
3**	1.39	1.33	1.48	8**	1.16	1.20	1.12
	1.39	1.39	1.49		1.10	1.21	1.20
4	1.64	1.49	1.55	9*	2.77	2.88	2.86
	1.59	1.50	1.57		2.79	2.90	2.83
5	0.85	0.85	0.95	10*	3.19	3.19	3.24
	0.84	0.89	0.98		3.29	3.25	3.20

The results obtained for the titrimetric, gravimetric, and spectrophotometric methods for diisopropyl phosphite in ten samples of sebacate-base lubricants are shown in Table I. The samples were from seven manufacturers (samples 2*, 9*, and 10* were different lots from the same company several months apart; samples 3** and 8** were different lots from a second company several months apart). It is seen that the three methods check each other reasonably well and that the precision of all three methods is satisfactory.

As was specified in the method, the theoretical factor was used for converting phosphorus to diisopropyl phosphite. As will be pointed out later, the phosphorus content of commercial diisopropyl phosphite may differ somewhat from the theoretical phosphorus content (18.64 %). However, the difference is not sufficient to cause a significant error insofar as the determination of the diisopropyl phosphite in the lubricant is concerned. Also, it would not always be feasible to determine the phosphorus content of the diisopropyl phosphite used in making a specific batch of lubricant, even if the intent were to calculate an empirical factor for converting phosphorus to diisopropyl phosphite.

As a further check on the validity of the perchloric acid attack, three synthetic sebacate-base lubricants containing 0.00 %, 1.03 %, and 2.98 % diisopropyl phosphite were prepared and the samples analyzed by the titrimetric procedure. Recoveries of 0.00 %, 1.07 %, and 2.98 % were obtained.

TABLE II

RESULTS FOR PHOSPHORUS IN DIISOPROPYL PHOSPHITE

Sample	*Phosphorus* (%)			
	Titrimetric	*Av.*	*Gravimetric*	*Av.*
A	18.67		18.62	
	18.56	18.62	18.61	18.62
B	17.73		17.62	
	17.58	17.66	17.66	17.64
C	18.52		18.54	
	18.55	18.54	18.57	18.56
D	16.91		16.81	
	16.67	16.79	16.74	16.78
E	18.07		18.23	
	18.16	18.12	18.16	18.20
F	18.36		18.58	
	18.44	18.40	18.42	18.50
G	17.92		18.06	
	17.94	17.93	18.03	18.05
H	18.41		18.60	
	18.50	18.46	18.50	18.55

The results obtained for phosphorus in eight samples of diisopropyl phosphite from eight different vendors and users (not necessarily manufacturers) by the titrimetric and gravimetric methods are shown in Table II. It is seen that the two methods check each other reasonably well and that the precision of the two methods is satisfactory. The phosphorus content of the samples ranged from a low of 16.67 % to a high of 18.67% (equivalent to 89.44% and 100.16% diisopropyl phosphite, respectively).

The authors are indebted to Joseph F. Messina for furnishing the samples and giving advise, and to Samuel Sitelman for his suggestions. This work was conducted under an Army Materials Testing Technology Project (AMS Code 4931.OM.6350).

SUMMARY

Methods are proposed for the determination of diisopropyl phosphite in sebacate-base lubricants titrimetrically, gravimetrically, and spectrophotometrically. Organic matter is destroyed by treating with nitric and perchloric acids. In the titrimetric and gravimetric methods, ammonium molybdophosphate is precipitated, and empirical factors established by carrying potassium dihydrogen phosphate through the procedures are used. In the spectrophotometric method, the vanadomolybdophosphate color developed in a perchloric acid medium is used. All three methods yield results in reasonable agreement. Phosphorus in diisopropyl phosphite is determined by treating the sample with a mixture of bromine and nitric acid, evaporating to fumes of perchloric acid, and determining the phosphorus titrimetrically or gravimetrically.

RÉSUMÉ

Des méthodes titrimétriques, gravimétriques et spectrophotométriques sont proposées pour le dosage du diisopropylphosphite dans des lubrifiants à base sébaçate La substance organique est détruite par traitement au mélange acide nitrique–acide perchlorique. Les dosages titrimétriques et gravimétriques sont basés sur la précipitation du molybdophosphate d'ammonium. La méthode spectrophotométrique utilise la coloration du vanadomolybdophosphate, en milieu acide perchlorique. Le phosphore du diisopropylphosphite est dosé par traitement de l'échantillon par un mélange brome–acide nitrique, évaporation aux fumées d'acide perchlorique et dosage titrimétrique ou gravimétrique du phosphore.

ZUSAMMENFASSUNG

Es werden titrimetrische, gravimetrische und spektrophotometrische Methoden für die Bestimmung von Diisopropylphosphit in Schmierstoffen auf Sebacatbasis vorgeschlagen. Die organische Substanz wird durch Behandlung mit Salpeter- und Perchlorsäure zerstört. Bei der titrimetrischen und gravimetrischen Methode wird Ammoniummolybdatophosphat gefällt, wobei empirische Faktoren benutzt werden, die durch Anwendung des Verfahrens auf Kaliumdihydrogenphosphat ermittelt worden sind. Bei der spektrophotometrischen Methode wird die in perchlorsaurem Medium erhaltene Vanadatomolybdatophosphat-Färbung zur Bestimmung ausgenutzt. Die Ergebnisse aller drei Methoden stimmen recht gut überein. Phosphor in Diisopropylphosphit wird titrimetrisch oder gravimetrisch bestimmt, nachdem die Probe mit einem Gemisch von Brom und Salpetersäure behandelt und bis zum Rauchen der Perchlorsäure eingedampft worden ist.

REFERENCES

1 *Military Specification, Lubricating Oil, Semi-Fluid (Automatic Weapons), MIL-L-46000B,* March 1970.
2 American Soc. for Testing and Materials, *Standard Methods of Test for Phosphorus in Lubricating Oil and Additives*, ASTM Designation D1091-64 (Reapproved 1968), Philadelphia, Pa., 1970.
3 American Soc. for Testing and Materials, *1970 Book of ASTM Standards, Part 32, Chemical Analysis of Metals; Sampling and Analysis of Metal Bearing Ores*, Philadelphia, Pa., 1970, p. 325.
4 W. F. HILLEBRAND, G. E. F. LUNDELL, H. A. BRIGHT AND J. I. HOFFMAN, *Applied Inorganic Analysis*, John Wiley, New York, 1953, p. 706, 707.
5 J. A. BRABSON, J. H. KARCHMER AND M. S. KATZ, *Ind. Eng. Chem., Anal. Ed.*, 16 (1944) 553.
6 E. J. CENTER AND H. H. WILLARD, *Ind. Eng. Chem., Anal. Ed.*, 14 (1942) 287.
7 R. A. KOENIG AND C. R. JOHNSON, *Ind. Eng. Chem., Anal. Ed.*, 14 (1942) 155.
8 K. P. QUINLAN AND M. A. DESASA, *Anal. Chem.*, 27 (1955) 1626.

Anal. Chim. Acta, 56 (1971) 385–392

Analytica Chimica Acta
Elsevier Publishing Company, Amsterdam
Printed in The Netherlands

TRACE DETERMINATION OF MERCURY IN GEOLOGICAL MATERIALS BY FLAMELESS ATOMIC ABSORPTION SPECTROSCOPY

SVERRE H. OMANG AND PER E. PAUS
Central Institute for Industrial Research, Oslo 3 (Norway)

(Received 5th May 1971)

In connection with the detection of certain types of ore deposits, special attention has been focussed on mercury. Saukov[1] discovered that many hydrothermal sulphide ore deposits contain abnormal concentrations of mercury, originating from the ease of migration of this metal. Mercury can therefore be used as a pathfinder in searching for undiscovered mineral deposits when extremely sensitive analytical methods are available.

Neutron activation methods are very useful in such work, but require expensive equipment and special safety precautions in the laboratory. Spectrophotometric methods based on dithizone extraction[2,3] have been widely used because of their high sensitivity, despite the strong interferences encountered from other metals. Pyrih and Bisque[4] combined dithizone extraction with direct atomic absorption spectroscopy in the organic layer and achieved a detection limit of 0.05 p.p.m. mercury in the rock samples.

Vaughn and McCarthy[5] developed a method in which the mercury vapour produced by direct heating of the sample was measured by atomic absorption. Deposition of mercury vapour as an amalgam on copper or gold and subsequent release by heat and light absorption measurements in the gas phase have been used by Warren *et al.*[6] and Brandenberger and Bader[7]. Hatch and Ott[8] passed the mercury vapour released from the sample solution directly through a light absorption cell. These authors decomposed the sample by treating the rock with sulphuric acid and hydrogen peroxide in unstoppered flasks, thus only acid-soluble mercury was determined and the possibility of loss by evaporation was not eliminated. This is also true for several other procedures developed for determination of trace mercury.

In this laboratory, satisfactory results have been obtained for traces of mercury in water and sulphuric acid by flameless atomic absorption spectroscopy[9], and a special decomposition bomb for silicate materials, ferro alloys and sulphide materials has been designed[10]. Decomposition procedures for such materials have been described by Langmyhr and Paus[11,12]. The present paper describes the combination of the two techniques into a simple, rapid, reliable and sensitive method for trace determination of mercury in different geological materials.

EXPERIMENTAL

Equipment and reagents

A Perkin-Elmer decomposition bomb, made of aluminium with a Teflon-lined inner vessel of 110 ml volume was used for sample decomposition. A Perkin-Elmer Model 303 atomic absorption spectrophotometer, equipped with an automatic recorded readout accessory and a Hitachi–Perkin-Elmer Recorder Model 159 together with a Perkin-Elmer Intensitron hollow-cathode lamp and a 8.7-cm long square gas cell made of PVC of 4.8 cm^2 cross-section with quartz windows was used for absorption measurements. Small aliquots were taken with Eppendorf Marburg micropipettes. An aeration system identical with the one described by Omang[9] was used. All chemicals were of reagent grade quality.

Mercury solutions

A 5-p.p.m. mercury standard solution was prepared from a 1000-p.p.m. stock solution of mercury(II) chloride; 1 ml of 1 + 1 sulphuric acid and 0.5 ml of aqueous 2% (w/v) potassium permanganate solution were added per 100 ml as preservative. This solution was stable for weeks in a stoppered bottle.

Procedure

Weigh out 200 mg of finely ground sample (< 200 mesh) and transfer it to the teflon vessel in the decomposition bomb. Add 5 ml of hydrofluoric acid (38–40 %) and 0.5 ml of concentrated nitric acid. In the case of sulphide ores and minerals add 2 ml of hydrofluoric acid, 2 ml of hydrochloric acid and 1 ml of nitric acid instead. Seal the bomb tightly, heat to 120° on a hot plate for 5–10 min and then cool to room temperature. To the completely decomposed sample add 50 ml of saturated boric acid to complex excess of fluoride and heat the solution until the precipitate dissolves. For sulphide ores, 20 ml of saturated boric acid is satisfactory. After dilution with distilled water to 100 ml in a volumetric flask, transfer 10-ml aliquots to a wash bottle containing 70 ml of distilled water, 2 ml of 1 + 1 sulphuric acid and 2 ml of 10% (w/v) tin(II) chloride dihydrate solution in 1 *M* hydrochloric acid. This mixture is prestripped for possible mercury contaminant from reagents by passing air through the solution. Shake the sample aliquot and the reduction mixture well for 20 sec, connect the flask to the aeration apparatus and record the absorption peak. When the recorder pen has returned to the base line, *i.e.* after 2 min, add an aliquot, *e.g.* 20 μl of the standard 5-p.p.m. mercury solution, and repeat the aeration step. In this way, the standards and samples are measured in essentially the same volume, a necessary procedure because a higher total volume produces a lower absorption peak. Draw a standard curve after conversion of the percentage peak absorption to absorbance and evaluate the sample content. The sensitivity obtained is about 38% absorption for 100 ng of mercury at scale expansion 3 on the instrument.

For samples with mercury contents unsuited for the recommended aliquots, take other aliquots and adjust the water volume in the flask correspondingly. It is also possible to decompose more than the 200 mg recommended if more hydrofluoric acid is added.

Interfering substances

Lindstedt[13] describes in detail the effect of various different interfering substances on the mercury peak height. Of these, only gold, palladium, platinum and silver are possible constituents of geological material. The influence of these ions was examined in the present mixture of acids and sample components, by adding various known amounts to 5 ml of sulphide ore sample solution. The results in Table I show that there is no need to take interferences from these metals into consideration even in accurate analysis of the usual ores.

TABLE I

INFLUENCE OF VARIOUS INTERFERING ELEMENTS ON THE MERCURY DETERMINATION

Interfering element	*Amount added (µg)*	*Peak height in percent of same peak height without interference*[a]
Au (as $HAuCl_4$)	0.1	100
	1	96
	10	78
Pt (as H_2PtCl_6)	1	97
	50	85
Pd (as $PdCl_2$)	1	92
	50	67
Ag (as $AgNO_3$)	100	100

[a] 10 mg of ASK-Kismalm (sulphide ore) containing 84.5 ng mercury was present in the solution.

The same small effects were also obtained when these ions were added to the sample in the bomb before decomposition.

All interferences found were somewhat less than described by Lindstedt[13]. This probably is due to the smaller volumes, and therefore higher concentrations in solution, used by him, even if the total amounts of mercury and noble metal were about the same. The difference in matrix may be another cause.

Applications

The described method was used in the analysis of different geological materials *e.g.* U.S. Geological Survey reference rock samples W-1 and AGV-1, the Nordic reference sample ASK-Kismalm (sulphide ore from Bleikvassli, Norway) and a Norwegian pyrite (local deposits, Sulitjelma, Norway).

The AGV-1 had a very low mercury content; 400-mg samples were weighed out for analysis and decomposed in 7 ml of hydrofluoric acid and 0.5 ml of nitric acid. Boric acid solution (40 ml) was added and the entire solution was taken for analysis. In this way a 12% signal was produced at scale expansion 10, indicating a limit of determination lower than 0.01 p.p.m. in rocks and minerals. With these instrumental conditions less than 2% blank absorption was registered.

Test for evaporation loss

Mercury is extremely volatile and escapes readily from dilute solutions if the conditions are not strongly oxidizing. In order to examine if the acid decomposition mixture was sufficiently oxidizing and if any mercury escaped after the bomb had been opened, 20 µl of 100-p.p.m. mercury solution was added to the ASK-Kismalm sample before the bomb was closed and heated. A 5-ml aliquot of the final solution thus contained 100 ng of mercury from the added standard and about 85 ng from the sample itself, according to Table II. The determined sum was 187.7 ng, in excellent agreement with the expected result. The same agreement was obtained when

TABLE II

RESULTS OBTAINED ON U.S.G.S. ROCKS AND NORWEGIAN LOCAL DEPOSITS

Sample		*Mercury (p.p.m.)*			
		Proposed method	*Atomic absorption*	*Emission spectroscopy*	*Spectro-photometry*
W-1 diabase	$\bar{X}$[a]	0.26	0.34[14]		0.17; 0.16[8]
	C[b]	3.8			
AGV-1 andesite	$\bar{X}$	0.027	0.015[15]		
	C	—			
ASK-Kismalm sulphide ore	$\bar{X}$	8.45		7[16]	
	C	2.1			
Pyrite local deposits	$\bar{X}$	0.34			
	C	2.9			

[a] $\bar{X}$ = Mean value.
[b] C = Rel. stand. deviation.

5 μl of standard 100-p.p.m. solution was added to the ore sample before decomposition; 108.2 ng was determined in the 5-ml aliquot, corresponding to 25 ng from the standard and 83.2 ng from the sample itself.

Elimination of blank

When very low concentration ranges are used, care must be taken to avoid contamination from reagents and glassware. The described method has considerable advantages in this respect over the usual chemical methods. As mentioned in the procedure, the possible contamination from the reduction mixture can be removed by prestripping it with air. Moreover, the boric acid, the hydrochloric acid and other chemicals not used as oxidants can, if necessary, be purified separately by adding a little tin(II) chloride and bubbling air through the solution. In this way, essentially no blank value was obtained even when only a few nanograms of mercury were measured.

RESULTS AND DISCUSSION

The results shown in Table II are in good agreement with the other values listed. As mentioned earlier, a frequently adopted procedure for mercury determinations is to take only the acid-soluble part of the sample for analysis. When the proposed method thus leads to somewhat higher results for some samples than found by other methods, this is probably due to the complete decomposition of all silicates that occurs under the high pressure in the bomb. The fact that the tightly sealed bomb eliminates any loss due to evaporation during the dissolution step, also promotes higher mercury values. Such loss is always a danger when dilute mercury solutions are treated in open vessels.

The precision and accuracy obtained is very good and a single dissolution and analysis can be accomplished in 20 min or less for easily decomposable materials.

Since a Coleman MAS 50 mercury analysis system was available, the ASK-Kismalm with the highest mercury content was also measured on this instrument.

The values found lay within the interval of the other values listed. However, the sensitivity of the instrument was not high enough to allow analysis of the AGV-1 sample.

The authors are indebted to the Royal Norwegian Council for Scientific and Industrial Research for support of this work.

SUMMARY

A rapid and sensitive method for determination of traces of mercury in geological material is described. The samples are decomposed with hydrofluoric acid and nitric acid in a tightly sealed Teflon-lined aluminium bomb and mercury is reduced to the metal with tin(II) chloride after addition of excess of boric acid. Air is then passed through the solution and mercury vapour is determined by cold-vapour atomic absorption measurements at 253.7 nm. The lower limit of determination for mercury in rocks and minerals is less than 0.01 p.p.m. with the aeration system employed. A single analysis requires 20 min. Data obtained on reference rock samples are presented and chemical interferences examined.

RÉSUMÉ

On décrit une méthode pour le dosage rapide et sensible de traces de mercure dans des substances géologiques. Les échantillons sont décomposés à l'aide d'acide fluorhydrique et d'acide nitrique dans une bombe d'aluminium, scellée au teflon. Le mercure est réduit en métal par le chlorure d'étain(II), après addition d'acide borique en excès. L'air est envoyé à travers la solution; la vapeur de mercure est déterminée par absorption atomique (vapeur froide) à 253.7 nm. La limite pour le dosage du mercure dans les roches et minerais est inférieure à 0.01 p.p.m., avec le système d'aération proposé. Une analyse se fait en 20 min. On examine les interférences chimiques.

ZUSAMMENFASSUNG

Es wird eine schnelle und empfindliche Bestimmungsmethode für Quecksilberspuren in geologischem Material beschrieben. Die Proben werden mit Flusssäure und Salpetersäure in einer dichtverschlossenen, mit Teflon ausgefütterten Aluminiumbombe zersetzt. Das Quecksilber wird mit Zinn(II)-chlorid nach Zugabe eines Überschusses Borsäure zum Metall reduziert. Dann wird Luft durch die Lösung geleitet und der Quecksilberdampf durch Messung der Atomabsorption nach der Kaltdampfmethode bei 253.7 nm bestimmt. Die untere Bestimmungsgrenze für Quecksilber in Gesteinen und Mineralen ist bei dem angewandten System kleiner als 0.01 p.p.m. Eine einzelne Analyse dauert 20 min. Es werden mit Vergleichsgesteinsproben erhaltene Ergebnisse vorgelegt und chemische Störungen untersucht.

REFERENCES

1 A. A. SAUKOV, *Akad. Nauk SSSR, Min. Geochem.*, Ser. No. 17 (1946) 129.

2 H. IRVING, G. ANDREW AND E. J. RISDON, *J. Chem. Soc.*, (1949) 541.
3 M. HINKLE, K. W. LEONG AND F. N. WARD, *U.S. Geol. Surv. Profess. Paper 550-B*, 1966, p. 135.
4 R. Z. PYRIH AND R. E. BISQUE, *Econ. Geol.*, 64 (1969) 825.
5 W. W. VAUGHN AND J. H. MCCARTHY, JR., *U.S. Geol. Surv. Profess. Paper 501-D*, 1964, p. 123.
6 H. V. WARREN, R. E. DELAVAULT AND J. BARAKSO, *Econ. Geol.*, 61 (1966) 1010.
7 H. BRANDENBERGER AND H. BADER, *Helv. Chim. Acta*, 50 (1967) 1409.
8 W. R. HATCH AND W. L. OTT, *Anal. Chem.*, 40 (1968) 2085.
9 S. H. OMANG, *Anal. Chim. Acta*, 53 (1971) 415.
10 P. E. PAUS, *Atomic Absorption Newsletter*, 10 (1971) 44.
11 F. J. LANGMYHR AND P. E. PAUS, *Anal. Chim. Acta*, 43 (1968) 397.
12 F. J. LANGMYHR AND P. E. PAUS, *Anal. Chim. Acta*, 50 (1970) 515.
13 G. LINDSTEDT, *Analyst*, 95 (1970) 264.
14 M. FLEISCHER, *Geochim. Cosmochim. Acta*, 29 (1965) 1263.
15 F. J. FLANAGAN, *Geochim. Cosmochim. Acta*, 33 (1969) 81.
16 G. SUNDKVIST, private communication, 1970.

Anal. Chim. Acta, 56 (1971) 393–398

Analytica Chimica Acta
Elsevier Publishing Company, Amsterdam
Printed in The Netherlands

POLY-(TRIAMINOPHENOLGLYOXAL) AS A CHELATING POLYMER IN THE DETERMINATION OF TRACES OF NICKEL

A. ZLATKIS, W. BRUENING AND E. BAYER

Chemistry Department, University of Houston, Houston, Texas 77004 (U.S.A.)

(Received 12th May 1971)

One of the major objectives in trace analysis is to improve the detection limits of the elements. Although modern instrumentation of analytical methods is constantly being developed there are still many instances in trace metal analysis in which the instrumentation cannot fulfill all demands for detection limits.

Quite often, the problem can be solved by the application of chelating polymers. These polymers are able to perform a preconcentration of the sample very conveniently by a column filtration procedure. Furthermore, the preconcentration of the sample can be simultaneously connected with a trace separation procedure which is based on the metal selectivity of the chelating polymers. This selectivity is due to differences in stability of the complexes formed between metal ion and the chelating polymer and can be varied to a large extent by changing the analytical conditions such as pH value, temperature, and addition of complex forming compounds.

Bayer *et al.*[1-8] have published several papers dealing with the synthesis and application of poly-(triaminophenolglyoxal), but the properties of this chelating polymer for the analysis of nickel have never been extensively investigated. This paper provides basic information concerning nickel chelation and elution properties of poly-(triaminophenolglyoxal), making this chelating polymer accessible to various trace concentration and trace separation problems. Because of its suitability for nickel, atomic absorption spectrophotometry was used as a means of measuring the nickel concentration[9].

EXPERIMENTAL

Column

The preparation of the column and the packing material have been described elsewhere[2]. The only difference was the suspension of 8 g of polymer instead of 4 g.

Apparatus

A Perkin-Elmer Model 303 atomic absorption spectrophotometer equipped with a nickel hollow-cathode lamp and the conventional burner atomizer was used to obtain the experimental data. The following instrumental parameters were used: wavelength 232.0 nm; slit 0.3 mm; source 25 mA; air flow 19 l $\min^{-1}$; acetylene flow 4 l $\min^{-1}$.

Chemicals

A standard stock solution (0.1 mg ml^{-1}) of nickel(II) was made by dissolving nickel chloride hexahydrate (reagent grade) in water. The 0.1% ammonium pyrrolidine dithiocarbamate (APDC) solution was prepared by dissolving the corresponding amount of reagent in water. The extraction solution consists of 1 ml of this APDC solution and 10 ml MIBK. Chromosorb W (acid washed, 45/60 mesh; Supelco, Inc., Bellefonte, Pa.) was used. The chelate polymer was prepared by condensing 2,4,6-triaminophenol with glyoxal by the method of Bayer[4].

Concentration procedure

Basically, the same procedure was used as published previously[2]. The only differences were the following: the pH of the sample was adjusted to 5.0, the sample flow rate was 5 ml min^{-1}, and after the elution and regeneration of the column with 0.1 *M* hydrochloric acid, the pH of the eluent was adjusted to 2–4.

RESULTS AND DISCUSSION

The polymer was coated on an inactive support (Chromosorb W) and then used in the column filtration process. The pH range of quantitative chelation is a function of the nickel concentration and the flow rate. In order to investigate these effects, both parameters were used in their extremes. The quantitative chelation range at pH 6 was found to be 0–100 p.p.b., and, therefore, 10 and 100 p.p.b. nickel were chosen as the two extremes of concentration and 2 and 12 ml min^{-1} (maximal flow rate of the column) as the extremes of flow rate.

Chelation

Figure 1 shows the influence of nickel concentrations and flow rates on the chelation range of pH.

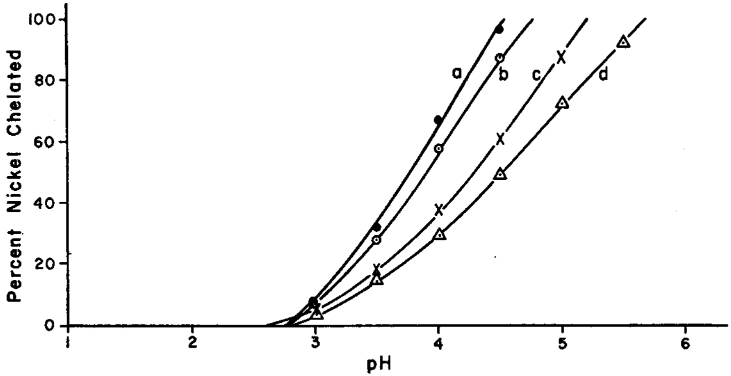

Fig. 1. Effect of pH on chelation. (a) 10 p.p.b. nickel, flow rate 2 ml min^{-1}; (b) 10 p.p.b. nickel, flow rate 12 ml min^{-1}; (c) 100 p.p.b. nickel, flow rate 2 ml min^{-1}; (d) 100 p.p.b. nickel, flow rate 12 ml min^{-1}.

Nickel standard solutions (1 l of each containing 10 and 100 p.p.b.) were adjusted to suitable pH values of the chelation range, with dilute hydrochloric acid and 10 ml of buffer solution of the corresponding pH. These solutions were passed through the columns at flow rates of 2 and 12 ml min^{-1}. The chelated nickel was eluted with 50 ml of 0.1 *M* hydrochloric acid and its concentration measured after extraction into MIBK by atomic absorption spectrophotometry. The concentration values were plotted *vs.* pH and the corresponding curves are shown in Fig. 1. They indicate that the beginning of the chelation is only slightly affected by concentration and flow rate because the origin of all four curves lies within a relatively small range of pH. However, there is a larger effect of concentration on quantitative chelation (at 100%), as indicated by the shift of the curves to higher pH values at increased nickel concentrations. The flow rate has a relatively small effect on quantitative chelation at 10 p.p.b. and a larger effect at 100 p.p.b. The ability of the column to chelate nickel is expected to be larger at 10 p.p.b. than at 100 p.p.b., which is the limit of quantitative chelation.

Elution

Figure 2 shows the influence of nickel concentration and flow rates on the elution range of pH. The columns were saturated with nickel by passing through 1 l of nickel standard solutions (containing 10 and 100 p.p.b., respectively) at pH 6 and a flow rate of 2 ml min^{-1}, thereby providing quantitative chelation. The nickel was then eluted from the column with 50 ml of acidic solutions of different pH values, prepared from dilute hydrochloric acid and the corresponding buffer solution. Flow rates of 2 and 12 ml min^{-1} were used. Atomic absorption spectrophotometry was used to measure the nickel concentration of the eluate and the corresponding curves are given in Fig. 2. The elution and chelation curves bear the same characteristics. The beginning of the elution is only affected by the nickel concentration and not by the flow rate. The completion of the elution is significantly affected by both concentration and flow rate. In contrast to the chelation curves, there is a shift to lower pH values. Only 50 ml of acid solution was used to elute the nickel in these experiments. Therefore, by increasing this volume the elution range of curve b and d (high flow rate) could probably be reduced.

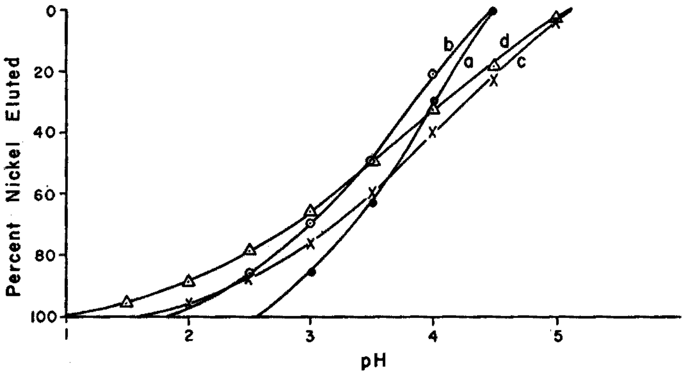

Fig. 2. Effect of pH on elution. (a, b, c, d) Concentrations and flow rates as in Fig. 1.

Conclusions concerning chelation and elution

An examination of Figs. 1 and 2 indicates that the column material for nickel is better analytically for the lower concentration range (0–10 p.p.b.), because the pH range of quantitative chelation and the effect of flow rate is smallest here (only about

2 pH units). The corresponding quantitative elution can be performed with 50 ml of 0.1 *M* hydrochloric acid even at a flow rate of 12 ml min^{-1} (Fig. 2, curve b).

Applications

The method was applied to the determination of nickel in distilled and sea waters. The poly-(triaminophenolglyoxal) column was used in both cases as a means of trace concentration, making atomic absorption accessible for measuring the nickel concentration. Since sea water contains numerous metals other than nickel, the column was also functioning as a means of trace separation.

The analysis of distilled water in this laboratory resulted in a value of 3.2 p.p.b. nickel. Consequently, all distilled water used for column washing and the preparation of standard solutions and reagents was first passed through the columns in order to cancel out the interferences of its nickel content.

TABLE I

EFFECT OF SALT CONCENTRATION ON QUANTITATIVE CHELATION

% Sea water	*Relative absorbance*
0	0.1024
20	0.0991
40	0.0985
60	0.1007
80	0.1035
100	0.1007

The measurements given in Table I should indicate whether or not the column functions independently of the salt content during the concentration procedure. The nickel content of the sea water was first lowered below the detection limit by passing it at pH 5 through the columns. The same water was then used again for the preparation of new 1-l samples containing different amounts of sea water but constant amounts of ionic material (5 p.p.b.). Their pH value was adjusted to 4 and they were passed with a flow rate of 2 ml min^{-1} through regenerated columns. Table I shows the results which indicate no dependence of quantitative chelation on salt concentration. The relative standard deviation is 1.7%. The nickel content of sea water samples taken at Galveston, Texas, was found to be 3.5 p.p.b.

The method shows suitability for other problems of nickel determination concerned with trace concentration and trace separation, such as in river water, drinking water, and industrial waters which are subject to pollution control. Further, this technique could be used for determination of trace nickel in biological fluids.

Interferences

Copper, cobalt, and uranium are also chelated by the column material. Experiments showed that interferences occur at pH 5 if their concentration is two orders of magnitude larger than that of the nickel. Although this indicates some limitations in trace separation of the column material, it does not actually restrict its analytical usefulness. The metal separation can easily be performed by instrumental methods, *e.g.*, atomic absorption spectrophotometry. However, in order to be able to apply these methods, a preconcentration of the sample may be necessary and this can be done quite conveniently by chelating polymers.

This investigation was supported in part by an endowment from the Robert A. Welch Foundation.

SUMMARY

The chelation and elution properties of poly-(triaminophenolglyoxal) have been studied for the determination of traces of nickel. Column chromatography and atomic absorption spectrophotometry were used to determine the nickel concentration. The analysis can be used for concentrations at the 0–10 p.p.b. level.

RÉSUMÉ

Une étude est effectuée sur les propriétés de chélation et d'élution de poly-(triaminophénolglyoxal) en vue du dosage de traces de nickel. On utilise chromatographie sur colonne et spectrophotométrie par absorption atomique pour l'analyse du nickel (concentrations de l'ordre de 0 à 10 p.p.b.).

ZUSAMMENFASSUNG

Für die Bestimmung von Spurenmengen Nickel wurden die Chelatisierungs- und Elutionseigenschaften von Poly-(triaminophenolglyoxal) untersucht. Die Bestimmung des Nickelgehalts erfolgte durch Säulenchromatographie und Atomabsorptionsspektrophotometrie. Die Methode eignet sich für Konzentrationen im Bereich 0–10 p.p.b.

REFERENCES

1 A. Zlatkis, W. Bruening and E. Bayer, *Anal. Chem.*, 41 (1969) 1692.
2 A. Zlatkis, W. Bruening and E. Bayer, *Anal. Chem.*, 42 (1970) 1201.
3 E. Bayer, *Angew. Chem.*, 69 (1957) 107, 240; 73 (1961) 533; *Chem. Ber.*, 90 (1957) 2325.
4 E. Bayer, *Chem. Ber.*, 90 (1957) 2785.
5 E. Bayer and H. Moellinger, *Angew. Chem.*, 71 (1959) 426.
6 E. Bayer and G. Schenk, *Chem. Ber.*, 93 (1960) 1184.
7 E. Bayer and H. Fiedler, *Angew. Chem.*, 72 (1960) 921.
8 E. Bayer, H. Fiedler, L.-L. Hock, D. Otterbach, G. Schenk and W. Voelter, *Angew. Chem., Intern. Ed.*, 3 (1964) 325.
9 J. E. Allen, *Nature*, 187 (1960) 1110.

Analytica Chimica Acta
Elsevier Publishing Company, Amsterdam
Printed in The Netherlands

ADSORPTION CHARACTERISTICS OF RADIONUCLIDES ON ZIRCONIUM HEXACYANOFERRATE(II)

SHOICHI KAWAMURA, SADAO SHIBATA AND KATSUMI KUROTAKI

Chemistry Division, National Institute of Radiological Sciences, 9-1, 4-Chome, Anagawa, Chiba-shi (Japan)

(Received 29th March 1971)

It has been shown[1-17] that several compounds containing hexacyanoferrate(II) selectively adsorb radionuclides, especially ^{137}Cs, and some, therefore, have been mainly used for selective adsorption of cesium from a mixture of radionuclides. Reactions of zirconyl chloride with hexacyanoferrates(II) of alkali metals have been studied in an aqueous phase[18,19]. Current analytical techniques for radionuclides in concentrated salt solutions include ion exchange, precipitation and solvent extraction, etc., most of which require tedious and time-consuming chemical separation of the radionuclides. Characteristic procedures with inorganic ion exchangers are based on adsorption of the radionuclide, followed by measurement of radioactivity of the adsorbed radionuclide. Otherwise, radionuclides adsorbed on an inorganic ion-exchanger column are suitably eluted, and the radioactivity of the eluant is measured. Recently developed high-resolution lithium-drifted germanium detectors have a high potential for radiochemical determination without chemical separation of the radionuclides.

In a study of the adsorption characteristics of zirconium hexacyanoferrate(II) (abbreviated to FeZr in the following paragraphs), it was found that ^{59}Fe, ^{60}Co, ^{65}Zn, ^{137}Cs and ^{95}Zr in concentrated salt solutions were adsorbed by FeZr and that FeZr was dissolved with 25% EDTA solution on heating for 10 min.

In the present paper, a procedure is described for a rapid and simple determination of ^{59}Fe, ^{60}Co, ^{65}Zn, ^{137}Cs, and ^{95}Zr, including ^{144}Ce, ^{106}Ru, ^{85}Sr in sea water, combined with a Ge(Li) detector after dissolution of the FeZr column on which the radionuclides are adsorbed. The chemical properties of FeZr, the adsorption rates for radionuclides, the pH–titration curves, the ion-exchange behavior and the distribution coefficients in concentrated salt solution are also discussed.

EXPERIMENTAL

Apparatus

Gross γ-ray measurements were made with Fujitsu Limited, well-type γ-ray scintillation counter. γ-Ray spectra were taken with a 20-cm^3 Ge(Li) detector (Ortec) coupled with a Nuclear Data 2200 1024-channel analyzer.

Preparation of zirconium hexacyanoferrate(II)

All reagents used in this study were of analytical grade. FeZr was prepared by mixing 2.25 l of 3 *M* hydrochloric acid containing 386.69 g of zirconyl chloride octahydrate (1.2 mole) and 2.25 l of aqueous solution containing 726.15 g of sodium hexacyanoferrate(II) decahydrate (1.5 mole). Yellow slurries were obtained by adding these solutions dropwise and simultaneously into a beaker for 30 min with stirring. The mixture was allowed to stand for 24 h, filtered, washed thoroughly and dried at 60° for 24 h. The adsorbent was ground, dry-sieved through a 200–300 mesh sieve, kept over saturated ammonium chloride solution and used for batch equilibrium studies. Adsorbent sieved through a 100–200 mesh sieve and kept over saturated ammonium chloride solution, was used for column studies. For the determination of the iron:zirconium ratio in FeZr, iron or zirconium was determined by radiochemical methods. ^{59}Fe-labeled or ^{95}Zr-labeled FeZr was prepared by mixing either zirconyl chloride–3 *M* hydrochloric acid solution with ^{59}Fe-labeled hexacyanoferrate(II) solution, or hexacyanoferrate(II) solution with ^{95}Zr-labeled solution under the conditions described above.

Batch equilibrium studies

Distribution coefficients (ml g^{-1}), K_d, of radionuclides were determined by batch equilibrium studies. The adsorbent (0.1 g) was weighed in a glass-stoppered test tube, to which 5 ml of the desired solution containing a radionuclide were added. After a given period of agitation at $25.0 \pm 0.5°$, the mixture was centrifuged at 8000 *g* for 1 min and the γ-activity in 2 ml of the supernate was counted with a well-type γ-ray scintillation counter.

pH–titration curve

FeZr (0.2 g) was weighed into a glass-stoppered test tube, to which graded amounts of 0.1 *M* sodium hydroxide were added to make a total volume of 20 ml with 0.1 *M* sodium chloride; the mixture was stirred for one day, and the pH was measured (with a Hitachi-Horiba pH meter, M-5).

Ratio of released hydrogen ion to adsorbed cesium

FeZr (1 g) was added to 10 ml of 0.005 *M* cesium chloride or 0.05 *M* cesium chloride containing ^{137}Cs and tritiated water. Another 1 g of FeZr was added to 10 ml of tritiated water and stirred for one day together with the above-mentioned mixture. After adsorption equilibrium had been reached, the supernate was separated by centrifugation, followed by the simultaneous measurement of ^{3}H or ^{137}Cs radioactivity in the supernates with a liquid scintillation counter (Nuclear-Chicago Mark 1). For the radioactivity measurement, "A" channel was set at L-U and "B" channel was set at L-∞ under the condition of power gain "B". Then, the counts per minute at the "A" or "B" channel were converted to ^{3}H or ^{137}Cs radioactivity on the basis of their detection efficiency. The radioactivity from released hydrogen (corresponding to hydrogen ion) was obtained by subtraction from the radioactivity of the total hydrogen in the supernate of the "cesium–tritiated water batch treatment", of that of "the tritiated water batch treatment". The amount of cesium taken up by FeZr was calculated from the ^{137}Cs decrease in the supernate.

Column studies

FeZr (7 g of 100–200 mesh) was slurried with 0.1 *M* hydrochloric acid and poured into a conventional glass column (i.d. 1.5 cm), pulled to a tip and plugged with glass wool. Sea water (1 l with hydrochloric acid added to give 0.1 *M*) spiked with a single or several radionuclides (*ca.* $2 \cdot 10^5$ c.p.m. each) was passed through the column at a flow rate of 1 l per 3 h. FeZr in the column was transferred to a beaker, to which was added 56 ml of 25% EDTA solution (tetrasodium salt), and dissolved by heating for 10 min, then transferred to a glass planchet (diam. 3 cm) to be evaporated to dryness under an infrared lamp for γ-activity measurement.

RESULTS AND DISCUSSION

Chemical properties

The mesh size of FeZr available was suitable for column treatment. FeZr gave a characteristic X-ray pattern. Although FeZr was appreciably soluble in water, it was not easily soluble in concentrated solutions of sodium hydroxide, hydrochloric acid, nitric acid or sulfuric acid; 5 g of FeZr could be dissolved in 40 ml of 25% EDTA solution on heating for 10 min. Such a selective solubilization and adsorbability of radionuclides combined with the Ge(Li) detector made it possible to use FeZr for a rapid and simple determination of some radionuclides. One of the starting materials, zirconyl chloride, used for the present work was dissolved in 3 *M* hydrochloric acid; dissolution in water yielded mechanically unstable FeZr. Since FeZr was difficult to decompose and the subsequent chemical procedure was tedious and time-consuming, the ratio of iron to zirconium was determined radiochemically rather than chemically. Iron (mmole) per g of ^{59}Fe-labeled FeZr was calculated from the specific activity (c.p.m. mmole^{-1}) of ^{59}Fe-labeled sodium hexacyanoferrate(II) solution, and zirconium (mmole) per g of ^{95}Zr-labeled FeZr was calculated from the specific activity (c.p.m. mmole^{-1}) of ^{95}Zr-labeled zirconyl chloride–3 *M* hydrochloric acid solution. Table I shows that the iron (mmole) and zirconium (mmole) content per gram of the labeled FeZr is 2.3 and 2.2, respectively, indicating that the mole ratio of iron to zirconium in FeZr is 1 : 1. The great discrepancy of the mole ratio between the present study and that of Tananaev *et al.*[18,19] probably comes from the difference in experimental conditions; the final concentration of hydrochloric acid in the aqueous phase in the present study was 1.5 *M*, whereas Tananaev's was 3 *M*, and the iron and zirconium were determined after isolation from the aqueous phase in the present work, whereas Tananaev's determinations were in the aqueous phase.

TABLE I

IRON TO ZIRCONIUM RATIO IN ZIRCONIUM HEXACYANOFERRATE(II)

^{9}Fe-labeled zirconium hexacyanoferrate(II) (abb. ^{59}Fe-FeZr) was prepared by mixing ^{59}Fe-labeled $Na_4Fe(CN)_6$ solu-on and $ZrOCl_2$ solution in 1/10 scale of the unlabeled zirconium hexacyanoferrate(II). ^{95}Zr-labeled zirconium hexa-yanoferrate(II) (abb. ^{95}Zr-FeZr) was prepared by mixing ^{95}Zr-labeled $ZrOCl_2$ solution and $Na_4Fe(CN)_6$ solution in /10 scale of the unlabeled zirconium hexacyanoferrate(II))

pecific activity of starting aterials	*Resultant zirconium hexacyanoferrate(II)*		
	Specific activity		*Fe/Zr ratio*
p.m. ^{59}Fe/mmole Fe	c.p.m. ^{59}Fe/g of ^{59}Fe-FeZr	mmole Fe/g of ^{59}Fe-FeZr	
46,238 ± 500	569,979 ± 755	2.31	
p.m. ^{95}Zr/mmole Zr	c.p.m. ^{95}Zr/g of ^{95}Zr-FeZr	mmole Zr/g of ^{95}Zr-FeZr	≃1
,312,145 ± 1,146	2,843,700 ± 1,687	2.17	

Adsorption rates of radionuclide in 0.1 *M hydrochloric acid and sea water*

Carrier-free ^{59}Fe, ^{60}Co, ^{65}Zn, ^{144}Ce, ^{137}Cs or ^{95}Zr were added to 0.1 *M* hydrochloric acid and to sea water (with addition of hydrochloric acid up to 0.1 *M*). Adsorption rates of the radionuclides in 0.1 *M* hydrochloric acid were compared with those in the sea water (Fig. 1). The adsorption rate decreased in the following order: Cs > Zn > Co > Zr > Fe > Ce. In the case of cerium, 3 h were necessary to attain adsorption equilibrium. The low quantity of adsorbed cerium in the FeZr column described later may be caused by the slow adsorption rate.

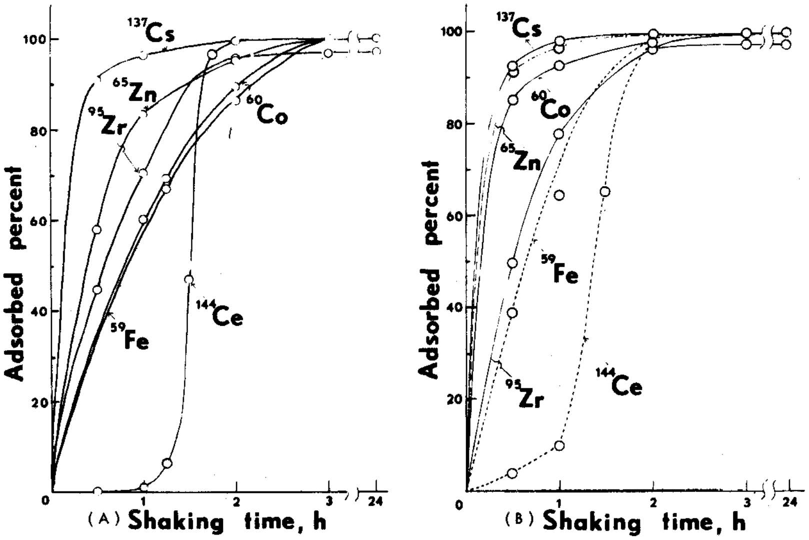

Fig. 1. Adsorption rates of several radionuclides in 0.1 *M* hydrochloric acid (A) and those in sea water adjusted to 0.1 *M* in hydrochloric acid (B).

Sea water comprises various inorganic elements; the concentrations in g l^{-1} are 10.5 sodium, 1.3 magnesium, 0.4 calcium, 0.38 potassium, $1 \cdot 10^{-5}$ aluminum, $1 \cdot 10^{-5}$ iron, $5 \cdot 10^{-7}$ cobalt, $1 \cdot 10^{-5}$ zinc, $4 \cdot 10^{-7}$ cerium, $5 \cdot 10^{-7}$ cesium, $8 \cdot 10^{-3}$ strontium, etc.[20]. The adsorption rates in the sea water were slightly faster than those in 0.1 *M* hydrochloric acid probably because the adsorption rate in sea water is accelerated by the presence of carriers corresponding to the radionuclides or by the coexistence of concentrated salts, the latter effect being more important.

pH–titration curve

In order to characterize the properties of FeZr in solution, the pH values of the aqueous phase in equilibrium with various zirconium-containing adsorbents are plotted in Fig. 2 against the quantities of sodium hydroxide added per g of zirconium-containing adsorbents. No clear-cut end-points of FeZr are distinguishable and the exchangeable hydrogens display a range of acidities. FeZr has the property of a weak cation exchanger. The fact that zirconyl chloride (one of the starting materials of FeZr) was associated with readily hydrolyzable zirconium and hydrogen ions were released through an ion-exchange process makes the pH–titration curve for FeZr fairly similar to those for other zirconium-containing adsorbents. However, no generally acceptable rule covering these adsorbents was found from these pH–titration curves. The pH–titration curve of FeZr was similar to those of zirconium molybdate and zirconium tungstate, somewhat similar to that of zirconium phosphate, but considerably different from that of hydrous zirconium oxide.

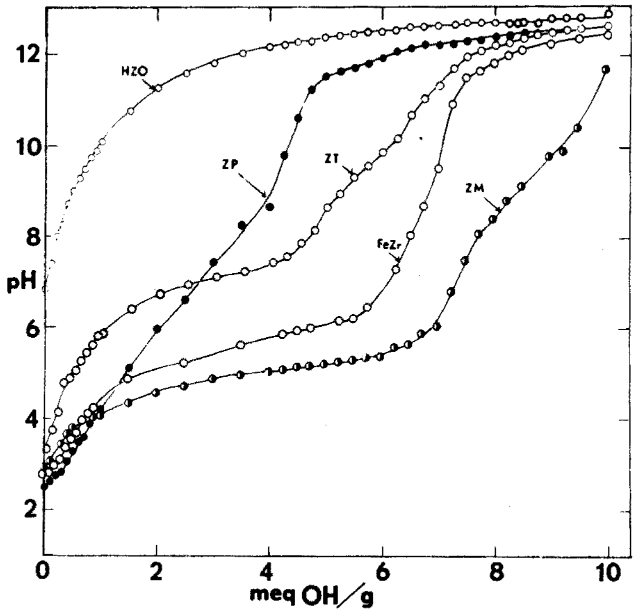

Fig. 2. pH–titration curve of zirconium-containing inorganic ion exchangers. HZO, Bio-Rad HZO-1 50–100 mesh; ZP, Bio-Rad ZP-1 100–200 mesh; ZT, Bio-Rad ZT-1 100–200 mesh; ZM, Bio-Rad ZM-1 100–200 mesh; FeZr, zirconium hexacyanoferrate(II).

Ion-exchange behavior

The adsorption of radionuclides on FeZr may arise from ion exchange, hence the kinds of released ions and the ratio of the amount of released ions to the amount of adsorbed metal ion were determined by batch equilibrium studies. Initially, the possibilities of exchanges of Co–Fe, Zn–Fe, ZrO–Fe and Cs–Fe were determined by mixing 0.1 g of ^{59}Fe-labeled FeZr in 0.1 *M* Co, Zn, ZrO or Cs solutions, and those of Co–Zr, Zn–Zr, ZrO–Zr and Cs–Zr were determined by mixing 0.1 g of ^{95}Zr-labeled FeZr in 0.1 *M* Co, Zn, ZrO or Cs solutions. Table II shows that no radioactivity was found in the external solutions except in the case of 0.1 *M* iron(III) chloride, indicating that no exchange occurred between Fe or Zr in FeZr and the metal ions in the solutions. With 0.1 *M* iron(III) chloride, released radioactivity of ^{59}Fe or ^{95}Zr from FeZr and an intense blue coloration were observed in the external solution, probably because of breakdown within the solid phases. When the pH values of the external solutions in equilibrium with FeZr were determined, they were lower than those of water or 0.1 *M* sodium chloride solution as shown in Table II. Since ^{22}Na-labeled sodium ion was not adsorbed appreciably by FeZr in another batch study, sodium chloride solution was used as the reference solution. From the results described above,

TABLE II

PERCENTAGE RELEASED FROM ZIRCONIUM HEXACYANOFERRATE(II) AND pH OF THE EXTERNAL SOLUTION IN EQUILIBRIUM

(0.1 g of FeZr spiked with either 382,054 ± 610 c.p.m. ^{59}Fe (abb. ^{59}Fe-FeZr) or spiked with 356,713 ± 597 c.p.m. ^{95}Zr (abb. ^{95}Zr-FeZr) was shaken with 5 ml of the external solution. Percentage released = (total radioactivity of ^{59}Fe or ^{95}Zr in the external solution)/(total radioactivity of ^{59}Fe- or ^{95}Zr-FeZr))

External solution	*Percentage released*		*pH in the external solution*
	^{59}Fe-FeZr	*^{95}Zr-FeZr*	
H_2O	$\simeq 0$	$\simeq 0$	2.60
0.1 *M* NaCl	$\simeq 0$	$\simeq 0$	2.62
0.1 *M* $FeCl_3$	14	37	1.67
0.1 *M* $CoCl_2$	$\simeq 0$	$\simeq 0$	2.45
0.1 *M* $ZnCl_2$	$\simeq 0$	$\simeq 0$	2.30
0.1 *M* $ZrOCl_2$	$\simeq 0$	$\simeq 0$	1.15
0.1 *M* CsCl	$\simeq 0$	$\simeq 0$	2.49

TABLE III

RATIO OF HYDROGEN ION RELEASED TO CESIUM ADSORBED

External solution	*H^+ released (mmole)*	*Cs adsorbed (mmole)*	*Exchange ratio H/Cs*
0.005 *M* CsCl	0.039 ± 0.008	0.044 ± 0.010	$\simeq 1$
0.05 *M* CsCl	0.039 ± 0.008	0.216 ± 0.126	0.18

it was concluded that only hydrogen ions were liberated from FeZr during the adsorption process.

Next, with 0.005 *M* cesium chloride, the exchange ratio of hydrogen ion in FeZr to cesium in the external solution was determined (Table III). The amount of released hydrogen from FeZr was nearly equal to the amount of cesium taken up by FeZr. This indicates that 1 : 1 exchange takes place between hydrogen ion in FeZr and cesium in the external solution. On the other hand, with 0.05 *M* cesium chloride, the amount of cesium taken up by FeZr was about five times the amount of released hydrogen. Such a retention of cesium by other means than ion exchange has also been observed in adsorption by zinc hexacyanoferrate(II) analogues[21].

Distribution coefficients in concentrated salt solutions

Table IV shows the variation in K_d values for several radionuclides on addition of concentrated salts to 0.1 *M* hydrochloric acid. K_d values for the radionuclides except those for ^{85}Sr and ^{106}Ru are still high after addition of concentrated salts. The individual K_d values of FeZr are rather high compared to those of nickel[22] or molybdenum hexacyanoferrate(II)[23]. Although the K_d values for cerium on FeZr are considerably higher than those on the nickel or molybdenum analogues, relatively long periods of shaking (4 h) are necessary to attain adsorption equilibrium. The K_d value for ^{95}Zr on FeZr is extremely high compared to the nickel or molybdenum analogues.

TABLE IV

INFLUENCE OF THE ADDITION OF CONCENTRATED SALTS ON THE DISTRIBUTION COEFFICIENTS

(Shaking time, 24 h)

Nuclide	*Distribution coefficient*		
	0.1 *M HCl*	0.1 *M HCl*+ 0.5 *M* NH_4Cl[a]	0.1 *M HCl*+ *sea water*[b]
^{59}Fe	$2.0 \cdot 10^4$	$5.0 \cdot 10^3$	$1.9 \cdot 10^4$
^{60}Co	$1.0 \cdot 10^4$	$5.0 \cdot 10^3$	$9.9 \cdot 10^3$
^{65}Zn	$2.6 \cdot 10^4$	$8.3 \cdot 10^3$	$1.6 \cdot 10^4$
^{85}Sr	3	< 1	< 1
^{95}Zr	$6.5 \cdot 10^4$	$4.4 \cdot 10^4$	$5.4 \cdot 10^4$
^{106}RuNO	5	3	2
^{137}Cs	$1.8 \cdot 10^4$	$5.4 \cdot 10^2$	$1.3 \cdot 10^4$
^{144}Ce	$6.0 \cdot 10^3$	$1.0 \cdot 10^3$	$6.6 \cdot 10^2$

[a] Dissolution of NH_4Cl in 0.1 *M* HCl to make 0.5 *M* solutions.

[b] Addition of HCl to sea water up to a molar concentration of 0.1.

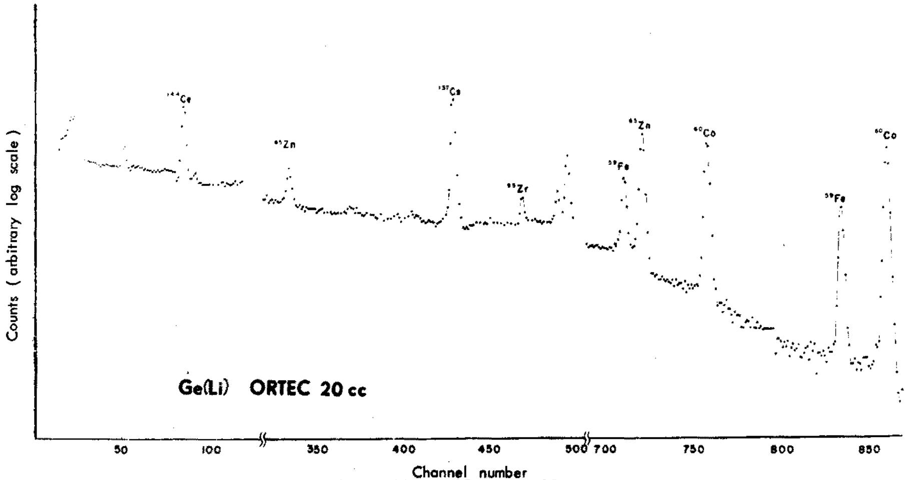

Fig. 3. Ge(Li) spectra of ^{59}Fe, ^{60}Co, ^{65}Zn, ^{144}Ce, ^{137}Cs and ^{95}Zr in zirconium hexacyanoferrate(II) matrix. FeZr (7 g) spiked with the six radionuclides was dissolved with 56 ml of 25% EDTA solution, evaporated to dryness, followed by measurement of the γ-activity.

Simultaneous radiochemical determination in sea water

There are two main advantages in using FeZr for adsorbing radionuclides from sea water. First, a FeZr column not only adsorbs some radionuclides from concentrated salt solution, but these radionuclides can be dissolved in the column by a one-step operation. A variety of mesh sizes of an adsorbent are often required according to experimental demands; it is quite easy to prepare any desired mesh size of FeZr. Secondly, when elution is inapplicable, accurate radioactivity can be measured by batch processes as in the present study, the radioactivity being measured with a Ge(Li) detector; a typical spectrum is shown in Fig. 3.

Before the measurement with the Ge(Li) detector, 1 l of sea water (adjusted to 0.1 *M* in hydrochloric acid) spiked with a single radionuclide was passed through the FeZr column and the percentage adsorbed was measured by a well-type γ-ray scintillation counter. Percentages adsorbed of ^{59}Fe, ^{60}Co, ^{65}Zn, ^{95}Zr or ^{137}Cs were found to be about 95%, and those of ^{85}Sr, ^{106}RuNO, ^{106}Ru or ^{144}Ce were 0.5, 2.0, 1.9, or 1.0, respectively (Table V). When 1 l of sea water (adjusted to 0.1 *M* in hydrochloric acid) containing these radionuclides was passed through the FeZr column, 95.3, 95.1, 95.4, 97.5 and 94.9% recovery was achieved by Ge(Li) detector with ^{59}Fe, ^{60}Co, ^{65}Zn, ^{95}Zr and ^{137}Cs, respectively (Table V). These recoveries are the average values of 3–5 independent determinations; the recoveries of mixed radionuclides showed some scatter owing to errors of measurement with the Ge(Li) detector. However, the simultaneous determination combined with Ge(Li) detector is simple and 6–7 h is adequate for a complete analysis.

TABLE V

PERCENTAGE RECOVERED OF SINGLE OR MIXED RADIONUCLIDES FROM SEA WATER WITH FeZr COLUMN

Nuclide	*Percentage recovered*	
	Single[a]	*Mixture*[b]
^{59}Fe	94.9	95.3
^{60}Co	95.1	95.1
^{65}Zn	95.2	95.4
^{85}Sr	0.5	
^{95}Zr	94.8	97.5
^{106}RuNO	2.0	
^{106}Ru	1.9	
^{137}Cs	95.4	94.9
^{144}Ce	1.0	

[a] Single: 1 l of sea water (0.1 *M* in HCl) spiked with a single radionuclide was passed through the FeZr column (1.5 × 5 cm, 100–200 mesh, 7 g). The radioactivity was determined by a well-type γ-ray scintillation counter.

[b] Mixture: 1 l of the sea water containing the radionuclides described above was passed through the FeZr column. The radioactivity was determined by a Ge(Li) detector.

The authors wish to express their gratitude to Dr. Masami Izawa for his interest and encouragement. We are also indebted to Mr. Yasushi Oami for his cooperation.

SUMMARY

Zirconium hexacyanoferrate(II) (FeZr) was prepared and shown to be a weak cation exchanger; definite mesh sizes are readily made. The mole ratio of iron to zirconium in the FeZr is 1 : 1. Adsorption rates of ^{59}Fe, ^{60}Co, ^{65}Zn, ^{144}Ce, ^{137}Cs and ^{95}Zr in 0.1 *M* hydrochloric acid and sea water were investigated by batch studies. K_d values of these radionuclides in 0.1 *M* hydrochloric acid and in concentrated salt solutions were determined together with those of ^{85}Sr and ^{106}RuNO. Batch studies indicated that only hydrogen ions are liberated in the exchange reaction. A Ge(Li) detector combined with adsorption on a FeZr column was used for a rapid and simple determination of ^{59}Fe, ^{60}Co, ^{65}Zn, ^{137}Cs, and ^{95}Zr in 1 l of sea water, the recoveries of these radionuclides being about 95%.

RÉSUMÉ

On a préparé l'hexacyanoferrate(II) de zirconium; il se comporte comme un échangeur faible de cations. Le rapport moléculaire fer–zirconium est de 1:1. On examine les vitesses d'adsorption de ^{59}Fe, ^{60}Co, ^{65}Zn, ^{144}Ce, ^{137}Cs et ^{95}Zr dans l'acide chlorhydrique 0.1 *M* et dans l'eau de mer. Un détecteur Ge(Li) combiné à la colonne d'adsorption à l'hexacyanoferrate de zirconium permet un dosage simple et rapide de ces radionuclides.

ZUSAMMENFASSUNG

Es wurde Zirkoniumhexacyanoferrat(II) (FeZr) hergestellt, welches ein schwacher Kationenaustauscher ist und leicht in definierten Korngrössen erhalten werden kann. Das Molverhältnis von Eisen zu Zirkonium in FeZr ist 1:1. Die adsorptionsgeschwindigkeiten von ^{59} Fe, ^{60}Co, ^{65}Zn, ^{144}Ce, ^{137}Cs und ^{95}Zr in 0.1 *M* Salzsäure und in Meerwasser wurden untersucht. K_d-Werte dieser Radionuklide in 0.1 *M* Salzsäure und in konzentrierten Salzlösungen wurden zusammen mit jenen von ^{85}Sr und ^{106}RuNO bestimmt. Die satzweise durchgeführten Versuche ergaben, dass bei der Ionenaustauschreaktion nur Wasserstoffionen freigesetzt werden. Ein Ge(Li)-Detektor in Verbindung mit Adsorption auf einer FeZr-Säule ermöglichte die schnelle und einfache Bestimmung von ^{59}Fe, ^{60}Co, ^{65}Zn, ^{137}Cs und ^{95}Zr in 1 l Meerwasser bei einem erfassten Anteil von etwa 95%.

REFERENCES

1 I. V. Tananaev, M. A. Glushkova and G. B. Seifer, *Khim. Redkikh Elementov, Akad. Nauk SSSR*, 1 (1954) 58.
2 I. V. Tananaev and N. V. Bausova, *Khim. Redkikh Elementov, Akad. Nauk SSSR, Inst. Obshch. i Neorgan. Khim.*, 3 (1957) 41.
3 V. Kouřím, J. Rais and B. Million, *J. Inorg. Nucl. Chem.*, 26 (1964) 1111.
4 V. Kouřím, J. Rais and J. Stejskal, *J. Inorg. Nucl. Chem.*, 26 (1964) 1761.
5 J. Krtil, *J. Inorg. Nucl. Chem.*, 27 (1965) 1862; *J. Chromatogr.*, 20 (1965) 384; 21 (1966) 85; *Radiochim. Acta*, 7 (1967) 30.
6 W. E. Prout, E. R. Russell and H. J. Groh, *J. Inorg. Nucl. Chem.*, 27 (1965) 473.
7 K. Watari, *J. At. Energy Soc. Japan*, 12 (1970) 718.
8 V. Kouřím and B. Million, *Collection Czech. Chem. Commun.*, 30 (1965) 2848.
9 A. L. Boni. *Anal. Chem.*, 38 (1966) 89.
10 T. Shigematsu, *Chemistry (Kagaku)*, 21 (1966) 215.
11 S. Kawamura, K. Kurotaki, H. Kuraku and M. Izawa, *J. Chromatogr.*, 26 (1967) 557.
12 V. I. Baranovskii, Y. Viza, G. S. Katykhin and M. K. Nikitin, *Radiokhimiya*, 9 (1967) 698.
13 H. G. Petrow and H. Levine, *Anal. Chem.*, 39 (1967) 360.
14 S. Kawamura, K. Kurotaki and M. Izawa, *Bull. Chem. Soc. Japan*, 42 (1969) 3003.
15 D. Huys and L. H. Baetsle, *J. Inorg. Nucl. Chem.*, 26 (1964) 1329.
16 L. H. Baetslé, D. van Deyck and D. Huys, *J. Inorg. Nucl. Chem.*, 27 (1965) 683; 28 (1966) 2385.
17 L. H. Baetslé, D. van Deyck, D. Huys and A. Guery, *Proc. Intern. Conf. Peaceful Uses At. Energy, 3rd, Geneva, 1964*, Vol. 10, United Nations, 1965, p. 580.
18 I. V. Tananaev and E. A. Ionova, *Zh. Neorgan. Khim.*, 2 (1957) 2468.
19 E. A. Ionova and I. V. Tananaev, *Zh. Neorgan. Khim.*, 7 (1962) 791.
20 G. G. Polikarpov, English translation edited by V. Schultz and A. W. Klement Jr., *Radioecology of Aquatic Organisms*, North-Holland, Amsterdam–Reinhold, New York, 1966.
21 S. Kawamura, H. Kuraku and K. Kurotaki, *Anal. Chim. Acta*, 49 (1970) 317.
22 S. Kawamura, unpublished work.
23 S. Kawamura and K. Kurotaki, *J. Chromatogr.*, 45 (1969) 331.

Analytica Chimica Acta
Elsevier Publishing Company, Amsterdam
Printed in The Netherlands

THE SOLVENT EXTRACTION OF COBALT WITH 6-NITROSO-3-DIMETHYLAMINOPHENOL

SHOJI MOTOMIZU

Department of Chemistry, Faculty of Science, Okayama University, Tsushima, Okayama-shi (Japan)

(Received 17th May 1971)

Nitroso derivatives of phenols and naphthols are widely used as the precipitating, extracting, color-producing and colorimetric reagents for cobalt. In general, such compounds react selectively with cobalt and iron(II) to form the red and the green complexes, respectively. The compounds which have been most widely used are 1-nitroso-2-naphthol, 2-nitroso-1-naphthol, nitroso-R salt, *o*-nitrosophenol, etc.[1].

In a previous paper[2] the coloration of some metal ions with 12 nitroso derivatives was reported. All these compounds react very sensitively with the cobalt ion. Of these compounds, 1-nitroso-2-hydroxy-3-naphthoic acid (nitroso-HNA) and nitroso-R salt were the most sensitive for cobalt. Later, the solvent extraction of cobalt with four nitroso derivatives, *i.e.* 6-nitroso-3-dimethylaminophenol (nitroso-DiMAP), 1-nitroso-2-naphthol, nitroso-HNA, 1-nitroso-2,7-dihydroxynaphthalene was reported[3]. Among these four compounds, nitroso-DiMAP and its cobalt complex were readily extracted into organic solvents of high dielectric constant, such as 1,2-dichloroethane, benzyl alcohol and nitrobenzene. This cobalt complex shows maximal absorption at 456 nm in 1,2-dichloroethane and at this wavelength the molar absorptivity is $6.0 \cdot 10^4$, which is 1.5–2 times larger than the others. Moreover, the extracted complex is not decomposed by hydrochloric acid solution and is stable in the organic phase, whereas the excess of reagent dissolves in the acidic aqueous solution. Thus, nitroso-DiMAP is a very useful reagent for cobalt. However, since Möhlaw reported this compound[4], no detailed investigation has been reported.

In this work, the acid dissociation constants, the formation constant of the cobalt complex, the distribution ratios of the reagent and of the cobalt complex and other relevant properties were studied.

EXPERIMENTAL

Reagents

Nitroso-DiMAP. The reagent was obtained by the nitrosation of *m*-dimethylaminophenol in hydrochloric acid solution with sodium nitrite[4]. The crude nitroso-DiMAP obtained was recrystallized from hydrochloric acid solution. The purified nitroso-DiMAP hydrochloride salt (nitroso-DiMAP·HCl) had yellow needle-like crystals. (Found: C, 47.6; H, 5.7; N, 13.5%. Calcd. for $C_8H_{11}N_2O_2Cl$: C, 47.4; H, 5.5; N, 13.8%.)

Standard cobalt solution. This was prepared from cobalt chloride hexahydrate and was standardized by EDTA titration.

To adjust the pH, hydrochloric acid, acetic acid–sodium acetate buffer, potassium dihydrogenphosphate–disodium hydrogenphosphate buffer, sodium hydrogencarbonate–disodium carbonate buffer, and potassium hydroxide were used.

All the reagents used were of analytical grade.

Apparatus

A Hitachi-Horiba model F-5 pH meter equipped with a combined electrode, 6026-05T, was used for measuring the pH. A Hitachi–Perkin Elmer model 139 spectrophotometer and Hitachi model EPS-3T recording spectrophotometer were used for measuring absorbance in glass cells of 1 mm, 5 mm or 10 mm pathlengths.

Stability of nitroso-DiMAP

It has been said that nitroso-DiMAP is not very stable. However, in the solid state, nitroso-DiMAP·HCl was stable for at least two years. In aqueous solution (*ca.* pH 6), the absorbance of the reagent (10^{-4} *M*) decreased with time, the decrease being about 1.5% during 4 h. Accordingly, the reagent was dissolved in acidic solution.

Nitroso-DiMAP·HCl was dissolved in 0.01 *M* hydrochloric acid solution to give a $5 \cdot 10^{-5}$ *M* solution. The reagent solution (5 ml) was pipetted into a glass-stoppered test tube, and 1 ml of aqueous $5 \cdot 10^{-3}$ *M* cobalt solution and 5 ml of buffer solution (1 *M* KH_2PO_4–0.5 *M* Na_2HPO_4) were added. The test tube was shaken vigorously for 30 sec. After 20 min, 5 ml of 1,2-dichloroethane was added and shaken for 30 sec. Then the organic phase was filtered through dry filter paper and the absorbance was measured at 456 nm in 5-mm glass cells. The absorbances obtained remained almost unchanged for 37 days; absorbances measured after 10 min, 14 days and 37 days were 0.479, 0.482 and 0.478, respectively. Accordingly, acidic solutions of this reagent appear to be stable for at least a month, and in this work, the stock solution of nitroso-DiMAP was prepared by dissolving in hydrochloric acid solution above 0.01 *M*.

The dissociation constants, pK_{a1} and pK_{a2}, of nitroso-DiMAP·HCl

Nitroso-DiMAP·HCl dissociates in aqueous solution as follows:

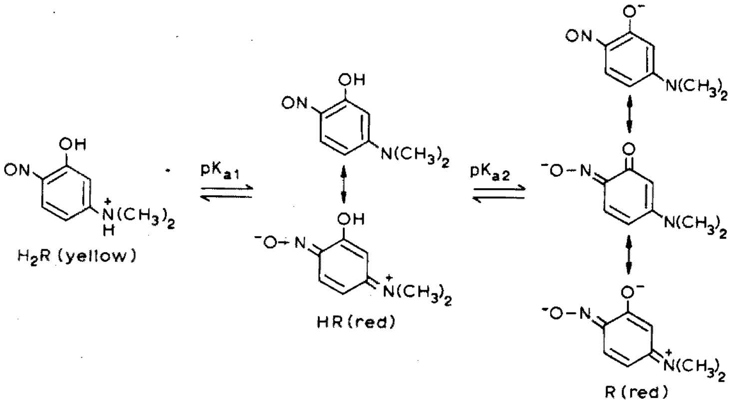

The first dissociation constant, pK_{a1}. The reagent stock solution (5 ml of $1 \cdot 10^{-3}$ *M*) was pipetted into a 25-ml volumetric flask, 1 *M* potassium chloride solution was added to adjust the ionic strength ($\mu = 0.1$) and hydrochloric acid or potassium hydroxide was added to adjust the pH. Then the solution was diluted to the mark with distilled water. The absorbance at 500 nm was measured in a 10-mm glass cell and simultaneously, the pH was measured in another portion of the solution. The absorbance spectra and other results obtained are shown in Figs. 1 and 2. An isosbestic point was found at 419.5 nm.

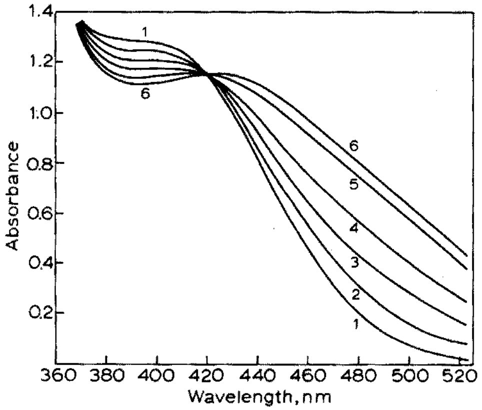

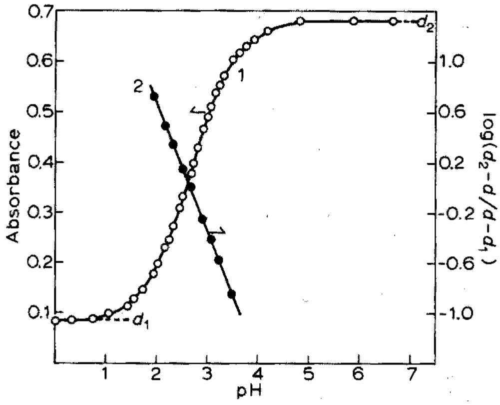

Fig. 1. The absorbance spectra of the reagent in aqueous solution. [Reagent] $2 \cdot 10^{-4}$ *M*. pH; (1) 0.0, (2) 1.97; (3) 2.46; (4) 2.83; (5) 3.65; (6) 5.90.

Fig. 2. The plots of the absorbance *vs.* pH and $\log\{(d_2-d)/(d-d_1)\}$ *vs.* pH at 500 nm in 1-cm cell. $\mu = 0.1$. (1) Absorbance *vs.* pH; (2) $\log\{(d_2-d)/(d-d_1)\}$ *vs.* pH.

The dissociation constant, pK_a, was calculated from eqn. (1).

$$\mathrm{p}K_a = \mathrm{pH} + \log \frac{d_2-d}{d-d_1} \tag{1}$$

or

$$\log \frac{d_2-d}{d-d_1} = \mathrm{p}K_a - \mathrm{pH} \tag{1'}$$

where d_1, d_2 and d are the absorbances of the acid-form solution, the base-form solution and the mixed solution, respectively.

In Fig. 2 is also shown the plot of $\log\{(d_2-d)/(d-d_1)\}$ against pH, which is a straight line of slope -1.0. According to eqn. (1), the pK_{a1} ($= -\log([\mathrm{H}][\mathrm{HR}]/[\mathrm{H_2R}])$) was calculated to be 2.69 ± 0.03.

The second dissociation constant, pK_{a2}. The reagent stock solution (10 ml of $8 \cdot 10^{-5}$ *M*) was pipetted into a 25-ml volumetric flask and phosphoric and carbonic acid buffer were added to adjust the pH. The ionic strength of the solution was adjusted to 0.2 by adding potassium chloride, and the solution was diluted to the mark with distilled water. Then, the absorbances at 376 nm and the absorbance spectra were measured in a 10-mm cell, and the pH was measured in another portion of the solution. The absorbance spectra and the absorbance–pH curve are shown in Figs. 3 and 4,

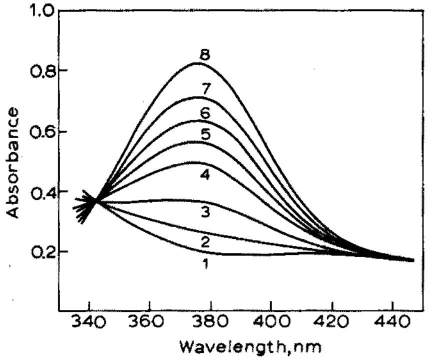

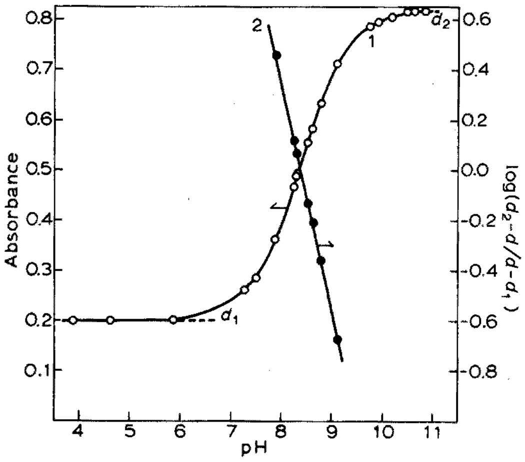

Fig. 3. The absorbance spectra of the reagent in the aqueous solution. [Reagent] $3.2\cdot10^{-5}$ M. 1-cm cell. pH: (1) 4.61; (2) 7.29; (3) 7.89; (4) 8.31; (5) 8.54; (6) 8.80; (7) 9.12; (8) 10.60.

Fig. 4. The plots of the absorbance *vs.* pH and log $\{(d_2-d)/(d-d_1)\}$ *vs.* pH at 376 nm in 1-cm cell. $\mu=0.2$. (1) Absorbance *vs.* pH; (2) log $\{(d_2-d)/(d-d_1)\}$ *vs.* pH.

respectively. The isobestic point is at 342 nm. In Fig. 4 is also shown the plot of log $\{(d_2-d)/(d-d_1)\}$ against pH. This plot is a straight line of slope -1.0. Finally, the pK_{a2} was calculated to be 8.40 ± 0.05.

The reaction of cobalt ion with nitroso-DiMAP

Cobalt ion reacts with nitroso-DiMAP to form a red complex. In Fig. 5 are shown the absorbance spectra of the complex and the reagent in aqueous solution.

In general, the reaction of cobalt(II) ion and the ligand is slow. When the concentrations of cobalt and the reagent were $1\cdot10^{-5}$ M and $3\cdot10^{-5}$ M, respectively, the absorbance of the solution was constant after 90 min. When an excess of cobalt

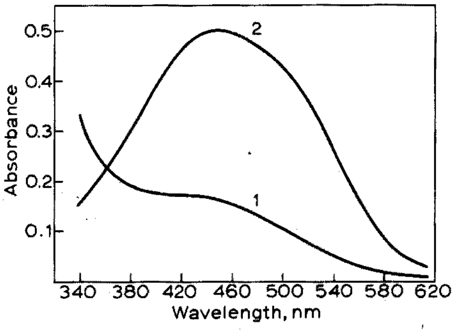

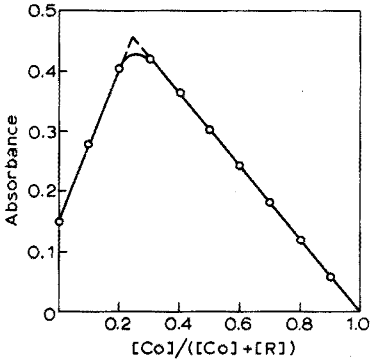

Fig. 5. The absorbance spectra of the complex and the reagent in the aqueous solution. pH=6.3, 1-cm cell. (1) [Reagent] $3\cdot10^{-5}$ M; (2) [reagent] $3\cdot10^{-5}$ M, [Co] $1\cdot10^{-5}$ M. These spectra were obtained 3 h later after the solutions had been prepared.

Fig. 6. Continuous variation method in the aqueous solution at 500 nm in 1-cm cell. pH = 6.4, [Co] + [R] = $5\cdot10^{-5}$ M.

was present, *i.e.* cobalt and the reagent were $1 \cdot 10^{-4}\,M$ or $1 \cdot 10^{-3}\,M$ and $3 \cdot 10^{-5}\,M$, respectively, 150 min was necessary for complete reaction at 20° and the final absorbance of the complex (>150 min) was 0.444 at 456 nm. Probably, complete reaction would be reached more rapidly at increased temperature. When an excess of reagent was present, *i.e.* cobalt and the reagent were $1 \cdot 10^{-5}\,M$ and $1 \cdot 10^{-4}\,M$ respectively, the absorbances after 10 and 100 min of the complex calculated by subtracting the absorbance of the excess reagent were 0.441 and 0.444 at 20°, respectively, and 0.443 and 0.444 at 60°, respectively. The fact that the absorbances were all essentially equal indicates that only one cobalt–nitroso-DiMAP complex was formed regardless of whether excess cobalt or reagent was present. The composition of this complex was determined by the continuous variation method. From Fig. 6, it follows that one mole of cobalt reacts with three moles of nitroso-DiMAP.

The formation constant of the cobalt–nitroso-DiMAP complex, log K_{MR_3}

Since the mole ratio of the cobalt complex is 1 : 3, the reactions of cobalt with nitroso-DiMAP can be written as follows (the charges of the metal and reagent are omitted):

$$\mathrm{pH} > \mathrm{p}K_{a2} \qquad \mathrm{M} + 3\mathrm{R} \rightleftharpoons \mathrm{MR_3} \qquad \mathrm{K} = \frac{[\mathrm{MR_3}]}{[\mathrm{M}][\mathrm{R}]^3} \tag{2}$$

$$\mathrm{p}K_{a2} > \mathrm{pH} > \mathrm{p}K_{a1} \qquad \mathrm{M} + 3\mathrm{HR} \rightleftharpoons \mathrm{MR_3} + 3\mathrm{H} \qquad K'_1 = \frac{[\mathrm{MR_3}][\mathrm{H}]^3}{[\mathrm{M}][\mathrm{HR}]^3} \tag*{(2)$'$}$$

$$\mathrm{p}K_{a1} > \mathrm{pH} \qquad \mathrm{M} + 3\mathrm{H_2R} \rightleftharpoons \mathrm{MR_3} + 6\mathrm{H} \qquad K'_2 = \frac{[\mathrm{MR_3}][\mathrm{H}]^6}{[\mathrm{M}][\mathrm{H_2R}]^3} \tag*{(2)$''$}$$

where M and R are the cobalt ion and the reagent, respectively.

When the absorbance of metal ion is neglected, the measured absorbance, Abs., is represented as follows:

$$\mathrm{Abs.} = \varepsilon_{MR_3} \cdot C_{MR_3} + \varepsilon_R \cdot C_R \tag{3}$$

where ε_{MR_3}, ε_R, C_{MR_3} and C_R are the molar absorptivities of the complex and the reagent, and the concentration of the complex and the reagent, respectively.

The total concentrations of the reagent and the metal, C_R^T and C_M^T, respectively, can be represented as follows:

$$C_R^T = C_R + 3C_{MR_3} \tag{4}$$

$$C_M^T = C_M + C_{MR_3} \tag{5}$$

From eqns. (3) and (4):

$$C_{MR_3} = \frac{\mathrm{Abs.} - \varepsilon_R \cdot C_R^T}{\varepsilon_{MR_3} - 3\varepsilon_R} \tag{6}$$

The apparent formation constant, K'_{MR_3}, is given by:

$$K'_{MR_3} = \frac{C_{MR_3}}{C_M \cdot C_R^3} = \frac{[\mathrm{MR_3}]}{[\mathrm{M}][\mathrm{R}]^3 \alpha_{R(H)}^3} = \frac{K_{MR_3}}{\alpha_{R(H)}^3} \tag{7}$$

or

$$\log K'_{MR_3} = \log K_{MR_3} - 3 \log \alpha_{R(H)} \qquad (7)'$$

where $\alpha_{R(H)} = C_R/[R] = 1 + ([H]/K_{a2}) + ([H]^2/K_{a1} \cdot K_{a2})$. From eqns. (4), (5), (6), and (7), K'_{MR_3} can be calculated.

The experiments were carried out as follows. In a 25-ml volumetric flask, the reagent and cobalt solutions were pipetted ([Co] $1 \cdot 10^{-5}$ *M*, [reagent] $3 \cdot 10^{-5}$ *M*), and potassium chloride solution was added to adjust the ionic strength ($\mu = 0.1$). Then buffer solution and hydrochloric acid solution were added to adjust the pH, and the solution was diluted to the mark with water. These solutions were thermostated at 60° for 3 h, then cooled to 25°, and the absorbances were measured at 500 nm. The pH value was measured in another portion. Reagent blanks were determined in the same way.

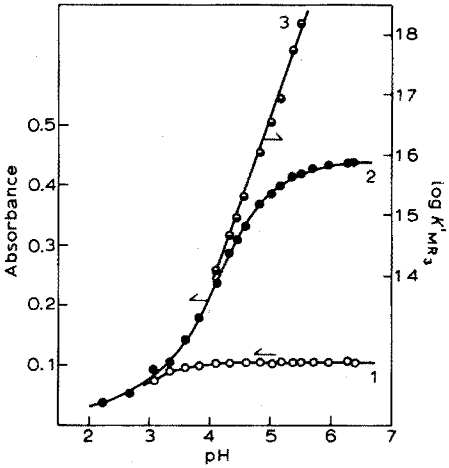

Fig. 7. The plots of the absorbance *vs.* pH and log K'_{MR_3} *vs.* pH. (1) [Reagent] $3 \cdot 10^{-5}$ *M*, 1-cm cell, 500 nm; (2) [reagent] $3 \cdot 10^{-5}$ *M*, [Co] $1 \cdot 10^{-5}$ *M*, 1-cm cell, 500 nm; (3) log K'_{MR_3} *vs.* pH. The absorbances were measured at 25° after the solutions had been heated at 60° for 3 h.

In Fig. 7 are shown the plots of the absorbance against pH and log K'_{MR_3} against pH. The plot of log K'_{MR_3} against pH gives a straight line with a slope of about 2.9, which is in fair agreement with the slope of 3.0 expected from eqn. (7) or (7)'. The formation constant, K_{MR_3}, calculated from eqn. (7)' was 26.77 ± 0.12.

The distribution of nitroso-DiMAP between 1,2-dichloroethane and water

The reagent itself is also extracted into the organic phase. The absorbance spectra of the reagent in the organic phase, which was extracted from aqueous phases at various pH (0.4–11.9), were all of the same type and showed maximal absorption at 404 nm. Thus only one species of the reagent, HR, is extracted into the organic phase, and, for all pH values the distribution ratio of the reagent, q_R, can be represented by:

$$q_R = \frac{C_{R(o)}}{C_{R(a)}} = \frac{[HR]_o}{[H_2R]_a + [HR]_a + [R]_a} = D_{HR}\left(1 + \frac{[H]}{K_{a1}} + \frac{K_{a2}}{[H]}\right)^{-1} \qquad (8)$$

where the subscripts o and a refer to the organic and the aqueous phases, and D_{HR} is the partition coefficient defined as:

$$D_{HR} = \frac{[HR]_o}{[HR]_a} \tag{9}$$

In the various pH regions, eqn. (8) is as follows:

(*a*) when $[H] > K_{a1}$, *i.e.*, $pH < pK_{a1}$,

$$q_R = \frac{D_{HR} \cdot K_{a1}}{[H]_a}$$

or

$$\log q_R = \log (D_{HR} \cdot K_{a1}) + pH \tag{8$'$}$$

(*b*) when $K_{a1} > [H] > K_{a2}$, *i.e.*, $pK_{a1} < pH < pK_{a2}$,

$$q_R = D_{HR}$$

or

$$\log q_R = \log D_{HR} = \text{constant} \tag{8$''$}$$

(*c*) when $K_{a2} > [H]$, *i.e.*, $pK_{a2} < pH$,

$$q_R = \frac{D_{HR} \cdot [H]}{K_{a2}}$$

or

$$\log q_R = \log (D_{HR}/K_{a2}) - pH \tag{8$'''$}$$

The experiments were carried out as follows. In the 25-ml volumetric flask, potassium chloride solution was pipetted to adjust the ionic strength ($\mu = 0.1$), and buffer solution was added. Then, 5 ml of reagent stock solution ($5.0 \cdot 10^{-3}\,M$) was added and the solutions were diluted to the mark. Aliquots (5 ml) of these solutions were pipetted into glass-stoppered test tubes and 5 ml of 1,2-dichloroethane was pipetted into each tube. The tubes were shaken for 30 min and the organic phase was then filtered through dry filter paper. The absorbance was measured at 404 nm. In the aqueous phase, when the pH was below about 7 and above about 7, the absorbances were measured at the isosbestic points, *i.e.*, 419.5 nm and 341 nm, respectively. At the same time, the pH was also measured.

The results obtained are shown in Fig. 8, from which it can be seen that the

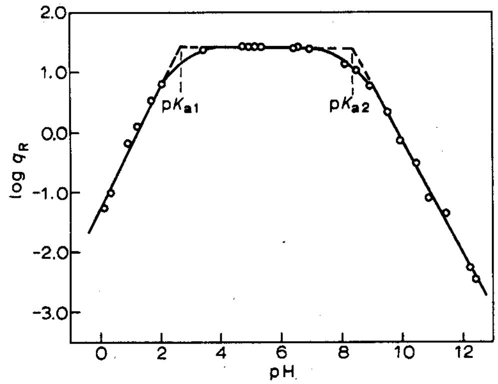

Fig. 8. The plot of log q_R *vs.* pH. [Reagent] $1 \cdot 10^{-3}\,M$.

plot of log q_R against pH has break points at pH = 2.7 (pK_{a1}) and 8.4 (pK_{a2}), and the plots below pH 2.7 and above pH 8.4 are straight lines with slopes of 1.0 and −1.0, respectively; between pH 2.7 and 8.4, the slope is zero. Accordingly, eqns. (8), (8)′, (8)″ and (8)‴ are proved to be reasonable. The calculated value of log D_{HR} is 1.42 ± 0.02.

Removal of the reagent extracted into the organic phase

The large excess of reagent in the organic phase causes errors in determining the absorbance of the cobalt complex, hence its removal is necessary. Other commonly used nitroso compounds are normally removed by alkaline solutions. In the case of nitroso-DiMAP, however, the excess of reagent can be removed with either alkaline or acidic solution. From Fig. 8, the regions where the reagent is more than 99% in the aqueous phase, are below pH −0.8 or above pH 12. Hence, the reagent in the organic phase was stripped with sodium hydroxide solution or hydrochloric acid solution. When the reagent ($1 \cdot 10^{-3}$ *M*) in 1,2-dichloroethane was stripped once with 1 *M* sodium hydroxide or with (1+2) hydrochloric acid solution, the residual absorbance of the organic phase was 0.001 and 0.004 at 456 nm, respectively. The cobalt complex, however, remained stable in the organic phase. In Fig. 9 are shown the absorbance spectra of the complex and the reagent blank after the removal of the reagent. The maximal absorbance of the complex is about 456 nm and that of the reagent blank is negligible. In this work, the excess of reagent was removed by stripping once with (1+2) hydrochloric acid solution.

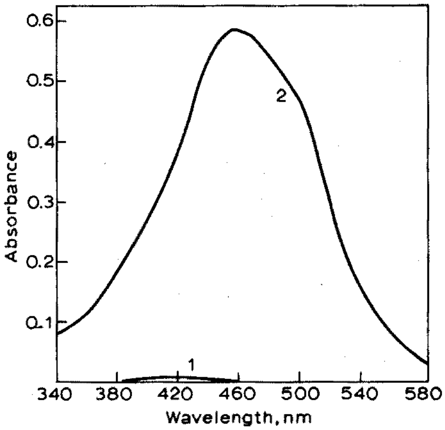

Fig. 9. The absorbance spectra of the complex and the reagent blank. (1) Reagent blank; (2) complex. These were washed out with (1+2) HCl or 1 *M* NaOH.

The composition and stability of the cobalt–nitroso-DiMAP complex in the organic phase

As reported previously[3], the absorbance of the extracted complex remained constant between pH 5 and 7, hence the composition of the extracted complex was determined at about pH 6 by the mole ratio and continuous variation methods. In all cases 5 ml each of organic and aqueous phase were used. The results (Figs. 10 and 11)

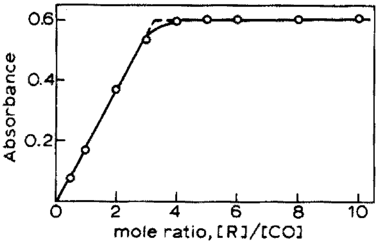

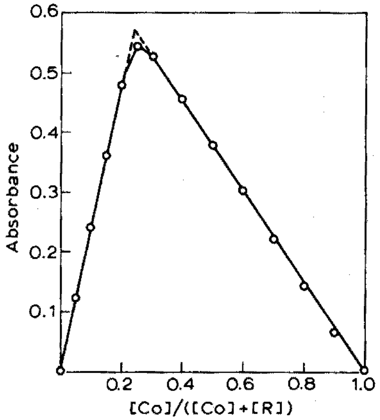

Fig. 10. Mole ratio method in the organic phase at 456 nm in 1-cm cell. pH = 6.2, [Co] + [R] = $4 \cdot 10^{-5}$ M.

Fig. 11. Continuous variation method in the organic phase at 456 nm in 1-cm cell. pH = 6.2, [Co] + [R] = $4 \cdot 10^{-5}$ M.

show conclusively that the extracted complex is of 1 : 3 composition, as in aqueous solution.

To examine the stability of the complex, the absorbance of the organic phase containing cobalt–nitroso-DiMAP complex ($1 \cdot 10^{-5}$ M) was measured in a stoppered 10-mm cell at 456 nm. During 7 and 10 days, the decrease of the absorbance was about 0.6 and 3%, respectively.

Distribution of the cobalt complex

From Fig. 8, most of the reagent is present in the organic phase in the pH range at which the complex is formed. The red complex formed is also readily extracted into the organic phase. The following equilibrium was therefore considered. When $pK_{a2} > pH > pK_{a1}$,

$$M_{(a)} + 3HR_{(o)} \rightleftharpoons MR_{3(o)} + 3H_{(a)} \qquad K_e = \frac{[MR_3]_o[H]_a^3}{[M]_a[HR]_o^3} \tag{10}$$

From eqn. (10), eqn. (10)′ can be derived:

$$\log K'_e = \log \frac{[MR_3]_o}{[M]_a[HR]_o^3} = \log K_e + 3\text{ pH} \tag*{(10)′}$$

The plot of log K'_e against pH must be linear and its slope should be 3.0.

For experimental verification, 5 ml of $5 \cdot 10^{-5}$ M cobalt solution was mixed with potassium chloride to give $\mu = 0.1$, buffer solution and 5 ml of $1.5 \cdot 10^{-4}$ M reagent solution before dilution to 25 ml with water; 5 ml of these solutions and 5 ml of 1,2-dichloroethane were shaken at 25°. At least 20 min was required for equilibrium to be achieved, and a shaking period of 3 h was used for safety. The results are shown in Fig. 12. The plot of log K'_e against pH shows a good linearity and the slope is 2.8, which indicates that eqns. (10) and (10)′ are reasonable. The calculated value of log K_e is 0.42 ± 0.22.

The partition coefficient of the complex, D_{MR_3}, is calculated from eqn. (11).

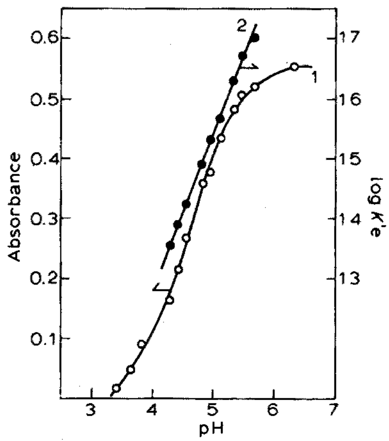

Fig. 12. The plots of the absorbance *vs.* pH and log K'_e *vs.* pH at 456 nm in 1-cm cell. [Co] $1\cdot10^{-5}$ *M*, [reagent] $3\cdot10^{-5}$ *M*. (1) Absorbance *vs.* pH; (2) log K'_e *vs.* pH.

$$K_e = \frac{D_{MR_3}\cdot K_{MR_3}\cdot K_{a2}^3}{D_{HR}^3}$$

or

$$\log D_{MR_3} = \log K_e - \log K_{MR_3} + 3\mathrm{p}K_{a2} + 3\log D_{HR} \qquad (11)$$

When the values obtained in this work were substituted into eqn. (11), log $D_{MR_3}=3.11$ was obtained.

DISCUSSION

Nitroso-DiMAP has usually been thought to be very unstable, and so has not been studied or used as an organic analytical reagent. The reagent is, however, very stable in 0.01 *M* hydrochloric acid solution. Accordingly, it was worthwhile to determine the various constants, such as the acid dissociation constants, the formation constant of the cobalt complex, the partition coefficients of the reagent and the complex, and to examine the mechanism of the extraction. The constants obtained are shown in Table I. It is clear that the reagent is a dibasic acid, and so is very soluble in water, especially in solutions of high or low pH. The reagent is extracted into the organic

TABLE I

THE CONSTANTS OBTAINED

ε_{MR_3}	$6.0\cdot10^4$ at 456 nm
pK_{a1}	2.69 ± 0.03 ($\mu=0.1$)
pK_{a2}	8.40 ± 0.05 ($\mu=0.2$)
log D_{HR}	1.42 ± 0.02 ($\mu=0.1$)
log K_{MR_3}	26.77 ± 0.12 ($\mu=0.1$)
log K_e	0.42 ± 0.22 ($\mu=0.1$)
log D_{MR_3}	3.11

phase in the form HR and can be stripped with acidic or basic solutions. The very stable complex formed with cobalt is soluble in water and is easily extracted into an organic phase of high dielectric constant; the complex is stable in the organic phase, even when washed with (1+2) hydrochloric acid. The structure of the cobalt complex can be considered as I.

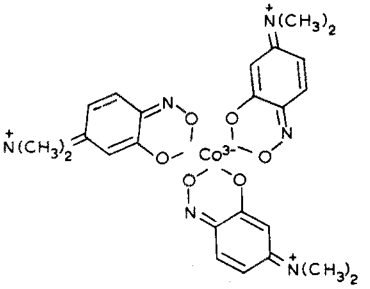

(I)

In general, the complex of cobalt with 2-nitroso-1-naphthol has been said to have the largest molar absorptivity of the various nitroso compounds. Needleman determined cobalt in iron and steel[5] and Ssekaalo determined cobalt in plant materials[6]; they reported that the molar absorptivity of the cobalt complex was $3.6 \cdot 10^4$ at 362 nm and $4.4 \cdot 10^4$ at 367 nm, respectively. However, as shown in Table II the molar absorptivity of the cobalt–nitroso-DiMAP complex is the largest ($6.0 \cdot 10^4$).

TABLE II

THE MOLAR ABSORPTIVITIES OF COBALT COMPLEXES

Reagent	*Molar absorptivity* $(\cdot 10^4)$	*Ref.*
2-Nitroso-1-naphthol	4.4 (367 nm, $CHCl_3$)	6
1-Nitroso-2-naphthol	2.5 (420 nm, $CHCl_3$)[a]	3
1-Nitroso-2-hydroxy-3-naphthoic acid	3.2 (428 nm, benzene)[a]	3
1-Nitroso-2,7-dihydroxy-naphthalene	2.7 (450 nm, nitrobenzene)[a]	3
Nitroso-DiMAP	5.3 (460 nm, 1,2-dichloroethane)[a]	3
	6.0 (456 nm, 1,2-dichloroethane)[b]	This work

[a] Absorbances were measured against a reagent blank as reference[3].
[b] Excess of reagent was washed out with (1+2) HCl.

With the other nitroso compounds used commonly, the excess of reagent extracted into the organic phase must be back-extracted with alkaline solution and then an acidic solution must be used to decompose other extracted complexes, *e.g.* those of iron, nickel and copper. With nitroso-DiMAP, however, the excess of reagent can be back-extracted with acidic solution, the other extracted complexes being removed simultaneously. The time required to determine cobalt is thus advantageously shortened.

The author is greatly indebted to Professor Kyoji Tôei of Okayama University for his valuable advice and discussion.

SUMMARY

6-Nitroso-3-dimethylaminophenol (nitroso-DiMAP) and its cobalt complex have been studied in detail. The reagent is stable in 0.01 *M* hydrochloric acid solution for at least a month. Its acid dissociation constants, pK_{a1} and pK_{a2}, were determined to be 2.69±0.03 and 8.40±0.05, respectively. A 1 : 3 complex is formed with cobalt, the formation constant, $\log K_{MR_3}$, being 26.77±0.12. The reagent is extracted into 1,2-dichloroethane in the form HR, the partition coefficient, $\log D_{HR}$, being 1.42±0.02. The partition coefficient of the complex, $\log D_{MR_3}$, is 3.11. The extracted cobalt complex is stable to back-extraction with (1+2) hydrochloric acid, whereas excess of reagent is removed to the aqueous phase. The molar absorptivity of the complex in the organic phase is $6.0 \cdot 10^4$ at 456 nm.

RÉSUMÉ

Une étude est effectuée sur le complexe cobalt–nitroso-6-diméthylamino-3-phenol (nitroso-DiMAP). Ce réactif, en solution dans l'acide chlorhydrique 0.01 *M*, est stable un mois au moins. Ses constantes de dissociation acide pK_{a1} et pK_{a2} sont respectivement 2.69±0.03 et 8.40±0.05. Un complexe 1:3 est formé, avec une constante de formation $\log K_{MR_3}$ de 26.77±0.12. On examine également extraction et coefficient de partage. Le coefficient d'extinction molaire du complexe, en phase organique est de $6.0 \cdot 10^4$ à 456 nm.

ZUSAMMENFASSUNG

6-Nitroso-3-dimethylaminophenol (Nitroso-DiMAP) und dessen Kobaltkomplex wurden im einzelnen untersucht. Das Reagenz ist in 0.01 *M* Salzsäure mindestens einen Monat lang beständig. Die Säuredissoziationskonstanten pK_{a1} und pK_{a2} wurden zu 2.69±0.03 bzw. 8.40±0.05 bestimmt. Mit Kobalt entsteht ein 1:3-Komplex; die Bildungskonstante ist $\log K_{MR_3} = 26.77 \pm 0.12$. Das Reagenz wird mit 1,2-Dichloräthan in der Form HR extrahiert; der Verteilungskoeffizient ist $\log D_{HR} = 1.42 \pm 0.02$. Der Verteilungskoeffizient des Komplexes ist $\log D_{MR_3} = 3.11$. Der Reagenzüberschuss wird durch Reextraktion mit Salzsäure (1+2) aus der organischen Phase entfernt, ohne dass hierdurch die Beständigkeit des extrahierten Kobaltkomplexes beeinträchtigt wird. Der molare Extinktionskoeffizient des Komplexes in der organischen Phase ist $6.0 \cdot 10^4$ bei 456 nm.

REFERENCES

1 F. D. SNELL AND C. T. SNELL, *Colorimetric Methods of Analysis*, 3rd Edn., 1958, p. 352.
2 K. TÔEI AND S. MOTOMIZU, *Nippon Kagaku Zasshi*, 92 (1971) 92.
3 S. MOTOMIZU, *Japan Analyst*, 20 (1971) 590.
4 R. MÖHLAW, *Ber.*, 25 (1859) 1059.
5 M. NEEDLEMAN, *Anal. Chem.*, 38 (1966) 915.
6 H. SSEKAALO, *Anal. Chim. Acta*, 51 (1970) 503.

Analytica Chimica Acta
Elsevier Publishing Company, Amsterdam
Printed in The Netherlands

EXTRACTION OF SEVERAL ELEMENTS WITH TRIOCTYLMONOMETHYLAMMONIUM CHLORIDE

KAORU UENO AND AKIRA SAITO

Chemistry Division, Japan Atomic Energy Research Institute, Tokai, Ibaraki (Japan)

(Received 26th April 1971)

During the last decade, quaternary organic ammonium salts have been investigated extensively as liquid–liquid extraction reagents for both chemical and chemical engineering purposes. Review articles on this subject have been published[1,2]. Seeley *et al.*[3] reported the partition of uranium(VI) between trioctylmonomethylammonium chloride (TOMA-Cl) and sodium carbonate solution. The Adogen-464–ammonium carbonate extraction system has been used for purification of beryllium[4]. However, no systematic study has been made on extractions from ammonium carbonate or ammonium sulfate solution.

In the present work, the extraction of 25 inorganic ions from ammonium carbonate or ammonium sulfate solutions with 10% TOMA-Cl in toluene has been studied. Separation methods for uranium-237 from fission products with these extraction systems are also described.

EXPERIMENTAL

All experiments were carried out at room temperature (25±2°).

Reagents

Trioctylmonomethylammonium chloride (TOMA-Cl; K & K Laboratories, Inc., U.S.A.). Used without further purification and diluted with toluene to give a 10% (v/v) solution.

Both ammonium carbonate and ammonium sulfate were of analytical grade. The distribution ratios were measured at 0.1, 0.2, 0.3, 0.5, 1.0 and 2.0 *M* for both salts and 3.0 *M* for ammonium sulfate.

Radioactive tracers

Thorium-234 was milked from natural uranium. Uranium-237 was obtained by γ-ray bombardment of a natural uranium target in the linear accelerator of JAERI. Other radioactive nuclides, ^{45}Ca, ^{56}Mn, ^{55}Fe, ^{60}Co, ^{75}Se, ^{85}Sr, ^{95}Zr–Nb, ^{99}Mo,^{99m}Tc, ^{106}Ru, ^{131}I, ^{134}Cs, ^{139}Ba, ^{144}Ce, ^{153}Sm, ^{152,154}Eu, ^{170}Tm, ^{177}Lu, ^{233}Pa, ^{239}Np, ^{239}Pu, ^{241}Am and ^{242}Cm were obtained either by irradiating the target materials of the respective elements in JRR-2 or by importing from U.S.A.

The radiochemical purity of these nuclides was checked by their half-lives, and by their α- or γ-ray spectra. The tracer was added in 1–2 drops of dilute ammonium carbonate or ammonium sulfate solution. Pretreatments were sometimes performed to obtain a definite ionic species. The most common species were generally chosen.

Determination of the distribution ratios.

The distribution ratios (K_d) defined as the concentration in the organic phase divided by that in the aqueous phase at equilibrium, were determined by ordinary radiometric method[5,6]. In this determination, a portion of an ammonium carbonate or ammonium sulfate solution of a given concentration containing the radioactive tracer was shaken with a portion of the pre-equilibrated organic solvent, and the two layers were separated. Most of the data in this experiment were obtained by shaking for 3 min.

Separation of uranium-237 from the fission products

Uranium dioxide target (*ca.* 20 mg) of natural isotopic ratio was irradiated with 20-MeV bremsstrahlung for 1 h. After cooling for one day, the irradiated sample was dissolved in concentrated nitric acid. About 10 mg each of lanthanum and zirconium were added to the solution as carriers, and then the solution was neutralized with dilute ammonia solution. After centrifugation, the supernatant solution was discarded. Uranium was leached with 1.5 ml of 1 *M* sodium carbonate solution from the precipitate, and then the solution was transferred to a 10-ml graduated cylinder. After dilution of the solution with water to 5 ml, an equal volume of the 10% TOMA-Cl–toluene solution was added; the organic solution had been pretreated with 0.3 *M* sodium carbonate solution. After shaking vigorously for about 3 min, the aqueous phase was discarded; then the organic phase was scrubbed twice with 5 ml of a fresh 0.3 *M* ammonium carbonate solution. Finally, uranium was back-extracted into 1 *M* ammonium nitrate solution. An aliquot of the aqueous uranium solution thus obtained was placed in a test tube for measurements of γ-ray spectra and decay.

When the sulfate extraction system was used, the precipitate containing uranium-237 was dissolved in a small amount of dilute hydrochloric acid, and then to this solution was added 5 ml of 1 *M* ammonium sulfate solution. The mixed solution was centrifuged and the white precipitate was discarded. The solution was transferred to a 10-ml graduated cylinder, and then the uranium was extracted by the same method as above except for the use of ammonium sulfate.

RESULTS AND DISCUSSION

Variation in the time of extraction

The dependence of the K_d value for thulium on the mixing time was first studied for the TOMA-Cl–toluene–ammonium carbonate and the TOMA-Cl–toluene–ammonium sulfate systems.

As seen in Fig. 1, the K_d value for thulium is nearly constant in the former extraction system after about 1 min, and in the latter system after about 2 min. A time of 3 min was therefore used for convenience in shaking the extraction system.

TOMA-Cl–ammonium carbonate system

The results are summarized in Fig. 2 as a series of graphs of K_d *vs.* M where K_d is the distribution ratio and M the molarity of ammonium carbonate. As can be seen, the K_d values for each ion usually depended on the inverse power of the carbonate concentration, except for cesium ion.

Cesium gave very low K_d values in the whole carbonate concentration range

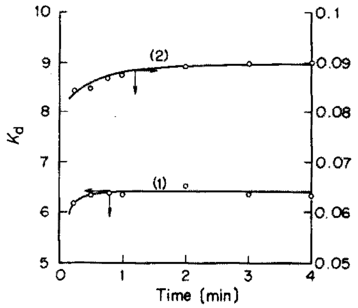

Fig. 1. Dependence of K_d values for ^{170}Tm on the mixing time. (1) Aq. phase, 0.3 M $(NH_4)_2CO_3$; (2) aq. phase, 0.3 M $(NH_4)_2SO_4$.

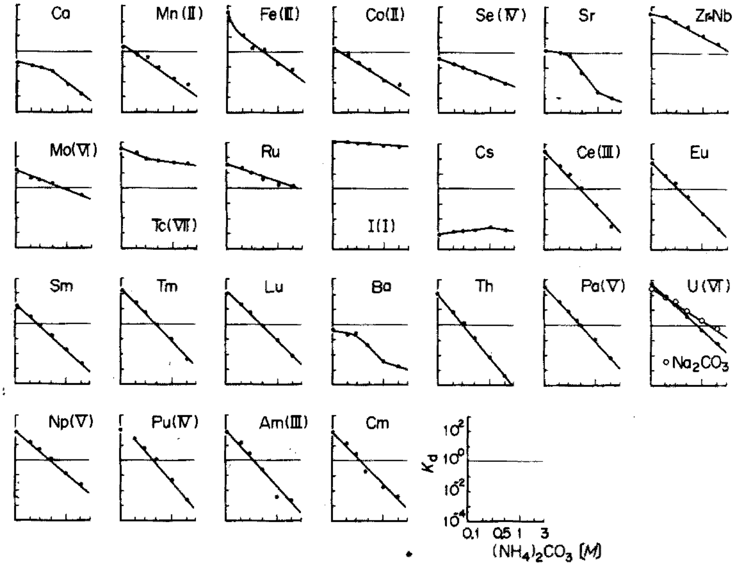

Fig. 2. Dependence of K_d values for 10% TOMA-Cl systems on the ammonium carbonate concentration.

studied. The extractability of calcium, strontium and barium decreased gradually in the range 0.1–0.3 M carbonate, and then decreased rapidly with increasing concentration of ammonium carbonate. Although the curves for manganese(II), iron(III) and cobalt(II) were similar in shapes, the K_d values for iron(III) were almost 10 times those for manganese and cobalt in the whole carbonate concentration range studied. The K_d values for selenium, molybdenum and ruthenium had an inverse dependence on the first power carbonate concentration and the extractability decreased in the following order: ruthenium > molybdenum > selenium. Zirconium–niobium, technetium(VII) and iodine(I) were readily extracted in this system, iodine exhibiting a nearly horizontal K_d curve.

The K_d values for selected trivalent lanthanide and actinide cations in the system varied inversely with the 3.5 power of the carbonate concentration in the

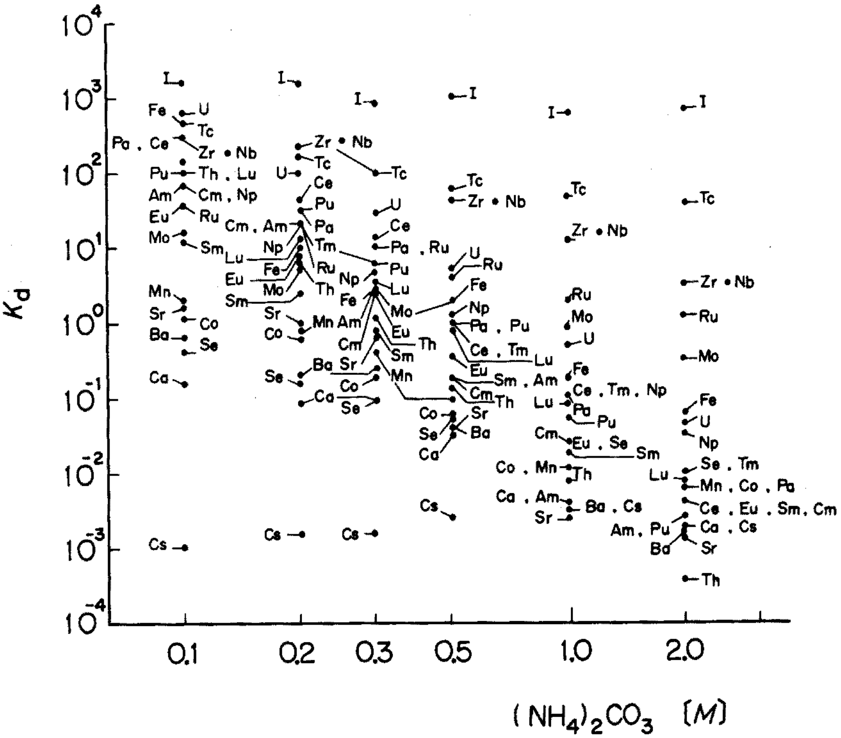

Fig. 3. K_d values in 10% TOMA-Cl–toluene–$(NH_4)_2CO_3$ systems.

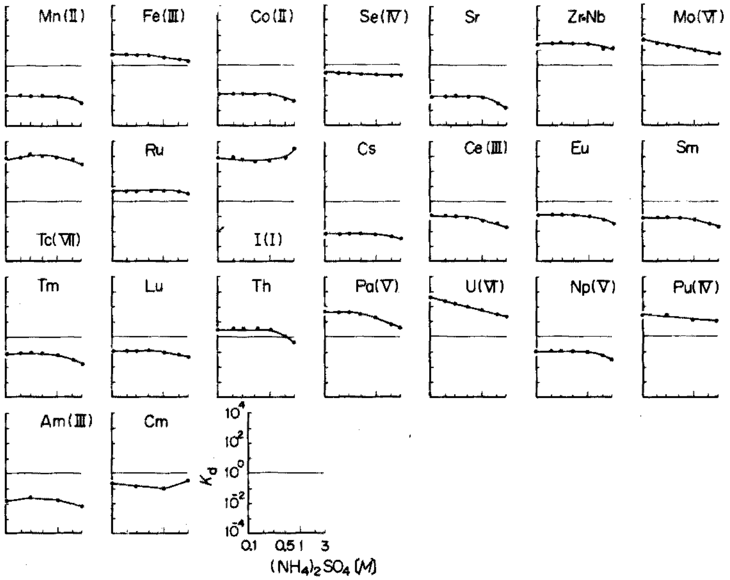

Fig. 4. Dependence of K_d values for 10% TOMA-Cl systems on the ammonium sulfate concentration.

aqueous phase. The K_d values for thorium and plutonium(IV) were dependent on the fourth power of the carbonate concentration; for protactinium(V) the 3.5 power, and for neptunium(V) the 2.5 power.

The K_d value for uranium(VI) was inversely proportional to the third power of the ammonium carbonate concentration in the aqueous solution, and in the sodium carbonate solution to the second power, as also reported by Seeley *et al.*[3].

In Fig. 3 are shown more accurate K_d values; this figure may be convenient for selecting a suitable separation scheme.

TOMA·Cl–ammonium sulfate system

The results for this system are given in Fig. 4 in an analogous way to Fig. 2. As can be seen, the shapes of the curves roughly follow two types. In the first type, the K_d value was unaffected by the sulfate concentration in the aqueous phase in the range below about 0.5 *M* and then decreased with increasing sulfate concentration. In the second type, the K_d value decreased inversely with the sulfate concentration in the aqueous phase.

The K_d values for cesium, strontium, manganese, iron, cobalt, zirconium–niobium, technetium, ruthenium, trivalent lanthanides, thorium, protactinium, neptunium, plutonium and americium were of the first type and the values for molybdenum and uranium were of the latter type.

The distribution ratios were very low for cesium, strontium, manganese(II) and cobalt(II) in the whole sulfate concentration range studied. Iron, zirconium–

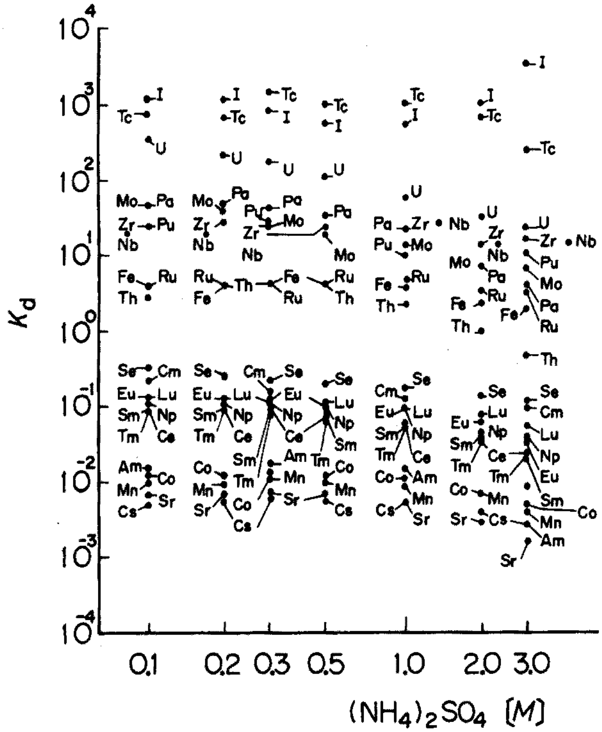

Fig. 5. K_d values in 10% TOMA-Cl–toluene–$(NH_4)_2SO_4$ systems.

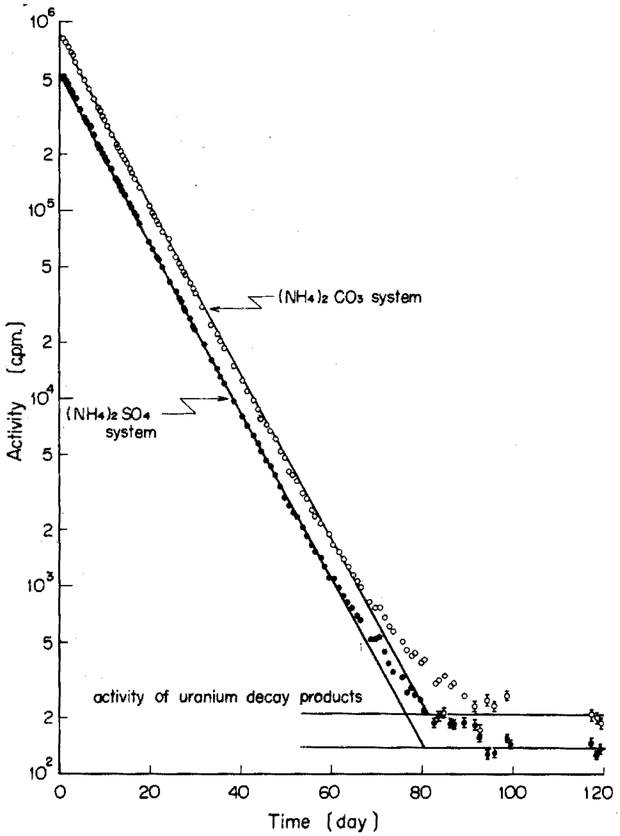

Fig. 6. Radioactive decay of uranium-237.

niobium, molybdenum(VI) and ruthenium were extracted in this extraction system, and the K_d values at 0.3 M ammonium sulfate were 3.0, 100, and 10 for iron, zirconium–niobium, molybdenum and ruthenium, respectively. Technetium(VII) and iodine(I) had very high K_d values. The curves for the selected lanthanide elements were similar in shapes and the values were generally low. Protactinium(V) and neptunium(V) showed similar K_d curves; the values for protactinium were almost 250 times as high as those for neptunium in the same extraction conditions. Americium and curium have low K_d values similarly to the cases of the lanthanide ions. Thorium, uranium(VI) and plutonium(IV) were extracted, the extractability decreasing in the order uranium > plutonium > thorium.

In general, the K_d values obtained in the present work were relatively high compared with the values reported for the TIOA–sulfuric acid system[8].

Figure 5 shows the precise K_d values obtained in this extraction system. This may be convenient for examining the possibility or efficiency for the separation of a pair of arbitrary elements.

Separation of uranium-237

The γ-ray spectra of the uranium fractions separated by the procedure described under *Experimental* were measured with a 3 × 3 in NaI(Tl) crystal covered with a plastic absorber, and a 1024-channel pulse-height analyzer. The spectra showed peaks at 0.06, 0.102, 0.165, 0.208, 0.270 and 0.332 MeV. These energy peaks are in good agreement with the data on uranium-237 reported by other workers[7]. As can be seen in Fig. 6, the decay curves of the uranium fraction had a half-life of 6.7 days, which agreed well with the values reported previously[7]. The activities of the long-lived components in the decay curves may correspond to those of decay products grown in the natural uranium sample.

The authors wish to thank Dr. Tomitaro Ishimori, JAERI for his helpful guidance.

SUMMARY

Radiochemical studies of the solvent extraction behavior of twenty-five elements in the ammonium carbonate or ammonium sulfate–trioctylmonomethylammonium chloride–toluene systems were performed. The distribution ratios were determined in 0.1–2.0 *M* ammonium carbonate solutions and in 0.1–3.0 *M* ammonium sulfate solutions. The K_d value for each element generally depends on the inverse power of the carbonate concentration in the aqueous phase, while the K_d value is essentially unaffected by the sulfate concentration in the aqueous phase. Separation methods for uranium-237 from fission products with these extraction systems are presented.

RÉSUMÉ

Une étude radiochimique est effectuée sur le comportement de 25 éléments, lors d'extractions en système carbonate ou sulfate d'ammonium–chlorure de trioctylmonométhylammonium–toluène. Les coefficients de partage varient suivant la concentration en carbonate dans l'eau; par contre celle des sulfates n'a pas d'influence. On propose des méthodes de séparation de l'uranium-237 de produits de fission à l'aide de ces systèmes d'extraction.

ZUSAMMENFASSUNG

Es wurde die Verteilung von 25 Elementen in den Systemen wässrige Ammoniumcarbonatlösung oder Ammoniumsulfatlösung–Trioctylmonomethylammoniumchlorid–Toluol radiochemisch untersucht. Die Verteilungsverhältnisse wurden für 0.1–2.0 *M* Ammoniumcarbonatlösungen und 0.1–3.0 *M* Ammoniumsulfatlösungen bestimmt. Der K_d-Wert jedes Elements ist allgemein der reziproken Carbonatkonzentration in der wässrigen Phase proportional, während die Sulfatkonzentration in der wässrigen Phase keinen wesentlichen Einfluss hat. Es werden Methoden zur Abtrennung von Uran-237 aus Spaltprodukten unter Verwendung dieser Extraktionssysteme beschrieben.

REFERENCES

1 I. D. Eubanks, *At. Energy Rev.*, 7 (1969) 49.
2 W. Müller, *Actinides Rev.*, 1 (1967) 71.
3 F. G. Seeley, F. J. Hurst and D. J. Crouse, *ORNL-3106*, 1962.
4 *ORNL-4145*, 1967, p. 215.
5 D. F. Peppard, G. M. Mason and J. L. Maier, *J. Inorg. Nucl. Chem.*, 3 (1956) 215.
6 D. F. Peppard, W. J. Driscoll, R. J. Sironen and S. McCarty, *J. Inorg. Nucl. Chem.*, 4 (1957) 326.
7 C. M. Lederer, J. M. Hollander and I. Perlman, *Table of Isotopes*, 6th Edn., John Wiley, 1968, p. 428.
8 T. Ishimori, E. Akatsu, W. P. Cheng, K. Tsukuechi and T. Osakabe, *JAERI-1062*, 1964.

Analytica Chimica Acta
Elsevier Publishing Company, Amsterdam
Printed in The Netherlands

STUDIES WITH DITHIZONE

PART XXV. SECONDARY COPPER(II) DITHIZONATE

H. M. N. H. IRVING AND A. M. KIWAN
Department of Inorganic and Structural Chemistry, University of Leeds, Leeds 2 (England)

(Received 10th May 1971)

It is well known that copper(II) forms two types of complexes with dithizone (3-mercapto-1,5-diphenylformazan, H_2Dz), whose composition depends on the pH of the aqueous phase used in the preparation and on the relative concentrations of the components[1]. Purple primary copper(II) dithizonate ($Cu(HDz)_2$; λ_{max} 545 nm in chloroform) is formed from copper(II) and two molecular equivalents of dithizone in fairly acidic media and has been thoroughly studied[2-4]. The structure of this complex, formerly and misleadingly termed a keto-dithizonate, has been shown by X-ray crystallography[5] to be derived from the thiol tautomer of dithizone by replacing the HS-proton to give a Cu–S bond, square planar 4-coordination being completed through a nitrogen atom as shown in (I).

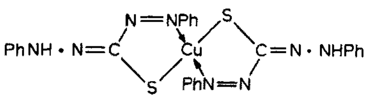

(I)

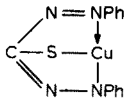

(II)

The position of the imino hydrogen atom (as shown in (I) or on the nitrogen atom directly coordinated to copper) is not fixed unambiguously since the structure was solved in projection only and data on interatomic distances and planarity are lacking. The presence of the :NH group is well attested by the infrared spectrum[6] which shows the stretching frequency at 3220 cm^{-1} and the :N–H bend at 1530 cm^{-1}.

Secondary copper(II) dithizonate (formerly termed the enol-dithizonate) is brown in colour (λ_{max} 445–450 nm in chloroform) and contains copper and dithizone in the molecular proportions 1 : 1. Its formation in alkaline solutions when copper is in excess has also been studied[2-4], though in less detail. Its structure has yet to be established although the balance of evidence has hitherto been consistent with its formation from the anion Dz^{2-} formed from dithizone by loss of both the thiol- and the imino-protons. The absence of an :NH group is clear from its infrared spectrum[6-9]. A formula such as (II) which appears in a number of papers and standard text-books is clearly unacceptable on stereochemical grounds.

Quite recently, Freiser and Freiser[10] have challenged the accepted view that secondary copper(II) dithizonate is a copper(II) complex and have concluded that "the so-called keto–enol equilibrium[4] for copper(II) dithizonate is really a Cu(II)–Cu-

(I) redox equilibrium". We do not agree with this view; and since we even disagree with these authors' interpretations of their own experiments it seems desirable to present their arguments in turn and to discuss them before introducing fresh evidence.

1. Dithizone ($pK_1 = 4.7$) has been shown[4] not to lose a proton from the anion HDz^- below pH 14. Although they are aware that "the acid-strengthening influences on organic ligands produced by metal chelation are frequently large", Freiser and Freiser feel that the loss of the remaining N-attached proton from $Cu(HDz)_2$ when the secondary complex is formed is "highly unlikely"[10].

There are innumerable examples in the literature of complexes of formazans, $ArNH \cdot N{=}CR \cdot N{=}NAr$, formed by replacing the imino-proton by a metal[11,12]. Certainly the formazans are very weak acids with pK values in anhydrous methanol of 16.5, 18.3, 18.3 and 18.6 for $Ar = C_6H_5$ and $R = H$, Cl, Me or Et, respectively[13]. When referred to water as a solvent, these values must be reduced by *ca.* 5.5 log units. Whereas the difficulty of removing a proton from the imino-group of the singly charged anion, HDz^- ($R = S^-$) of the weak acid dithizone ($pK_1 = 4.7$) will naturally lead to a value for $pK_2 > 11$, this need not be the case for the formally neutral metal complexes such as $Cu(HDz)_2$, particularly if there is overlap between the copper and sulphur orbitals leading to a decreased electron density on the non-metal. The extreme lability of the corresponding proton in primary mercury(II) dithizonate, $Hg(HDz)_2$, has been confirmed by its ready replacement by deuterium; it is an important factor in the photochromism of this and other dithizonates[6,14].

That such ionisation of the imino-hydrogen of a primary metal dithizonate actually takes place has been demonstrated in the case of phenylmercury(II) dithizonate, $C_6H_5Hg(HDz)$ which behaves as a weak acid in 52.75% (v/v) aqueous–ethanol, wherein the value $pK = 11.47$ was obtained spectrophotometrically[15]. Other arylmercury primary dithizonates have also been shown to form secondary complexes[16].

More recently[17] primary mercury(II) dithizonate has been shown to react with excess of silver ions to give a mixed complex $Hg(AgDz)_2$ and what are also presumably secondary complexes containing $C_6H_5Hg^+$ and Ag^+ have been obtained in solution, although their stoicheiometry could not be demonstrated[18]. It is quite impossible to explain the formation of such species if the loss of a proton from the species HDz^- and from a formally uncharged ligand in a primary metal dithizonate is regarded as unlikely.

2. If secondary copper dithizonate is a simple monomeric complex, CuDz, derived from the components Cu^{2+} and Dz^{2-} it should be paramagnetic in view of the unpaired electron from the metal. Freiser and Freiser state[10] that a $5 \cdot 10^{-4}$ *M* solution of the purple primary dithizonate exhibited a normal e.s.r. spectrum characteristic of copper(II) (a quartet with $g = 2.059$), whereas the brown secondary complex "gave no signal indicating that it was diamagnetic, *and, therefore was a copper(I) chelate*" (our italics).

Freiser and Freiser attempted to measure the molecular weight of these complexes by vapour pressure osmometry and arrived at values of 3,100 ± 200 for primary copper(I) dithizonate and 6,300 ± 300 for the brown secondary or "enol" complex from copper(II); they noted that copper may achieve a coordination number of four through intermolecular bonding. However despite this apparent evidence for extensive association, these authors conclude[10] that: "although the possibility exists that the diamagnetism observed with the copper(II) enol complex results from metal–metal bonding with consequent electron pairing, it would seem to be impossible because of the need for dithizone to lose a second proton to form an uncharged $CHCl_3$-soluble species".

Measurements by the Gouy method in these laboratories[19] gave the values $\mu_{eff} = 1.8$ B.M. for solid $Cu(HDz)_2$ and 0.63 B.M. for a solid sample of the secondary complex, which suggests that under these conditions it can be regarded as a complex of copper(II) with some metal–metal interaction sufficient to reduce the paramagnetism but not to quench it completely. The possibility that the observed paramagnetism is due to the presence of copper(II) as an impurity in "diamagnetic CuDz" seems highly unlikely. We shall refer later to molecular weight determinations which show secondary copper(II) dithizonate to be a dimer in chloroform solution.

3. Having prepared primary copper(I) dithizonate and shown that it has a single absorption band at 478 nm, Freiser and Freiser[10] noted that the spectrum of the enol chelate, *i.e.* that of the secondary dithizonate derived from copper(II), "was quite similar but its band maximum displaced to 446 nm". Essentially, Freiser and Freiser claim that the observed spectrum of brown secondary copper(II) dithizonate (λ_{max} 446 nm) is actually a summation of that produced by an equivalent amount of primary copper(I) dithizonate (λ_{max} 478)* and an oxidation product, diphenylthiocarbadiazone (DTD), absorbing maximally at 425 nm and responsible for the hypsochromic shift.

Now what was formerly termed diphenylthiocarbadiazone has been shown to be the mesoionic compound 2,3-diphenyl-2H-tetrazolium-5-thiolate (III) with $\lambda_{max} =$ 468 nm, and not 425 nm as Freiser and Freiser assume[10]. As such, it might well have caused a hypsochromic shift in the maximum but since its molar absorptivity is so low ($\varepsilon_{468} = 1{,}200$) in comparison to that of the copper(I) complex Cu(HDz) ($\varepsilon_{max} = 28{,}200$) it would hardly cause any detectable change in the alleged composite spectrum in the visible region.

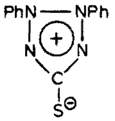

(III)

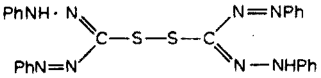

(IV)

There is, however, another well-defined oxidation product of dithizone, *viz.* the disulphide (IV), which does absorb in the region of 425 nm ($\varepsilon_{max} = 40{,}000$ in chloroform) at 420 nm[20,21]. It is uniquely characterised by its ease of spontaneous thermal fission (half-life period, 1.5 h at room temperature)[21] to give an equimolecular mixture of the mesoionic compound (III) and dithizone itself ($\lambda_{max} = 610$ nm; $\varepsilon_{max} = 40{,}000$). Its presence would be shown unambiguously by a progressive decrease in absorption at 420 nm and a large increase at 610 nm. However, the spectrum of a brown solution of secondary copper(II) dithizonate does not change over a period of days proving that this oxidation product is not present.

4. Freiser and Freiser state that "equilibrating the chloroform solution of the copper(II) enol complex with aqueous hydroxylamine at pH 4–5 which might be expected to reduce DTD or other oxidation products to dithizone, resulted in the

---

* In our hands these wavelength maxima occur at 490 nm in $CHCl_3$ and 480 nm in CCl_4.

formation of some normal purple copper(II) dithizonate". However, if the solution of the "copper(II) enol complex" consisted—as these authors contend—of a mixture of primary copper(I) dithizonate and "DTD" it is difficult to see why the addition of a *reducing* agent could possibly increase the oxidation state of copper from (I) to (II).

The conditions under which this experiment was carried out are not specified[10] and we detected no change in the spectrum of pure secondary copper(II) dithizonate when its chloroform solution was equilibrated with hydroxyammonium chloride or with very dilute hydrochloric acid at pH *ca.* 4.8. With stronger acid (0.5 M hydrochloric acid) complete conversion to primary copper(II) dithizonate takes place, thus:

$$2(CuDz)_{org} + 2H^+ \rightarrow (Cu(HDz)_2)_{org} + Cu^{2+} \qquad (1)$$

This stoicheiometry had previously been thoroughly established by Geiger and Sandell[4] and it has now been confirmed by a study of the back-reaction. When, for example, a solution of primary copper(II) dithizonate in chloroform is equilibrated with various amounts of aqueous copper(II) sulphate, the spectrum gradually changes to that of secondary copper(II) sulphate and there are isosbestic points at 492 and 638 nm conforming the equilibrium between the two coloured species (Fig. 1).

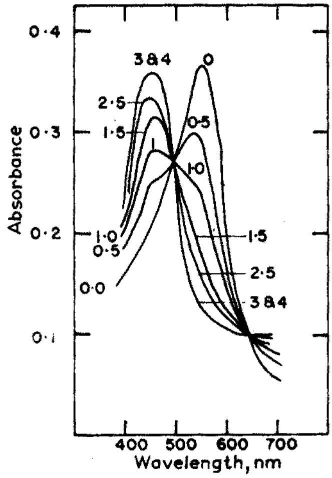

Fig. 1. The reaction after 30 min between 10 ml of 8.01 · 10^{-6} M primary copper(II) dithizonate in chloroform and 0, 0.5, 1.0, 1.5, 2.5, 3 and 4 ml of 4.0 · 10^{-5} M copper(II) sulphate made up to 10 ml with 0.1 M sodium acetate and adjusted to pH 10.75 with NaOH.

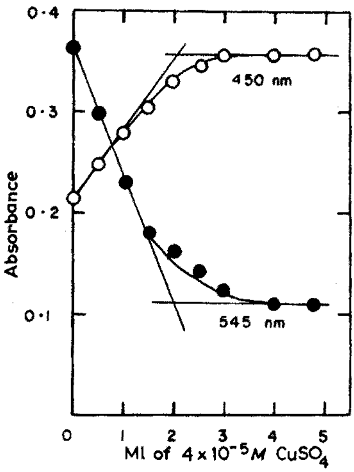

Fig. 2. The extractive titration of 10 ml of 8.01 · 10^{-6} M primary copper(II) dithizonate with aqueous copper sulphate at pH 10.75. Data from Fig. 1.

From the changes in absorption spectra at 545 nm (λ_{max} for primary copper(II) dithizonate) and at 450 nm (λ_{max} for the secondary dithizonate), it is possible to plot extractive titration curves (Fig. 2), from which it is clear that 8.01 · 10^{-5} mM of $Cu(HDz)_2$ reacts with 2.0 ml of 4.0 · 10^{-5} M copper sulphate, *i.e.* with 8.0 · 10^{-5} mM of copper(II) to give 16.01 mM of secondary dithizonate, CuDz. In complete contrast to the hypothesis put forward by Freiser and Freiser[10], no redox change of any sort is involved.

5. Freiser and Freiser state that the addition of dithizone to a solution of copper(I) dithizonate resulted in the formation of some purple copper(II) chelate "proving that the so-called keto–enol equilibrium... is really a copper(II)–copper(I) redox equilibrium". But if dithizone can oxidise copper(I) to copper(II), it must itself be easily reduced. And in our hands the admixture of primary copper(I) dithizonate and dithizone gave a composite spectrum which showed no evidence of interaction.

Whereas so far we have only shown that the evidence in favour of the redox equilibrium postulated by Freiser and Freiser is capable of different and simpler interpretations, we shall now adduce experimental evidence that proves conclusively that primary copper(I) dithizonate cannot be a constituent of the brown secondary complex.

Table I shows the effect of equilibrating chloroform solutions of authentic primary copper(I) dithizonate, authentic primary copper(II) dithizonate, and brown secondary copper(I) dithizonate with aqueous solutions of various reagents.

TABLE I

DISTINGUISHING REACTIONS OF INDIVIDUAL COPPER–DITHIZONE COMPLEXES

Reagent in the aqueous phase	*Primary copper(I) dithizonate*	*Primary copper(II) dithizonate*	*Secondary copper(II) dithizonate*
0.1 *M* NaOH	Pale brown ppt. and dithizonate ions appear in aq. phase. After 30 min "CuDz" formed	Partial conversion to CuDz	No reaction at all
2 *M* KI (neutral solution)	Immediate reversion to green H_2Dz in org. phase and Cu(I) complexes in aq. phase	No reaction	No reaction
0.5 *M* $Na_2S_2O_3$ (neutral solution)	Immediate reversion to H_2Dz in org. phase and Cu(I) complexes in aq. phase	No significant reaction	Partial conversion to $Cu^{II}(HDz)_2$
0.5 *M* KCN (alkaline solution)	Immediate reversion in each case giving dithizone mainly as dithizone ions in aq. phase together with copper(I)–cyanide complexes		

The reactions of the three chelate complexes towards different reagents reflect on the one hand differences in the respective stability and extraction coefficients of the species Cu(HDz), $Cu(HDz)_2$ and CuDz, and on the other hand the stability of the complexes formed by copper with iodide, thiosulphate and cyanide. In each case, copper(I) complexes are formed in the aqueous phase and although measurements of stability constants have not been made under identical conditions of temperature and ionic strength, the range of published values[22] makes it possible at least to produce a consistent order of increasing complexing ability, *viz.* I^- ($\log \beta_2 = 8$–9; $\log \beta_3 = 9$–10) $< S_2O_3^{2-}$ ($\log \beta_2 = 10$–12; $\log \beta_3 = 12$–14) $\ll CN^-$ ($\log \beta_2 = 21.7$–24; $\log \beta_3 = 21.6$–28.6; $\log \beta_4 = 22.8$–30.3).

It is obvious from Table I that potassium iodide is the reagent of choice for detecting the presence of primary copper(I) dithizonate in mixtures. If, as Freiser and Freiser postulate[10], secondary copper dithizonate is only a mixture of primary copper(I) dithizonate and an oxidation product (DTD), equilibration with aqueous 2 *M* potassium iodide should immediately liberate dithizone. In practice, no such reaction takes place, which proves the complete absence of any primary copper(I) dithizonate in the brown solution of the secondary complex and disproves the "redox hypothesis".

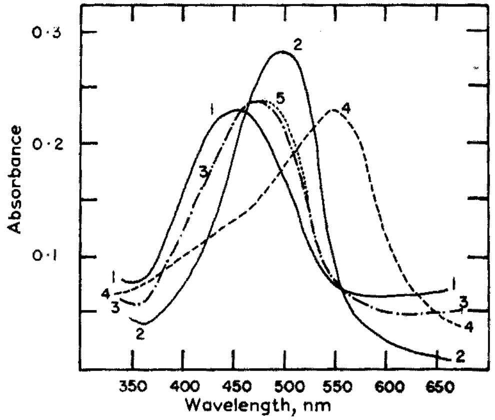

Fig. 3. Reaction between an equimolecular mixture of secondary copper(II) dithizonate and copper(I) dithizonate dissolved in chloroform with aqueous 2 *M* potassium iodide. (1) 10^{-5} *M* secondary copper(II) dithizonate; (2) 10^{-5} *M* primary copper(I) dithizonate; (3) 1 : 1 mixture (v/v) of 1 and 2; (4) spectrum of product ($\mathrm{Cu(HDz)_2}$) obtained by equilibrating this mixture for 30 min with an equal volume of 2 *M* potassium iodide; (5, dotted line) calculated spectrum for equimolar mixture of secondary copper(II) dithizonate and primary copper(I) dithizonate assuming no interaction.

This conclusion is supported by another experimental result. Secondary copper(II) dithizonate (5 ml of 10^{-5} *M*) (Fig. 3, curve 1) was mixed with an equal volume of primary copper(I) dithizonate of the same concentration (Fig. 3, curve 2). The mixture had substantially the same absorption spectrum (Fig. 3, curve 3) as that calculated (dotted curve 5) on the assumption that Beer's law holds for both complexes and that there is no interaction. Curve 4 is the spectrum of the organic phase after the mixture had been equilibrated for 30 min with aqueous 2 *M* potassium iodide. This corresponds exactly to that of a 10^{-5} *M* solution of primary copper(I) dithizonate. Clearly the rapid quantitative reaction

$$(\mathrm{Cu^I(HDz)})_{\mathrm{org}} \xrightarrow{\mathrm{I^-}} (\mathrm{H_2Dz})_{\mathrm{org}} + \Sigma \mathrm{Cu^I I}_j \qquad (2)$$

is followed quantitatively by

$$(\mathrm{Cu^{II}Dz})_{\mathrm{org}} + (\mathrm{H_2Dz})_{\mathrm{org}} \rightarrow (\mathrm{Cu^{II}(HDz)_2})_{\mathrm{org}} \qquad (3)$$

Had Freiser and Freiser's hypothesis been correct, the 10^{-5} *M* solution of secondary copper dithizonate would be $0.667\cdot10^{-5}$ *M* in copper(I) dithizonate and $0.333\cdot10^{-5}$ *M* in DTD. The admixture with primary copper(I) dithizonate (Fig. 3, curve 3) would thus have been $0.8335\cdot10^{-5}$ *M* in copper(I) dithizonate and $0.1665\cdot10^{-5}$ *M* in DTD. On equilibration with potassium iodide one would have expected the immediate appearance of $0.8335\cdot10^{-5}$ *M* dithizone in the organic phase with copper(I) complexes in the aqueous phase. As Fig. 3 shows, no dithizone whatsoever is set free.

There is one further piece of evidence to disprove the presence of copper(I) dithizonate as a component of secondary copper(II) dithizonate. The i.r. spectrum of the copper(I) complex does display the characteristic :NH stretching frequency at 3220 cm^{-1} and bending frequency at 1525 cm^{-1}; the spectrum of secondary copper(II) dithizonate shows an :NH group to be absent[6–9].

Although there can be no doubt that Freiser's concept of secondary copper(II) dithizonate as a mixture of copper(I) dithizonate and some oxidation product of dithizone must be rejected, the problem of its actual structure remains. This must contain no :NH group, must satisfy the normal coordination number of copper and must provide for electron pairing to secure a lower paramagnetism than 1.8 B.M.

Some years ago the dimeric structure (VIII) was suggested[9,23]. It is known that for steric reasons the stabilities of 1:1 complexes of copper(II) with 1,2-diaminoalkanes decrease with increasing alkyl substitution on the nitrogen atoms[24] until a point is reached with N,N,N′-triethylethylenediamine when a bis-complex cannot be formed; at the high pH engendered by excess of the very basic ligand, a proton ionises from water coordinated to the copper(II) and the resultant unipositively charged species (V) dimerises through hydroxyl bridges, thus:

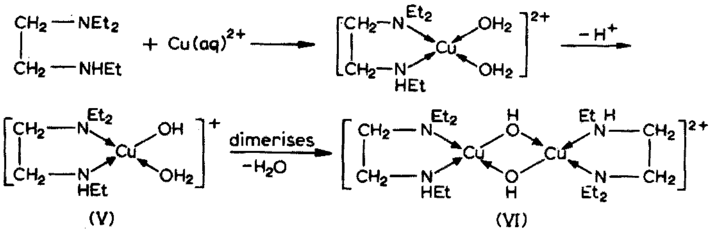

The copper atoms in the bridged structure (VI) must be closer together even than in the dimer of copper(II) acetate monohydrate (VII) where electron pairing is well established[25].

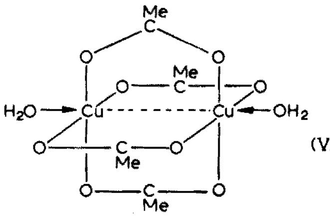
(VII)

Precisely similar conditions occur in the formation of secondary copper dithizonate *viz.* a deficiency of dithizone relative to copper and a high pH. The sequence of reactions can be envisaged as follows:

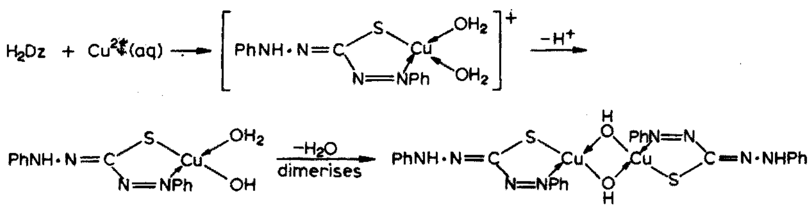

(VIII)

The dimer (VIII) will have the same ultimate composition as the monohydrate $CuDz \cdot H_2O$. The compositions CuDz (Duncan) and $CuDz \cdot 2H_2O$ (Sandell) have been proposed for the solid, but, as can be seen from Table II the published figures do not distinguish unambiguously between the various possibilities, though they favour, on the whole, the composition $CuDz \cdot H_2O$. Table II includes analyses for two solid samples prepared by Ramakrishna[23], one (A) according to Geiger and Sandell's procedure[4], the second (B) by a modified procedure in which great care was taken to obtain a dry sample. It should be emphasised that the spectra obtained for solutions of these solids in chloroform were identical with those obtained by liquid–liquid extraction.

TABLE II

ANALYSES OF SOLID PREPARATIONS OF SECONDARY COPPER(II) DITHIZONATE

Author	*Formula proposed*	*Found*					
		C	*H*	*N*	*S*	*Cu*	*M*
Duncan and Thomas[8]	CuDz	43.9, 43.9	3.3, 3.5	—	9.5, 9.6	19.3, 19.6[a]	—
Geiger and Sandell[4]	$CuDz \cdot 2H_2O$	—	—	—	—	19.4	—
Ramakrishna[23] (A)	$CuDz \cdot 2H_2O$	44.85	3.13	—	—	18.0	589[c]
(B)	$CuDz \cdot H_2O$	46.41	3.52	16.75	—	18.3	610[c]
Meriwether *et al.*[6]	$CuDz \cdot 2H_2O$	46.64	3.50	14.16[b]	—	17.7	—
Calc. for CuDz		49.12	3.17	17.64	10.08	20.00	317
$CuDz \cdot H_2O$		46.49	3.60	16.68	9.54	18.92	335
$CuDz \cdot 2H_2O$		44.12	3.99	15.83	9.06	17.99	353

[a] Calculated from weight of ash. [b] This must be a typographical error. [c] See experimental section.

By isopiestic measurements in chloroform (see *Experimental*) with azobenzene as a comparison solute, the molecular weights of samples A and B were found to be 589 and 610, respectively, pointing to a dimerised species which dissociated to some extent in solution and favouring the composition Cu_2Dz_2.

We have not been able to obtain unambiguous proof of the presence of the elements of water in secondary copper dithizonate. Infrared measurements on solid samples do not settle the point owing to the difficulty of obtaining truly anhydrous samples. It is, however, significant that the spectrum of a sample in $CDCl_3$ that had been equilibrated with H_2O could not be distinguished from one that had been shaken with D_2O.

Formula (VIII) must, however, be rejected on other grounds for all i.r. studies (*v.s.*) have failed to detect either in solution in CS_2 or in the solid state any trace of the

:N–H stretching frequency at 3200 cm^{-1} or of the :N–H bending frequency at 1525 ± 10 cm^{-1} which are found in all the primary metal dithizonates[6,9]. The only formula consistent with the analyses, with the low or negligible paramagnetism, with the molecular weight and the absence of :NH groups would appear to be the resonance hybrid (IX) of which two canonical forms are shown as (IXa) and (IXb). This formula was proposed quite independently by Alsop[19].

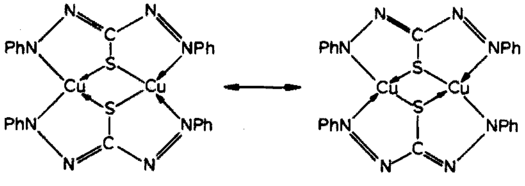

(IXa) (IXb)

Clearly all C–N bonds, all N–N bonds, and all Cu–S bonds should have the same bond order and, in contrast to the situation with primary metal dithizonates where the two phenyl groups are distinguishable, the four phenyl groups in IX are equivalent. It should be possible to study this point by a careful analysis of the deformation vibrations δ(C–H) of the phenyl groups or by high-resolution n.m.r. with a sufficiently soluble homologue of dithizone as the ligand. A reduction or cancellation of the paramagnetism due to the unpaired electron in each of the two copper atoms could result from sideways overlap of appropriately orientated orbitals or by superexchange via the intervening sulphur atoms[25]. A plot of the observed magnetic susceptibility decreased from 80 to 220 K and then increased with temperature: it could be explained if the antiferromagnetic sample (IX) was contaminated with about 4% of a paramagnetic impurity (possibly I). However, the confirmation of the postulated structure (IX) and the possibility that each molecule of the dimer involves two molecules of water must await a full X-ray crystallographic investigation of a single crystal.

If formula (IX) is acceptable for secondary copper dithizonate, a similar structure could be proposed for those formed by Hg(II), Pt(II) and Pd(II). For the secondary complexes derived from uninegative cations such as Ag$^+$, Cu$^+$ and ArHg$^+$, we propose the formula (X)

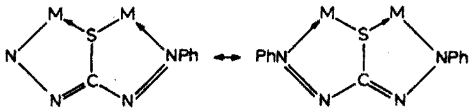

(M = Ag$^+$, Cu$^+$, ArHg$^+$)

where the coordination requirements of the metal may be completed by intermolecular bonding.

EXPERIMENTAL

Reagents

Dithizone, chloroform and aqueous buffers were purified as described in previous papers in this series and the customary precautions were taken in cleaning all glassware and optical cells for use with dithizone and its metal complexes. Absorptiometric measurements were carried out in matched 1-cm silica cells with a Unicam SP500 spectrophotometer and spectra were also recorded with the SP700.

Primary copper(II) dithizonate

This was prepared by equilibrating purified dithizone in chloroform (10 ml of $2.18 \cdot 10^{-5}$ *M*) with an equal volume of AnalaR copper(II) sulphate of the same concentration at pH *ca.*·2.5 for 30 min. The phases were allowed to separate and the absorption spectrum of the organic phase was measured to give λ_{max} 545 nm, ε_{max} 45,000 in agreement with other authors[3-7,23].

Secondary copper(II) dithizonate

Solutions were prepared from primary copper(II) dithizonate by equilibrating its chloroform solution (10 ml of $1.09 \cdot 10^{-5}$ *M*) with an equal volume of 0.1 *M* sodium acetate containing a 10-fold excess of copper(II) for 30 min. After the phases had separated the organic layer was removed. From the absorption spectrum, $\lambda_{max} = 450$ nm and $\varepsilon_{max} = 23{,}000$. Various values appear in the literature *viz.* 455[3], 448[7], 450 and 560[26], 445[5,6], 442 nm and $\varepsilon_{max} = 22{,}570$[23].

Solid sample A was prepared by the method given by Geiger and Sandell[4] and dried over magnesium perchlorate (m.p. 175–178°; found: C, 44.85%, H, 3.13%, Cu, 17.99%). A sample dissolved in chloroform (0.04072 g l^{-1}) gave a spectrum with λ_{max} 442 nm and absorbance 1.095 (1-cm cell) corresponding to $\varepsilon_{max} = 18{,}300$ if the formula is taken as $(CuDz \cdot H_2O)_2$, M = 671.8.

Solid sample B was prepared by dissolving highly purified dithizone (0.5 g; peak ratio 2.59) in pure chloroform (50 ml) and shaking mechanically with a solution of copper sulphate (25 g) in water (100 ml) to which aqueous ammonia (25 ml) had been added to give pH *ca.* 6. A violet precipitate formed first and then basic copper salt separated. After 2 h the organic layer was withdrawn and washed several times with deionised water until this remained perfectly clear. It was then dried over anhydrous sodium sulphate and the solvent removed by suction in a vacuum desiccator equipped with a small heating coil. The brown residue (0.4 g, m.p. 190–192°) was dissolved in chloroform (5 ml) and the dark brown solid precipitated by adding hexane was dried *in vacuo* over magnesium perchlorate (m.p. 198–200°; found: C, 46.41%; H, 3.52%; N, 16.75%; Cu, 18.30%).

A sample dissolved in chloroform (0.0368 g l^{-1}) had an absorbance of 1.262 at 442 nm corresponding to $\varepsilon_{max} = 23{,}000$.

The molecular weight was determined isopiestically as described by Morton *et al.*[27]. In this method a solution of the secondary copper dithizonate in chloroform (Sample A, 0.0125 g) contained in a small weighing bottle and a solution of azobenzene (0.0051 g) in a second weighing bottle were placed in a container containing chloroform from which the air had been removed, and gently rocked in a thermostat at 20°. At intervals the weighing bottles were removed, capped and weighed to obtain the concentration of each of the solutions. The molecular weight was calculated after equilibrium had been reached, when the weights of chloroform were 5.1510 and 6.7980 g respectively.

Time (h)	30	48	72	96
Calculated molecular weight				
Sample A	530.8	578.0	588.9	589.1
Sample B	580.0	604.8	610.0	610.0

Primary copper(I) dithizonate

A solution of copper(II) sulphate (10 ml of $2.10 \cdot 10^{-5}$ M) was first reduced by adding a large excess of 10% hydroxyammonium chloride and then shaken with an equal volume of a solution of purified dithizone of the same concentration ($2.10 \cdot 10^{-5}$ M) for 3 min. The organic phase was then separated and its spectrum recorded (λ_{max} 490 nm, $\varepsilon_{max} = (27.9 \pm 1) \cdot 10^3$).

The reaction between primary copper(II) dithizonate and copper(II)

Aliquot portions (10 ml) of $8.01 \cdot 10^{-6}$ M primary copper(II) dithizonate in chloroform were equilibrated for 30 min with x ml of $4 \cdot 10^{-5}$ M $CuSO_4$ and $(10-x)$ ml of 0.1 M sodium acetate that had been adjusted to pH 10.75 by adding sodium hydroxide. After phase separation the organic layers were removed and their spectra recorded. Results are shown in Figs. 1 and 2.

The reaction between secondary copper(II) dithizonate and dithizone

Aliquot portions (5 ml) of a $1.055 \cdot 10^{-5}$ M solution of secondary copper(II) dithizonate in chloroform were mixed with x ml of a $4.45 \cdot 10^{-5}$ M solution of dithizone and $(5-x)$ ml of chloroform and equilibrated (30 min) with 10 ml of 0.1 M acetic acid. After the phases had separated the spectrum of the organic layer was recorded.

The reaction between secondary copper(II) dithizonate, primary copper(I) dithizonate, and potassium iodide

The details are given in the legend to Fig. 3.

We gratefully acknowledge the loan of a Unicam SP700 recording spectrophotometer by the Royal Society and financial support from Imperial Chemical Industries Ltd. We also wish to thank Drs. Ramakrishna and Alsop for allowing us to quote unpublished results from their doctoral theses and Dr. A. Earnshaw for measuring the temperature dependent magnetic susceptibility of secondary copper dithizonate.

SUMMARY

Secondary copper(II) dithizonate has been prepared and its composition and reactions reinvestigated. The solid complex is shown to be a dimer in chloroform solution and the analysis is consistent with the composition $CuDz \cdot xH_2O$ where $x = 1$ or less. A new structural formula is proposed which is consistent with the absence of any frequencies from an :N–H group in the infrared spectrum, and which accounts for the electron pairing indicated by the low paramagnetic moment, $\mu_{eff} = 0.63$ B.M. Secondary copper(II) dithizonate is shown to react stoicheiometrically with copper(II) to give primary copper(II) dithizonate. No reaction takes place between equimolecular amounts of secondary copper(II) dithizonate and primary copper(I) dithizonate until potassium iodide is added, when primary copper(II) dithizonate (and no dithizone) is formed quantitatively in the organic phase. Reactions of primary copper(II) dithizonate, primary copper(I) dithizonate and secondary copper(II) dithizonate with OH^-, I^-, $S_2O_3^{2-}$ and CN^- are reported. The possibility that secondary copper(II) dithizonate is actually a mixture of primary copper(I) dithizonate with an oxidation product of dithizone is shown to be untenable.

RÉSUMÉ

Le dithizonate de cuivre(II) secondaire a été préparé; sa composition et ses réactions sont examinées. Le complexe solide est un dimère, en solution dans le chloroforme: $CuDz \cdot xH_2O$ où $x=1$ ou moins. Une nouvelle structure est proposée.

ZUSAMMENFASSUNG

Es wurde sekundäres Kupfer(II)-dithizonat hergestellt; seine Zusammensetzung und seine Reaktionen wurden erneut untersucht. Der Komplex liegt in Chloroform dimer vor; die Analyse stimmt mit der Zusammensetzung $CuDz \cdot xH_2O$ überein, wobei $x=1$ oder kleiner. Es wird eine neue Strukturformel vorgeschlagen, die mit dem Fehlen von Frequenzen einer :N–H-Gruppe im Infrarotspektrum in Einklang steht und die die Elektronenpaarung berücksichtigt, die durch das niedrige paramagnetische Moment, $\mu_{eff}=0.63$ B.M. angezeigt wird. Sekundäres Kupfer(II)-dithizonat reagiert mit Kupfer(II) stöchiometrisch zum primären Kupfer(II)-dithizonat. Zwischen äquimolaren Mengen von sekundärem Kupfer(II)-dithizonat und primärem Kupfer(I)-dithizonat findet keine Reaktion statt, ausser wenn Kaliumjodid zugefügt wird, wobei quantitativ primäres Kupfer(II)-dithizonat (und kein Dithizon) in der organischen Phase gebildet wird. Es wird über Reaktionen von primärem Kupfer(II)-dithizonat, primärem Kupfer(I)-dithizonat und sekundärem Kupfer(II)-dithizonat mit OH^-, J^-, $S_2O_3^{2-}$ und CN^- berichtet. Die Ansicht, dass sekundäres Kupfer(II)-dithizonat in Wirklichkeit ein Gemisch von primärem Kupfer(I)-dithizonat mit einem Oxidationsprodukt von Dithizon sei, wird widerlegt.

REFERENCES

1 G. Iwantscheff, *Das Dithizon und seine Anwendung in der Mikro- und Spurenanalyse*, Verlag Chemie, Weinheim, 1958.
2 H. Fischer, *Angew. Chem.*, 50 (1937) 919.
3 F. Koroleff, *Merentutkimuslaitoksen Julkaisu Havsforskningsinstitutets*, No. 145, Helsinki, 1950.
4 R. W. Geiger and E. B. Sandell, *Anal. Chim. Acta*, 42 (1953) 197.
5 R. F. Bryan and P. M. Knope, *Proc. Chem. Soc.*, (1961) 203.
6 L. S. Meriwether, E. C. Breitner and N. B. Colthup, *J. Amer. Chem. Soc.*, 87 (1965) 4448.
7 A. Dyferman, *Acta Chem. Scand.*, 17 (1963) 1609.
8 J. F. Duncan and F. G. Thomas, *J. Chem. Soc.*, (1960) 2814.
9 H. M. N. H. Irving and R. S. Ramakrishna, unpublished observations.
10 B. Freiser and H. Freiser, *Anal. Chem.*, 42 (1970) 305.
11 A. W. Nineham, *Chem. Rev.*, 55 (1955) 380.
12 H. Irving, J. B. Gill and W. R. Cross, *J. Chem. Soc.*, (1960) 2095 and refs. therein.
13 J. B. Gill and A. Prescott, to be published.
14 L. S. Meriwether, E. C. Breitner and C. L. Sloan, *J. Amer. Chem. Soc.*, 87 (1965) 4441.
15 H. M. N. H. Irving and A. M. Kiwan, *Anal. Chim. Acta*, 45 (1969) 19.
16 A. M. Kiwan and M. F. Fouda, *J. Organometallic Chem.*, 23 (1970) 19.
17 H. M. N. H. Irving and T. Nowicka-Jankowska, *Anal. Chim. Acta*, 54 (1971) 55.
18 A. M. Kiwan and H. M. N. H. Irving, *Anal. Chim. Acta*, in press.
19 P. A. Alsop, *Ph.D. Thesis*, London, 1971.
20 H. M. N. H. Irving, A. M. Kiwan, D. C. Rupainwar and S. S. Sahota, *Anal. Chim. Acta*, in press.
21 A. M. Kiwan and H. M. N. H. Irving, *J. Chem. Soc., B*, (1971) 901; *Chem. Commun.*, (1970) 928.
22 *Stability Constants*, Chem. Soc. Spec. Publ. No. 17, 1964.
23 R. S. Ramakrishna, *D. Phil. Thesis*, Oxford, 1961.
24 H. Irving and J. T. Griffiths, *J. Chem. Soc.*, (1954) 213 and refs. therein.
25 A. Earnshaw, *Introduction to Magnetochemistry*, Academic Press, London and New York, 1968.
26 T. Ashizawa, *Bunseki Kagaku*, 10 (1961) 350.
27 J. E. Morton, A. N. Campbell and T. S. Ma, *Analyst*, 78 (1953) 722.

Analytica Chimica Acta
Elsevier Publishing Company, Amsterdam
Printed in The Netherlands

A SYRINGE DILUTION METHOD OF CALIBRATION FOR THE GAS CHROMATOGRAPHIC ANALYSIS OF GASES

O. F. FOLMER Jr.
Research and Development Laboratories, Ponca City, Okla. 74601 (U.S.A.)

(Received 7th May 1971)

The analysis of gases, particularly for trace components, is an application to which gas chromatography is well suited. Such analyses are frequently hampered by the lack of suitable quantitative standards for calibration. Reliable standards containing the required compounds in concentrations of a few parts per million are difficult to obtain and frequently expensive. For this reason several techniques have been devised to permit the analyst to make up his own calibration standards.

An apparatus for the calibration of detectors based on the exponential decay of the concentration of a gaseous substance was described by Lovelock[1] in 1960. The apparatus basically consists of a flask with an internal stirrer into which a measured amount of a test gas is placed. Carrier gas flows through the flask at a constant rate to the detector under test. The flowing carrier gas both dilutes the test gas and sweeps it into the detector. The concentration of the test gas in the flask is related to time as described by the following equation:

$$C = C_0 e^{-\frac{QT}{V}} \tag{1}$$

where C is the concentration in the flask at time T, C_0 is the concentration immediately after addition of the test gas, Q is the flow rate of the carrier gas, and V is the volume of the flask. Assuming no slow desorption or adsorption of test gas on the walls of the apparatus, this equation can be used to calculate the concentration of the test gas in the flask at any given time. Test gases are usually chosen so that sorptive effects are negligible.

Roske and Fuller[2] describe a variation of the Lovelock device in which sample gas as well as carrier gas can be added continuously. Thus, two modes of operation are possible, exponential increase of sample concentration as well as exponential decrease.

Varian Aerograph markets a device which is described by Hartmann *et al.*[3,4] as being similar to that of Lovelock.

Fowlis and Scott[5] describe a procedure in which the sample is partitioned between a liquid and the gas in a volume above the liquid. The gaseous volume is swept by a carrier gas leading to an exponential dilution of the sample.

Scaringelli *et al.*[6] describe the use of permeation devices for preparing gas standards in the p.p.m. to p.p.b. concentration range. While excellent accuracy can be obtained in standards prepared in this manner, the procedures are exacting, and a precise control over environmental conditions such as temperature is necessary.

Another method, also requiring careful technique and precise control of parameters, is that reported by Angely *et al.*[7]. In this method the binary gas mixtures are prepared by combining two very carefully regulated separate flows of the pure gases. Accuracy appears to be very good but is dependent on exact control of gas flows and exact measurement of various gas pressures, including atmospheric pressure.

This paper reports a simple procedure in which successive dilutions are made in a syringe. Such a series of dilutions gives rise to a series of exponentially decreasing concentrations which can range from 100% to the limit of detection of the chromatographic system used.

EXPERIMENTAL

Equipment

Various syringes were used to make series of dilutions. These were a 0.5-ml syringe with replaceable needle, a 0.5-ml syringe with fixed needle (both made by Precision Sampling Corp., P. O. Box 15119, Baton Rouge, La. 70815); a Hamilton No. 750 syringe of 0.5 ml capacity (Hamilton Company, Whittier, Calif.); a Becton-Dickenson, 1-ml tuberculin syringe, No. 1YT; and a Becton-Dickenson, $\frac{1}{4}$-ml tuberculin syringe, No. 2001 (Becton, Dickenson and Company, Rutherford, N.J.).

The chromatograph used was an F & M model 810 (F & M Scientific Company, now Hewlett-Packard Company, Avondale Division, Avondale, Pa.), modified by the addition of a pair of Aerograph (Varian Aerograph, Walnut Creek, Calif.) flame ionization detectors including the dual electrometer from the Aerograph 660 chromatograph.

Peak area was measured by an Infotronics Digital Readout System, Model CRS-104 (Infotronics Corporation, Houston, Texas). The electrometer attenuation for nearly all of this work was × 100. A few series were run at × 1000.

Chromatographic columns

Several columns and conditions were used in this work, from a 223-cm (7-ft), 0.25-cm i.d. (3/16-in. o.d.) column at 70° to a 91-cm (3-ft), 0.25-cm i.d. (3/16-in. o.d.) column at room temperature. The packing of these columns was 10% UCW-98 on 70–80 mesh Anakrom ABS. Flow in the long column was about 40 ml min^{-1}, and flow in the short column was about 12 ml min^{-1}; nitrogen was used in both cases. Some work was also done with a short open tube at room temperature with about 12 ml min^{-1} flow of nitrogen.

Gases

The gases used as samples were Phillips (Phillips Petroleum Company, Bartlesville, Okla.) pure grade, except for acetylene, ethyl chloride, and methyl chloride. The acetylene was welding-grade samples from a welding torch; the ethyl chloride and methyl chloride were obtained from the Matheson Company, La Porte, Texas. Two gas mixtures obtained from Scott Research Laboratories, Inc., Perkasie, Pa., were used to check calibration accuracy at the 5–10 p.p.m. level.

Procedure

A syringe, such as the 1-ml tuberculin syringe, is flushed with the desired sample gas either by repetitive filling and emptying of the syringe or by flowing the sample gas through the syringe. Any of several techniques may be used so long as all of the air is eliminated and the syringe is filled (approximately to capacity) with sample gas.

Just before making an injection, the excess of sample is expelled leaving only the amount to be injected, *e.g.* 0.1 ml. This amount (0.1 ml) is then injected, and the syringe is laid aside until all the components of the sample have eluted.

At this time the syringe plunger is drawn back to exactly 0.1 ml, drawing in this amount of air. Then 0.1 ml of the resulting mixture is immediately injected and comprises the first dilution of the original sample.

The syringe is again laid aside until all the sample components have eluted, and again 0.1 ml of air is drawn into the syringe and 0.1 ml of the resulting mixture in the syringe is injected.

This procedure can be repeated until the component peaks become too small to measure.

An alternative procedure differs from the original procedure in that the syringe is flushed and filled with the original sample after each injection. The first injection of the original sample concentration is done as before. The syringe is then refilled with original sample and the deliverable contents expelled into the air. The plunger is drawn back to fill the syringe with air to the volume to be injected. This injection is the first dilution. The syringe is refilled again with original sample, and the deliverable volume is expelled, the syringe filled with air to the volume previously injected and the deliverable volume expelled again. A second time air is drawn into the syringe to the volume previously injected and this time injected into the chromatograph. This is the second dilution. The syringe is again filled with original sample, and a third dilution is made. This procedure can be continued through as many stages of dilution as are required.

The alternative procedure has several advantages over the original. Multiple, independent injections of each dilution can be prepared; this allows better accuracy. An error in technique at any point does not ruin the whole dilution series, merely one step, which can be re-done. More reproducible results are obtained with the alternative procedure when used with gas chromatographic columns requiring high head pressure. The sole disadvantage of the alternative procedure is that it is somewhat longer than the original procedure.

With either procedure it is sometimes better to use a pure grade of inert gas (such as nitrogen) from a cylinder instead of laboratory air for preparing dilutions. There can be impurities in the air of such nature and quantity that serious interference with the component peaks of interest occurs.

RESULTS AND DISCUSSION

If the peak areas resulting from a series of injections as described in the *Experimental* are plotted on semi-log graph paper against the number of the injection (the injection number being on the linear scale), then these points fall on a straight sloping line An example of this is shown in Fig. 1. The points are from a series of dilutions of Phillips Mixture No. 34 and indicate the peak areas obtained from propane, which amounted to 8 mol-% in the original mixture. Similar plots result when a series of such dilutions are made with samples of acetylene, ethane, normal butane, isobutane, and ethyl chloride. Impurities present in the original gas sample provide peak areas which show the same relationship with injection number. Figure 2

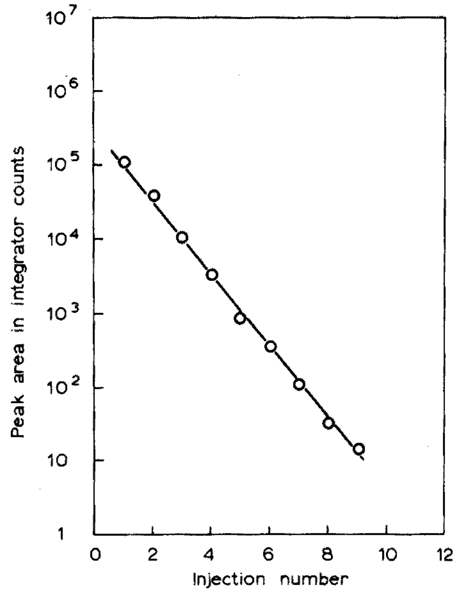

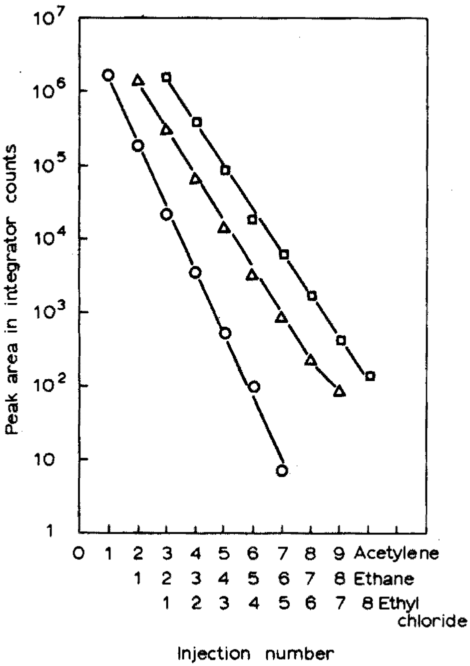

Fig. 1. Exponential dilution of propane contained in Phillips Mixture No. 34.

Fig. 2. Exponential dilutions of acetylene (○), ethane (△) and ethyl chloride (□).

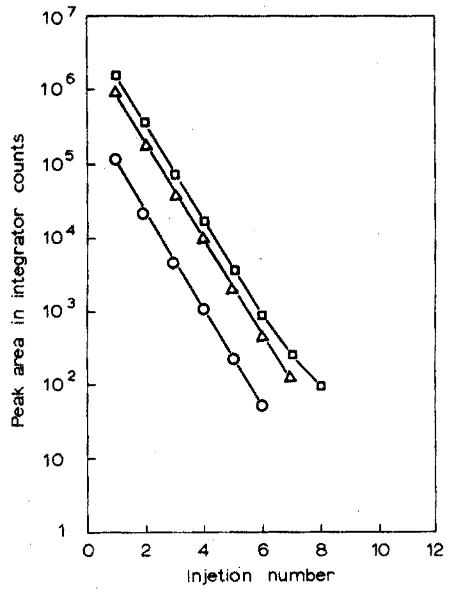

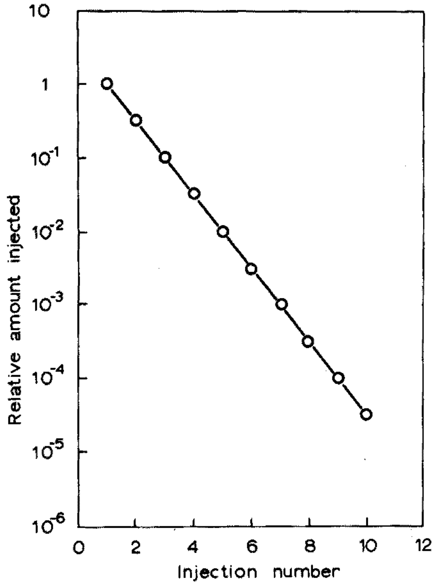

Fig. 3. Exponential dilution of Phillips Mixture No. 34. (○) Propane; (□) isobutane and isobutene; (△) *n*-butane and *n*-butenes.

Fig. 4. Calculated relative amount of propane injected in the dilution series plotted in Fig. 1.

shows plots made with dilutions of acetylene, ethane, and ethyl chloride. Figure 3 shows a plot of the three major peaks from Phillips Mixture No. 34. The slope in Fig. 3 is different from that in Fig. 1 because a different syringe was used.

These results indicate that the amount of material in successive injections decreased in an inverse exponential fashion. Since the same volume was injected each time, then, necessarily, the concentration decreased in an exponential manner.

A reasonable explanation can be based on the fact that some residual gas remains in a syringe when the plunger has been completely depressed. If a measured volume of air is drawn into the syringe, the residual gas will be diluted by a factor depending on the volume of air and the amount of residual gas. If this volume is expelled (the syringe plunger completely depressed again) and another equal volume of air drawn in, then a second dilution will take place with the same dilution factor as before.

For example, let the volume injected be 0.1 ml and the amount of residual gas be X ml. The concentration of gas in any injection is a product of the concentration of the gas in the previous injection and the dilution factor. In this case the dilution factor is $X/(0.1+X)$.

Initially, the syringe contains only the sample gas, and the concentration is 1 (the original concentration of the gas used); the dilution factor is 1 since the sample is undiluted. In the first dilution (the second injection) the concentration is 1 times the dilution factor, $X/(0.1+X)$. The volume injected remains constant at 0.1 ml. For the third injection the concentration is $[X/(0.1+X)][X/(0.1+X)]$ or $[X/(0.1+X)]^2$. Table I shows the dilution factors and the concentrations injected for ten injections.

TABLE I

CALCULATION OF QUANTITIES INJECTED

Injection no.	*Concentration in previous injection*	*Dilution factor*	*Concentration in the volume injected*
1	1.000[a]	1.000	1.000
2	1.000[a]	$X/(0.1+X)$	$X/(0.1+X)$
3	$X/(0.1+X)$	$X/(0.1+X)$	$[X/(0.1+X)]^2$
4	$[X/(0.1+X)]^2$	$X/(0.1+X)$	$[X/(0.1+X)]^3$
5	$[X/(0.1+X)]^3$	$X/(0.1+X)$	$[X/(0.1+X)]^4$
6	$[X/(0.1+X)]^4$	$X/(0.1+X)$	$[X/(0.1+X)]^5$
7	$[X/(0.1+X)]^5$	$X/(0.1+X)$	$[X/(0.1+X)]^6$
8	$[X/(0.1+X)]^6$	$X/(0.1+X)$	$[X/(0.1+X)]^7$
9	$[X/(0.1+X)]^7$	$X/(0.1+X)$	$[X/(0.1+X)]^8$
10	$[X/(0.1+X)]^8$	$X/(0.1+X)$	$[X/(0.1+X)]^9$

[a] This is a relative value; the absolute value depends on the concentrations of the component in question in the gas sampled.

The numerical value of the dilution factor can be derived from a semi-log plot of injection number *versus* the integrated detector response such as shown in Fig. 1. The dilution factor is the antilog of the slope of this line. Taking the original gas concentration to be 1.000 and using the experimentally derived dilution factor, relative concentrations for successive dilutions can be calculated. A semi-log plot is shown in Fig. 4.

A least-squares linear regression analysis of the log of the integrated response and the log of the calculated concentrations for the data in Fig. 1 gives the following equation:

$$\log Q = 0.999 \log R - 5.01 \tag{2}$$

where Q is the calculated concentration and R is the integrated response. This equation can be considered a sufficiently close approximation to

$$\log Q = 1.000 \log R - 5.00 \tag{3}$$

which is the equation of a straight line, $Q = 10^{-5} \cdot R$. This indicates that there is a linear relationship between concentration and response over the range of dilutions performed and that the smallest concentrations can be calculated from the concentration of the original gas and the experimentally derived dilution factor.

Although the relationship between response and amount injected is a linear one, both for convenience and precision, it should be treated as a log–log function. The values cover such a wide range (10^4 or 10^5 to 1) that linear plotting is out of the question; two semi-log plots or one log–log plot is necessary for graphical treatment. A least-squares linear regression analysis of Q and R provides a very poor fit at the lower values; order-of-magnitude inaccuracy can occur. A least-squares linear regression analysis of $\log Q$ and $\log R$ gives an error of only 21% (relative) for the lowest value of Q.

As a check on the preceding reasoning, two independent standards were run and calculated on the basis of the series of dilutions of propane plotted in Fig. 1.

The propane dilution series (Figs. 1 and 4) will be used as an example of the method of calculation.

The peak area of the sample peak and the graph in Fig. 1 are used to find an "Injection number" corresponding to the peak area. This "Injection number" is then used with the graph in Fig. 4 to find the relative quantity injected. The following formula is then used to calculate the concentration of the sample peak:

$$C_s = Q \cdot \frac{V_Q}{V_s} \cdot P$$

where P = concentration of compound used in dilution series, C_s = concentration of sample peak, Q = relative quantity injected, determined from graphs, V_Q = volume injected in dilution series, and V_s = volume injected of mixture containing sample peak.

In calculating the concentration of propylene in standard Mixture No. 14, the following values were used: $P = 8$ mol-%, $Q = 8 \cdot 10^{-4}$, $V_Q = 0.1$, $V_s = 1.0$. Substituting these values in the above formula gives:

$$C_s = 8 \cdot 10^{-4} \cdot \frac{0.1}{1.0} \cdot 8 \cdot 10^{-2}$$
$$= 6.4 \cdot 10^{-6} \text{ or } 6.4 \text{ p.p.m.}$$

Note that this concentration is in the same units as P, in this case mol p.p.m. or volume p.p.m.

An alternative procedure is to use the equation obtained from a least-squares linear regression analysis of $\log Q$ and $\log R$ to determine Q. One way of doing this is to make a least-squares linear regression analysis using log R and the injection number to obtain the log of the dilution factor, which is the slope of the line. The series of values for log Q is obtained by calculating the series 0, slope, 2 × slope, 3 × slope, etc. Then the least-squares linear regression analysis is performed to obtain an equation relating log Q to log R.

TABLE II

ANALYSIS OF SCOTT MIXTURE NO. 14, PROPYLENE IN NITROGEN

Peak area average of six runs	*Concentration (p.p.m.) calculated from*		*Nominal concn.*
	Graphical plots	*Least-squares equation*[a]	
93 ± 2.2[b] ± 12.0[c]	Conc. 6.4 ± 0.1[b] ± 0.8[c] Relative error 32 %	Conc. 7.2 ± 0.2[b] ± 0.9[c] Relative error 23 %	9.4 ± 0.5

[a] Later work gave an average of 8.5 p.p.m. from two runs using the alternative procedure of independent dilutions.

[b] 50 % confidence level.

[c] 99 % confidence level.

One standard, No. 14, contained only propylene in nitrogen. The results of six runs are shown in Table II. A second standard contained methane, ethane, propane, isobutane, and normal butane. The results of three runs of this standard are given in Table III.

The assumption of linearity made previously appears to have been valid since it leads to concentration figures which agree reasonably well with those given by the manufacturer of the gas mixtures.

There does not seem to be any particular advantage to the equation obtained from a least-squares regression analysis over the graphic plots as a means of calculation. The equation appears to give slightly better results, but t tests show that there is no statistical reason for choosing it.

The choice of method of calculation must then be based on convenience and other information obtained. The least-squares regression analysis provides statistical data such as goodness of fit of the data to a straight line and precision limits on the equation parameters as well as the calculated data points. The graphic method is faster and easier even though the least-squares regression analysis is available as a program (CØLNR$***) in the General Electric Library of Mark I computer programs.

Of the different types of syringe used, a glass syringe with a ground glass plunger and barrel, such as made by Becton-Dickenson and Company, seems to work best. A Hamilton gas-tight syringe also works well in this application. Unfortunately, Precision Sampling Corporation syringes do not seem to work so well. Dilutions made from pure gases with these syringes give a series of points of which only the first four or five fall on a straight line. The later points deviate in a curve toward greater peak area than would be expected.

TABLE III

ANALYSES OF SCOTT MIXTURE NO. 32, C_1 TO C_4 PARAFFINS IN NITROGEN

Compound	*Concentration calculated from*						*Nominal concn. (p.p.m., vol)*
	Graphic plots			*Least-squares equation*			
	p.p.m. (vol)	*99% conf.*	*Relative error*	*p.p.m. (vol)*	*99% conf.*	*Relative error*	
Methane+ethane[a]	14.2	±22.0	−20.0%	16.0	±25.0	−10.1%	17.8±0.9
Propane	9.7	± 0.7	+ 7.8%	10.6	± 1.1	+17.8%	9.0±0.5
Isobutane	8.4	± 0.7	− 4.5%	9.8	± 0.8	+11.4%	8.8±0.4
n-Butane	7.8	± 1.1	−14.3%	8.7	± 1.2	− 4.4%	9.1±0.5
Total	40.1	±13.5	−10.3%	45.1	±15.2	+ 0.9%	44.7±2.2

[a] There were interfering substances present whose effect could not be accurately removed. This probably accounts for the extremely poor precision of these values.

This behavior begins to appear at about the same peak area in different series of dilutions. It appears that some of the sample is adsorbed from the concentrated sample and later desorbs into the more dilute sample. This hypothesis is strengthened by the fact that if in the series of dilutions a longer than usual delay between injections occurs, then the next injection produces a much larger peak area than would be expected, based on the previous peak areas. This deviation from a straight line does not occur with components of small concentration in the original sample. Since Precision Sampling syringes have a relatively great surface area of Teflon, a substance known to be porous and absorptive of gases[8], absorption–desorption phenomena appear to be a reasonable explanation for these deviations from a straight line.

Such deviations generally do not appear with the other two types of syringe, although in several cases a very small deviation at a much lower peak area level has been observed.

SUMMARY

A simple method for the preparation of standard gas samples for gas chromatography is described. It is shown that successive dilutions of pure sample gas with air or an inert gas in an injection syringe yields linear calibration plots of sufficient precision. The determination of various organic gases is considered.

RÉSUMÉ

On décrit une méthode simple de préparation d'échantillons standards pour la chromatographie en phase gazeuse. Des dilutions successives de gaz pur avec l'air ou avec un gaz inerte dans une seringue d'injection permet d'obtenir un calibrage linéaire de précision suffisante. On examine le dosage de divers gaz organiques.

ZUSAMMENFASSUNG

Es wird eine einfache Methode für die Herstellung von Standard-Gasproben für die Gaschromatographie beschrieben. Es wird gezeigt, dass die sukzessive Verdünnung des reinen Probengases mit Luft oder einem Inertgas in der Injektionsspritze zu linearen Eichkurven mit genügender Reproduzierbarkeit führt. Die Bestimmung verschiedener organischer Gase wird erörtert.

REFERENCES

1 J. E. Lovelock, in R. P. W. Scott, *Gas Chromatography, 1960*, Butterworths, Washington, 1960, p. 26.
2 R. W. Roske and D. H. Fuller, *ISA Journal*, March, 1963, p. 73.
3 C. Hartmann and P. Dimick, *J. Gas Chromatogr.*, 4 (1966) 163.
4 C. H. Hartmann and K. Thompson, *Aerograph Research Notes*, Spring, 1967, p. 1.
5 I. A. Fowlis and R. P. W. Scott, *J. Chromatogr.*, 11 (1963) 1.
6 F. P. Scaringelli, A. E. O'Keeffe, E. Rosenberg and J. P. Bell, *Anal. Chem.*, 42 (1970) 871.
7 L. Angely, E. Levart, G. Guiochon and G. Peslerbe, *Anal. Chem.*, 41 (1969) 1446.
8 R. S. Juvet Jr., private communication, October 10, 1969.

Analytica Chimica Acta
Elsevier Publishing Company, Amsterdam
Printed in The Netherlands

SHORT COMMUNICATIONS

An improved technique for the preparation of pellets for X-ray spectrographic analysis on ion-exchange resins

The procedure described previously for the preparation of pellets from ion-exchange resins may be applied with good results to any resin that can be dried and will retain the adsorbed elements[1]. Disadvantages of this method are the dilution of the sample by the addition of a binder (paraffin) and the friable nature of the pellets. Recently, it has been found possible to produce pellets of excellent quality from Chelex-100 resin without the use of any binder compound. Resin treatment is the same as described previously except that the resin is quantitatively aliquoted. The combination of quantitative treatment of the resin and reproducible pelletization has virtually eliminated the need for an internal standard. The counting rate for a given element is essentially a function of the amount of that element in the resin pellet.

Quantitative treatment of resin

Chelex-100 resin comes with a water content of about 75%. This resin is first washed with a hot 0.1 *M* EDTA solution to remove trace amounts of iron and other transition metals. It is then partially dried at 50° and finally stored in a desiccator over a saturated sodium hydrogensulfate solution to provide constant humidity. The resin attains a constant water content and shows little variation in weight after storage for 2 days. Aliquots of resin are weighed to ± 1 mg. Aliquots of 180–200 mg of resin make good pellets, but all aliquots of resin used for an analysis must have the same weight.

Preparation of pellets

The ion-exchange resin is equilibrated with solutions as described previously[1].

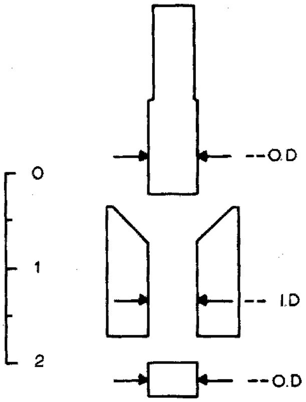

Fig. 1. Cross-section of cylindrical die for making 0.5-in diameter ion-exchange resin pellets. Parts are made of type 440 C stainless steel hardened to Rockwell C 62. Die body was honed and piston faces are polished with 1 μm diamond paste. I.d. of cylinder = o.d. pistons +0.0005 in.

The resin is separated from the solutions on a glass frit, washed with distilled water, dried for 2 h at 80° and then transferred to a warm die (Fig. 1). The die is then put into a hydraulic press and 5,000 to 7,000 pound force applied. The die is then heated with a hot air gun until it reaches 150°–180° (about 10 min). Cool air is then blown over the die, and the pressure is released after the die has cooled. This treatment results in the production of hard translucent pellets which show good stability against swelling, water uptake or crumbling. The surface of the pellet appears to be partially fused.

TABLE I

X-RAY INTENSITIES SHOWING REPRODUCIBILITY FOR CHELEX-100 RESIN PELLETS

(Analyses were made with a tungsten target on a Philips PW 1410 vacuum spectrograph; X-ray spectral lines and operating conditions were: barium $K\alpha$ line, operated at 100 kV, 35 mA; bismuth $L\alpha$ line, operated at 100 kV, 35 mA; chromium $K\alpha$ line, operated at 70 kV, 50 mA)

Element and amount in pellet	*Net (counts sec^{-1})*	*Aver. (counts sec^{-1})*	*Dev. (counts sec^{-1})*	*% Rel. dev. (counts sec^{-1})*	*Std. dev. (counts sec^{-1})*	*95% C.I. (counts sec^{-1})*
Barium	4593	4591.3	1.7	0.04	19.6	48.6
3 μmole	4610		18.7	0.41		
	4571		−20.3	−0.44		
Barium	146.7	147.6	−0.86	−0.58	3.56	5.66
0.1 μmole	145.9		−1.68	−1.14		
	152.8		5.23	3.54		
	144.9		−2.68	−1.82		
Bismuth	5025	5017	8.0	0.16	12.3	12.9
1 μmole	5020		3.0	0.06		
	5030		13.0	0.26		
	4998		−19.0	−0.38		
	5023		6.0	0.12		
	5006		−11.0	−0.22		
Chromium	9127	9169	−42.0	−0.46	36.9	58.7
1 μmole	9199		30.0	0.33		
	9149		−20.0	−0.22		
	9201		32.0	0.35		
Chromium	945	909.5	35.5	3.90	27.3	43.4
0.1 μmole	896		−13.5	−1.48		
	915		5.5	0.60		
	882		−27.5	−3.02		
Chromium	4685	4653.3	31.8	0.68	40.2	64.0
0.5 μmole	4596		−57.3	−1.23		
	4655		1.8	0.04		
	4677		23.8	0.51		

In Table I, typical results of X-ray analysis of pellets produced in the above manner are tabulated for a number of elements. Reproducibility of counting rates between pellets with the same element content are good. Repeated analysis and handling of the pellets does not alter their counting rates. However, pellets should be stored in a desiccator over anhydrous calcium sulfate to prevent slow moisture pick up.

Note added in proof

It has recently been found that pellets with better physical stability result when the dried resin absorbs some moisture by being placed in the constant humidity desiccator for 2 h before pressing.

This work was supported in part by NSF Grant GA 001667 and NSF Grant GP-24311.

Department of Geology,
Department of Chemistry,
University of Georgia,
Athens, Ga. 30601 (U.S.A.)

C. W. Blount
R. E. Channell
D. E. Leyden

1 C. W. Blount, W. R. Morgan and D. E. Leyden, *Anal. Chim. Acta*, 53 (1971) 463.

(Received 13th April 1971)

Anal. Chim. Acta, 56 (1971) 456–458

Spectrochemical analysis of thin films of binary alloys of Ni–Ta and Ni–B

This work was undertaken to meet the demand for a convenient method of determining alloying elements in various stages of the production of nickel-based thin-film alloys. Since it would be advantageous to perform the analysis with simultaneous general checking of the purity of the fabricated material, and generally only small samples were available, a spectrochemical method seemed to be most suitable. The Scheibe–Rivas technique for solutions was applied, this procedure having the necessary sensitivity and being simple and rapid enough for routine use.

Preparation of standards and samples

Specpure nickel metal was dissolved in 25% (v/v) nitric acid with heating and diluted with water to give a stock solution containing 1 mg Ni ml^{-1}. Stock solutions of niobium (for use as internal standard) and tantalum were obtained by electrolytic dissolution of the metals[1,2]. The boron solution was prepared by dissolving Specpure boric acid (Johnson-Matthey) in water.

The sets of boron and tantalum standards were prepared by mixing suitable aliquots of the stock solutions with a given volume of the nickel stock solution. Niobium was added to the tantalum standards to serve as internal standard because of the chemical and spectrochemical similarity of niobium and tantalum.

The samples to be analyzed were dissolved in 25% nitric acid with addition of 40% hydrofluoric acid and diluted to give a solution containing 1 mg of alloy per ml, like the standards.

Excitation and photometric conditions

A 0.05-ml portion of the standard or sample solution was dried on the flat end

TABLE I

EXCITATION AND DEVELOPING CONDITIONS

Spectrograph	Jarrell Ash Grating Spectrograph, Ebert Mounting, 3.4-m focal distance, grating 600 grooves mm^{-1}, first order.
Analytical lines[a]	Ta II 2635.58 Å B II 3451.28 Å Nb II 2620.45 Å Ni II 3454.16 Å
Slit width	0.030 mm
Mode of illumination	The image of the source on the collimator mirror.
Electrical parameters	Inductance: residual Capacitance: 0.0025 μF Secondary resistance: not added Auxiliary spark gap: 7 mm Analytical gap: 2 mm R.F. current: 10.6 A
Electrodes	Upper and lower: graphite rods, flat, 6 mm diam., UCP Spectrotech for Ta, ultra pure for B determination
Exposure time	45 sec
Photographic plates	Eastman SA-1
Developing	D-19, 20°, 5 min

[a] The wavelength given for boron is as corrected by the present author.

of both graphite electrodes, coated with a thin layer of collodion, and excited under the conditions given in Table I.

The transmittances of the spectral lines were measured with a non-recording Jarrell Ash microphotometer. The photographic emulsion was calibrated with a 7-step filter in the region of the analytical lines. Percentage transmittance values were

BLE II

ULTS OF PHOTOMETRIC MEASUREMENTS[a]

nent	c (%)	n	$\overline{\Delta Y}$	$S_{\Delta Y} = \sqrt{\frac{\Sigma (\Delta Y - \overline{\Delta Y})^2}{n-1}}$	$\overline{S_{\Delta Y}} = S_{\Delta Y}/\sqrt{n}$	$S_c/c = 2.303 \cdot b^{-1} \cdot S_{\Delta Y} \cdot 100$	$\overline{S_c}/c = S_c/c\sqrt{n}$
ıtalum	1.0	9	−0.15	0.071	0.024	11.1	
	2.0	4	0.31	0.064	0.037	10.0	5.0
	2.5	13	0.42	0.044	0.012	6.9	1.9
	3.0	13	0.56	0.057	0.016	8.9	2.5
	4.0	16	0.81	0.053	0.013	8.3	2.1
	5.0	12	0.88	0.037	0.011	5.8	1.7
on	0.5	10	−0.61	0.068	0.021	15.7	4.9
	1.0	12	−0.37	0.079	0.023	18.2	5.2
	1.5	9	−0.20	0.063	0.021	14.5	4.8
	2.5	9	0.03	0.070	0.023	16.1	5.4
	3.0	6	0.22	0.114	0.046	26.5	10.8
	5.0	6	0.65	—	—	—	—

= wt-% of Ta or B in the standard.
= number of measurements.
$\overline{Y}$ = mean value of the log of the intensity ratio of the analytical line pair.
/c = coefficient of variation for a single determination.
/c = relative mean standard deviation.
= the slope of the analytical curve. In the present work $b = 1.4$ for Ta and $b = 1.0$ for B.

converted to Seidel function values[3]. Corrections for background were applied throughout.

Results

The results of the photometric measurements are given in Table II. The analytical curves based on these data are straight lines. The concentration of tantalum or boron in the sample is read from the graphs.

The method covers the ranges 0.4–5% for tantalum and 0.5–3% for boron. The lower and upper limits can be varied according to interest by changing the concentration of the samples and standard solutions.

The coefficient of variation for a single determination of tantalum is about 10%; 4 determinations are sufficient to obtain a precision of 5%. For boron determination such precision can be achieved only with 10 measurements. When the concentration of boron in the alloy is higher than 3%, the precision is low and the samples to be analyzed should be diluted with nickel standard solution in order to achieve the desired concentration range.

The method described has been used for the analysis of numerous films and has proved helpful in guiding the choice of the best conditions for preparation of the alloy films.

Soreq Nuclear Research Center,
Yavne (Israel)

I. Schoenfeld

1 A. Aladjem, *Anal. Chem.*, 91 (1969) 989.
2 I. Schoenfeld, to be published.
3 D. C. Gordingley, L. I. Lacey and P. I. Sandiford, *Appl. Spectrosc.*, 8 (1954) 92.

(Received 3rd May 1971)

Analytica Chimica Acta
Elsevier Publishing Company, Amsterdam
Printed in The Netherlands

The determination of thulium(III) in borate and phosphate glasses

Methods which have been developed in this laboratory for the determination of rare earths in glasses[1–4] have been extended to the determination of thulium in sodium borate and sodium metaphosphate glasses.

Since thulium has been shown to transfer energy to erbium in these glasses[5], the fluorescence of thulium in the presence of erbium has also been studied.

Apparatus

A spectrofluorimeter built in this laboratory[1] and the Turner 210 "Spectro" spectrofluorimeter were used. Fluorescence was viewed at 135° to the excitation beam, since this was found to give the best signal-to-noise ratio. A Cary 14 spectrophotometer was used for the absorption measurements with undoped glasses as blanks. The decay times were measured as described previously by Reisfeld *et al.*[6].

Reagents

Sodium tetraborate decahydrate (Riedel), boric acid (Frutarom), sodium dihydrogenphosphate monohydrate (Mallinckrodt, 99.5% pure) and thulium oxide and erbium oxide (Molycorp., 99.9% pure) were used.

Preparation of glasses

Borate glasses. Dry thulium oxide was mixed with borax and boric acid in glass vials. Three series of mixtures were prepared:

(I) thulium only, ranging from 0.001 to 2.0 wt.%;

(II) thulium and erbium in equal concentrations, ranging from 0.25 to 2.0 wt.% of each;

(III) thulium at 1% and erbium varying from 0.25 to 2.0 wt.%.

Further details concerning borate glasses can be found in previous papers[1–4].

Phosphate glasses. Dry sodium dihydrogen phosphate was mixed with dry thulium oxide as described above. Two series of mixtures were prepared:

(IV) thulium only, ranging from 0.0005 to 1.65 wt.%;

(V) thulium at 1% and erbium varying from 0.25 to 2.0 wt.%.

Absorption, excitation and emission spectra

The absorption spectra of thulium and erbium in borate glass are shown in Fig. 1. Figure 2 presents the corrected emission and excitation spectra of thulium. The excitation spectrum from the 454-nm emission band of thulium in borate and phosphate glasses consists of bands peaking at 263, 275, 287 and 358 nm. Table I shows the relative intensities of the excitation peaks and the experimental lines compared to the centers of gravity of thulium(III) energy levels, as calculated by Carnall *et al.*[7].

The emission spectrum excited at 263 nm consists of 5 lines, peaking at 292, 350, 453, 478, and 513 nm, and the emission spectrum excited at 358 nm consists of 4 lines at 455, 478, 515, and a broad band at 650–670 nm. Table II gives the assignments of the emission spectrum and the relative intensities at 263-nm excitation.

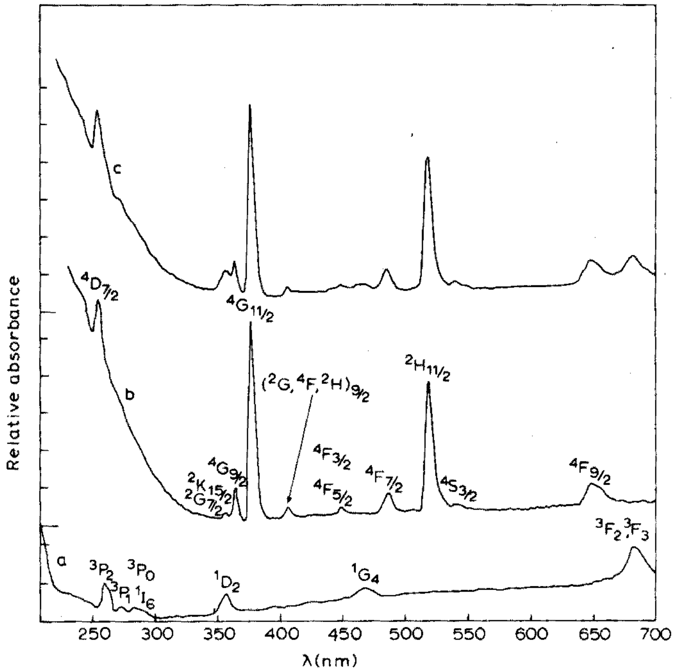

Fig. 1. Absorption spectrum in borate glass. (a) Thulium, (b) erbium, (c) thulium and erbium.

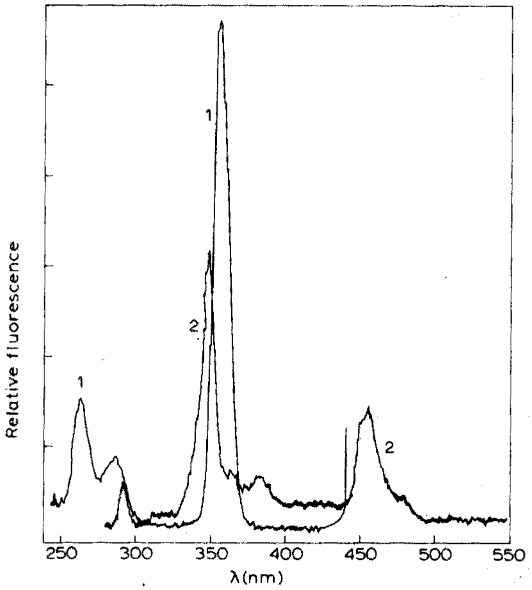

Fig. 2. Corrected excitation and emission spectra of thulium in phosphate glass. (1) Excitation spectrum at 454-nm fluorescence; (2) emission spectrum at 263-nm excitation.

TABLE I

EXCITATION SPECTRUM OF 454-nm FLUORESCENCE AND THE ENERGY LEVELS OF THULIUM

Assigned levels	*Wavenumber (cm^{-1})*		*Wavelength (nm)*	*Relative intensity*
	Literature[7]	*This work*		
${}^3H_6 \to {}^3P_2$	38171–38451	38023	263	18
${}^3H_6 \to {}^3P_1$	36472–36587	36727	275	7
${}^3H_6 \to {}^1I_6, {}^3P_0$	34403–35160	34835	287	10
${}^3H_6 \to {}^1D_2$	27956–28346	27930	358	83

TABLE II

EMISSION SPECTRUM OF THULIUM EXCITED AT 263 nm (XENON SOURCE)

Assigned levels	*Literature source*	*Wavelength (nm)*	*Wavenumber (cm^{-1})*	*Relative intensity*
${}^3P_1, {}^1I_6 \to {}^3H_6$	8	292	34248	8
${}^3P_1, {}^1I_6 \to {}^3H_4$	8,9	350	38571	45
${}^1D_2 \to {}^3H_4$	8,9	454	22026	18
${}^1G_4 \to {}^3H_6$	8,9	478	20920	3
${}^1G_4 \to {}^3H_4$ ${}^1D_2 \to {}^3F_4$	9	660	15151	0.2

Because of its low intensity, the 660-nm band could be measured only in the laboratory-built apparatus. The excitation spectrum from the 660-nm emission band consists of lines peaking at 365 and 473 nm with the strongest band at 360 nm.

Determination of thulium

Borate glasses. Fluorescence intensities as a function of thulium concentration for Series I and II, obtained by excitation at 358 nm (xenon source), are shown in Fig. 3. The relative fluorescence intensities for Series I obtained by excitation at 265 nm (mercury lamp) were only about one-third of those obtained by excitation at 358 nm, though the linear range was similar. The scattering of the experimental points with xenon excitation was much lower than that found with mercury excitation, probably because of excitation of impurities with the latter.

Phosphate glasses. Fluorescence intensity measurements as a function of the thulium concentration were obtained at 358 nm with xenon excitation only. The results are shown in Fig. 3. Linear concentration dependence was observed over the range 0–0.25 wt.% for phosphate glasses and 0–0.1 wt.% for borate glasses. The concentration range of 0.25–1.1 wt.% in phosphate glasses and 0.1–0.75 wt.% in borate glasses also showed linear dependence, but the slope was smaller. At higher concentrations, a quenching effect was observed. The decay curves of thulium(III) in phosphate glasses and in borate glasses, were simple exponentials. The measured decay times for 1 wt.% of thulium(III) in borate and phosphate glasses were 0.0135 and 0.0145 msec, respectively.

The presence of erbium affects the fluorescence of thulium, and this effect is more pronounced in phosphate glasses. The measurements shown in Table III were made at 454 nm with excitation at 358 nm.

TABLE III

RELATIVE FLUORESCENCE (RF) OF THULIUM AS A FUNCTION OF THE CONCENTRATION OF ERBIUM

$[Er^{3+}]$ (wt. %)	Borate glasses		Phosphate glasses	
	RF	I_0/I[a]	*RF*	I_0/I[a]
0	2150	1	2410	1.0
0.25	2005	1.07	2060	1.17
0.5	1720	1.25	1960	1.42
0.75	1548	1.38	1310	1.76
1.0	1290	1.66	1070	2.25
1.25	1290	1.66	975	2.52
1.5	1350	1.55	1150	2.1

[a] Ratio of maximum fluorescence of 1 wt. % of thulium (I_0) to its fluorescence at varying concentrations of erbium (I).

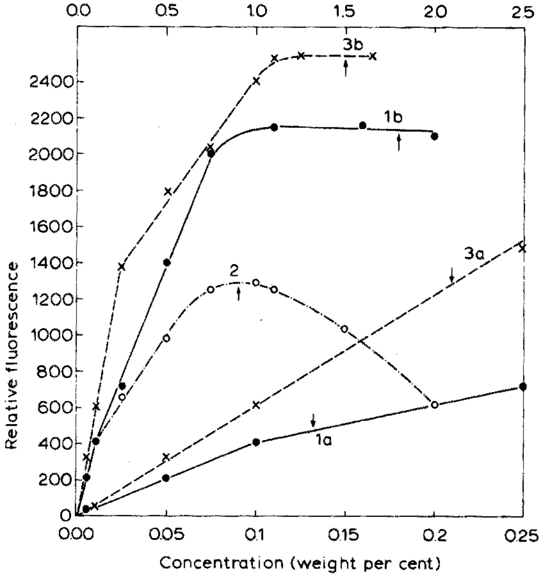

Fig. 3. Fluorescence dependence on concentration at 358-nm excitation; fluorescence at 454 nm. (1) Thulium in borate glass: (a) concentration range 0–0.25 wt. %, (b) concentration range 0–2.0 wt. %; (2) thulium and erbium in borate glass at equal concentrations, range 0.25–2.0 wt. %; (3) thulium in phosphate glass: (a) concentration range 0–0.25 wt. %, (b) concentration range 0–1.65 wt. %.

Discussion

Since the fluorescence intensity of thulium(III), both alone and with erbium in glasses, shows a linear dependence on the concentration of thulium within the range of 0–0.75 wt. % in borate glasses and 0–1.0 wt. % in phosphate glasses, these concentration ranges can be used for simple determinations. At higher concentrations, where quenching occurs, thulium can be determined by means of calibration curves as described above. The different excitation bands existing in the spectrum of thulium permit excitation at the optimal wavelength in order to prevent excitation of interfering elements.

The concentration quenching appears to be effective at distances where the energy transfer becomes appreciable. In the case described, two kinds of energy transfer exist: nonradiative transition between various electronic levels of thulium, and energy transfer between thulium and erbium, as can be seen by comparing the energy levels of these elements given by Dieke and Crosswhite[8]. The self-quenching of thulium is stronger in the borate glasses, as has been previously explained for other rare earth elements[10]. The interaction between thulium and erbium is stronger in phosphate glasses, however, as the energy transfer is promoted by the phosphate matrix.

The authors are grateful to Dr. Rance Velapoldi for measuring the spectra on the Turner instrument. This work was performed under NBS contract (G)-103.

Department of Inorganic
and Analytical Chemistry,
Hebrew University, Jerusalem (Israel)

Renata Reisfeld
Y. Eckstein

1 R. Reisfeld and E. Greenberg, *Anal. Chim. Acta*, 47 (1969) 155.
2 R. Reisfeld and E. Biron, *Talanta*, 17 (1970) 105.
3 R. Reisfeld, Z. Gur-Arieh and E. Greenberg, *Anal. Chim. Acta*, 50 (1970) 249.
4 R. Reisfeld, E. Greenberg and S. Kraus, *Anal. Chim. Acta*, 51 (1970) 133.
5 R. Reisfeld and Y. Eckstein, submitted for publication.
6 R. Reisfeld, A. Honigbaum, G. Michaeli, L. Harel and M. Ish-Shalom, *Israel J. Chem.*, 7 (1969) 613.
7 H. T. Carnall, P. R. Fields and K. Rajnak, *J. Chem. Phys.*, 49 (1968) 4424; H. T. Carnall, P. R. Fields, J. Morrison and R. Sarup, *ibid.*, 52 (1970) 4054.
8 G. H. Dieke and H. M. Crosswhite, *Appl. Opt.*, 2 (1963) 675.
9 S. Ibuki and D. Langer, *J. Chem. Phys.*, 40 (1964) 796.
10 R. Reisfeld, E. Greenberg, L. Kirshenbaum and G. Michaeli, *8th Rare Earth Conference Proc., Vol. II*, 1970, p. 743.

(Received 14th December 1970)

Analytica Chimica Acta
Elsevier Publishing Company, Amsterdam
Printed in The Netherlands

The direct determination of cadmium and mercury in the atmosphere

Numerous compounds of cadmium and mercury are poisons which have become of concern to the environmentalist. Each of these metals and their salts is widely used in industrial processes and their presence in the world's atmosphere is well documented. Mercury, because of its high vapor pressure at room temperature, is particularly hazardous. Cadmium, from an environmental health standpoint, is one of the most dangerous of the atmospheric pollutants. Cardiovascular disease has been related to inhaled doses of cadmium approximating those suffered in average urban situations[1].

The mercury concentration in the atmosphere of a Russian thermometer plant was determined as 17 μg Hg m^{-3} of air[2]. The atmosphere of some dental surgeries contained 100 μg Hg m^{-3} air[3]. The average concentration of cadmium in the atmosphere of the United States was 0.002 μg Cd m^{-3}, while the maximum concentration reported was 0.420 μg Cd m^{-3}[4].

Most of the recorded methods for the determination of mercury or cadmium in the atmosphere involve scrubbing large volumes of air. These methods are notoriously time-consuming and subject to numerous interferences. In order to eliminate these analytical problems, the instrument previously reported as successful for the direct determination of lead in the atmosphere[5] was modified for the determination of mercury and cadmium.

Equipment

The construction of the instrument has been described previously[5]. However, for present work, a commercial Barnes demountable hollow-cathode lamp was used in the studies on mercury and cadmium to provide a strong steady signal.

Calibration

In order to effect calibration it was necessary first to remove the mercury and cadmium from the air samples and then add known quantities of these elements back to the purified air. This eliminated the problems involved with variable amounts of mercury or cadmium present in air samples and permitted preparation of samples of known metal concentrations.

Removal of mercury and cadmium from air. Several scrubbing agents were investigated for the removal of the metals from the airstream. It was found that both activated charcoal and dilute nitric acid removed mercury from the air to a level below the detection limit of the instrument at flow rates of 1.0 l or less per min. A magnesium sulfate scrubber was 94% efficient under the same conditions. Based on these data, charcoal was used as a pre-scrubbing agent to supply "zero air" for calibration purposes.

After the airstream had been purified, known amounts of mercury were added before introduction into the atomizer. The results are shown in Table I and a linear plot through the origin is obtained. Similar calibration curves for cadmium were obtained (Table II). The analytical range of the determination is seen to cover those concentrations of the metals found in polluted air.

TABLE I

CALIBRATION OF THE INSTRUMENT WITH RESPECT TO MERCURY

($\lambda = 253.7$ nm. Flow rate $= 1.0$ l min^{-1}. Standard deviation is calculated for 10 separate runs at each concentration)

Concentration (μg *Hg* m^{-3})	*Absorbance*[a]	σ
30.0	0.122	0.003
54.5	0.225	0.005
161.0	0.652	0.009
188.0	0.750	0.009

[a] Average of 10 determinations.

TABLE II

CALIBRATION OF THE INSTRUMENT WITH RESPECT TO CADMIUM

($\lambda = 228.8$ nm. Flow rate $= 1.2$ l min^{-1}. Standard deviation is calculated for 5 separate runs at each concentration)

Concentration (μg *Cd* m^{-3})	*Absorbance*[a]	σ
0.98	0.221	0.013
2.51	0.509	0.025
4.42	0.921	0.028

[a] Average of 10 determinations.

Calibration for mercury. The instrument was calibrated for the determination of mercury by using elemental mercury vapor. A pool of mercury was placed in a diffusion chamber and the chamber was immersed in a constant temperature water bath held at $25° \pm 0.1°$ [5,6]. The air flow rate through the chamber was held at 1.0 l min^{-1}, and the weight of mercury diffusing out of the chamber was determined by weight losses over long periods of time. These data were used to calculate the concentration of mercury in the airstream supplied to the atomizer by this method. The calibration data and the precision of the procedure are shown in Table I.

Calibration for cadmium. Cadmium chloride was placed within a resistance heater described previously[4] and vaporized at controlled temperatures. Air was passed through the furnace at 1.2 l min^{-1} and the effluent of this injection furnace was passed serially through two nitric acid scrubbers. These solutions were then analyzed by conventional atomic absorption. No cadmium was found in the second scrubber and the data obtained from the first solution were used to calculate the concentration of cadmium in the airstream issuing from the furnace. Air containing known amounts of cadmium chloride was then fed directly into the atomizer. The calibration data and the precision of the procedure are shown in Table II.

Analytical sensitivity

Mercury. The sensitivity of the procedure for mercury was determined by diluting the flow of the effluent of the injection apparatus with pre-scrubbed air from a compressed air tank.

Air was passed into the diffusion chamber at 1.0 l min^{-1}, emerging with a mercury concentration of 30 μg Hg m^{-3}. This standard air sample was mixed with a pre-scrubbed airstream flowing at 24.0 l min^{-1}. The analytical sensitivity (1% absorption) was obtained with a mixed sample flowing at 1 l min^{-1} provided a concentration of 1.2 μg Hg m^{-3} (0.147 p.p.b.). The total weight of mercury in the absorption tube was $2 \cdot 10^{-10}$ g.

Cadmium. Cadmium-free air was prepared by scrubbing with charcoal. The pure air was then impregnated with cadmium and diluted to the desirable concentration with more pure air. One percent absorption of the 228.8-nm cadmium resonance line was measured at a concentration of 0.02 μg Cd m^{-3} (0.004 p.p.b.). The total weight of cadmium in the absorption tube was $4 \cdot 10^{-12}$ g.

Direction determination of mercury and cadmium in the atmosphere

Laboratory air samples were drawn into the instrument on various days and the resultant absorptions were measured. Based on the calibration curves, the concentrations of mercury and cadmium in the ambient atmosphere were obtained. The results are shown in Table III.

TABLE III

DETERMINATION OF MERCURY AND CADMIUM IN AIR IN BATON ROUGE, LA.

Date	*Absorbance*	*Metal concentration* ($\mu g\ m^{-3}$)
Mercury		
2-11-69	0.019	4.7
2-20-69	0.013	3.2
3-5-69	0.007	1.9
3-19-69	0.012	3.0
Cadmium		
4-15-70	0.062	0.27
4-20-70	0.040	0.18
4-24-70	0.066	0.29

Interference studies

Organic vapor interferences. In order to study the effects of the organic vapors in the atmosphere on the determination of mercury or cadmium, organic vapors were injected into the airstreams. The concentration of the vapor in the air was approximately 30 mg m^{-3}. This was well above the pollutant concentration normally encountered in the atmosphere. The effects of these vapors on the absorption of mercury at the 253.7-nm and 252.8-nm lines and on the absorption of cadmium at the 228.8-nm and 226.4-nm lines were measured. No interferences were encountered from hexane, heptane, isopropanol, *n*-butanol, *n*-butyl sulfide, acetone, acetonitrile, pyridine, benzene, nitrobenzene, toluene, bromotoluene or methyl iodide. In the determination of mercury, carbon tetrachloride caused a 2% change in percentage absorption whereas chloroform caused a 1% change. For the determination of cadmium 60 mg m^{-3} of these compounds caused changes in percentage absorption of 4% and 2%, respectively. In all cases with these chloro compounds, equal absorption of resonance and non-resonance lines was observed. This indicated molecular absorption by the chloro-compounds rather than an indirect effect on the mercury or cadmium absorption. Ambient concentrations of organic chlorine compounds do not normally approach the levels used in this study, and these compounds would not normally interfere with atmospheric determination.

Chemical interferences caused by the incomplete reduction of molecular compounds to ground-state atoms are sources of major interferences in atomic absorption. Several chemical forms of mercury and cadmium were examined. The method used for sample injection is described in the calibration of cadmium. The effluent of the injector was passed through a nitric acid scrubber, and the scrubbing solutions were analyzed by atomic absorption. From these data the concentrations of the metals in the airstream were calculated; the concentrations were then determined by absorption. The results are given in Table IV. The data in the right column were obtained by analysis of the scrubbing solutions, the data in the adjacent column by comparing the absorption of resonant radiation with the appropriate calibration curve. No evidence of interferences caused by the chemical form of the mercury was detected for the compounds studied.

TABLE IV

INTERFERENCE OF ANIONS ON MERCURY ABSORPTION AT 253.7 nm AND ON CADMIUM ABSORPTION AT 228.8 nm

Anion	*Absorbance*	*Concentration of metal by*	
		Absorption ($\mu g\ m^{-3}$)	*Scrubbing* ($\mu g\ m^{-3}$)
Mercury			
Chloride	0.524	132	133
Sulfate	0.585	146	147
Nitrate	0.288	74	73
Cadmium			
Chloride	0.221	0.98	0.99
Chloride	0.509	2.51	2.50
Nitrate	0.347	1.67	1.66
Sulfide	0.260	1.23	1.22
Sulfate	0.125	0.59	0.60

Conclusions

This method provides a rapid, sensitive and reproducible method for the continuous determination of atmospheric mercury and cadmium. The lower limit of sensitivity appears to be 1.2 μg m^{-3} and 0.02 μg m^{-3} for mercury and cadmium, respectively. The method is applicable to a wide variety of metals and their determination is presently under investigation.

The authors wish to acknowledge that this investigation was supported by Research Grant AP 00866-02, Air Pollution Control Office, Environmental Protection Agency.

Department of Chemistry,
Louisiana State University,
Baton Rouge, La. 70803 (U.S.A.)

C. M. Christian, II
J. W. Robinson

1 R. E. Carroll, *J. Amer. Med. Assoc.*, 198 (1966) 267.
2 Y. G. Sonnov, *Tr. Tsent. Inst. Usoversh. Vrachei*, 103 (1967) 19.
3 M. M. Joselow, L. J. Goldwater, A. Alverez and J. Herndon, *Arch. Environ. Health*, 17 (1) (1968) 39.
4 *Air Quality Data from the National Air Sampling Network and Contributing State and Local Networks, 1964–1965*, U.S. Dept. of Health, Education, and Welfare, 1966.
5 H. P. Loftin, C. M. Christian and J. W. Robinson, *Spectrosc. Lett.*, 3 (7) (1970) 161.
6 A. P. Altshuller and I. R. Cohen, *Anal. Chem.*, 32 (1960) 803.

(Received 6th May 1971)

Anal. Chim. Acta, 56 (1971) 466–470

The determination of vanadium and nickel in mineral oils by flameless graphite tube atomization

The development of analytical methods for certain heavy metals in mineral oils has recently become of particular interest. Special attention has been focused on vanadium and nickel principally because the ratio of these two metals in crude petroleums differs according to the geographical source of the petroleum. Their determination can therefore provide valuable information for identification of crude oils and pollution samples originating from petroleum oils[1].

Vanadium and nickel are also important constituents of common engine alloys, and their determination in worn lubricating oils can indicate the state of condition of the engine. Nickel is a serious catalyst "poison" and large amounts of vanadium in fuel oils present corrosion problems. Control of the contents of the two metals in such oils is therefore also important.

Several methods can be used, but atomic absorption spectrophotometry has been widely applied in the petroleum industry, particularly in the determination of nickel[2–6], but also in vanadium determinations[4,7]. The common analytical procedures all include dilution of the sample with an organic solvent such as xylene or methyl isobutyl ketone, followed by direct aspiration of the solution into a flame. Standard solutions are made from organic metal complexes of known composition dissolved in the same solvent. These methods have disadvantages in that very careful calibration is essential, and the required sample size can be a limiting factor in pollution work.

The graphite furnace technique for flameless atomic absorption[8] has recently been applied to urine analysis[9] and to the determination of lead in air[10]. This method offers the possibility of analysing small biological and other organic samples directly without a prior ashing or preconcentration step, the organic matter being destroyed in the graphite tube. Most of the usual contamination and loss encountered in ordinary trace element analysis is thus avoided.

In this laboratory a method has been worked out for vanadium and nickel determination in the small oil lumps picked up by the Papyrus Ship Ra II in 1970. The full analytical data obtained will be published elsewhere; the application of the flameless graphite cell atomization technique to small amounts of organically bound vanadium and nickel compounds in mineral oils is described below.

Experimental

Equipment and reagents. A Perkin–Elmer Model 303 Atomic Absorption Spectrophotometer equipped with a Perkin–Elmer (Bodenseewerk) Graphite Cell HGA 70, an automatic recorder readout accessory and a Hitachi–Perkin–Elmer Recorder Model 159 was used. A deuterium arc background corrector was applied in the procedure for nickel. Small sample aliquots were injected into the graphite tube by means of Eppendorf-Marburg micropipettes. Flame atomic absorption measurements were carried out on the instrument equipped with a Boling burner head. Vanadium and nickel single-element hollow-cathode lamps were used as light source. The xylene was of laboratory-reagent quality (Merck) and other chemicals were of reagent-grade quality.

Vanadium and nickel solutions. Stock solutions (1000 p.p.m.) were prepared from ammonium vanadate and nickel sulphate hexahydrate dissolved in 0.1 *M* nitric acid. More dilute (1.0 and 0.1 p.p.m.) standard solutions containing 5 ml of nitric acid per 100 ml were prepared daily by suitable dilution.

Measurement conditions. Before samples were atomized in the graphite tube, any solvent, organic material or other unwanted component of the matrix was removed by heating the tube in stages to certain temperatures; otherwise false signals could be obtained. The optimal times and temperatures of the various stages were found to be as follows: the sample solutions were dried at 100° and then charred at 1100°, by means of program 7 on the HGA 70 with a 30-sec sequence duration; for the atomization stage 2400° (8 V) was selected for nickel and 2700° (10 V) for vanadium.

Procedure. Weigh out a suitable quantity, *e.g.* 1 g, of oil into a 10-ml volumetric flask and dilute to volume with xylene. In the case of pollutants contaminated with insoluble material, centrifuge or filter the suspension, take 2 ml in a platinum crucible, and evaporate the xylene on a hot plate at very low heat; weigh the oil left in order to evaluate the quantity dissolved.

For vanadium inject 5–50 μl of 1-p.p.m. standard solution into the graphite tube and measure the absorption peak using program 7, 10-V atomization voltage, 30-sec sequence duration and the 318.2-nm analytical line.

For nickel inject 5–50 μl of 0.1-p.p.m. standard solution and record the peak using program 7, 8-V atomization voltage, 30-sec duration and the 232.0-nm analytical line.

Record blank values at the same instrumental settings and substract them from the analytical value after conversion to absorbance. 20 ng of vanadium or 5 ng of nickel produce about 20 % absorption at scale expansion 1. Prepare calibration graphs and measure 10-μl sample volumes in the same way. If necessary, inject several 10-μl aliquots successively before the charring and atomization steps but always dry the solvent at 100° between each loading.

For vanadium calculate the concentration directly from the calibration graph after converting peak heights to absorbance and subtracting the blank. For nickel, make a new absorption peak reading at 231.6 nm and subtract the scattering signal from the analytical value before calculating the concentration by means of the calibration curve. If available, use a deuterium arc background corrector to avoid measuring at two different wavelengths.

Factors influencing the results. Sample volumes up to 100 µl of aqueous solutions can be injected into the tube without difficulty, but when xylene/oil solutions were used, the sample spread immediately over the entire length of the tube at the drying stage. If more than 10 µl of solution was used, the solution reached the graphite cone connections before the solvent had evaporated. The results were then low, probably because of different distribution of the sample throughout the tube, varying temperature along the tube, and losses in the cone connections. Accordingly, only 10-µl samples were injected; if larger samples were needed, a drying step at 100° for 20–30 sec was used between injections. Well shaped reproducible peaks were then obtained and total sample volumes of desired magnitude could be injected. No difference in absorption between this multiple loading technique and the constant concentration, single addition technique, mentioned by Manning and Fernandez[11], was found. The dilution of the samples with xylene, recommended above, might seem unnecessary. However, no other way was found for accurate injection of small amounts of the solid oil lumps or thick liquids available for analysis.

Light scattering. Light scattering contributed (less than 5 %) to the absorption signal for nickel at 232.0 nm. This had to be compensated for, either by using a deuterium arc background corrector or by measuring later at the non-absorbing line 231.6 nm and subtracting the signal from the analytical value; the two methods showed good agreement. The standard solutions should be checked for zero absorption at the non-absorbing line. For vanadium the 318.3-, 318.4- and 318.5-nm lines were applied and no absorption was recorded.

TABLE I

RESULTS FOR VANADIUM AND NICKEL IN MINERAL OILS

Oil sample	*Graphite furnace, proposed method*		*Graphite furnace, ashing–dissolution*		*Flame atomic abs., APDC/MIBK extract*
	Vanadium (p.p.m.)	*Nickel (p.p.m.)*	*Vanadium (p.p.m.)*	*Nickel (p.p.m.)*	*Nickel (p.p.m.)*
Venezuela	225	30.5	229	28.5	29.5
Middle East	22.1	8.7	22.7	7.7	—
Nigeria	<0.2	5.6	<0.2	4.9	—
Unknown 1	37.9	11.9	37.2	12.4	11.1
Unknown 2	27.2	9.8	26.4	7.8	—

Results and discussion

Welz and Wiedeking[9] mention carbide formation in the determination of lithium in blood. This phenomenon can also be experienced in vanadium and nickel determinations, according to information given by the instrument manufacturer. In order to check the described method for this and other possible systematic errors, some oil samples were analysed by the same technique after the oil had been ashed at low temperature in platinum crucibles and the ash dissolved in nitric acid. Nickel was also determined in some of the same solutions by flame atomic absorption after extraction of its complex with ammonium pyrolidine dithiocarbamate (APDC) into methyl isobutyl ketone (MIBK)[12].

The results for a few typical crude oil and pollution samples (Table I) show reasonable agreement between the various methods employed. The rather poor precision for the lower concentrations can be explained by the very small samples of oil, usually 50–100 μg, taken.

For comparison with other methods than atomic absorption, a fuel oil analysed previously by optical spectrography on the ash, was also employed directly in the graphite tube. The results found by the proposed method, 86.6 and 7.0 p.p.m. vanadium and nickel, respectively, compare favourably with the earlier data, 110 p.p.m. vanadium and 6 p.p.m. nickel.

The proposed method offers considerable advantages in speed of analysis, in ability to handle minute quantities of material, and in low detection limits.

Central Institute for
Industrial Research,
Oslo 3 (Norway)

Sverre H. Omang

1 V. V. Brunnock, D. F. Duckworth and G. G. Stephens, *J. Inst. Petrol.*, 54 (1968) 310.
2 D. J. Trent and W. Slavin, *Atomic Absorption Newsletter*, 3 (1964) 131.
3 J. D. Kerber, *Appl. Spectrosc.*, 20 (1966) 212.
4 J. A. Burrows, J. C. Heerdt and J. B. Willis, *Anal. Chem.*, 37 (1965) 579.
5 E. A. Means and D. Ratcliffe, *Atomic Absorption Newsletter*, 4 (1965) 174.
6 S. Slavin and W. Slavin, *Atomic Absorption Newsletter*, 5 (1966) 106.
7 L. Capacho-Delgado and D. C. Manning, *Atomic Absorption Newsletter*, 5 (1966) 1.
8 B. V. L'vov, *Spectrochim. Acta*, 24B (1969) 53.
9 B. Welz and E. Wiedeking, *Z. Anal. Chem.*, 252 (1970) 111.
10 S. H. Omang, *Anal. Chim. Acta*, in press.
11 D. C. Manning and F. Fernandez, *Atomic Absorption Newsletter*, 9 (1970) 65.
12 W. Slavin, *Atomic Absorption Spectroscopy*, Interscience, New York, 1968, p. 137.

(Received 7th May 1971)

Anal. Chim. Acta, 56 (1971) 470–473

Determination of the nitrogen content of grains by means of fast neutron activation analysis

The nitrogen content of agricultural products, such as grain, which is related to the amount of contained protein, has been determined advantageously by various nuclear methods[1-4]. Nuclear techniques have been found to be superior as regards rapidity to the kind of analysis typified by the classical Kjeldahl technique. By means of the 14-MeV neutron activation method, nitrogen can be determined with a high degree of precision, as has been demonstrated by Wood *et al.*[6] and Kosta *et al.*[2]. Moreover, since the analysis is non-destructive the seed can be retained in viable condition, and used for example for breeding purposes.

By means of proton activation with a 185-MeV synchrocyclotron, nitrogen has been determined[3] by the $^{14}N(p,d)^{13}N$ reaction through spectroscopic analysis of promptly emitted deuterons. It has also been demonstrated that the nitrogen content of grain samples can be favourably determined by photonuclear activation analysis with a betatron[4].

A study of the flux density near the target of a neutron generator has shown that the 14-MeV neutron flux decreases with the square of the distance beyond 10 cm from the target[5]. In the irradiation volume close to the target, the attenuation of the neutron flux is less pronounced. The aim of the present study has been to optimize the irradiation conditions by irradiating several samples simultaneously in a position close to the target. This improved neutron economy might be of importance for analysis with generators with conventional tritium targets as well as those with sealed neutron tubes.

In order to facilitate quantitative evaluation, as well as to account for the non-uniform fast neutron distribution, each sample was provided with a flux monitor. In this study copper threads were used as monitors since the threshold energy for the reaction $^{63}Cu(n,2n)^{62}Cu$ is about the same as that for the reaction $^{14}N(n,2n)^{13}N$, namely about 10 MeV[6]. Further, the excitation functions for these reactions show similarities in shape[6].

In organic matter ^{13}N can also be produced from carbon or oxygen through proton reactions occurring from fast neutron interactions, such as $^{13}C(p,n)^{13}N$ or $^{16}O(p,\alpha)^{13}N$[7]. In order to evaluate this effect, samples with a zero nitrogen content but with a composition otherwise similar to that of the grains were simultaneously irradiated and the induced ^{13}N activity measured. In this case, glucose was chosen as a suitable "background" sample.

Experimental

Samples. The grain samples contained nitrogen in quantities of 5.32% (mustard grain) and 1.77% (wheat grain). The samples were contained in plastic vials and amounted to about 5 g. A copper thread monitor was mounted in each vial as shown in Fig. 1. Single beans weighing about 80 mg were also irradiated and analyzed.

Irradiations. The samples were irradiated for periods of 10 min in front of a 5-Ci tritium target of a Kaman-1250 neutron generator with a maximum neutron output of about $2 \cdot 10^{11}$ n sec^{-1} over 4π solid angle. The irradiations were carried out at about 1/10 maximal flux. The fast flux was measured by means of copper foils according to the technique adopted by the Texas convention[8].

Measurements. The measurements were begun roughly 10 min after the end of irradiation, to accommodate the decay of ^{30}P ($T_{\frac{1}{2}} = 2.6$ min). The annihilation radiation of the ^{13}N and ^{62}Cu nuclides, with half-lives of 10.0 and 9.9 min respectively, was measured with a 2 × 2 in NaI (Tl) crystal coupled to a 512-channel pulseheight analyzer (Nuclear Data). The copper thread monitors were curled to spheres before the activity was measured.

Results and discussion

The geometrical arrangement for simultaneously irradiating seven samples together with their copper monitors is shown in Fig. 1. The use of copper foils placed in each sample in front of the target was also studied, but reproducible results were not

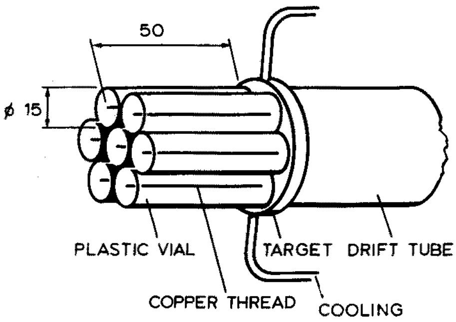

Fig. 1. Geometrical arrangement for simultaneous irradiation of seven samples.

obtained by this method of monitoring. After irradiation each sample was transferred to a new vial, before being counted in order to avoid nitrogen contamination introduced by contact with air. According to an investigation by Kosta *et al.*[2], atmospheric nitrogen adsorbed into and trapped in loosely packed powdered samples can produce an error of about 10%.

Table I lists values for the ratio of the ^{13}N activity in the grain to the corresponding ^{62}Cu monitor activity for the geometrical arrangement applied. The mean values of the ratios obtained for the two series studied, containing 1.77 and 5.32% nitrogen were 1.28 and 3.91, respectively (Table I). Considering the relationship between these ratios and the corresponding nitrogen contents, namely $3.91:1.28 = 3.05$ and $5.32:1.77 = 3.00$, good agreement is observed for the results obtained by the fast neutron activation technique compared to those obtained by the Kjeldahl method.

Decay analysis of the 0.51-MeV peak confirmed the 10-min activity of ^{13}N for a period of about 50 min after irradiation for the grain samples containing 5.3% nitrogen. Consequently, the nitrogen content of an unknown product may be evaluated by combining the results of two measurements, the one being the ^{13}N activity of the grain sample, and the other the ^{62}Cu monitor activity. Each measurement requires 1 min, and the whole analysis can be completed in under 30 min.

In the analysis of grain samples of unknown nitrogen composition, it may be appropriate to include a standard as one of the samples in the geometrical arrangement.

Single beans of about 80 mg weight were also irradiated. The decay of the 0.51-MeV peak was measured, and the 10-min ^{13}N activity was confirmed. At neutron fluxes above $5 \cdot 10^8$ n cm^{-2} sec^{-1}, sufficient activity seems to be induced in the beans to permit an analysis to be made on single specimens.

At a nitrogen concentration of roughly 2–5%, nitrogen could be determined with a standard deviation for the single value of about 3%. In samples with high potassium contents interference was experienced from ^{38}K ($T_{\frac{1}{2}} = 7.7$ min) which is formed by the $^{39}K(n,2n)^{38}K$ reaction. This entails making separate corrections to the activity measurements[1]. The background activity of ^{13}N formed in the glucose samples was found to correspond to an apparent nitrogen concentration in the sample of 0.30%.

The proposed fast neutron activation method requires about the same time as the photon activation method[4], which is based on the $^{14}N(\gamma,n)^{13}N$ reaction, and the activities are measured by similar techniques. ^{38}K is formed from any ^{39}K in both

TABLE I

RATIO OF ^{13}N ACTIVITY IN GRAINS TO CORRESPONDING ^{62}Cu MONITOR ACTIVITY FOR THE GEOMETRICAL ARRANGEMENT DESCRIBED[a]

^{13}N activity in grain/^{62} Cu activity of monitor		
Sample	*Wheat grains* (1.77% *N*)	*Mustard grains* (5.32% *N*)
1	1.23	3.82
2	1.25	3.82
3	1.26	3.83
4	1.27	3.86
5	1.29	4.00
6	1.30	4.00
7	1.35	4.05
	Mean value: 1.28 Stand. dev. of single value: 0.04	Mean value: 3.91 Stand. dev. of single value: 0.10

[a] Corrections have been applied for the ^{13}N activity induced by recoil proton effects.

methods; in the photonuclear activation method, a suitable maximal brehmstrahlung energy must be selected to suppress the formation of ^{38}K. The flux distribution in front of the target of the fast neutron or photon facility is characterized by non-uniformity, which necessitates the use of a rotated sample device or accurate flux monitoring. The latter was chosen for its simplicity in the present work.

This work was supported under the International Atomic Energy Agency Technical Assistance Programme.

Instituto de Asuntos Nucleares,
Bogotà (Colombia)

Dag Brune*
Alfredo Arroyo

1 D. E. Wood, P. L. Jessen and R. E. Jones, *52nd Annual Meeting of The American Association of Cereal Chemists, April 2–6, 1967, Los Angeles, Calif., U.S.A.*
2 L. Kosta, V. Ravnik and J. Dumanovic, *New Approaches to Breeding for Improved Plant Protein, Proc. of a Panel, Rostånga, Sweden, June 17–21, 1968*, FAO, IAEA, Vienna, 1969, p. 161–168.
3 A. Johansson, B. Larsson, G. Tibell and L. Ehrenberg, *New Approaches to Breeding for Improved Plant Protein, Proc. of a Panel, Rostånga, Sweden, June 17–21, 1968*, FAO, IAEA, Vienna, 1969, p. 169–171.
4 D. Brune, L. During, B. Larsson and H. Lundquist, to be published.
5 P. E. Wilkniss and G. J. Wynne, *Intern. J. Appl. Radiation Isotopes*, 18 (1967) 77.
6 P. Jessen, M. Bormann, F. Dryer and H. Neuert, *Nuclear Data*, 1 (2) (1966) 166.
7 D. C. Aumann and H. J. Born, *Modern Trends in Activation Analysis, Proc. Intern. Conf., College Station, Texas, U.S.A., April 19–22, 1965*, p. 265–71.
8 R. L. Heath, *Modern Trends in Activation Analysis, Proc. Intern. Conf., College Station, Texas, U.S.A., April 19–22, 1965*, p. 389–90.

(Received 2nd April 1971)

---

* On leave from AB Atomenergi, Studsvik, Nyköping, Sweden.

Analytica Chimica Acta
Elsevier Publishing Company, Amsterdam
Printed in The Netherlands

An investigation of ion-selective electrodes prepared for titration purposes by precipitation of a metal sulphide on a silver sulphide surface

The membranes of many of the commercially available selective metal ion electrodes consist of a polycrystalline mixture of a sulphide of the metal with silver sulphide, the role of the latter, owing to the high conductivity of silver ions in the silver sulphide crystal lattice, being primarily to promote electrical conductance. Although this type of electrode has been found to behave satisfactorily, such electrodes have been constructed only for relatively few metal ions. In order to see whether or not sulphide electrodes could be successfully constructed for other metals, *e.g.* nickel and cobalt, and to examine possible sources of interference with existing electrodes, different methods of preparing metal sulphide electrodes have been investigated. Some results of these investigations are reported in this paper.

Reagents and apparatus

All reagents were of analytical grade.

All titrations were performed with a semi-automatic titrator[1] equipped with a high-impedance digital voltmeter of resolution ±0.1 mV. Discrete increments of titrant were added from syringe burets, it being possible to pre-set the volume of each titrant increment and the time between each new addition of titrant.

In all measurements a calomel reference electrode (Radiometer K 401) was used.

Preparation of the electrodes

A silver rod was anodically oxidized in a dilute solution of sodium sulphide until its surface was completely coated with silver sulphide, the resulting electrode being sensitive both to silver and sulphide ions. This silver sulphide electrode could be made sensitive to a specific metal ion by immersing it in a dilute solution of sodium sulphide and then adding a solution of the metal nitrate until the free metal ion concentration was greater than the free sulphide concentration and of the order of 0.01 M. The electrode was then carefully rinsed in doubly distilled water and stored in a saturated solution of the metal sulphide. The preparation of electrodes for copper, cadmium, lead, mercury(II), nickel, cobalt and zinc was attempted by this procedure.

Calibration of the electrodes

The electrodes were calibrated against increasing free concentration of the relevant metal ion by a titration procedure. Titrant increments of 0.01 M metal nitrate were added to 100 ml of a solution buffered at pH 4.5 with sodium acetate–acetic acid, until the total metal concentration was approximately 0.001 M. In order to cover the high metal ion concentration range the solution was then titrated with increments of 0.25 M metal nitrate. The free metal ion concentration in each calibration point, M_{calc}, was then calculated from the total amount of metal ion added, neglecting the acetate complexes, and pM_{calc} was plotted against the corresponding e.m.f. reading, E mV. The results of the calibration curves obtained for the different metal electrodes are shown in Fig. 1.

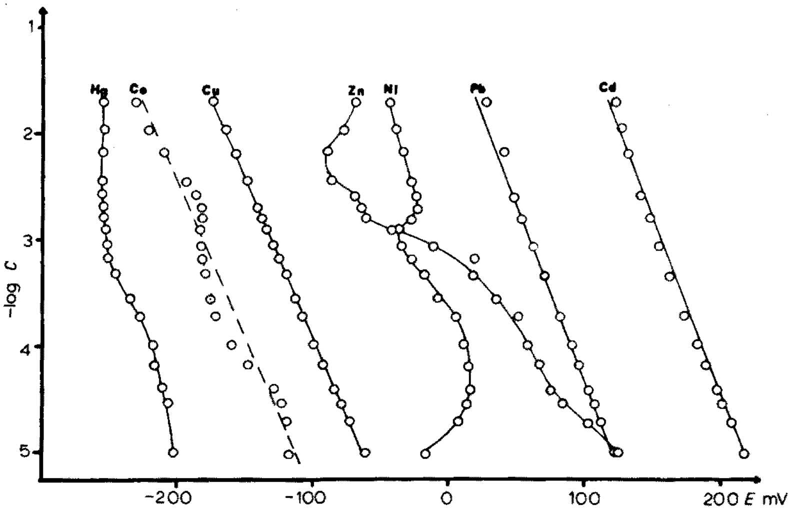

Fig. 1. Calibration curves for the electrodes prepared. The E_0 values have been chosen arbitrarily to make it possible to illustrate all the calibration curves in the same figure.

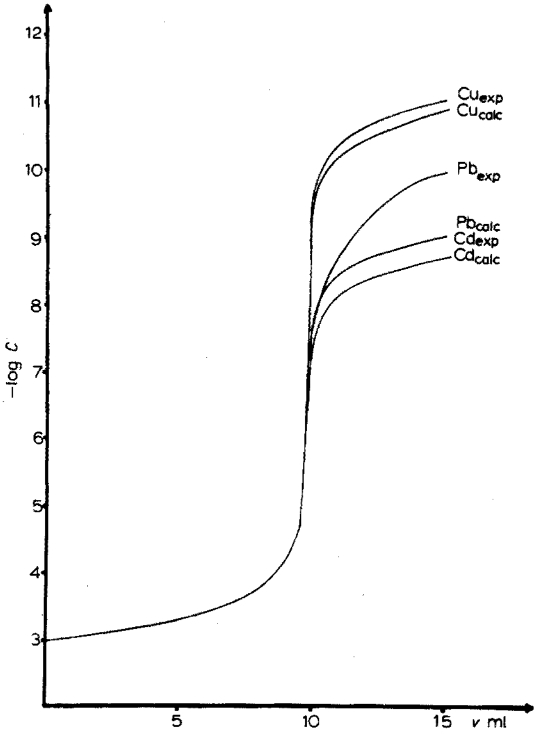

Fig. 2. Experimental and calculated titration curves for the titration of 100 ml 0.001 *M* metal nitrate with *v* ml 0.01 *M* EDTA in 0.005 *M* acetic acid–sodium acetate buffer.

Titrations with the electrodes

The copper, cadmium and lead electrodes were each used as sensor in a titration procedure. Titrant increments of v ml of 0.01 M Na_2H_2Y (H_4Y = EDTA) were added to 100 ml of a solution containing 0.001 M metal nitrate, buffered with 0.005 M sodium acetate–acetic acid. The three titration curves ($-\log[M]$ *versus* v ml of titrant added) thus obtained are shown in Fig. 2.

Theoretical titration curves. The forms of the theoretical titration curves were calculated with the computer program HALTAFALL[2]. The stability and solubility constants used in the computation are specified in Table I.

TABLE I

STABILITY CONSTANTS USED IN THE CALCULATION OF THE THEORETICAL TITRATION CURVES FOR THE TITRATION OF 100 ml 0.001 M COPPER, CADMIUM OR LEAD NITRATE WITH 0.01 M DISODIUM-EDTA AT pH 4.5

Equilibrium	*Log. of stab. const.*	*Reference*
$H+Y \rightleftharpoons HY$	10.27	3
$2H+Y \rightleftharpoons H_2Y$	16.43	3
$3H+Y \rightleftharpoons H_3Y$	19.10	3
$4H+Y \rightleftharpoons H_4Y$	21.10	3
$H_2O \rightleftharpoons H+OH$	−13.89	
$Cu+Y \rightleftharpoons CuY$	18.80	4
$Cd+Y \rightleftharpoons CdY$	16.60	5
$Pb+Y \rightleftharpoons PbY$	17.00	6

Results

Calibration curves. As seen from the calibration curves shown in Fig. 1, the copper, cadmium and lead electrodes exhibit approximately Nernstian behaviour in the pM range 5–1.7. Moreover, these electrodes show a rapid response to changes in the free metal ion concentration, the copper electrode being superior in this respect to the other two. All three electrodes gave stable potential readings in each calibration point. In order to verify that each electrode was selective for the relevant metal ion, the electrodes were also calibrated in solutions containing high concentrations of other metal ions. The copper electrode gave, for instance, a calibration curve identical with that shown in Fig. 1, even in media containing 0.01 M cadmium nitrate. The cobalt electrode showed a slow, but irreproducible response towards changes in the free cobalt ion concentration while no logical response at all was obtained with the nickel, zinc and mercury "electrodes". All these "electrodes" together with the cobalt electrode, showed a continuous drift in e.m.f. reading with time and the calibration points shown in Fig. 1 are those obtained approximately 3 min after the addition of a new increment of titrant in the calibration procedure.

Titration curves. The experimental titration curves obtained with the copper, cadmium and lead electrodes are shown in Fig. 2, together with the corresponding theoretical titration curves. From the figure it can be seen that the copper and cadmium electrodes can be successfully used for end-point detection in potentiometric titrations, while the lead electrode is less satisfactory. The magnitudes of the potential jumps around the equivalence point are, moreover, of the same order of magnitude as those predicted theoretically. Since the form of the theoretical titration curve is very sensitive to the pH value chosen in the computation, and since, moreover, the stability constants specified in Table I are not exactly relevant to the experimental conditions, no attempt is made to explain the slight discrepancies between the computed and experimental titration curves.

Discussion

The electrodes can be considered to consist of a layer of metal sulphide, $MS_{(s)}$, on silver sulphide, and can be illustrated schematically:

$$MS_{(s)}/Ag_2S_{(s)}/Ag$$

The formation of the sulphide layer on the silver sulphide surface can be assumed to take place in either of two ways. With an excess of metal ions, M^{2+}, as is the case in the preparation of the electrodes, the reaction

$$M^{2+} + Ag_2S_{(s)} \rightarrow MS_{(s)} + 2\,Ag^+ \quad (1)$$

will occur, provided that the metal ion concentration is high enough for the solubility product of the metal sulphide to be exceeded. Reaction (1), since it involves two solid phases, is likely to proceed slowly, whereas the experiments indicated a rapid formation of the metal sulphide layer. It is well-known that sulphide ions are enriched at the contact surface between silver sulphide and a solution containing excess of sulphide. Addition of metal ions which can form a sparingly soluble metal sulphide will cause the sulphide ions to precipitate as metal sulphide on the silver sulphide surface. This mechanism, since it is likely to be more rapid than reaction (1), would seem to be more probable.

It is obvious that metal sulphides will also be precipitated on silver sulphide membranes. A silver sulphide membrane electrode can thus be converted to, for instance, a copper electrode by the procedure described above. The reason why only the (silver), copper, cadmium and lead electrodes, which are those mixed sulphide electrodes available commercially, show response to the concentration of their respective metal ions is not apparent. The most probable explanation seems to be that for the other metal sulphides the reaction between the metal ion and its solid sulphide is not established owing to kinetic hindrance as suggested by Ross[7]. It is of course also possible that no precipitate is formed on the silver sulphide surface or, more likely, that the metal sulphides have weak mechanical properties causing the sulphide layer to flake off.

Interferences. There has been much discussion concerning modes of interference with metal sulphide electrodes. Such discussions have, moreover, often been complicated by a tendency to forget that the electrode reactions must obey the law of mass action. If, for instance, an electrode consisting of a layer of $M_IS_{(s)}$ on a silver sulphide matrix is used to measure the M_I^{2+} concentration in a solution containing M_{II}^{2+} ions, the following equilibrium may be established

$$M_IS_{(s)} + M_{II}^{2+} \rightleftharpoons M_{II}S_{(s)} + M_I^{2+} \quad (2)$$

provided that $K = [M_{II}^{2+}]/[M_I^{2+}]$ reaches a certain critical value[7]. The M_I-electrode will then be sensitive to changes in the free M_{II}^{2+} concentration since this concentration determines the free sulphide concentration in the solution. After a prolonged exposure of the $M_IS_{(s)}$ electrode to such a solution the electrode would presumably be converted to a $M_{II}S$ electrode. The critical K value depends mainly on the ratio between the solubility products for M_IS and $M_{II}S$. In a rigorous calculation of the critical K value all soluble species in the M_I–M_{II}–proton–sulphide system ought, of course, to be included. It should, thus, in principle, be possible to predict by computer calculation the extent of the interference of a particular metal ion with a metal sulphide electrode. Such calculations are, however, difficult to carry out in practice, owing to the lack of relevant stability constants.

Department of Analytical Chemistry,
University of Göteborg,
40220 Göteborg 5 (Sweden)

Torbjörn Anfält
Daniel Jagner

1 D. Jagner, *Anal. Chim. Acta*, 50 (1970) 15.
2 N. Ingri, W. Kakolowicz, L. G. Sillén and B. Warnqvist, *Talanta*, 14 (1967) 1261.
3 R. Skochdopole and S. Chakerek, *J. Inorg. Nucl. Chem.*, 11 (1959) 222.
4 G. Schwarzenbach, R. Gut and G. Anderegg, *Helv. Chim. Acta*, 37 (1954) 937.
5 G. Schwarzenbach and G. Anderegg, *Helv. Chim. Acta*, 40 (1957) 1773.
6 V. L. Hughes and A. E. Martell, *J. Phys. Chem.*, 57 (1953) 694.
7 J. W. Ross, in R. A. Durst, *Ion-Selective Electrodes*, Dept. of Commerce, National Bureau of Standards, Special Publ. 314.

(Received 27th May 1971)

The photometric titration of uranium with cerium(IV) or chromium(VI)

Uranium in solution is generally determined by reduction in sulphuric acid solution to the tetravalent state with a metallic reductor followed by oxidimetric titration. The induction of the atmospheric oxidation of uranium(IV) by several metals, *e.g.* iron and copper, has often been described as a serious interference; the exclusion of air from the column as well as from the effluent and the titration solution is regarded as essential by most authors. In the present investigations it was shown that when *ca.* 10^{-3} M solutions of uranium(IV) are titrated, the induction is not caused by the presence of metal ions only, but is very probably due to the combined presence of metal ions and hydrogen peroxide.

Experimental

A Jones reductor as described by Kolthoff and Belcher[1] was used in a modified way. Instead of washing the column after the reduction successively with dilute sulphuric acid and water, only washing with dilute sulphuric acid was applied. Washing with water has been reported to introduce hydrogen peroxide in the effluent[2]. This was confirmed in the present work: washing with water resulted in a considerable reagent blank whereas no reagent blank was observed when the column was washed with dilute sulphuric acid.

Cerium(IV) was used as the titrant. End-points were detected photometrically, which at low concentrations has distinct advantages over some other methods, as has been pointed out previously[3,4]. For reasons of selectivity, the absorbance was measured at 650 nm, where uranium(IV) has a maximum in the absorption curve ($\varepsilon = 50$ in 1 *M* sulphuric acid). Titrations were done in 10-ml cells with 2-cm optical pathlength on a Zeiss PMQ II spectrophotometer or a Zeiss Elko II filter photometer.

Results

Operating the column as described above makes possible the selective determination of uranium in the presence of other metals, without exclusion of air from the column and the effluent. Dilute ($5 \cdot 10^{-4}$ *M*) solutions of uranium(IV) appeared to be stable for more than 24 h in the presence of other metal ions, even when air was blown through the solution. When 10-ml aliquots of the effluent containing *ca.* 1 mg of uranium were titrated, the standard deviation was 0.5%. At this concentration level, uranium(III) was not detected in the effluent, probably because the column was operated at a low flow rate (1 drop per sec). When present in 30-fold amounts iron, aluminium, cobalt, nickel, manganese and chromium did not interfere. Titanium, copper and nitrate could be tolerated in equal amounts to uranium. Vanadium, molybdenum and tungsten interfered. Large amounts of copper interfered with the reduction in the column.

Determinations in phosphoric acid solutions

Some other photometric titrations of uranium were carried out by reduction in 11.5 *M* phosphoric acid medium with iron(II) followed by titrations with potassium dichromate. These determinations have been done previously with potentiometric end-point detection by Gopala Rao *et al.*[5]. In this case photometric end-point detection at 650 nm also has some advantages. The determination of 2 mg of uranium in 10 ml of solution was possible with a standard deviation of 1%. No interference was observed from 100-fold amounts of cobalt, nickel and iron, 10-fold amounts of chromium and titanium, or equal amounts of copper and tungsten. Manganese, vanadium and molybdenum interfere.

Laboratory for Analytical Chemistry,
University of Amsterdam,
Amsterdam (The Netherlands)

G. J. van Rossum
G. den Boef
H. Poppe

1 I. M. Kolthoff and R. Belcher, *Volumetric Analysis III*, Interscience, New York, 1957, p. 189.
2 W. L. Burdick, *J. Amer. Chem. Soc.*, 48 (1926) 1179.
3 T. M. Florence, *Anal. Chim. Acta*, 23 (1960) 282.
4 C. E. Bricker and P. B. Sweetser, *Anal. Chem.*, 25 (1953) 764.
5 G. Gopala Rao, P. Kanta Rao and M. A. Rahman, *Talanta*, 12 (1965) 953.

(Received 29th April 1971)

Analytica Chimica Acta
Elsevier Publishing Company, Amsterdam
Printed in The Netherlands

Direct EDTA titration of scandium, yttrium and some rare earth metals with iron–N-benzoyl-N-phenylhydroxylamine as indicator

One of the most interesting types of direct EDTA titration is exemplified by the use of copper–1-(2-pyridylazo)-2-naphthol as indicator in the determination of Cd, Pb, In, Ga, etc.[1,2]. The success of such a titration depends on the stability constants of the various metal–reagent complexes present. In general, any metal ion (M) which forms a colourless complex with an organic reagent (R) can be titrated with EDTA employing the coloured complex of a second metal (M′) with the same reagent (R) as indicator, provided that (*a*) the stability of the M–EDTA chelate is greater or nearly equal to that of the M′–EDTA complex at a particular pH, and (*b*) the stability of the M′–R complex is greater than that of the M–R complex at the same pH.

Although EDTA has been employed as a complexing agent in the separation of some individual rare earths[3], it is usually applicable only as a group titrant. Eriochrome black T[4], PAN[5,6], chrome azurol S[7], thorin[8], xylenol orange[9] and some modifications of those dyes[10] have been suggested as indicators for such titrations. In the work described here, the strongly coloured iron(III)–N-benzoyl-N-phenylhydroxylamine (BPHA) complex in ethanolic solution was studied as indicator for the titration of scandium, yttrium, and some rare earth metals. The application of iron–BPHA as indicator in direct titrations of indium, thallium and thorium was reported earlier[11].

Since the complexes formed by BPHA with scandium, yttrium, lanthanum, cerium(III), europium, erbium, neodymium and samarium are all colourless, the end-point of the titration of those metals with EDTA is indicated by a sharp change of colour of the indicator (iron–BPHA) from reddish violet to colourless in the pH range 4.8–5.4. Scandium can, however, be titrated in a wider pH range, *i.e.* 3.0–5.4. Large amounts of beryllium, magnesium, calcium and barium and small amounts of manganese(II) and uranium(VI) do not interfere. Only europium, erbium, yttrium and scandium can be titrated in presence of aluminium, zinc or cadmium whereas scandium can be determined even in presence of small amounts of cobalt and nickel. It is possible to titrate thorium and the above metals successively by the control of pH.

Reagents and chemicals

Standard metal solutions. Extra-pure oxides of scandium, yttrium and the rare earths in known amounts were dissolved separately in hydrochloric acid and made up to volume with water. Cerium(III) and thorium solutions were prepared by dissolving the corresponding nitrates in water containing a few ml of dilute nitric acid and were standardised by the oxide and oxalate methods, respectively.

Indicator solution. 1 ml of 0.002 *M* iron(III) solution and 4 ml of ethanolic 1% BPHA solution were used for each titration.

All other chemicals employed were of A.R. quality.

Procedure

Dilute an aliquot of the standard solution of the required metal ion to 50 ml with distilled water. Adjust the pH to 4.8–5.4 by addition of 10% sodium acetate solution or dilute hydrochloric acid and then introduce the indicator solutions. The solution should turn reddish violet or wine red. Add 10–15 ml of ethanol to prevent precipitation of the metal–BPHA complex. Warm the solution gently to 40–45° and titrate with standard 0.01 *M* EDTA solution to a colourless end-point. An indicator correction of 0.16 ml of 0.01 *M* EDTA was found.

Results

The upper limits for the titration of scandium, yttrium and the rare earths were found to be 3.8 mg, 4.0 mg and *ca.* 5.2 mg, respectively. When more indicator solution was added, larger amounts of these metals could be titrated, but the end-points became generally less sharp. The results are shown in Table I.

Effect of pH. The pH of the solutions to be titrated was adjusted to different values in the range 1.0–6.0 with 10% sodium acetate solution or 4 *M* hydrochloric acid and to higher pH values with sodium potassium tartrate solution, before the addition of indicator. All the metal ions mentioned above could be titrated successfully in the pH range 4.2–6.2, the optimal range being 4.8–5.4. Below pH 4.2 the reactions of the rare earth ions and of yttrium with EDTA were not quantitative, owing to the low stability of the corresponding chelates. Scandium could, however, be titrated quantitatively at a pH as low as 3.0. Above pH 6.5 the colour intensity of the indicator was reduced.

Effect of foreign ions. In studies of the effect of diverse metal ions, titrations were carried out at pH 4.8, as described in the *Procedure*. It was found that La^{3+} (3.90 mg), Ce^{3+} (3.42 mg), Nd^{3+} (4.80 mg), Sm^{3+} (4.20 mg), Eu^{3+} (5.19 mg), Er^{3+} (4.50 mg), Y^{3+} (3.75 mg), or Sc^{3+} (3.40 mg) could be titrated without interference from Be^{2+} (80 mg), Mg^{2+} (100 mg), Ca^{2+} (80 mg), Ba^{2+} (80 mg), Mn^{2+} (12 mg) or U^{6+} (3 mg). In titrations of the heavier rare earths (Eu^{3+} and Er^{3+}), yttrium and scandium,

TABLE I

EDTA TITRATION OF SCANDIUM, YTTRIUM AND SOME RARE EARTHS

Metal taken (mg)		*Volume of* 0.008895 *M EDTA required (ml)*	*Metal found (mg)*	*Error (mg)*
La^{3+}	1.30	1.04	1.29	−0.01
	3.90	3.16	3.90	0.00
Ce^{3+}	1.14	0.92	1.15	+0.01
	3.42	2.74	3.41	−0.01
Nd^{3+}	1.60	1.24	1.59	−0.01
	4.80	3.72	4.77	−0.03
Sm^{3+}	1.40	1.06	1.42	+0.02
	4.20	3.16	4.23	+0.03
Eu^{3+}	1.73	1.28	1.73	0.00
	5.19	3.82	5.16	−0.03
Er^{3+}	1.50	1.02	1.52	+0.02
	4.50	3.04	4.50	0.00
Y^{3+}	1.25	1.56	1.23	−0.02
	3.75	4.68	3.70	−0.05
Sc^{3+}	0.85	2.14	0.86	+0.01
	3.40	8.50	3.40	0.00

even appreciable quantities of Al^{3+} (6 mg), Zn^{2+} (7 mg) or Cd^{2+} (5 mg) could be tolerated. Scandium could be quantitatively titrated with EDTA at pH 3.0 even in the presence of Co^{2+} (6 mg) or Ni^{2+} (3 mg). Larger amounts of uranium interfered, owing to the formation of a red uranium–BPHA complex at the end-point. Even traces of titanium, molybdenum and vanadium interfered, perhaps because of the greater stability of their BPHA complexes compared to that of the iron–BPHA complex. Phosphates, fluorides, cyanides and citrates interfered in these titrations of scandium, yttrium and the rare earth metals.

Simultaneous determination of thorium and rare earth metals (*including Sc and Y*). A known amount of thorium nitrate was mixed with the required amount of the scandium, yttrium or the rare earth solution and the resulting mixture was diluted to 50 ml. The pH of the solution was adjusted to 2.0 with sodium acetate or hydrochloric acid, the usual iron(III) and BPHA indicator solutions were added, and the titration was carried out with standard 0.01 *M* EDTA solution to the colourless end-point. The pH was then raised to 5.0, 10 ml of ethanol and more indicator were added and the titration with EDTA was completed as before. The first titration value indicated the amount of thorium present and the second value was due to the corresponding amount of the rare earth yttrium or scandium. Typical results are shown in Table II.

TABLE II

SIMULTANEOUS DETERMINATION OF THORIUM AND SOME RARE EARTHS

Thorium taken (mg)	*Rare earth metal taken (mg)*	*Thorium found (mg)*	*Rare earth metal found (mg)*	*Error in rare earth (mg)*
4.80	La^{3+} 3.90	4.78	3.93	+0.03
14.40	3.90	14.40	3.88	−0.02
14.40	Ce^{3+} 3.42	14.44	3.39	−0.03
19.20	3.42	19.22	3.40	−0.02
14.40	Nd^{3+} 4.80	14.44	4.74	−0.06
19.20	4.80	19.24	4.76	−0.04
14.40	Sm^{3+} 4.20	14.42	4.17	−0.03
14.40	Eu^{3+} 1.73	14.38	1.70	−0.03
14.40	Er^{3+} 4.50	14.40	4.46	−0.04
14.40	Y^{3+} 3.75	14.42	3.75	0.00
19.20	3.75	19.22	3.73	−0.02
4.80	Sc^{3+} 3.40	4.86	3.33	−0.07
19.20	3.40	19.20	3.42	+0.02

Chemical Laboratory,
Presidency College,
Calcutta (India)

B. Das*
S. C. Shome

1 H. Flaschka and H. Abdine, *Chemist-Analyst*, 45 (1956) 58.
2 H. Flaschka and H. Abdine, *Mikrochim. Acta*, (1956) 770.

---

[*] Present address: Department of Soil Science and Chemistry, Faculty of Agriculture, Kalyani University, Nadia (West Bengal).

3 R. C. Vickery, *Chemistry of the Lanthanons*, Butterworths, London, 1953.
4 H. Flaschka, *Chemist-Analyst*, 47 (1958) 52.
5 K. L. Cheng, *Chemist-Analyst*, 44 (1955) 96.
6 K. L. Cheng and R. H. Bray, *Anal. Chem.*, 27 (1955) 782.
7 M. Malat and M. Tenorova, *Chem. Listy*, 51 (1957) 2135.
8 L. Erdey and G. Rady, *Z. Anal. Chem.*, 152 (1956) 253.
9 E. A. C. Crouch and I. G. Swainbank, *U.K. At. Energy Authority Rept. AERE-C/R-2843*, 1959.
10 J. T. Baker Chemical Co., *The EDTA Titration*, Nov. 1957.
11 H. R. Das and S. C. Shome, *Anal. Chim. Acta*, 43 (1968) 140.

(Received 21st April 1971)

Anal. Chim. Acta, 56 (1971) 483–486

The filtration and extraction of non-volatile air and water sensitive solids

A principal operation in the pre-analytical treatment of a material is purification. When the substance is non-volatile and air and water sensitive, special precautions are required. A filtration and extraction method is discussed which permits

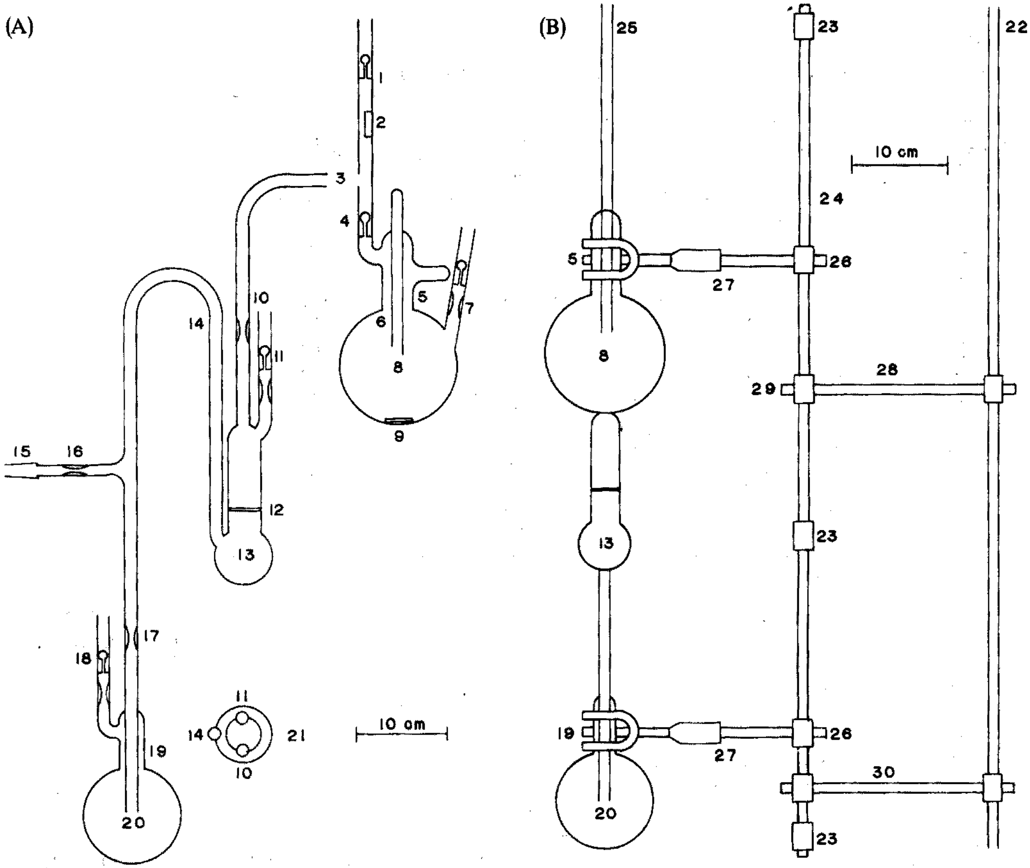

Fig. 1. Filtration apparatus, (A) front view; (B) side view including support rod.

Anal. Chim. Acta, 56 (1971) 486–488

the protracted manipulation of organic solvents in an all-glass system free of stopcocks. The operating principle is the hand manipulation of an apparatus to that solutions and solids are transferred under the force of gravity from one region to another.

Apparatus

The apparatus shown in Fig. 1 comprises the following three primary units: the raw mixture vessel 8 (designated previously[1] as the reactor), the filter 12, and the receiver-trap 20. When the filtration–washing–extraction process is complete, these parts are sealed off at the constricted points 10 and 17 so that the contents of each may be examined independently. The basic unit of 8 and 20 is either a 500-ml or 1-l round-bottom flask. The sintered filter 12 is generally M grade, and 35 mm o.d. Its base is enlarged with a 100-ml round-bottom flask. The dimensions of the filter section, both horizontally and vertically, are such that a 1-l Dewar (68 mm i.d.) may be safely placed around the filter and raised to point 14. The three primary units are positioned so that Dewars may be raised and lowered vertically without striking the corresponding lower unit. Most connecting tubing is 12 mm o.d. In the front view (Fig. 1A), the position of the fragile bulb break seal 11 is distorted. The top view of the filter section 21 illustrates the orientation of the three tubes 10, 11, and 14 connected to it. The entire apparatus is connected to a ½-in aluminum rod about 1 m long by two large three-finger clamps 27, one positioned at 5 and the other at 19. Figure 1B shows a side view of the apparatus 25 connected to the supporting aluminum rod 24 which is itself connected to a fixed lattice 22.

Method of use

Most of the manipulations are carried out by clamping the apparatus rod 24 slightly above its center of gravity at 29 to the rotation rod 28 which is fixed on the lattice 22. The longer end of the apparatus rod is fixed to the lattice by the auxiliary rod 30. At all times the major apparatus plane is in the vertical position. Except when the apparatus is being rotated, the auxiliary rod 30 is clamped to both rod 24 and the lattice 22. The apparatus may also be completely separated from the rods 28 and 30 and rotated in the hands of an operator. In this case the tightly screwed clamp holders 23 serve as handles and permit the exertion of the leverage necessary to prevent twisting of the major apparatus plane to the horizontal position.

Initially, the raw mixture vessel 8 is sealed onto the filtration apparatus at 3. Since it may be necessary to carry out a number of operations, some expected and some not, on the contents of vessel 8, provision should be made for re-entry by sealing on fragile bulb 1. The filtration–washing–extraction apparatus is pumped down to $< 10^{-5}$ Torr via the inner standard taper joint 15. The last traces of moisture are removed by flaming out. If required, solvent is distilled from the vacuum line and condensed in the receiver-trap 20. The constriction 16 is then sealed off and fragile bulb 4 is smashed by the Teflon (Du Pont) coated bar magnet 2 which until now has been arrested in position by an externally taped bar magnet.

The filtration–washing–extraction of products is carried out after condensation of the solvent in 8 by a cold bath when the major apparatus axis is in the vertical position. The mixture is warmed to room temperature and stirred by the magnetic bar 9. Filtration of the solid or extraction of the more dense solution is effected in approximately the same manner. The apparatus is rotated about its center of gravity in a counter-clockwise direction (with respect to a facing operator) so as to pass the solution through 4 and onto the filter 12. If the operation involves extraction, the apparatus is rotated only to the point that the more dense layer does not go over the lip 6 of the raw mixture vessel 8. Transfer of a dense oil onto the filter would probably result in clogging. In the case of filtration, two extreme conditions, or any intermediate one, are possible. All the products are placed on the filter initially or else the bulk remains as a result of its settling action, in bulb 8. In the early washing stages, the latter is preferred because it permits a greater ease of precipitate washing and leaching and more rapid filtration. The filtrate collects in 13 and is then decanted into the receiver-trap 20. Since the degree of counter-clockwise rotation in the second decantation step is not as great as in the first, material is not decanted from 8 onto 12. Repetition of the decantation process is necessary if a large quantity of solvent is used.

On completion of the filtration–washing–extraction, the solvent in 20 is condensed back in 8 by a dry ice or liquid nitrogen bath. The raw mixture vessel 8 should not be so rapidly cooled that bumping of the filtrate in 20 occurs. The solvent is warmed to room temperature and the cycle repeated as many times as the experiment requires. The filtrate can be monitored for solute by color or by collecting a sample in 13 and then evaporating the solvent. At any stage before transfer of the filtrate to the receiver-trap 20, it can be returned to the original vessel 8. As the inner tube of the receiver-trap 20 is intended to prevent filtrate flow back, the total solvent volume cannot exceed one half the volume of 20. In the later washing stages, the precipitate is transferred in a slurry to filter 12.

When filtration into 13 is slow, there is a temptation to use a pressure difference accomplished by cooling 13 to increase the filtration rate. Solvent evaporation with consequent filter plugging may occur especially when concentrated solutions are used. This possibility can be reduced by cooling the entire filter section to point 14, *e.g.* with an ice bath. If pressure difference is required to increase filtration rate, it is far better to heat the solution in 8 slightly and thus "push rather than pull". However, such manipulation should only be used as a last resort.

This apparatus was designed for, and extensively used in, the separation of products from the reaction of an ethereal solution of iron(III) chloride with phenyl Grignard under an atmosphere of hydrogen[2]. Initially a dense black oil separated from the ether solution. This oil was repeatedly extracted with ether and eventually it solidified to a powdery solid which was filtered from the solvent.

Department of Chemistry,
University of Victoria,
Victoria, British Columbia (Canada)

S. G. Gibbins

1 S. G. Gibbins, *J. Catalysis*, in press.
2 S. G. Gibbins, *161st National American Chemical Society Meeting, Los Angeles, Calif., March 1971*, Abstr. Inorg. Chem. 155.

(Received 22nd April 1971)

Analytica Chimica Acta
Elsevier Publishing Company, Amsterdam
Printed in The Netherlands

BOOK REVIEWS

James W. McCoy, *Chemical Analysis of Industrial Waters*, Macdonald & Co., Ltd., London, 1969, xi+292 pp., price £6.25.

This book aims to deal with the chemical analysis of industrial water. Part I discusses the necessity for treating boiler feed water and cooling water; part II is concerned with the determination of mineral constituents of industrial waters; part III deals with the special procedures of importance in water treatment; and part IV covers the chemical analysis of scales, sludges and deposits.

Whilst the main emphasis of this book is directed to the methods used by service chemists in petroleum refineries, some attempt has been made to generalize the treatment, and to utilize classical methods wherever possible. Much of the information is drawn from the author's own experience at the Richmond refineries of the Standard Oil Company, and may not be too relevant to other industrial situations. Many of the chemical procedures seem rather out-dated but these appear to be more the type of procedure required for use by plant operatives than the best existing, and perhaps more elaborate, processes.

This book is a projection of the author's long experience in handling the water problems of a large refinery. Some useful chemistry is presented, which makes the book a reasonable additional source of information to those chemists involved in the examination of water for industrial purposes. There is little here for the environmentalist concerned with water pollution.

W. I. Stephen (Birmingham)

Anal. Chim. Acta, 56 (1971) 489

Four-Language Technical Dictionary of Chromatography, Edited by H.-P. Angelé, Pergamon Press, Oxford and VEB Verlag Technik, Berlin, 1970, 119 pp., price £5.00 ($12.50).

This small book covers the terminology of all types of chromatography. In the major part of the book, the selected English words are listed alphabetically, and their German, French and Russian equivalents are given. In later sections, the German, French and Russian terms are listed alphabetically and reference is made to the English section.

Large numbers of chromatographic terms are of course given, but so are many chemical names which have dubious special relationship to chromatography, as well as many terms relating to general chemical technique. There are few terms in this book which could not be readily interpreted with the aid of the ordinary technological dictionaries, which would be needed anyhow in the translation of most chromatographic texts, except by expert linguists. Accordingly, the book cannot be wholeheartedly recommended.

A. M. G. Macdonald (Birmingham)

Anal. Chim. Acta, 56 (1971) 489

Analytica Chimica Acta
Elsevier Publishing Company, Amsterdam
Printed in The Netherlands

BOOK REVIEWS

Paul Nangniot, *La Polarographie en Agronomie et en Biologie*, Editions J. Duculot, Gembloux (B), 1970, 396 pp., BF. 450.00.

Il y a un nombre considérable de livres traitant de la polarographie. C'est une preuve de l'importance de cette méthode analytique. Pourtant je ne connais pas d'ouvrage d'application de celle-ci à l'agronomie et à la biologie (sauf dans une certaine mesure celui de Brezina et Zuman).

L'auteur a fait un choix qui nous paraît judicieux; il donne les bases théoriques fondamentales et évite toutes considérations secondaires qui n'ont pas directement trait au sujet qu'il s'est imposé. Ceci permet au non spécialiste de se documenter rapidement et de mettre en pratique sans difficulté toute méthode susceptible de résoudre les problèmes qui lui sont posés.

Dans une introduction générale, l'auteur expose les principes des diverses polarographies: de la classique à la polarographie différentielle, ainsi que de la technique oscillographique, à courant imposé, à onde carrée et à impulsion; il insiste sur la souplesse d'une telle méthode, montre comment ou peut la rendre sélective et donne des indications concernant la sensibilité et la précision. Une foule de renseignements en quelque 47 pages.

Le chapitre 2 a pour objet les manipulations telles que la purification du mercure et les dangers que présente cet élément, les différentes électrodes dont celle à goutte de mercure, le dégazage des solutions pour éliminer O_2, l'élimination des maxima etc. Les réactions anodiques et cathodiques sont étudiées de même que les différents types de courant rencontrés en polarographie (courant catalytique, courant d'adsorption).

La deuxième partie a pour titre: le dosage des éléments mineurs en agronomie et en biologie; chacun connaît l'importance des oligo-éléments. Comme milieu, l'auteur a choisi les eaux, les boissons et les aliments. Il donne en bref la méthode pour chaque élément et pour plus de détails une bibliographie succincte. Peut-on reprocher à l'auteur de ne pas toujours donner la précision et la sensibilité de ces méthodes? Il est probable que dans la plupart des cas elles n'aient pas été déterminées de façon satisfaisante par les auteurs cités.

La troisième partie concerne un sujet particulièrement brûlant: le dosage des pesticides et, entre autres, les dérivés chlorés, les thiocarbamates, les dérivés nitrés, l'Euparen, les esters phosphoriques etc.

Enfin, la dernière partie dite *Dosages polarographiques divers* comprend le dosage dans les milieux biologiques de l'acide ascorbique, de l'oxygène dissous et une foule d'autres substances.

En fait, l'auteur s'en est tenu au titre proposé. Aussi, ce livre est-il facile à consulter, il donne tous les détails pratiques nécessaires et il sera d'un grand secours pour tous ceux qui désirent utiliser cette méthode, remarquable tant par sa sensibilité que par sa sélectivité et qui n'a pas toujours été utilisée comme elle le mérite, car elle peut paraître très délicate à ceux qui ne la connaissent pas.

Ce livre leur montrera qu'en fait l'application dans tous les milieux en est fort aisée.

Denys Monnier (Genève)

ANALYTICA CHIMICA ACTA, VOL. 56 (1971)

AUTHOR INDEX

ANALYTICA CHIMICA ACTA, VOL. 56 (1971)

SUBJECT INDEX

VOL. 56 NO. 3 ANALYTICA CHIMICA ACTA OCTOBER 1971

CONTENTS

Short communications

(continued on page 4 of cover)

Continued from inside page of cover